

FRANNY JONGBLOED



DIETARY RESTRICTION AS TREATMENT MODALITY

inducing resistance to ischemic and chemotherapy related stress

DIETARY RESTRICTION AS TREATMENT MODALITY

inducing resistance to ischemic and chemotherapy related stress



FRANNY JONGBLOED

Cover design & layout

Design Your Thesis

www.designyourthesis.com

Printing

Ridderprint

www.ridderprint.nl

ISBN: 978-94-6299-790-5

The printing of this thesis has been financially supported by:

Erasmus MC afdeling Heelkunde

Erasmus Universiteit Rotterdam

Maasstad Ziekenhuis Fonds Bariatrie

Maasstad Academie

RIVM

Nederlandse Transplantatie Vereniging

Pfizer

Chipsoft

Rabobank Medicidesk

This research was funded by the Strategic Research Program from the National Institute for Public Health and the Environment and the Ministry of Health, Welfare and Sport of the Netherlands (Protocol number: S/340005).

© Copyright by F. Jongbloed, Rotterdam, the Netherlands, 2017. All rights reserved.

No part of this thesis may be reproduced or transmitted in any form by any means without prior permission of the author.

DIETARY RESTRICTION AS TREATMENT MODALITY
inducing resistance to ischemic and
chemotherapy related stress

DIEETRESTRICTIE ALS BEHANDELINGSMODALITEIT
inductie van weerstand tegen ischemische en
chemotherapie-gerelateerde stress

PROEFSCHRIFT

ter verkrijging van de graad van doctor aan de

Erasmus Universiteit Rotterdam

op gezag van de rector magnificus

Prof.dr. H.A.P. Pols

en volgens besluit van het College voor Promoties.

De openbare verdediging zal plaatsvinden op

woensdag 13 december 2017 om 11:30 uur

door

Franny Jongbloed

geboren te Rotterdam, Nederland



Erasmus University Rotterdam

PROMOTIECOMMISSIE

Promotoren: Prof. dr. J.N.M. IJzermans
Prof. dr. H. van Steeg

Overige leden: Prof. dr. J.H.J. Hoeijmakers
Prof. dr. H. Pijl
Prof. dr. A.H.J. Mathijssen

Copromotoren: Dr. R.W.F. de Bruin
Dr. M.E.T. Dollé

TABLE OF CONTENTS

PART I. INTRODUCTION

Chapter 1	General introduction & aims and outline of this thesis	11
-----------	--	----

PART II. MECHANISMS OF DIETARY RESTRICTION

Chapter 2	Preoperative fasting protects against renal ischemia-reperfusion injury in aged and overweight mice <i>PLoS One. 2014 Jun 24;9(6):e100853</i>	23
Chapter 3	The transcriptomic response to irinotecan in fasted colon carcinoma bearing mice <i>Submitted</i>	51
Chapter 4	A signature of renal stress resistance induced by short-term dietary restriction, fasting, and protein restriction <i>Scientific Reports. 2017 Jan 19;7:40901</i>	79
Chapter 5	The role of protein and essential amino acids in the protection against hepatic ischemia-reperfusion injury in mice <i>Manuscript</i>	117

PART III. CLINICAL APPLICATIONS OF DIETARY RESTRICTION

Chapter 6	The effects of morbid obesity, metabolic syndrome and bariatric surgery on aging of the T-cell immune system <i>Submitted</i>	145
Chapter 7	Preoperative calorie and protein restriction is feasible and safe in healthy kidney donors and morbidly obese patients: a pilot study <i>Nutrients. 2016 May 20;8(5):306</i>	167
Chapter 8	Combined calorie and protein restriction improves outcome in living kidney donors and kidney transplant recipients <i>Submitted</i>	199

PART IV SUMMARY AND DISCUSSION

Chapter 9	Summary and discussion	241
Chapter 10	Nederlandse samenvatting	259

APPENDICES

Dankwoord	273
List of publications	279
Curriculum Vitae	281
PhD portfolio	283

PART I

INTRODUCTION

Chapter 1

General introduction & aims and outline of this thesis

CHAPTER 1

GENERAL INTRODUCTION &
AIMS AND OUTLINE OF THIS THESIS

GENERAL INTRODUCTION

Dietary restriction (DR) is defined as the reduction in food intake without causing malnutrition¹. As from the 1930s, the beneficial effects of DR became known when McCay et al. showed that reducing calorie intake extended the lifespan of laboratory rats by at least 30%² (Table 1). Much later, their results were extended to other animal species including yeast, fruit flies and rodents as well as non-human primates^{3,4}. These beneficial effects were seen by restricting calorie intake generally around 30%, starting from early adulthood. Although the extension of lifespan could not be replicated in every animal model, for instance in the normal housefly, the beneficial effects are thought to be derived from evolutionary conserved mechanisms^{3,5}. The average extension rate of the median lifespan by DR in healthy animals was around 30%³. This percentage was shown to be even higher in mice with deficiencies causing accelerated aging, including the *Ercc1*(Δ /-) mouse, in which the median and maximum lifespan could be tripled by DR⁶.

Shortly after the effects of DR on aging were discovered, scientists also demonstrated a reduction in incidence and severity of **age-related diseases**. One of the first acknowledgements of this was made in the 1940s, when Tannenbaum et al. demonstrated a reduction of both initiation and progression of spontaneous tumors in small rodents on long-term DR⁷. Indeed, various studies confirmed these results and showed a marked decrease in the incidence of tumor development and progression⁸⁻¹¹. Other well-established effects of DR are the decreased incidence and reversal of the metabolic syndrome, including insulin resistance and diabetes mellitus^{4,12}. Recently, two studies showed and compared these effects in non-human primates, demonstrating that rhesus monkeys on a normal diet had a three times higher and earlier rate of dying from an age-related cause, including cancer, cardiovascular disease and diabetes mellitus, than did monkeys on DR^{13,14}.

The beneficial and reproducible effects of long-term DR triggered scientists to search for the mechanisms inducing these benefits. Until now, the exact mechanisms underlying DR are still largely unknown. One of the effects of DR that has been established is a reduction of the formation of **reactive oxygen species (ROS) and increased resistance against oxidative stress**¹⁵. ROS, which are natural byproducts of the metabolism of oxygen, are overly present in times of increased oxidative stress which occurs for example during metabolic disturbances as hyperinsulinemia as well as chronic inflammation¹⁶.

Table 1. A list of the durations of dietary restriction (DR), maximum lifespan extension and health span benefits described in various animal species

Species	DR (%)	Maximum lifespan extension (%)	Health span	References
Yeast	20-60%	300%	Increased reproductive period	³
Worms	10-35%	200-300%	Increased stress resistance	³
Flies	20-30%	200%	None reported	³
Fish	33-58%	33%	Decrease in age-dependent learning and memory	¹⁷
Mice	30-60%	30-60%	Decrease in age-associated diseases, auto-immune, increased stress resistance	³
Rats	30-60%	30-60%	Decrease in age-associated diseases, increased stress resistance	¹⁸
Monkeys	25%	30%	Decrease in age-associated diseases, prevention of obesity	^{4,13,14}

Increased oxidative stress is also induced by **ischemia-reperfusion injury** (IRI), a phenomenon occurring for instance during organ transplantation and which is a major risk factor for damage to or even failure of the transplanted organ. After organ retrieval, cessation of the blood flow, ischemia, leads to hypoxia, nutrient deprivation, and thereby accumulation of metabolic waste products. Reperfusion of the ischemic organ increases the generation of reactive oxygen species, triggers apoptotic cell death, and starts an inflammatory response which may result in profound tissue injury^{19,20}. Especially the reperfusion period is thought to be a major player in the increased ROS production, which leads to high levels of oxidative stress²¹. Several studies have tried to use the increased stress resistance by DR in a therapeutic fashion. For instance, Sun et al. showed that rats subjected to 6 months of 40% DR are protected against the oxidative damage induced by a high dose of paraquat²². In addition, mice offered 40% DR during 8 months were protected against the toxicity of high doses of paracetamol²³. However, the therapeutic use of DR to protect against oxidative stress in humans was hampered by the long period of DR that was applied.

Since the kinetics of onset of oxidative stress resistance against IRI induced by DR were not yet known at this time, colleagues investigated whether short and clinically applicable periods of DR were able to induce resistance against oxidative stress induced by renal IRI in the mice. It was shown that both four and two weeks of 30% DR were capable of ameliorating renal IRI in mice¹. Mice showed significantly improved survival rate and kidney function after induction of IRI compared to mice that were allowed to eat ad libitum. Subsequently, a short period of 100% DR, namely three days of fasting, induced similar protective effects against renal IRI. Antioxidant and cytoprotective molecules, including heme oxygenase-1 (HO-1) and glutathione reductase (Gsr) were significantly induced by three days of fasting

compared to ad libitum fed mice, while pro-inflammatory markers, including interleukin-6, were significantly reduced after induction of renal IRI¹. These beneficial effects were reproduced in models of hepatic, cardiac, and cerebral IRI, showing that the effects of DR are not organ specific and might be applicable in multiple settings of acute stress²⁴⁻²⁶.

It did not take long before other research fields tried to exploit the beneficial effects of short-term DR, and started to apply it on different models of acute stress. One of these is **chemotherapy**, one of the treatments against cancer. Irinotecan, a chemotherapeutic agent used in the treatment of colorectal carcinoma, is known to induce severe and unpredictable side effects including myelosuppression, diarrhea, and in some cases even death as a complication of side effects, thereby severely reducing the applicability of the drug²⁷. Recently, it was shown that 3-day fasting prior to the administration of a high dose of irinotecan significantly prevented the occurrence of side effects in mice²⁸. Furthermore, tumor growth was reduced equally in ad libitum fed and fasted animals, indicating that the antitumor effect of the drug was unimpaired by the dietary preconditioning²⁹. The mechanisms underlying the beneficial effects of DR on chemotherapy have not yet been unraveled either, and further studies were more than warranted in order to understand the molecular mechanisms by which DR exerts its beneficial effects. Discovering these mechanisms may lead to regimens that are easier to apply in a clinical setting as well as the development of a dietary mimetic.

Despite the impressive body of evidence on the positive effects of DR, a high level of skepticism was present among clinicians about the **clinical translation** of DR to surgical patients³⁰. Not only would it be difficult for patients to voluntarily restrict themselves in their calorie intake, restricting food intake prior to surgery goes against the generally held beliefs that patients should be well fed before surgery to prevent malnutrition³. Even more so, since mice and men cannot be compared one to one, the ideal diet composition and duration needed for inducing similar effects in humans is not yet known³¹. In a pilot study in living kidney donors, Van Ginhoven et al. showed as one of the first that three days of 30% DR followed by 24 hours of fasting prior to kidney donation was feasible and safe, and that kidney donors were highly motivated and open to participate in such a study³². Unfortunately, the diet had only marginal beneficial effects on surgical outcome. Although serum insulin levels were significantly reduced by the diet compared to the control group, it was uncertain whether this was the result of the 4-day dietary intervention or the 24 hours of fasting only³³. Therefore, no clear set of objective markers for compliance to the diet was present up-to-date.

To improve efficacy of a diet in a clinical setting, experiments were initiated to discriminate whether the calorie restriction per se or absence of one of the **nutrients** is responsible for the effects of DR. Data from fruit flies in aging studies hint towards a different role of individual macronutrients, where *Drosophila* lived up to 50% longer when restricted in their protein intake³⁴. Further studies confirmed the key role of protein in the protective effects on both the long-term and short-term effects^{3,35}. In animal models of IRI, a protein-free diet given up to six days prior to IRI was found to be protective against oxidative stress and surgery-related outcome^{36,37}. However, mice on protein-restricted or protein-free diets restricted themselves in food, and thus calorie intake, which made it difficult to distinguish between the effects of protein restriction and calorie restriction³⁶. Also, the role of the other macronutrients, carbohydrates and fats, as well as the amino acids had not been investigated sufficiently to disentangle their contribution to the beneficial effects of DR³⁸⁻⁴⁰. Therefore, in the work described this thesis, my colleagues and I set out to further narrow down the duration and deprivation of nutrient components prior to acute stress-related injury in order to find a safe and effective diet that would be applicable to study in a clinical setting.

AIMS AND OUTLINE OF THIS THESIS

The aims of this thesis were to assess the effects of current short-term DR regimens in different mouse models, to investigate the effects of macronutrients and amino acids in the effects of DR, to broaden the knowledge about the molecular mechanisms underlying DR, and to develop a safe and effective DR regimen to investigate in a clinical surgical setting.

In **chapter 2**, we extended our previous studies on nutritional preconditioning by testing the hypothesis that preoperative fasting induces the same beneficial effects on renal IRI in mice of a different genetic background and that were overweight, aged, and of both male and female gender. We compared general changes on a transcriptional level between young-lean and aged-overweight male mice, and focused on pathways and individual genes that could be involved in the protective effect of DR on renal IRI. In **chapter 3**, the reduction of chemotherapy-related toxicity by fasting was investigated on a transcriptional level. Tumor-bearing mice were subjected to fasting and subsequent irinotecan treatment, and the transcriptome of both liver and tumor was compared to that of mice that were ad libitum fed and/or were not given any chemotherapy. In **chapter 4**, we investigated to role of short-term macronutrient-free diets on renal IRI on both a phenotypical and transcriptional level. Together with the gene expression profiles of DR and fasting, we collected an extensive dataset of different DR strategies that are either protective or non-protective against renal IRI. Microarray analyses enabled us to further unravel potential key pathways and transcription factors mediating the effects of DR, fasting and protein

restriction (PR). In **chapter 5**, we took a step further and studied the role of the building blocks of proteins, *i.e.* the essential amino acids leucine, tryptophan and methionine, on postoperative and transcriptional outcome after IRI of the liver.

To further understand the role of DR on surgical outcome, in **chapter 6** we used a human model that is the opposite of nutrient deprivation, *i.e.* morbid obesity, followed by a surgical form of DR, namely bariatric surgery. We investigated the detrimental effects of the metabolic syndrome on aging in morbidly obese patients. In particular, we examined the aging of the immune system and whether bariatric surgery is able to reverse these detrimental effects. We took blood samples of morbidly obese patients before and after bariatric surgery and measured relative telomere length and T-cell differentiation status, which are markers of cellular aging.

In **chapter 7**, a first step towards translation of short-term DR to humans was made by investigating the safety, feasibility of and compliance to a combined DR and PR diet in humans awaiting surgery. Healthy living kidney donors and morbidly obese bariatric surgery patients were offered a synthetic diet containing both DR and PR, or a synthetic placebo-diet that was isocaloric to the individual daily energy requirements. Effects of these diets were compared to those of a control group including donors whom were allowed to eat *ad libitum*, and were asked to fill in a diary of their nutritional intake. Safety, feasibility and compliance were tested via objective markers in blood samples, as well as subjective outcome in the form of questionnaires filled in before and after the application of the three dietary interventions. Since the DR and PR synthetic diet was considered safe and feasible, in **chapter 8**, the effects of this diet on clinical outcome as well as molecular changes was investigated in healthy living kidney donors and their kidney transplant recipients. This was done by examining kidney function and systemic inflammation markers in blood samples taken before, during and after surgery in both kidney donor and recipient. Effects on gene expression profiles were examined in kidney biopsies taken during surgery.

In **chapter 9**, a summary and discussion of the results described in this thesis are presented and emphasis is put on future perspectives of the research of DR in both the preclinical and clinical setting.

REFERENCES

1. Mitchell, J.R., et al. Short-term dietary restriction and fasting precondition against ischemia-reperfusion injury in mice. *Aging Cell* 9, 40-53 (2010).
2. McCay, C.M. Is Longevity Compatible with Optimum Growth? *Science* 77, 410-411 (1933).
3. Fontana, L., Partridge, L. & Longo, V.D. Extending healthy life span--from yeast to humans. *Science* 328, 321-326 (2010).
4. Colman, R.J., et al. Caloric restriction delays disease onset and mortality in rhesus monkeys. *Science* 325, 201-204 (2009).
5. Mockett, R.J., Cooper, T.M., Orr, W.C. & Sohal, R.S. Effects of caloric restriction are species-specific. *Biogerontology* 7, 157-160 (2006).
6. Vermeij, W.P., et al. Restricted diet delays accelerated ageing and genomic stress in DNA-repair-deficient mice. *Nature* 537, 427-431 (2016).
7. Tannenbaum, A. & Silverstone, H. The influence of the degree of caloric restriction on the formation of skin tumors and hepatomas in mice. *Cancer Res* 9, 724-727 (1949).
8. Weindruch, R. Dietary restriction, tumors, and aging in rodents. *J Gerontol* 44, 67-71 (1989).
9. Robertson, L.T. & Mitchell, J.R. Benefits of short-term dietary restriction in mammals. *Exp Gerontol* 48, 1043-1048 (2013).
10. Daniel, M. & Tollefsbol, T.O. Epigenetic linkage of aging, cancer and nutrition. *J Exp Biol* 218, 59-70 (2015).
11. Brandhorst, S. & Longo, V.D. Fasting and Caloric Restriction in Cancer Prevention and Treatment. *Recent Results Cancer Res* 207, 241-266 (2016).
12. Wang, J., et al. Nutrition, epigenetics, and metabolic syndrome. *Antioxid Redox Signal* 17, 282-301 (2012).
13. Colman, R.J., et al. Caloric restriction reduces age-related and all-cause mortality in rhesus monkeys. *Nat Commun* 5, 3557 (2014).
14. Mattison, J.A., et al. Caloric restriction improves health and survival of rhesus monkeys. *Nat Commun* 8, 14063 (2017).
15. Lopez-Torres, M. & Barja, G. Calorie restriction, oxidative stress and longevity. *Rev Esp Geriatr Gerontol* 43, 252-260 (2008).
16. Mittal, M., Siddiqui, M.R., Tran, K., Reddy, S.P. & Malik, A.B. Reactive oxygen species in inflammation and tissue injury. *Antioxid Redox Signal* 20, 1126-1167 (2014).
17. Terzibasi, E., et al. Effects of dietary restriction on mortality and age-related phenotypes in the short-lived fish *Nothobranchius furzeri*. *Aging Cell* 8, 88-99 (2009).
18. Masoro, E.J. Dietary restriction and aging. *J Am Geriatr Soc* 41, 994-999 (1993).
19. Kalogeris, T., Baines, C.P., Krenz, M. & Korthuis, R.J. Cell biology of ischemia/reperfusion injury. *Int Rev Cell Mol Biol* 298, 229-317 (2012).

20. Weight, S.C., Bell, P.R. & Nicholson, M.L. Renal ischaemia--reperfusion injury. *Br J Surg* 83, 162-170 (1996).
21. Jaeschke, H. & Woolbright, B.L. Current strategies to minimize hepatic ischemia-reperfusion injury by targeting reactive oxygen species. *Transplant Rev (Orlando)* 26, 103-114 (2012).
22. Sun, D., Muthukumar, A.R., Lawrence, R.A. & Fernandes, G. Effects of calorie restriction on polymicrobial peritonitis induced by cecum ligation and puncture in young C57BL/6 mice. *Clin Diagn Lab Immunol* 8, 1003-1011 (2001).
23. Harper, J.M., et al. Stress resistance and aging: influence of genes and nutrition. *Mech Ageing Dev* 127, 687-694 (2006).
24. Verweij, M., et al. Preoperative fasting protects mice against hepatic ischemia/reperfusion injury: mechanisms and effects on liver regeneration. *Liver Transpl* 17, 695-704 (2011).
25. Mattson, M.P., Duan, W., Lee, J. & Guo, Z. Suppression of brain aging and neurodegenerative disorders by dietary restriction and environmental enrichment: molecular mechanisms. *Mech Ageing Dev* 122, 757-778 (2001).
26. Mattson, M.P. & Wan, R. Beneficial effects of intermittent fasting and caloric restriction on the cardiovascular and cerebrovascular systems. *J Nutr Biochem* 16, 129-137 (2005).
27. Rothenberg, M.L. Efficacy and toxicity of irinotecan in patients with colorectal cancer. *Semin Oncol* 25, 39-46 (1998).
28. Huisman, S.A., Bijman-Lagcher, W., JN, I.J., Smits, R. & de Bruin, R.W. Fasting protects against the side effects of irinotecan but preserves its anti-tumor effect in *Apc15lox* mutant mice. *Cell Cycle* 14, 2333-2339 (2015).
29. Huisman, S.A., et al. Fasting protects against the side effects of irinotecan treatment but does not affect anti-tumour activity in mice. *Br J Pharmacol* 173, 804-814 (2016).
30. Brandhorst, S., Harputlugil, E., Mitchell, J.R. & Longo, V.D. Protective effects of short-term dietary restriction in surgical stress and chemotherapy. *Ageing Res Rev* (2017).
31. Demetrius, L. Of mice and men. When it comes to studying ageing and the means to slow it down, mice are not just small humans. *EMBO Rep* 6 Spec No, S39-44 (2005).
32. van Ginhoven, T.M., et al. Pre-operative dietary restriction is feasible in live-kidney donors. *Clin Transplant* 25, 486-494 (2011).
33. van Ginhoven, T.M., et al. Dietary restriction modifies certain aspects of the postoperative acute phase response. *J Surg Res* 171, 582-589 (2011).
34. Partridge, L., Piper, M.D. & Mair, W. Dietary restriction in *Drosophila*. *Mech Ageing Dev* 126, 938-950 (2005).
35. Mirzaei, H., Suarez, J.A. & Longo, V.D. Protein and amino acid restriction, aging and disease: from yeast to humans. *Trends Endocrinol Metab* 25, 558-566 (2014).
36. Peng, W., et al. Surgical stress resistance induced by single amino acid deprivation requires *Gcn2* in mice. *Sci Transl Med* 4, 118ra111 (2012).

37. Gallinetti, J., Harputlugil, E. & Mitchell, J.R. Amino acid sensing in dietary-restriction-mediated longevity: roles of signal-transducing kinases GCN2 and TOR. *Biochem J* 449, 1-10 (2013).
38. Solon-Biet, S.M., et al. Dietary Protein to Carbohydrate Ratio and Caloric Restriction: Comparing Metabolic Outcomes in Mice. *Cell Rep* 11, 1529-1534 (2015).
39. Solon-Biet, S.M., et al. Macronutrients and caloric intake in health and longevity. *J Endocrinol* 226, R17-28 (2015).
40. Verweij, M., et al. Glucose supplementation does not interfere with fasting-induced protection against renal ischemia/reperfusion injury in mice. *Transplantation* 92, 752-758 (2011).

PART II

MECHANISMS OF DIETARY RESTRICTION

Chapter 2

Preoperative fasting protects against renal ischemia-reperfusion injury in aged and overweight mice

PLoS One. 2014 Jun 24;9(6):e100853

Chapter 3

The transcriptomic response to irinotecan in fasted colon carcinoma bearing mice

Submitted

Chapter 4

A signature of renal stress resistance induced by short-term dietary restriction, fasting, and protein restriction

Scientific Reports. 2017 Jan 19;7:40901

Chapter 5

The role of protein and essential amino acids in the protection against hepatic ischemia-reperfusion injury in mice

Manuscript

CHAPTER 2

PREOPERATIVE FASTING PROTECTS AGAINST RENAL ISCHEMIA-REPERFUSION INJURY IN AGED AND OVERWEIGHT MICE

Franny Jongbloed, Ron W.F. de Bruin, Jeroen L.A. Pennings, César Payán-Gómez, Sandra van den Engel, Conny T. van Oostrom, Alain de Bruin, Jan H.J. Hoeijmakers, Harry van Steeg, Jan N.M. IJzermans, Martijn E.T. Dollé

PLoS One. 2014 Jun 24;9(6):e100853

ABSTRACT

Ischemia-reperfusion injury (IRI) is inevitable during kidney transplantation leading to oxidative stress and inflammation. We previously reported that preoperative fasting in young-lean male mice protects against IRI. Since patients are generally of older age with morbidities possibly leading to a different response to fasting, we investigated the effects of preoperative fasting on renal IRI in aged-overweight male and female mice. Male and female F1-FVB/C57BL6-hybrid mice, average age 73 weeks weighing 47.7 grams, were randomized to preoperative ad libitum feeding or 3-day fasting, followed by renal IRI. Body weight, kidney function and survival of the animals were monitored until day 28 postoperatively. Kidney histopathology was scored for all animals and gene expression profiles after fasting were analyzed in kidneys of young and aged male mice. Preoperative fasting significantly improved survival after renal IRI in both sexes compared with normal fed mice. Fasted groups had a better kidney function shown by lower serum urea levels after renal IRI. Histopathology showed less acute tubular necrosis and more regeneration in kidneys from fasted mice. A mRNA analysis indicated the involvement of metabolic processes including fatty acid oxidation and retinol metabolism, and the NRF2-mediated stress response. Similar to young-lean, healthy male mice, preoperative fasting protects against renal IRI in aged-overweight mice of both genders. These findings suggest a general protective response of fasting against renal IRI regardless of age, gender, body weight and genetic background. Therefore, fasting could be a non-invasive intervention inducing increased oxidative stress resistance in older and overweight patients as well.

INTRODUCTION

The rate of morbidity and mortality in patients with end-stage renal disease (ESRD) is greatly decreased by kidney transplantation, although it brings along its own set of complications like delayed graft function (DGF) and rejection¹. DGF, defined as the need of dialysis in the first week after transplantation, occurs in almost 25% of all kidney transplantations in the USA². Because elderly patients also benefit from a renal transplant, the number of transplantations performed in these patients has increased³. With the already existing shortage of donors, this has widened the gap between organ availability and demand. In an attempt to overcome this shortage, guidelines for extended donation are developed⁴. These extended criteria donors (ECD) are generally of older age, with existing morbidities like obesity and diabetes mellitus⁵. ECD kidneys show higher risks of DGF, acute rejection and graft failure, with recipient and donor age as independent risk factors^{6,7}. Hence, practices improving transplantation success rates are urgently needed.

Ischemia-reperfusion injury (IRI) is an unavoidable consequence of organ transplantation leading to a deleterious activation of cellular oxidases causing oxidative damage, tissue injury and inflammation^{8,9}. IRI has been identified as a major risk factor for the development of DGF and rejection, with ECD kidneys being even more vulnerable to ischemic damage¹⁰. A potentially protective intervention against IRI is dietary restriction (DR), a short-term reduction in caloric intake before induction of ischemia. Long-term DR has been shown to prolong both health- and lifespan^{11,12}. Although its mechanisms have not yet been elucidated, increased resistance to oxidative stress is likely to be involved. In addition, short-term DR and fasting as a more acute approach of DR have been found to increase resistance against oxidative damage as well, including IRI^{9,13}. Previously, we have shown that both three days of fasting and two weeks of 30% DR induce robust protection against renal IRI in mice^{9,14,15}. However, these studies have been conducted with healthy young-lean male mice. The relevance of these findings for a heterogeneous group of patients which are generally older and suffer from disease is uncertain since the response induced by fasting and DR under these conditions is unknown^{16,17}. Therefore, the aim of this study is to examine the effect of age, body weight, gender, and genetic background on the protection against renal IRI induced by fasting. We show that preoperative fasting protects against the effects of IRI in aged-overweight male and female mice comparable to young-lean mice. Subsequently, we compared gene expression profiles of kidneys of young-lean mice with those of aged-overweight mice before and after fasting and identified several metabolic processes including fatty acid oxidation and retinol metabolism as well as pathways involved in the oxidative stress response as likely candidates involved in the induction of increased stress resistance by fasting.

RESULTS

Fasted aged-overweight mice show a gradual weight gain after renal IRI

Male and female F1-FVB/C57BL6-hybrid mice were either fasted for three days by permitting water only or fed ad libitum (AL) preceding surgery. The mean baseline weight was 47.4 ± 5.1 and 48.0 ± 7.6 grams for male and female mice, respectively, demonstrating their overweight phenotype acquired by ad libitum conditions compared to their mean body weight at 12 weeks: 31.4 ± 3.1 (male) and 24.2 ± 2.4 (female) (data not shown). Fasting resulted in a net body weight loss of 8.2 ± 0.5 and 6.5 ± 0.9 grams in males and females, respectively, correlating with approximately 17% and 14% of their body weight before fasting (Figure 1A). After IRI, the fasted male and female mice showed a 5% and 10% weight loss, respectively, in the first five postoperative days (POD), after which their weight stabilized (Figure 1A). From POD7 on, they gradually gained weight and eventually reached their preoperative weight ($t=0$) at day 28. In contrast, the AL fed mice showed a larger and faster weight loss after IRI. The AL fed males lost 7% in three days, after which they had all died. The AL fed females lost slightly more relative weight during the same period (10%). By POD5, they had lost 21% of their weight, resulting in a total weight slightly below that reached by the fasted animals. After POD7, the single surviving AL fed female mouse showed a similar trend in body weight gain as the fasted mice.

Three-day fasting confers resistance to renal ischemia in aged-overweight mice

At surgery, bilateral renal ischemia was applied for 37 minutes in male and 60 minutes in female mice followed by reperfusion. Both male and female fasted mice had a significant improved survival compared to the AL fed groups (Figure 1B). All eight AL male mice died or were sacrificed because of morbidity indicative of kidney failure within three days following reperfusion, whereas 7/8 fasted males survived through POD7. At POD7, four male mice were sacrificed for pathological analysis and censored in Figure 1B. Two of the three remaining mice survived in good health through day 28. In the fasted female group, one mouse was found dead on POD1 after IRI because of secondary causes (sutures removed by animal) and was excluded from further analyses. One of the 11 ad libitum fed females survived the observation period, while the majority, nine in total, died or were sacrificed due to morbidity within three days following IRI. At 28 days, 7/10 fasted female mice were still alive and appeared healthy. All fasted mice that died showed indications of irreversible kidney failure (morbidity and loss of kidney function, see serum and histology data described further on).

Preoperative fasting leads to improved kidney function and recovery after IRI

To measure the effect of fasting on kidney function after IRI, serum urea and creatinine levels were measured at days 0, POD1 and if applicable, POD2 and POD7 after surgery. Compared to AL fed mice, serum urea levels in male and female fasted aged mice were lower on postoperative day one, which became significant on day 2 (males $P=0.001$; females $P=0.016$; Figure 2A). Significance could not be determined on day 7 post-IRI as only 2 AL females remained. Serum creatinine did not show statistically significant differences between groups (Figure 2B).

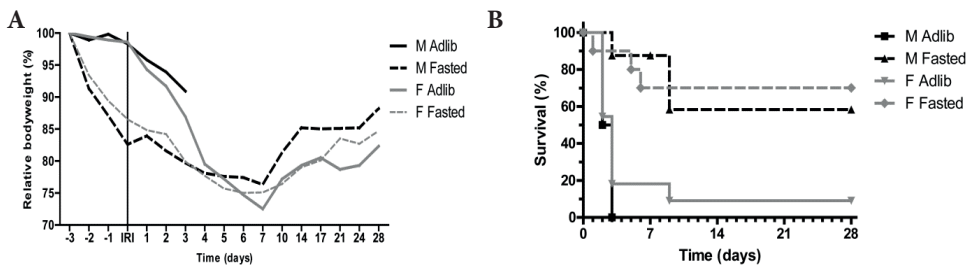


Figure 1. Relative body weight and survival. Relative body weight (A) and survival (B) of male and female mice undergoing 37 and 60 minutes of renal ischemia-reperfusion injury (IRI), respectively, preceded by 3-day fasting or ad libitum feeding. In the first week after surgery, both fasted groups gradually lost weight after which they slowly gained weight in the weeks thereafter. Both fasted groups show a significantly improved survival: $P=0.0171$ for males, $P=0.0040$ for females. M=male, F=female, Adlib=ad libitum fed.

Kidney damage after IRI was further assessed by histopathology. After sorting by cause of death, mice found dead and mice that were moribund and sacrificed showed severe acute tubular necrosis (Figure 3A), a major determinant of renal IRI. Median tubular necrosis scores in these groups, with 0 indicating no and 5 severe necrosis, were 5 and 4, respectively, with no significant differences between the two groups, demonstrating that moribund mice indeed suffered from severe kidney failure independent of the day histology was determined. In contrast, the surviving mice had a median pathology score of 1 ($P<0.001$) (Figure 3A).

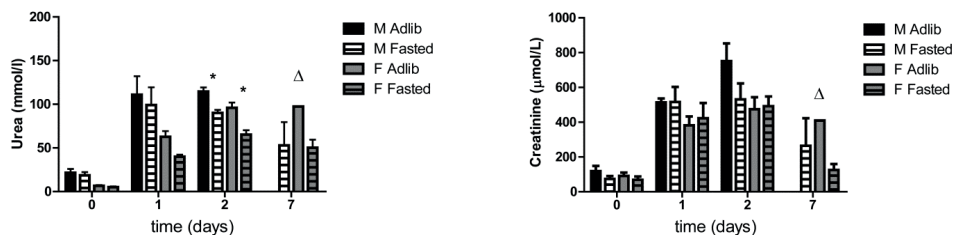


Figure 2. Kidney function of male and female mice after undergoing 37 and 60 minutes of bilateral renal IRI, respectively, preceded by 3-day fasting or ad libitum feeding. (A) Serum urea levels are significantly lower in fasted males and females on day 2 after renal IRI. (B) Serum creatinine levels show no significant differences between fasted and ad libitum fed mice. M=male, F=female, Adlib=ad libitum fed. Δ=no standard deviation is shown as only two animals comprised this group.

As time after IRI might influence the severity of the pathological changes, four fasted male mice were sacrificed at POD7 and histology was compared with mice that died due to kidney failure. The tubular necrosis score of these four sacrificed mice was identical to that of the mice sacrificed at day 28 (median score 1), showing a similar contrast with the mice that died due to kidney failure, indicative of an acute protective effect of the diet. The amount of tubular regeneration is scored between 0 and 4 with 4 as the strongest regenerative response. Mice found dead or moribund scored a median pathology score for tubular regeneration of 0.5 and 0, respectively, and the fasted mice had a median score of 3.5, including mice sacrificed at POD7 and at later time-points ($P < 0.0001$) (Figure 3B). When subdivided by gender and diet group, fasted male and female mice showed significantly less necrosis ($P = 0.0018$ and $P = 0.0035$, respectively) and significantly more regeneration ($P = 0.0089$ and 0.0036 , respectively) compared to the AL fed groups (Figures 3 C/D). Representative images of the pathological lesions observed in the different groups are shown in Figure 4.

Gene expression profiles in kidneys show overlap between young and aged male mice in response to fasting

Firstly, gene expression profiles were compared between kidneys of ad libitum fed and three days fasted aged male mice (without renal IRI) by whole-genome mRNA microarray analysis. The total number of probe sets differentially regulated was assessed. In total, 854 out of 45,141 probe sets were significantly differentially regulated ($FDR \leq 5\%$) in the fasted aged mice with a fold change ≥ 1.5 . Of these 854 probe sets, 454 probe sets were upregulated and 400 downregulated (Figure 5A). Secondly, since fasting was shown to confer resistance to IRI in young-lean male mice⁹, we performed a similar mRNA analysis in kidneys

young or aged mice were plotted against each other (Figure 5B). The majority of these probe sets (85%) had similar directional changes in kidneys of young and aged mice, although the fold changes of the aged kidneys were generally lower compared to young.

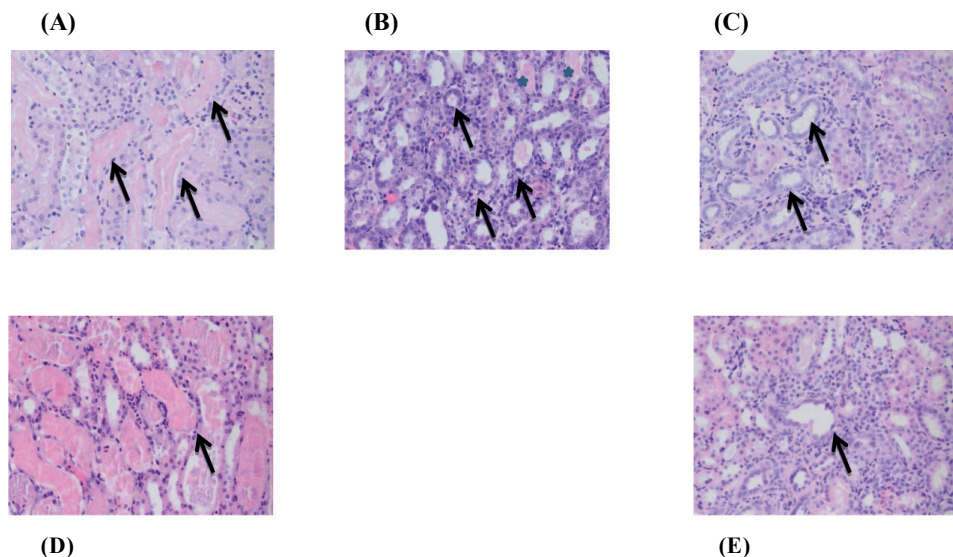


Figure 4. Representative images of HE stained kidney sections with acute tubular necrosis or tubular epithelial regeneration. (A) Multifocal severe acute tubular necrosis with typical diluted tubules, flattened epithelial lining and granular casts inside the tubules (arrows) in ad libitum fed male mouse four days after 37 minutes of IRI. (B) On day 7, male fasted mice already show a high degree of regeneration (arrows) with minimal necrosis (stars). (C) Multifocal tubular regeneration as shown by mitosis bodies along the epithelial line (arrows) in a fasted male mouse 28 days after 37 minutes of IRI. (D) Multifocal severe acute tubular necrosis in ad libitum fed female mouse four days after 60 minutes of IRI. (E) Multifocal tubular regeneration in a fasted female mouse 28 days after 60 minutes of IRI.

To determine the effect on a biological level, functional annotation and pathway overrepresentation analyses of probe sets with $FDR \leq 5\%$ and $FC \geq 1.5$, were performed with Ingenuity software. The top up- and downregulated genes ($FC \geq 5$) with corresponding P -values resulting from the functional annotation are provided as supplementary tables by age group (Table S1-S4). Pathway analysis in aged mice resulted in the highest overrepresented pathways being *LXR/RXR Activation*, *Cholesterol Biosynthesis* and *Fatty Acid β -Oxidation* (Table 1). The most overrepresented pathways in young-lean male mice were *Cholesterol*

Biosynthesis, NRF2-mediated Oxidative Stress Response and *LXR/RXR Activation*. Amongst the top 15 regulated pathways, six pathways are represented in both aged and young mice (Table 1), demonstrating the similarity of the individual pathway results.

The overlapping probe sets in both young and aged mice presumably contain those in the kidney that contribute to resistance to IRI. Therefore, the pathway overrepresentation was repeated for the 601 probe sets significantly expressed in both age groups (Table 2). The top overrepresented pathways involve *RXR Activation, Fatty Acid β -oxidation* or *NRF2-mediated stress response*, partly overlapping with the age group specific pathway analyses.

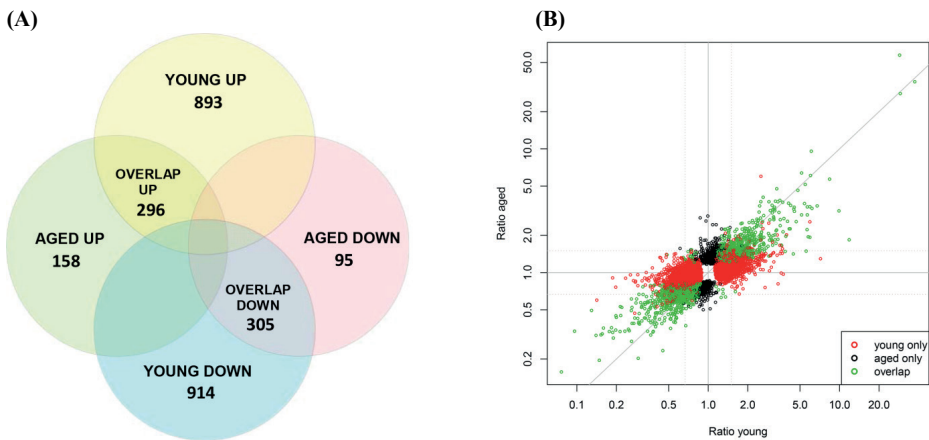


Figure 5. Venn diagram and scatterplot of microarray data after fasting in young and aged mice. (A) Venn diagram of the significantly differentially up- and downregulated ($FDR \leq 5\%$, $FC \geq 1.5$) and overlapping probe sets in kidneys of three days fasted aged and young mice in comparison with normal fed control mice. (B) Scatter plot comparing up- and downregulated trends and their fold ratios of probe sets significantly regulated ($FDR \leq 5\%$) in young-lean (red), aged-overweight mice (black) or overlapping in both groups (green). Without fold change cut-off, 85% of the genes showed the same directionality in both age groups. The grey solid line represents the reference diagonal (ratio young = ratio aged); the grey dotted lines show the 1.5-fold change cutoffs applied in 5A.

Because of their relatively high fold change and their involvement in processes regulated by fasting found in the analysis, *Ppara*, *Gst2*, *Cyp4a14* and *Sc4mol* were validated by qRT-PCR.

Table 1. Top 15 canonical pathways in kidney of aged and young mice in response to fasting compared with ad libitum

Canonical Pathways AGED	P-value	Genes Ratio
LXR/RXR Activation	9.68 ^E -08	17/139 (12.2%)
Fatty Acid β -oxidation I	1.30 ^E -07	9/45 (20.0%)
Superpathway of Cholesterol Biosynthesis	1.30 ^E -07	9/87 (10.3%)
LPS/IL-1 Mediated Inhibition of RXR Function	6.08 ^E -07	22/245 (9.0%)
Sterate Biosynthesis I (Animals)	6.32 ^E -06	8/49 (16.3%)
Cholesterol Biosynthesis I/II/III	2.31 ^E -05	5/40 (12.5%)
TR/RXR Activation	1.96 ^E -04	10/109 (9.2%)
NRF2-mediated Oxidative Stress Response	2.96 ^E -04	15/195 (7.7%)
Dopamine Degradation	5.84 ^E -04	5/38 (13.2%)
Androgen Biosynthesis	5.91 ^E -04	4/26 (15.4%)
Mevalonate Pathway I	7.87 ^E -04	4/29 (13.8%)
Alanine Degradation III/Biosynthesis II	8.86 ^E -04	2/6 (33.3%)
γ -linolenate Biosynthesis II (Animals)	1.31 ^E -03	4/24 (16.7%)
Superpathway of Geranylgeranyldiphosphate Biosynthesis I (via Mevalonate)	2.04 ^E -03	4/37 (10.8%)
Canonical Pathways YOUNG	P-value	Genes Ratio
Superpathway of Cholesterol Biosynthesis	1.19 ^E -08	14/87 (16.1%)
NRF2-mediated Oxidative Stress Response	3.46 ^E -07	35/195 (17.9%)
LXR/RXR Activation	4.46 ^E -07	27/139 (19.4%)
Cholesterol Biosynthesis I/II/III	1.16 ^E -06	8/40 (20.0%)
LPS/IL-1 Mediated Inhibition of RXR Function	6.87 ^E -06	37/245 (15.1%)
VDR/RXR Activation	8.03 ^E -05	17/88 (19.3%)
Acute Phase Response Signaling	1.04 ^E -04	28/181 (15.5%)
Glucocorticoid Receptor Signaling	1.24 ^E -04	38/299 (12.7%)
Xenobiotic Metabolism Signaling	2.70 ^E -04	38/288 (13.2%)
AMPK Signaling	2.75 ^E -04	23/181(12.7%)
Fatty Acid β -oxidation I	3.17 ^E -04	9/45 (20.0%)
GADD45 Signaling	5.23 ^E -04	7/24 (29.2%)
PPAR α /RXR α Activation	5.39 ^E -04	27/200 (13.5%)
Production of Nitric Oxide and Reactive Oxygen Species	6.44 ^E -04	27/212 (12.7%)
FXR/RXR Activation	8.48 ^E -04	16/110 (14.5%)

Canonical pathways differentially regulated by 3-day fasting in kidneys from aged mice and young mice compared to their ad libitum controls. Pathways are ranked by their corresponding *P*-value. Genes Ratio is the number of genes significantly differentially regulated in the pathway.

The qRT-PCR data confirmed the upregulation of *Ppara*, *Gst2*, *Cyp4a14* with fold increases of 2.5, 8.0 and 106 respectively in young and 2.2, 3.4 and 147, respectively in aged kidneys. The downregulation of *Sc4mol* was also validated with qRT-PCR and showed a significant 1.77-fold decrease in young and 1.72-fold in aged kidneys (Table 3).

Table 2. Top 15 canonical pathways overlapping in aged and young mice in response to fasting compared with ad libitum

Canonical Pathways OVERLAP	P-value	Genes Ratio
LPS/IL-1 Mediated Inhibition of RXR Function	7.85 ^E -07	18/245 (7.3%)
LXR/RXR Activation	1.27 ^E -06	13/139 (9.4%)
Fatty Acid β -oxidation I	2.00 ^E -06	7/45 (15.6%)
Superpathway of Cholesterol Biosynthesis	2.85 ^E -05	6/87 (6.9%)
Dopamine Degradation	1.10 ^E -04	5/38 (13.2%)
Androgen Biosynthesis	1.50 ^E -04	4/26 (15.4%)
Alanine Degradation III/Biosynthesis II	4.22 ^E -04	2/6 (33.3%)
Retinoate Biosynthesis I	4.57 ^E -04	5/37 (13.5%)
Sterate Biosynthesis I (Animals)	7.01 ^E -04	5/49 (10.2%)
NRF2-mediated Oxidative Stress Response	1.29 ^E -03	11/195 (5.6%)
Serotonin Degradation	1.56 ^E -03	6/78 (7.8%)
TR/RXR Activation	1.84 ^E -03	7/109 (6.4%)
FXR/RXR Activation	1.97 ^E -03	7/110 (6.4%)
Cholesterol Biosynthesis I	2.12 ^E -03	3/40 (7.5%)
Bile Acid Biosynthesis, Neutral Pathway	2.12 ^E -03	3/58 (5.2%)

Canonical pathways overlapping in aged and young mice after 3-day fasting with their corresponding geometric mean *P*-value and the percentage of regulated genes.

DISCUSSION

With publications dating back 80 years, DR is one of the most extensively investigated interventions in biology^{18,19}. Long-term DR leads to prolongation of health- and lifespan in many animal species¹¹ as well as an increase in acute stress resistance²⁰. Induction of organ ischemia is a widely used model to examine the effects of DR, since it has been shown to increase the resistance against ischemic injury in organs like heart and brain^{21,22}.

Previous research done in one of our laboratories showed that applying short periods of DR (two and four weeks 30% DR) as well as three days of fasting, conveyed strong protection against morbidity and mortality induced by IRI in the kidney as well as decreased morbidity and improved liver function in a non-lethal liver IRI model^{9,23,24}.

Table 3. Validation via qRT-PCR of four genes found to be significant in the array analysis

Gene	Aged (Affy)	Aged - qPCR	Young (Affy)	Young - qPCR
<i>Ppara</i>	2.53/ 3.00 ^E -09	2.5/6.83 ^E -07	2.74/1.45 ^E -05	2.2/0.0005
<i>Gsta2</i>	5.52/2.45 ^E -08	8.0/3.12 ^E -05	8.72/3.73 ^E -05	3.4/1.52 ^E -05
<i>Cyp4a14</i>	344.47/4.11 ^E -09	106/6.16 ^E -06	126.72/9.85 ^E -07	147/0.0003
<i>Sc4mol</i>	-2.64/5.16 ^E -07	-1.77/0.005	-4.98/1.69 ^E -06	-1.72/0.007

Fold ratios and corresponding *p*-values obtained via microarray analysis (Affy) and qRT-PCR (qPCR) of four genes found to be significant in the performed array analysis.

A drawback of the majority of reports is that for practical reasons the same animal model was utilized, namely healthy young (8-12 weeks) male mice of one genetic background (C57BL/6). These mice poorly represent the heterogeneous human population. In particular, this is valid for ECD whom are older and usually overweight. In this study, we showed that preoperative fasting strongly protects both male and female aged-overweight mice against renal IRI, with a significantly reduced mortality after IRI and better preserved kidney function and morphology. Compared to young mice, the recovery of body weight in fasted aged mice takes longer, probably at least in part due to their greater fat reserve and therefore reduced need to restore body weight in order to survive. Previously we observed that fasted young mice started eating shortly after surgery and showed a rapid increase in body weight. We showed that postoperative food intake and associated weight gain did not contribute to the observed protection⁹. The prolonged modest postoperative weight loss in the fasted aged mice provides additional evidence that postoperative feeding is not involved. In addition, the relative body weight loss in aged mice was less than in the young cohort, leaving these mice with more remaining body fat after fasting and IRI. These results indicate that weight loss and reduction of body fat coincide with but do not contribute to the protection against IRI induced by preoperative deprivation of food.

We compared and analyzed the overlap of gene expression data of young and aged mice via microarray analysis, narrowing down genes and pathways possibly involved in the effect of fasting. We found a striking corresponding directionality in overlapping genes of both groups with the changes being more pronounced and more often significant in the young group. Possibly, aged organs and tissues are not able to mount a more vigorous response as

seen in young animals. Alternatively, or in addition, it could be that fasting of overweight mice triggers less extreme responses because of the presence of larger reserves. Taken together, the survival and kidney function data as well as the gene expression findings suggest that fasting has a more robust effect in young mice, although in aged mice it is still sufficient to induce a protective effect against IRI.

Although ECD are getting more and more accepted as an alternative for optimal donors, the outcome after transplantation of an ECD kidney is worse, with higher risks of DGF, acute rejection and graft failure²⁵. Since age is a factor that cannot be influenced, reducing the consequences of ischemia is all the more warranted. To elucidate the mechanisms responsible for the protective effect induced by fasting, we performed microarray analysis after fasting. Our analysis revealed several interesting pathways regulated in kidneys from both young-lean and aged-overweight male mice, thereby being independent of age, weight and genetic background. After clustering of the pathways according to their known or predicted biological function, three biological processes stood out, namely: retinol biosynthesis, fatty acid oxidation and the stress response pathway *Nrf2* (see Tables 1 and 2). Upregulation of the retinoid X receptors (RXRs) together with retinol biosynthesis was responsible for over a quarter of all overrepresented pathways. RXRs are able to bind with multiple factors like the peroxisome proliferator-activated receptors (PPARs). Depending on the different complexes made, RXRs are involved in many processes. They are able to reduce inflammatory processes and contribute to the reduction of the acute phase response, an inflammatory response occurring after invasive surgery resembling renal IRI²⁶. Activation of RXR also stimulates fatty acid oxidation and transport and is thus partially responsible for the enrichment in fatty acid pathways found after short-term fasting, leading to reduced fat synthesis and storage and increased oxidation in order to burn fat for the production of energy as part of a redesign of metabolic processes upon lack of food²⁷. *Nrf2* and genes involved in the *Nrf2*-pathway were found to be significantly upregulated in kidneys of both young and aged mice after three days of fasting, although less pronounced in the aged cohort. *Nrf2*, nuclear factor-erythroid 2 p-45 related factor 2, is known to have both anti-oxidant and anti-inflammatory features and, more specific to IRI, a deficiency of *Nrf2* leads to aggravation of ischemic injury in mice²⁸⁻³⁰. Previously, we showed that a downstream product of *Nrf2*, heme oxygenase 1 (HO-1), is markedly increased by 3-day fasting in young mice⁹. Together with the pronounced *Nrf2*-mediated oxidative stress response pathway found in the current analysis, *Nrf2* is likely involved in the stress resistance phenotype after DR in both young-lean and aged-overweight mice. It was recently shown that a *Nrf2* activator, CDDO-imidazolide, is able to improve survival after a renal IRI model in mice, inducing similar outcome found with fasting in our mouse model³¹. Whether *Nrf2* induction would lead to the same beneficial effects induced by DR and would be safe and feasibly in the clinic, is to be elucidated.

The upregulation of pathways involved in stress resistance suggests that DR induces a protective state. In addition, we previously showed in young animals that this protection was associated with decreased levels of oxidative injury, cytokine production and inflammation and at six hours after IRI, levels of the pro-inflammatory cytokine interleukin 6 (IL-6) were significantly lower in DR compared to ad libitum fed mice^{9,24}. These early effects support the concept that DR preconditions a protective stress response resulting in a better recovery rather than a faster recovery per se.

In summary, we have shown that fasting induces a robust protection against renal IRI in aged-overweight F1-FVB/C57BL6-hybrid mice as it does in young-lean C57BL/6 mice. These findings suggest a general protective response induced by DR against IRI regardless of age, gender, body weight and genetic background. Gene expression profiles of kidneys of both young and aged mice after fasting show the involvement of retinol biosynthesis as well as stress response pathways. Whether these effects are cell-autonomous or influenced by systemic factors remains unknown and needs further clarification. Finally, contrary to common believe short-term preoperative DR rather than hyper alimentation improves stress resistance and recovery from surgically induced renal IRI. Therefore, translation of preoperative DR to the clinic seems to be the next logical step, whereby older and overweight patients do not have to be excluded from its benefits.

MATERIALS AND METHODS

Ethics statement

All animal experiments are done according to the Dutch National Experiments on Animal Act via the EU adopted Directive 86/609/EEC (1986) and had the approval of the local Animal Experiments Committee of the National Institute of Public Health and the Environment (RIVM), the Netherlands (protocol number: 201100308). To ameliorate suffering of the animals, the mice were given 0.5 ml PBS supplemented with 2.4 µg buprenorphine after surgery in order to compensate for fluid loss and provide analgesia and an identical analgesic dose of buprenorphine was administered in the morning after surgery. The method of sacrifice was exsanguination, done under anesthesia by intramuscular injection of a Ketamine–Rompun mixture.

Animals

All aged mice were bred, raised and kept under identical SPF conditions as described³². Male (n=16) and female (n=22) wild type FVB-C57BL/6J F1-hybrid mice, with an average age of 72 and 74 weeks and average weight of 48.0 and 47.4 grams, respectively, were used. Animals were kept under standard laboratory conditions (temperature ± 20°C, 12-hour

light/12-hour dark) with either one animal (male) or two animals (females) per cage and were allowed free access to water and food (Special Diet Services, UK) unless noted otherwise. The conditions of and procedures done in the young male C57BL/6J mice are described elsewhere⁹.

Preoperative fasting

Mice were pair-matched based on body weight and sex. Subsequently, the animals were randomly assigned to one of two groups. The first group had unlimited access to food and water preoperatively. The average amount of food eaten in the ad libitum fed male and female group was approximately 5.7 and 4.4 grams/day respectively. The second group was fasted for three days preoperatively with no access to food and unlimited access to water. Fasted animals did not show any morbidity due to the fasting. Directly after surgery, all mice had unlimited access to food and water. For the microarray analysis, 10 other male mice were also assigned to either ad libitum food or fasting for three days, after which the mice were sacrificed.

Surgical procedure

Renal IRI was performed as described previously^{9,14}. In brief, mice were anesthetized by isoflurane inhalation (5% isoflurane initially and then 2-2.5% with oxygen for maintenance). A midline abdominal incision was performed and the renal artery and vein of both kidneys were exposed. In the male mice, the pedicles of both kidneys were occluded for 37 minutes. As female mice are more resistant to ischemic renal damage^{33,34}, the ischemic time in female mice was extended to 60 minutes. Purple discoloration of the kidneys confirmed ischemia macroscopically. After removal of the clamps, reperfusion was confirmed when the kidney color turned back to normal. The incision was closed in two layers with 5/0 sutures. After closure, the animals were subcutaneously injected with 0.5 ml PBS supplemented with 2.4 µg buprenorphine in order to compensate for fluid loss and provide analgesia. An identical analgesic dose of buprenorphine was administered in the morning after surgery to ameliorate suffering. The mice used for microarray analysis did not undergo renal IRI, instead were sacrificed right after the dietary intervention.

Follow-up and serum measurements

The animals were followed up to 28 days postoperatively unless they died or were sacrificed as a result of morbidity (ruffled fur, decreased mobility, cold to the touch, excessive weight loss), or noted otherwise. During follow-up, they were inspected at least daily. Body weight was measured daily in the first postoperative week and on day 10, 14, 17, 21 and 28 if applicable. At day 28, all remaining animals were euthanized after which the abdominal cavity was opened for inspection of the kidneys. A blood sample of 50 µl was collected

by orbital puncture while the animals were anesthetized as well as on postoperative day 1, 2, 3, 7 and 28 if applicable. Serum urea and creatinine levels were measured using the QuantiChrom™ assay kits (DIUR-500 and DICt-500, Gentaur Europe, Brussels, Belgium). Statistical analysis was performed with IBM SPSS statistics version 20.0, GraphPad Prism version 5.0, R software and/or Microsoft Excel. Statistical significance was defined as $P < 0.05$ unless noted otherwise. For assessment of the kidney function, the one-way ANOVA was used including the Bonferroni test for multiple comparisons. Means were compared using either the non-parametric Mann-Whitney U test or the independent t-test for parametric data. The survival curves were compared using the Log-rank (Mantel-Cox) test and visualized by the Kaplan-Meier curve.

Histology

After euthanasia, both kidneys were harvested. Half of the left and the right kidney of each mouse were fixed in formalin for histological analysis in Hematoxylin and Eosin (HE) stained sections. Kidneys were analyzed in a blinded manner. Semi-quantitative scoring of the severity of the lesions was performed for acute tubular necrosis (0-5) and tubular epithelial regeneration (0-4). Scores were defined as: 0= none; 1=minimal; 2=mild; 3=moderate; 4=marked and, if applicable, 5=severe necrosis or regeneration. Pathology scores were analyzed with the Kruskal-Wallis test for K independent samples and the Dunn's test for multiple comparisons.

Microarray analysis

Of the 10 male mice used for microarray analysis, half of both the left and the right kidney (taken in longitudinal direction) were snap frozen in liquid nitrogen until further analysis directly after fasting. For gene expression analysis, total RNA was extracted from frozen kidney tissue using the QIAzol lysis Reagent and miRNAeasy Mini Kit (QIAGEN, Hilden, Germany), as described in the Qiagen protocol (males: fasted $n=5$, ad libitum $n=5$). Addition of wash buffers RPE and RWT (QIAGEN) was done mechanically by using the QIAcube (QIAGEN, Hilden, Germany) via the miRNeasy program. RNA was eluted in RNase free water and stored at -80°C . The concentration of RNA was measured by Nanodrop (Thermo Scientific). Quality assessment of the RNA was done using the 2100 Bio-Analyzer (Agilent Technologies, Amstelveen, the Netherlands). The quality of the RNA is expressed as the RNA integrity number (RIN, range 0-10). Samples with a RIN below 8 were excluded from analysis. RNA was further processed for hybridization to Affymetrix HT MG-430 PM Array Plates at the Microarray Department of the University of Amsterdam, the Netherlands according to Affymetrix protocols. Four to six biological replicates were used for each group. Quality control and normalization were performed using the pipeline at the www.arrayanalysis.org website (Maastricht University, the Netherlands). Normalization was done

via the Robust Multichip Average (RMA) algorithm. Normalization output consisted of data for 45,141 probe sets, with several probe sets corresponding to the same Entrez Gene ID. Complete raw and normalized microarray data and their MIAME compliant metadata have been deposited at GEO (www.ncbi.nlm.nih.gov/geo) under accession number GSE52982. Gene expression data were compared using ANOVA with correction for multiple testing using the false discovery rate (FDR) according to Benjamini and Hochberg³⁵. Fold changes are expressed as the geometric mean per fasted group against the corresponding ad libitum group. Cutoff values for a significant difference were put at $FDR < 5\%$. Functional annotation and overrepresentation analyses were performed with Ingenuity software (<http://www.ingenuity.com/products/ipa>). For comparison analysis with young male mice, the same procedure was performed in kidney tissue of male C57BL/6J mice (fasted $n=4$, ad libitum fed $n=5$). For the analyses done in the genes overlapping between aged-overweight and young-lean male mice, the mean fold ratios and geometric mean p -values of both groups were used. No female mice were available for the microarray analysis in young and aged mice.

REFERENCES

1. Tonelli M, Wiebe N, Knoll G, Bello A, Browne S, et al. (2011) Systematic review: kidney transplantation compared with dialysis in clinically relevant outcomes. *Am J Transplant* 11: 2093-2109.
2. Sharif A, Borrows R (2013) Delayed graft function after kidney transplantation: the clinical perspective. *Am J Kidney Dis* 62: 150-158.
3. Rao PS, Merion RM, Ashby VB, Port FK, Wolfe RA, et al. (2007) Renal transplantation in elderly patients older than 70 years of age: results from the Scientific Registry of Transplant Recipients. *Transplantation* 83: 1069-1074.
4. Carrier M, Lize JF (2012) Impact of expanded criteria donors on outcomes of recipients after kidney transplantation. *Transplant Proc* 44: 2227-2230.
5. Port FK, Bragg-Gresham JL, Metzger RA, Dykstra DM, Gillespie BW, et al. (2002) Donor characteristics associated with reduced graft survival: an approach to expanding the pool of kidney donors. *Transplantation* 74: 1281-1286.
6. Saxena R, Yu X, Giraldo M, Arenas J, Vazquez M, et al. (2009) Renal transplantation in the elderly. *Int Urol Nephrol* 41: 195-210.
7. Lim WH, Clayton P, Wong G, Campbell SB, Cohn S, et al. (2013) Outcomes of Kidney Transplantation From Older Living Donors. *Transplantation* 95: 106-113.
8. Eltzschig HK, Eckle T (2011) Ischemia and reperfusion--from mechanism to translation. *Nat Med* 17: 1391-1401.
9. Mitchell JR, Verweij M, Brand K, van de Ven M, Goemaere N, et al. (2010) Short-term dietary restriction and fasting precondition against ischemia-reperfusion injury in mice. *Aging Cell* 9: 40-53.
10. Kosieradzki M, Rowinski W (2008) Ischemia/reperfusion injury in kidney transplantation: mechanisms and prevention. *Transplant Proc* 40: 3279-3288.
11. Nakagawa S, Lagisz M, Hector KL, Spencer HG (2012) Comparative and meta-analytic insights into life extension via dietary restriction. *Aging Cell* 11: 401-409.
12. Colman RJ, Anderson RM, Johnson SC, Kastman EK, Kosmatka KJ, et al. (2009) Caloric restriction delays disease onset and mortality in rhesus monkeys. *Science* 325: 201-204.
13. Pamplona R, Barja G (2006) Mitochondrial oxidative stress, aging and caloric restriction: the protein and methionine connection. *Biochim Biophys Acta* 1757: 496-508.
14. Van Ginhoven TM, Huisman TM, van den Berg JW, Ijzermans JN, Delhanty PJ, et al. (2010) Preoperative fasting induced protection against renal ischemia/reperfusion injury is independent of ghrelin in mice. *Nutr Res* 30: 865-869.
15. Van Ginhoven TM, Van Den Berg JW, Dik WA, Ijzermans JN, De Bruin RW (2010) Preoperative fasting induces protection against renal ischemia/reperfusion injury by a corticosterone-independent mechanism. *Transpl Int* 23: 1171-1178.

16. Sohal RS, Weindruch R (1996) Oxidative stress, caloric restriction, and aging. *Science* 273: 59-63.
17. Rains JL, Jain SK (2011) Oxidative stress, insulin signaling, and diabetes. *Free Radic Biol Med* 50: 567-575.
18. Spindler SR (2010) Caloric restriction: from soup to nuts. *Ageing Res Rev* 9: 324-353.
19. McCay CM, Crowell MF, Maynard LA (1989) The effect of retarded growth upon the length of life span and upon the ultimate body size. 1935. *Nutrition* 5: 155-171; discussion 172.
20. Cruzen C, Colman RJ (2009) Effects of caloric restriction on cardiovascular aging in non-human primates and humans. *Clin Geriatr Med* 25: 733-743, ix-x.
21. Yu ZF, Mattson MP (1999) Dietary restriction and 2-deoxyglucose administration reduce focal ischemic brain damage and improve behavioral outcome: evidence for a preconditioning mechanism. *J Neurosci Res* 57: 830-839.
22. Yamagishi T, Bessho M, Yanagida S, Nishizawa K, Kusuhashi M, et al. (2010) Severe, short-term food restriction improves cardiac function following ischemia/reperfusion in perfused rat hearts. *Heart Vessels* 25: 417-425.
23. Van Ginhoven TM, Mitchell JR, Verweij M, Hoeijmakers JH, Ijzermans JN, et al. (2009) The use of preoperative nutritional interventions to protect against hepatic ischemia-reperfusion injury. *Liver Transpl* 15: 1183-1191.
24. Verweij M, van Ginhoven TM, Mitchell JR, Sluiter W, van den Engel S, et al. (2011) Preoperative fasting protects mice against hepatic ischemia/reperfusion injury: mechanisms and effects on liver regeneration. *Liver Transpl* 17: 695-704.
25. Akoh JA, Mathuram Thiagarajan U (2013) Renal Transplantation from Elderly Living Donors. *J Transplant* 2013: 475964.
26. Mandard S, Muller M, Kersten S (2004) Peroxisome proliferator-activated receptor alpha target genes. *Cell Mol Life Sci* 61: 393-416.
27. Goldstein JL, Zhao TJ, Li RL, Sherbet DP, Liang G, et al. (2011) Surviving starvation: essential role of the ghrelin-growth hormone axis. *Cold Spring Harb Symp Quant Biol* 76: 121-127.
28. Edwards MG, Anderson RM, Yuan M, Kendziorski CM, Weindruch R, et al. (2007) Gene expression profiling of aging reveals activation of a p53-mediated transcriptional program. *BMC Genomics* 8: 80.
29. Jaeschke H, Woolbright BL (2012) Current strategies to minimize hepatic ischemia-reperfusion injury by targeting reactive oxygen species. *Transplant Rev (Orlando)* 26: 103-114.
30. Sykiotis GP, Habeos IG, Samuelson AV, Bohmann D (2011) The role of the antioxidant and longevity-promoting Nrf2 pathway in metabolic regulation. *Curr Opin Clin Nutr Metab Care* 14: 41-48.
31. Liu M, Reddy NM, Higbee EM, Potteti HR, Noel S, et al. (2013) The Nrf2 triterpenoid activator, CDDO-imidazolide, protects kidneys from ischemia-reperfusion injury in mice. *Kidney Int*.

32. Dolle ME, Kuiper RV, Roodbergen M, Robinson J, de Vlugt S, et al. (2011) Broad segmental progeroid changes in short-lived *Ercc1(-/Delta7)* mice. *Pathobiol Aging Age Relat Dis* 1.
33. Hu H, Wang G, Batteux F, Nicco C (2009) Gender differences in the susceptibility to renal ischemia-reperfusion injury in BALB/c mice. *Tohoku J Exp Med* 218: 325-329.
34. Park KM, Kim JI, Ahn Y, Bonventre AJ, Bonventre JV (2004) Testosterone is responsible for enhanced susceptibility of males to ischemic renal injury. *J Biol Chem* 279: 52282-52292.
35. Benjamini Y, Hochberg Y (1995) Controlling the False Discovery Rate - a Practical and Powerful Approach to Multiple Testing. *Journal of the Royal Statistical Society Series B-Methodological* 57: 289-300.

SUPPLEMENTARY DATA

Table S1. Top genes upregulated in aged mice fasted for three days

Genes AGED upregulated	Symbol	Log FR	P-value
Cytochrome P450, family 4, subfamily a, polypeptide 14	Cyp4a14	5.842	5.46 ^E -06
3-hydroxy-3-methylglutaryl-CoA synthase 2	HMGCS2	5.125	1.48 ^E -06
Phosphoenolpyruvate carboxykinase 1	PCK1	3.260	1.83 ^E -04
Acyl-CoA thioesterase 1	ACOT1	2.609	6.18 ^E -06
Pyruvate dehydrogenase kinase, isozyme 4	PDK4	2.508	2.44 ^E -03
Solute carrier family 38, member 3	SLC38A3	2.365	5.57 ^E -05
Cytochrome P450, family 4, subfamily a, polypeptide 11	Cyp4a11	2.250	2.15 ^E -05
Mitochondrial amidoxime reducing component 1	MARC1	2.209	6.23 ^E -03
WD repeat and SOCS box containing 1	WSB1	2.020	3.64 ^E -06
Inhibitor of DNA binding 1	ID1	1.937	6.18 ^E -06
Kv channel-interacting protein 2	Kcni2	1.913	6.50 ^E -06
inhibitor of DNA binding 3	ID3	1.903	7.35 ^E -06
acyl-CoA thioesterase 1	Acot1	1.902	4.94 ^E -06
betaine--homocysteine S-methyltransferase	BHMT	1.890	2.60 ^E -02
insulin-like growth factor binding protein 1	IGFBP1	1.860	8.55 ^E -03
group-specific component (vitamin D binding protein)	GC	1.853	3.60 ^E -03
apolipoprotein D	APOD	1.808	3.82 ^E -03
fibrinogen alpha chain	FGA	1.802	9.00 ^E -04
microsomal glutathione S-transferase 1	MGST1	1.792	6.30 ^E -06
nuclear factor, erythroid 2-like 2	NFE2L2	1.767	4.56 ^E -03
fibrinogen gamma chain	FGG	1.766	1.29 ^E -02
complement component 3	C3	1.756	1.18 ^E -04
aldehyde dehydrogenase family 1, subfamily A7	Aldh1a7	1.722	2.02 ^E -06
glutathione S-transferase alpha 5	GSTA5	1.708	1.63 ^E -05
amylase, alpha 1A (salivary)	AMY1A	1.706	1.16 ^E -03
acyl-CoA thioesterase 2	ACOT2	1.705	1.48 ^E -06
ATP-binding cassette, sub-family B (MDR/TAP), member 1B	Abcb1b	1.662	5.84 ^E -06
aldehyde dehydrogenase 1 family, member A1	ALDH1A1	1.655	4.12 ^E -05
arginase 2	ARG2	1.641	8.57 ^E -05
cytochrome c oxidase subunit VIb polypeptide 2 (testis)	COX6B2	1.624	1.98 ^E -06

Top gene lists of upregulated genes in aged-overweight mice fasted for three days, with corresponding symbols, log fold ratios and *P*-values. All genes with a fold change >5 (log fold ratio (-)1.609) are listed.

Table S2. Top genes downregulated in aged mice fasted for three days

Genes AGED downregulated	Symbol	Log FR	P-value
Solute carrier family 22, member 7	SLC22A7	-2.670	7.74 ^E 05
Major facilitator superfamily domain containing 2A	MFSD2A	-2.357	2.03 ^E 04
Solute carrier family 8, member 1	SLC8A1	-2.302	1.76 ^E 04
Antisense Igf2r RNA	Airn	-2.097	1.17 ^E 05
Midkine	MDK	-1.850	2.84 ^E 04
Branched chain amino-acid transaminase 1	BCAT1	-1.686	1.64 ^E 03
Carbonix anhydrase IV	CA4	-1.680	2.62 ^E 06
Isopentenyl-disphosphate delta isomerase 1	IDI1	-1.674	2.25 ^E 05
Solute carrier family 9, subfamily A, member 8	SLC9A8	-1.647	1.29 ^E 06
Ring finger protein 183	RNF183	-1.606	6.58 ^E 05

Top gene lists of downregulated genes in aged-overweight mice fasted for three days, with corresponding symbols, log fold ratios and *P*-values. All genes with a fold change >5 (log fold ratio (-)1.609) are listed.

Table S3. Top genes upregulated in young mice fasted for three days

Genes YOUNG upregulated	Symbol	Log FR	P-value
3-hydroxy-3-methylglutaryl-CoA synthase 2 (mitochondrial)	HMGCS2	5.227	1.69 ^E -07
cytochrome P450, family 4, subfamily a, polypeptide 14	Cyp4a14	4.842	9.85 ^E -07
carbonyl reductase 3	CBR3	3.565	4.18 ^E -08
aldehyde dehydrogenase 1 family, member A1	ALDH1A1	3.307	5.82 ^E -09
pyruvate dehydrogenase kinase, isozyme 4	PDK4	3.071	4.25 ^E -07
cell death-inducing DFFA-like effector a	CIDEA	2.841	2.45 ^E -02
receptor accessory protein 6	REEP6	2.757	2.82 ^E -07
aldehyde dehydrogenase family 1, subfamily A7	Aldh1a7	2.625	2.57 ^E -07
phosphoenolpyruvate carboxykinase 1 (soluble)	PCK1	2.608	5.70 ^E -05
acyl-CoA thioesterase 1	ACOT1	2.590	8.71 ^E -07
carbonyl reductase 1	CBR1	2.573	8.78 ^E -08
nuclear factor, erythroid 2-like 2	NFE2L2	2.573	2.00 ^E -07
cytochrome P450, family 2, subfamily d, polypeptide 22	Cyp2d22	2.531	1.21 ^E -07
fibrinogen gamma chain	FGG	2.508	2.66 ^E -06
solute carrier family 25, member 25	SLC25A25	2.507	5.74 ^E -06
atonal homolog 7 (Drosophila)	ATOH7	2.478	3.35 ^E -08
solute carrier family 38, member 3	SLC38A3	2.456	4.25 ^E -07
group-specific component (vitamin D binding protein)	GC	2.437	5.65 ^E -06
monoamine oxidase B	MAOB	2.363	1.67 ^E -05
mitochondrial amidoxime reducing component 1	MARC1	2.270	1.94 ^E -05
arginase 2	ARG2	2.180	3.60 ^E -06
complement component 3	C3	2.176	9.85 ^E -07
glutathione S-transferase alpha 5	GSTA5	2.166	3.73 ^E -05
fibrinogen alpha chain	FGA	2.086	2.12 ^E -05
lectin, galactoside-binding, soluble, 4	LGALS4	2.051	5.67 ^E -06
insulin-like growth factor binding protein 1	IGFBP1	2.035	1.03 ^E -03
CCR4 carbon catabolite repression 4-like (<i>S. cerevisiae</i>)	CCRN4L	2.006	8.54 ^E -05
perilipin 5	PLIN5	1.981	1.05 ^E -06
abhydrolase domain containing 15	ABHD15	1.964	3.11 ^E -07
paternally expressed 3	PEG3	1.947	1.97 ^E -05
retinol dehydrogenase 1 (all trans)	Rdh1	1.916	4.25 ^E -07
early growth response 1	EGR1	1.901	2.54 ^E -02
pyridoxal (pyridoxine, vitamin B6) kinase	PDXK	1.894	1.15 ^E -05
betaine--homocysteine S-methyltransferase	BHMT	1.886	4.91 ^E -03

Table S3. (continued)

Genes YOUNG upregulated	Symbol	Log FR	P-value
suprabasin	SBSN	1.879	5.74 ^E -06
cold inducible RNA binding protein	CIRBP	1.875	1.38 ^E -05
regulation of nuclear pre-mRNA domain containing 2	RPRD2	1.850	3.04 ^E -06
period circadian clock 1	PER1	1.848	4.56 ^E -05
RIKEN cDNA 6030422H21 gene	6030422H21Rik	1.847	2.93 ^E -03
retinol saturase (all-trans-retinol 13,14-reductase)	RETSAT	1.825	8.77 ^E -07
chromosome 10 open reading frame 10	C10orf10	1.822	2.73 ^E -03
inhibitor of DNA binding 1	ID1	1.814	4.89 ^E -07
amyotrophic lateral sclerosis 2 (juvenile) chromosome region, candidate 12	ALS2CR12	1.814	1.21 ^E -04
cytochrome P450, family 4, subfamily A, polypeptide 11	CYP4A11	1.792	3.47 ^E -07
cytochrome c oxidase subunit VIIIb	Cox8b	1.769	4.64 ^E -02
ATP-binding cassette, sub-family C (CFTR/MRP), member 4	ABCC4	1.764	1.10 ^E -06
angiopoietin-like 4	ANGPTL4	1.748	2.64 ^E -05
zinc finger CCCH-type containing 6	ZC3H6	1.743	7.07 ^E -06
solute carrier family 22 (organic anion transporter), member 8	SLC22A8	1.730	3.19 ^E -05
Kv channel-interacting protein 2	Kcnp2	1.702	5.03 ^E -07
ganglioside-induced differentiation-associated-protein 10	Gdap10	1.690	5.67 ^E -06
NAD(P)H dehydrogenase, quinone 1	NQO1	1.688	7.41 ^E -07
ATP-binding cassette, sub-family B (MDR/TAP), member 1B	Abcb1b	1.686	3.40 ^E -07
acyl-CoA thioesterase 2	ACOT2	1.679	1.55 ^E -05
FBJ murine osteosarcoma viral oncogene homolog	FOS	1.660	4.41 ^E -02
2-hydroxyacyl-CoA lyase 1	HACL1	1.660	5.67 ^E -06
DAZ interacting zinc finger protein 1	DZIP1	1.657	1.08 ^E -03
butyrobetaine, 2-oxoglutarate dioxygenase 1	BBOX1	1.656	7.42 ^E -07
amylase, alpha 1A	AMY1A	1.644	6.26 ^E -06
ceruloplasmin (ferroxidase)	CP	1.641	4.15 ^E -06
fatty acid binding protein 4, adipocyte	FABP4	1.640	1.16 ^E -04
G0/G1switch 2	GOS2	1.629	1.05 ^E -06
vanin 1	VNN1	1.621	4.25 ^E -07
ethanolamine-phosphate phospho-lyase	ETNPPL	1.617	5.58 ^E -06
apolipoprotein D	APOD	1.617	6.81 ^E -04

Top gene lists of upregulated genes in young-lean mice fasted for three days, with corresponding symbols, log fold ratios and *P*-values. All genes with a fold change >5 (log fold ratio (-)1.609) are listed.

Table S4. Top genes downregulated in young mice fasted for three days

Genes YOUNG downregulated	Symbol	Log FR	P-value
Solute carrier family 22, member 7	SLC22A7	-3.713	8.28 ^E -08
Kinesin family member 20B	KIF20B	-3.379	4.11 ^E -06
Hydroxy-delta-5-steroid dehydrogenase 3, beta- and steroid-isomerase 1	HSD3B1	-2.950	1.04 ^E -06
Branched chain amino-acid transaminase 1	BCAT1	-2.838	1.94 ^E -05
Histone cluster 2, H3c	HIST2H3C	-2.818	5.05 ^E -07
major facilitator superfamily domain containing 2A	MFSD2A	-2.756	1.27 ^E -04
isopentenyl-diphosphate delta isomerase 1	IDI1	-2.712	2.96 ^E -08
solute carrier family 9, subfamily A, member 8	SLC9A8	-2.679	1.07 ^E -07
gamma-aminobutyric acid (GABA) A receptor, beta 3	GABRB3	-2.502	1.25 ^E -05
solute carrier family 7, member 13	SLC7A13	-2.418	3.09 ^E -02
heat shock transcription factor 2 binding protein	HSF2BP	-2.337	7.43 ^E -07
myosin VA (heavy chain 12, myosin)	MYO5A	-2.334	5.95 ^E -06
synapsin III	SYN3	-2.324	4.15 ^E -06
collagen, type III, alpha 1	COL3A1	-2.229	1.05 ^E -06
ST8 alpha-N-acetyl-neuraminide alpha-2,8-sialyltransferase 1	ST8SIA1	-2.212	7.42 ^E -07
chemokine ligand 9	CXCL9	-2.184	1.17 ^E -04
ornithine decarboxylase 1	ODC1	-2.106	4.25 ^E -07
cytochrome P450, family 51, subfamily A, polypeptide 1	CYP51A1	-2.088	2.82 ^E -07
family with sequence similarity 151, member A	FAM151A	-2.018	5.95 ^E -06
GRB10 interacting GYF protein 2	GIGYF2	-1.968	6.45 ^E -06
aldo-keto reductase family 1, member C3	AKRIC3	-1.943	1.11 ^E -04
C1q and tumor necrosis factor related protein 3	C1QTNF3	-1.943	1.60 ^E -06
midkine (neurite growth-promoting factor 2)	MDK	-1.937	6.72 ^E -05
kinesin family member 12	KIF12	-1.928	8.78 ^E -08
SLIT and NTRK-like family, member 6	SLITRK6	-1.890	9.74 ^E -05
McKusick-Kaufman syndrome	MKKS	-1.843	2.30 ^E -05
3-hydroxy-3-methylglutaryl-CoA reductase	HMGCR	-1.838	7.06 ^E -06
solute carrier family 35, member F1	SLC35F1	-1.809	6.67 ^E -07
solute carrier family 34, member 3	SLC34A3	-1.782	3.50 ^E -05
C-type lectin domain family 2, member h	Clec2h	-1.780	7.84 ^E -05
guanylate binding protein 6	Gbp6	-1.778	1.10 ^E -04
solute carrier family 8, member 1	SLC8A1	-1.770	6.25 ^E -06
UDP-Gal:beta GlcNAc beta 1,4- galactosyltransferase, polypeptide 5	B4GALT5	-1.755	6.58 ^E -07
protein Z, vitamin K-dependent plasma glycoprotein	PROZ	-1.745	9.18 ^E -07

Table S4. (continued)

Genes YOUNG downregulated	Symbol	Log FR	P-value
centromere protein J	CENPJ	-1.737	1.24 ^E -06
histone cluster 1, H2ab	Hist1h2ab	-1.708	5.22 ^E -05
UDP glucuronosyltransferase 2 family, polypeptide B15	UGT2B15	-1.680	6.53 ^E -04
annexin A13	ANXA13	-1.678	1.23 ^E -04
glycerate kinase	GLYCK	-1.611	7.42 ^E -07

Top gene lists of downregulated genes in young-lean mice fasted for three days, with corresponding symbols, log fold ratios and *P*-values. All genes with a fold change >5 (log fold ratio (-)1.609) are listed.

CHAPTER 3

THE TRANSCRIPTOMIC RESPONSE TO IRINOTECAN IN FASTED COLON CARCINOMA BEARING MICE

Franny Jongbloed, Martijn E.T. Dollé, Sander A. Huisman, Harry van Steeg,
Mirjam Luijten, Jeroen L.A. Pennings, Jan N.M. IJzermans, Ron W.F. de Bruin

Submitted

ABSTRACT

Irinotecan use is limited due to severe toxicity. Fasting protects against side effects of irinotecan while preserving its antitumor activity. The mechanisms underlying the effects of fasting still need to be elucidated. Here, we investigated the transcriptional responses to fasting and irinotecan in both tumor and healthy liver tissue. Male BALB/c mice were subcutaneously injected with C26 colon carcinoma cells. Twelve days after tumor inoculation, two groups were fasted for three days and two groups were allowed food ad libitum (AL). Within each diet group, one group received irinotecan intraperitoneally, the other vehicle. Twelve hours after injection mice were sacrificed, and blood, tumor and liver tissue were harvested. Blood samples were analyzed for side effects, tissues were used for microarray analyses. The AL irinotecan group had worsened organ function and leukocyte numbers. These effects were abated in fasted animals. A dampened transcriptional response to irinotecan was observed in liver of fasted compared to AL fed mice, including a decreased inflammatory and increased stress resistance response. Tumor tissue did not show a homogeneous response amongst groups. The transcriptional response after fasting as seen in liver was absent in tumor tissue. Fasting reduces toxicity of irinotecan by inducing a protective stress response in healthy liver but not in tumor tissue. These data further help to unravel the mechanisms involved in the effects of fasting on chemotherapeutic side effects and preservation of antitumor activity, and pave the way to improve outcome of chemotherapeutic treatment in cancer patients.

INTRODUCTION

Colorectal cancer (CRC) is the second most diagnosed cancer in women and the third most diagnosed in men. Estimated new colorectal cancer cases account for 1.4 million cases and 693,900 deaths worldwide occurring in 2012¹. At initial presentation, 15-20% of patients already has liver metastases and another 45% is diagnosed with liver metastases in the follow-up after resection of the primary tumor². Irinotecan is a pro-drug of the topoisomerase-I inhibitor SN-38, and is applied in first and second line chemotherapy treatment for colorectal carcinoma^{3,4}. Irinotecan can induce severe and unpredictable side effects including myelosuppression, diarrhea, and in some cases even death as a complication of side effects⁵.

Dietary restriction (DR) is a method to trigger highly conserved survival mechanisms that enhance the resistance of organisms against stressors and diseases⁶. We recently showed that 3-day fasting prior to a toxic dose of irinotecan significantly prevented the occurrence of side effects in *Apc*-mutant mice⁷. Furthermore, tumor size and proliferation were reduced equally in ad libitum (AL) fed and fasted animals. Levels of the active metabolite of irinotecan, SN-38, were significantly lower in plasma and liver tissue from fasted mice, indicating that dietary precondition was able to reduce the systemic toxicity of SN-38 while the phenotypic effect on tumor tissue remained unaltered^{7,8}. These data support the concept of differential stress resistance (DSS), which states that tumor cells are unable to elicit a protective response since they remain driven towards growth due to mutations in onco- and tumor suppressor genes^{8,9}. However, the molecular mechanisms that govern these processes remain largely unknown.

Insight into these mechanisms could facilitate translational research into the clinic since it may reveal alternative approaches to DR such as specialized forms of DR or DR mimetics which may induce similar effects without the disadvantages of fasting, including additional body weight loss in cancer patients. Therefore, in this study we investigated the transcriptional responses to fasting and irinotecan exposure in tumor and in healthy liver tissue.

RESULTS

Fasting induces a chemoprotective phenotype in the liver

Male BALB/c mice with subcutaneously injected C26 colon carcinoma tumors were divided in two groups of six mice each. One group was housed under AL food conditions, while the other group was fasted for three days prior to irinotecan administration. After

administration of either vehicle or irinotecan, all mice were fasted for two hours, after which they were given AL access to food for 10 hours until the moment of sacrifice. Food intake during this period was measured by weighing the food before and afterwards. The mice in both AL groups, AL vehicle and AL irinotecan, ate around three grams per mouse in this 10-hour period. The fasting vehicle group had the highest food intake, 4.3 grams per mouse, whereas the fasted irinotecan mice had an average intake of 3.5 grams per mouse.

The systemic toxic effects of irinotecan and the effects of fasting were analyzed via markers of common (LDH) and liver specific (ALT and AST) cellular injury, and kidney function (urea and creatinine). Levels of these markers in the serum increase upon cell damage and death. Leukocyte numbers were determined as markers of bone marrow toxicity. Administration of irinotecan increased markers of both liver (Figure 1A), and kidney injury (Figure 1B). These increases were suppressed in the fasted animals that received irinotecan.

A common side effect of irinotecan therapy is depletion of white blood cells from the blood. Irinotecan treatment caused a significant depletion of white blood cells, which was also ameliorated by fasting (Figure 1C). Collectively, these results demonstrate successful replication of the fasting induced chemo-protective phenotype in the liver as described before¹⁰.

Liver transcriptome analysis

Principal component analysis

To investigate variability between and within our experimental groups, we performed an unbiased principal component analysis (PCA) including all probe sets in the microarray of liver and tumor tissue samples. In the PCA plot of the liver samples, 50.77% of the variance was explained by principal component (PC) 1 and 16.81% by PC2 (Figure 2A). A pattern of distinct clustering of the four individual groups was seen, with the smallest intragroup variability in the fasting vehicle group. Using the AL vehicle group as reference, the fasting vehicle and fasting irinotecan groups diverged mainly by PC1, while the difference with the AL irinotecan group was for the most part by PC2. The fasting irinotecan group differed almost exclusively by PC1 from AL vehicle, in direction and distance similar to that of fasting vehicle, making fasting vehicle and fasting irinotecan the two groups in closest proximity. These data point towards a more differential regulated and homogeneous response to irinotecan in the liver due to fasting.

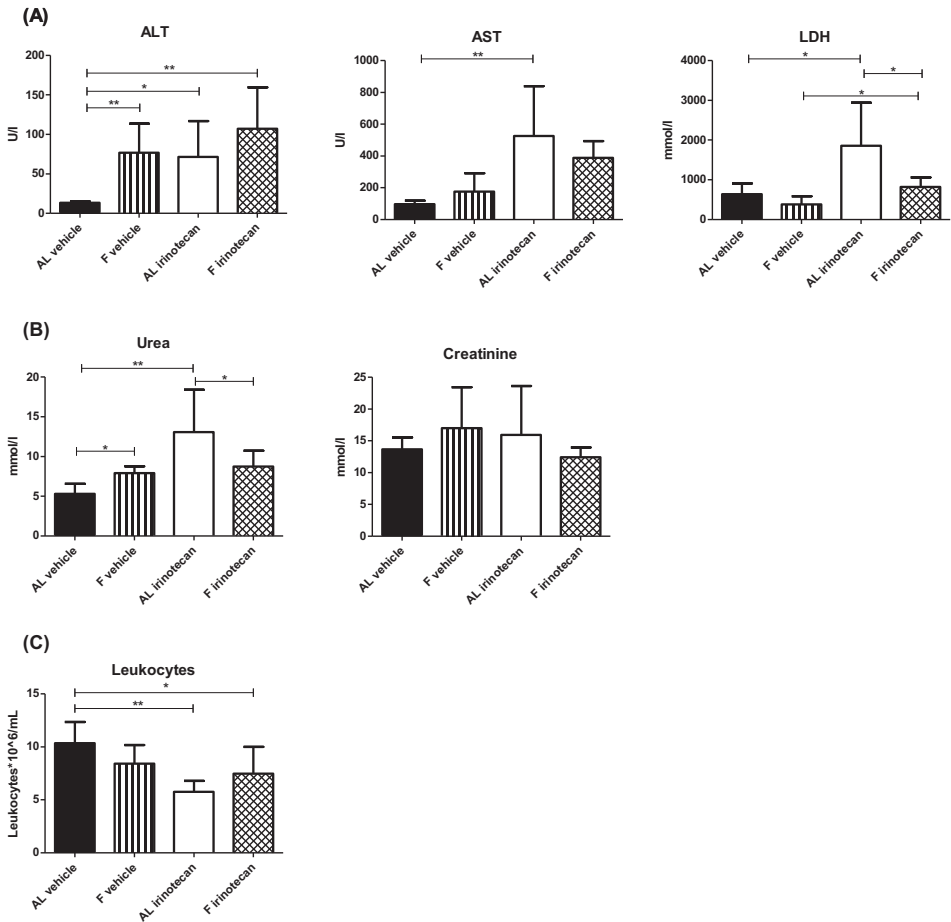


Figure 1. (A) Liver function of the different experimental groups, measured via serum AST, ALT and LDH levels. (B) Measurement of kidney function of the experimental groups via serum urea and creatinine levels. (C) Leukocyte numbers of all the experimental groups. All values correspond to time point 12 hours after administration of either vehicle or irinotecan. AST = aspartate transaminase, ALT = alanine transaminase, LDH = lactate dehydrogenase. * = $P < 0.05$, ** = $P < 0.01$.

Expression profiles

To compare expression profiles between the different experimental groups, the numbers of differentially expressed probe sets (DEPS) were calculated. In the liver, 2,667 DEPS were found between the AL vehicle and AL irinotecan group, with 1,144 DEPS downregulated and 1,523 upregulated (Figure 2B). The number of DEPS between fasting vehicle and fasting irinotecan was 754, a 3.5-fold lower number than found in the AL vehicle and AL

3

irinotecan comparison. Of these 754 genes, 459 DEPS were downregulated and 295 were upregulated. To analyze common expression patterns between the AL and fasting groups, the overlapping DEPS were visualized using a Venn diagram and a scatterplot. The Venn diagram showed that 329 DEPS overlapped between the AL irinotecan and fasting irinotecan groups, corresponding to 44% of the DEPS found after fasting, and only 14% of the DEPS after AL vehicle vs. AL irinotecan (Figure 2C). Directionality and expression intensity of the unique and overlapping genes were visualized in a scatterplot. This scatterplot showed that 83% of all DEPS had a similar directionality in both comparisons, but fold change expressions of the AL irinotecan groups (red symbols) were on average higher than the fasting irinotecan groups (green symbols). Of the overlapping DEPS (black symbols), 99% had a similar directionality (Figure 2D). Collectively, these results point towards a dampened response upon irinotecan exposure in the fasted group compared to that found in AL fed mice.

Pathway analyses

To explore the pathways regulated by irinotecan, the 2,667 DEPS resulting from the comparison of AL vehicle with AL irinotecan were analyzed. A total of 20 pathways were found to be regulated, defined as pathways with a significant *P*-value of <0.05 and a *z*-score of ≥ 1 or ≤ -1 (Table 1A). Of these 20 pathways, 17 were activated and three were inhibited. Analysis of these pathways resulted in an image of an activated genotoxic response. This genotoxic response revealed itself via the activation of multiple pathways involved in intracellular and second messenger signaling, including the RhoA DNA damage pathway. Both cellular stress and cytokine signaling pathways were activated as well, of which most notable eIF2 and interleukin signaling. Apoptosis was stimulated via activation of MAPK signaling. A similar pathway analysis between the fasting groups was performed after exposure to irinotecan which revealed 39 pathways, of which 35 were downregulated and four were upregulated (Table 1B). In contrast to the response in the AL fed animals, an overall inhibition of the response was shown. Comparison of the regulated pathways between the AL groups and the fasting groups revealed a near opposite image (Table 1).

Especially cytokine signaling and cellular immune response appeared downregulated, including chemokine signaling and the IL-8 signaling pathway. Irinotecan exposure in a fasting state also resulted in an inhibition of cellular growth and proliferation, including the inhibition of P70S6K signaling, indicating a decrease in activity of the nutrient-sensor mammalian target of rapamycin (mTOR). Xenobiotic metabolism appears reduced via an inhibition of the aryl hydrocarbon receptor (AHR) pathway, while the stress resistance inducing NRF2-pathway was upregulated.

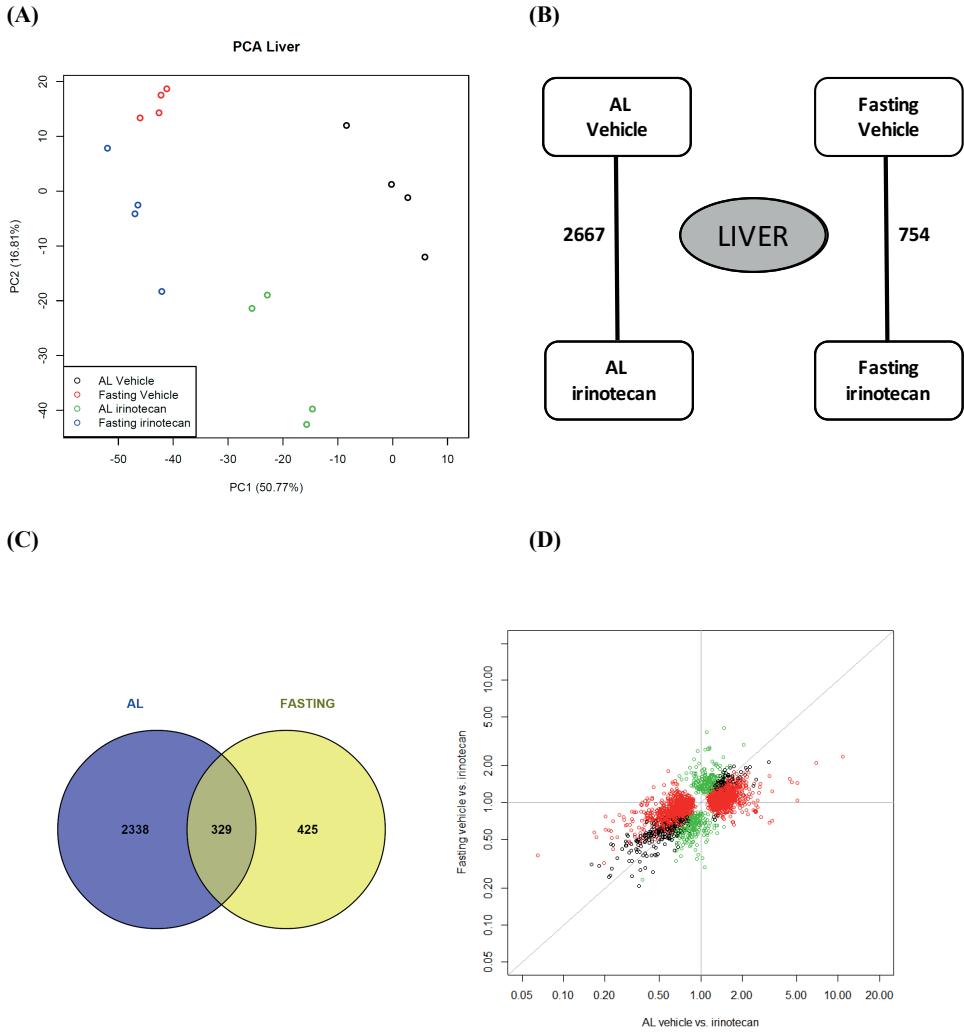


Figure 2. (A) Unbiased principal component analyses (PCA) of liver samples, based on all probe sets in the microarray. Principal component (PC) 1 is depicted on the x-axis and PC2 is depicted on the y-axis, including the percentage of variance explained by each PC. Each symbol represents one sample of one mouse. Samples of the same group are shown in the same color. AL = ad libitum. **(B)** Number of significantly differentially expressed probe sets (DEPS) in livers of AL and fasted mice. **(C)** Venn diagram of overlapping DEPS due to irinotecan exposure in AL and fasted mice. **(D)** Scatterplot of probe set fold expression changes with false discovery rates of 5% or less after irinotecan administration in liver of either AL fed mice (x-axis) or fasted mice (y-axis). Red symbols = AL groups; green symbols = fasting groups; black symbols = overlapping DEPS.

Table 1. Overview of the top overrepresented canonical pathways in liver ranked by their *P*-value

Canonical Pathway	Pathway classification	<i>P</i> -value	Genes Ratio	Z-score
<i>Liver – AL vehicle vs. AL irinotecan</i>				
Signaling by Rho Family GTPases	Intracellular and second messenger signaling	4.99 ^E -03	34/248 (13.7%)	+3.128
LPS/IL-1 Mediated Inhibition of RXR Function	Nuclear Receptor Signaling	2.74 ^E -03	32/221 (14.5%)	+2.840
RhoA Signaling	Intracellular and second messenger signaling	1.02 ^E -02	19/124 (15.3%)	+2.668
EIF2 Signaling	Intracellular and second messenger signaling; cellular stress and injury; cellular growth and proliferation and development	9.16 ^E -03	30/221 (13.6%)	+2.500
Role of NFAT in Cardiac Hypertrophy	Cardiovascular Signaling	4.72 ^E -03	28/193 (14.5%)	+2.000
Ephrin Receptor Signaling	Organismal growth and development; neurotransmitter and other nervous system signaling	2.12 ^E -03	27/174 (15.5%)	+1.789
Sumoylation Pathway	Cellular stress and injury; cellular growth and proliferation and development	1.36 ^E -03	18/96 (18.8%)	+1.604
IL-1 signaling	Cytokine Signaling	5.31 ^E -03	16/92 (17.4%)	+1.604
Integrin Signaling	Cell cycle regulation; intracellular and second messenger signaling; cellular growth and proliferation and development	8.08 ^E -03	30/219 (13.7%)	+1.512
Remodeling of Epithelial Adherens Junctions	Cellular growth and proliferation and development	3.40 ^E -02	11/69 (15.9%)	+1.414
LPS-stimulated MAPK Signaling	Apoptosis	3.61 ^E -02	13/87 (14.9%)	+1.387
fMLP Signaling in Neutrophils	Cytokine signaling; cellular immune response	1.25 ^E -04	24/123 (19.5%)	+1.279
NRF2-mediated Oxidative Stress Response	Cellular stress and injury	4.55 ^E -02	24/193 (12.4%)	+1.291
IL-8 Signaling	Cytokines signaling; cellular immune response	3.34 ^E -05	35/197 (17.8%)	+1.219
Sphingosine-1-phosphate Signaling	Organismal growth and development	2.20 ^E -02	18/125 (14.4%)	+1.213
CXCR4 Signaling	Cytokine signaling; cellular immune response	7.63 ^E -05	30/165 (18.2%)	+1.177
Phospholipase C Signaling	Intracellular and second messenger signaling	9.43 ^E -03	32/240 (13.3%)	+1.000
Calcium-induced T Lymphocyte Apoptosis	Apoptosis; cellular immune response	3.87 ^E -03	13/66 (19.7%)	-1.732
Huntington's Disease Signaling	Neurotransmitter and other nervous system signaling	3.06 ^E -02	30/243 (12.3%)	-1.606
eNOS Signaling	Cardiovascular Signaling	1.25 ^E -03	27/168 (16.1%)	-1.091

Table 1. (continued)

Canonical Pathway	Pathway classification	P-value	Genes Ratio	Z-score
<i>Liver – Fasting vehicle vs. Fasting irinotecan</i>				
RhoGDI Signaling	Intracellular and second messenger signaling	5.03 ^E -03	11/173 (6.4%)	+2.333
Toll-like Receptor Signaling	Apoptosis; humoral/cellular immune response	4.50 ^E -02	5/76 (6.6%)	+1.342
NRF2-mediated Oxidative Stress Response	Cellular stress and injury	4.63 ^E -04	14/193 (7.3%)	+1.000
PTEN Signaling	Apoptosis; cancer	3.51 ^E -03	9/119 (7.6%)	+1.000
Dopamine-DARPP32 Feedback in cAMP Signaling	Intracellular and second messenger signaling; neurotransmitter and other nervous system signaling	2.45 ^E -02	9/163 (5.5%)	-2.121
Aryl Hydrocarbon Receptor Signaling	Cell cycle regulation; apoptosis; xenobiotic metabolism; nuclear receptor signaling	2.76 ^E -02	8/140 (5.7%)	-2.121
GNRH Signaling	Neurotransmitters and other nervous system signaling	1.19 ^E -04	12/129 (9.3%)	-1.732
Huntington's Disease Signaling	Neurotransmitter and other nervous system signaling	1.00 ^E -02	13/243 (5.3%)	-1.732
Synaptic Long Term Potentiation	Neurotransmitter and other nervous system signaling	3.92 ^E -03	9/121 (7.4%)	-1.667
Chemokine Signaling	Cytokine signaling; organismal growth and development	9.55 ^E -03	6/71 (8.5%)	-1.633
Sperm Motility	Organismal growth and development	4.47 ^E -02	7/127 (5.5%)	-1.633
Cardiac Hypertrophy Signaling	Cardiovascular signaling	1.16 ^E -03	15.236 (6.4%)	-1.604
Signaling by Rho Family GTPases	Intracellular and second messenger signaling	6.85 ^E -04	16/248 (6.5%)	-1.508
Leukocyte Extravasation Signaling	Cellular Immune response	2.02 ^E -02	11/211 (5.2%)	-1.508
Colorectal Cancer Metastasis Signaling	Cancer	2.63 ^E -02	12/248 (4.8%)	-1.508
eNOS Signaling	Cardiovascular Signaling	1.13 ^E -02	10/168 (6.0%)	-1.414
STAT3 Pathway	Cellular growth and proliferation and development	4.09 ^E -02	5/74 (6.8%)	-1.342
Thrombin Signaling	Cardiovascular signalling	2.54 ^E -04	15/204 (7.4%)	-1.291
Glioma Signaling	Cancer	1.40 ^E -04	11/112 (9.8%)	-1.265
Renin-Angiotensin Signaling	Cardiovascular signaling; growth factor signaling	1.17 ^E -03	10/122 (8.2%)	-1.265
fMLP Signaling in Neutrophils	Cytokine signaling; cellular immune response	1.24 ^E -03	10/123 (8.1%)	-1.265
Tec Kinase Signaling	Intracellular and second messenger signaling	1.46 ^E -03	12/170 (7.1%)	-1.265
P2Y Purigenic Receptor Signaling Pathway	Cardiovascular signaling	2.23 ^E -03	10/133 (7.5%)	-1.265
Glioblastoma Multiforme Signaling	Cancer	8.21 ^E -03	10/160 (6.2%)	-1.265
Dendritic Cell Maturation	Cytokines signaling; cellular immune response	1.07 ^E -02	11/192 (5.7%)	-1.265
IL-8 Signaling	Cytokines signaling; cellular immune response	1.33 ^E -05	17/197 (8.6%)	-1.213



Table 1. (continued)

Canonical Pathway	Pathway classification	P-value	Genes Ratio	Z-score
Phospholipase C Signaling	Intracellular and second messenger signaling	9.09 ^E -03	13/240 (5.4%)	-1.155
Estrogen-Dependent Breast Cancer Signaling	Cancer	1.50 ^E -04	9/77 (11.7%)	-1.134
EGF Signaling	Growth Factor Signaling; cellular growth and proliferation and development	1.73 ^E -03	7/68 (10.3%)	-1.134
Androgen Signaling	Nuclear receptor signaling	2.19 ^E -03	9/111 (8.1%)	-1.134
Cholecystokinin/Gastrin-mediated Signaling	Neurotransmitters and other nervous system signaling	2.87 ^E -07	14/101 (13.9%)	-1.069
CXCR4 Signaling	Cytokine signaling; cellular immune response	2.30 ^E -05	15/165 (9.1%)	-1.069
Gaq Signaling	Intracellular and second messenger signaling	6.96 ^E -05	14/161 (8.7%)	-1.069
Production of Nitric Oxide and Reactive Oxygen Species in Macrophages	Cellular immune response	4.88 ^E -04	14/194 (7.2%)	-1.069
14-3-3-mediated Signaling	Cell Cycle Regulation; Apoptosis	2.00 ^E -03	10/131 (7.6%)	-1.000
P70S6K Signaling	Cellular stress and injury; cellular growth and proliferation and development	2.11 ^E -03	10/132 (7.6%)	-1.000
HGF Signaling	Growth Factor Signaling; cellular growth and proliferation and development; organismal growth and development	2.79 ^E -03	9/115 (7.8%)	-1.000
CREB Signaling in Neurons	Neurotransmitters and other nervous system signaling; cellular growth and proliferation and development	8.20 ^E -03	11/185 (5.9%)	-1.000
Agrin Interactions at Neuromuscular Junction	Neurotransmitters and other nervous system signaling	3.16 ^E -02	5/69 (7.2%)	-1.000

All canonical pathways with a z-score of ≤ -1.000 or $\geq +1.000$ are listed. Pathways with a significant z-score of ≤ -2.000 or $\geq +2.000$ are depicted in bold. Genes ratio=the number and percentage of genes differentially expressed in ratio to the total number of genes involved in the pathway.

A partial opposite response due to irinotecan administration presented itself via the upregulation of RhoGDI and PTEN signaling, indicative of growth suppression (Table 1A). The AHR pathway and the p70S6K signaling pathways were not regulated in the AL groups.

Tumor transcriptome analysis

Principal component analysis

Next, the transcriptomes of the tumor samples were analyzed using a similar approach as for the liver samples. With a total of 59.49% of the variance explained by PC1 and 10.88% by PC2, the PCA plot of the tumor samples of the four experimental groups showed high heterogeneity among the groups with large intragroup variability (Figure 3A). The individual groups were not clearly separated as clusters, and showed only minor differences between groups. The tumor tissue of the fasting vehicle group showed the smallest intragroup

variability. A shift on both the PC1 and PC2 axes could be detected between the AL vehicle and AL irinotecan groups, while the fasting comparison diverged more on the PC1 axis in an opposite direction but converging with the AL irinotecan group. Both irinotecan-treated groups showed high overlap and no clear clustering of groups. The data derived from these PCA plots show a heterogeneous response in tumor tissue treated with irinotecan, and this response could not be altered by three days of fasting.

Expression profiles

Calculation of the number of DEPS in the tumor groups was done similarly as in the liver. The comparison of AL vehicle and AL irinotecan showed 610 DEPS, of which 321 were downregulated and 289 upregulated (Figure 3B). The number of regulated DEPS between fasting vehicle and fasting irinotecan was 3,093, of which 1,922 were upregulated and 1,171 downregulated. A total of 138 DEPS overlapped between the AL vehicle vs. AL irinotecan and the fasting vehicle vs. fasting irinotecan comparison, corresponding to 23% of the DEPS in the AL groups and only 5% of the fasting groups (Figure 3C). All DEPS considered, only 17% had the same directionality in both comparisons, while the other DEPS had opposite directionalities (Figure 3D), contrasting sharply to the 83% similar directionality found in the liver (Figure 2D).

Pathway analyses

Similarly as done in the liver, pathway analyses were performed in tumor tissue using the DEPS of the AL comparison and the fasting comparison groups. The 610 DEPS as found between the AL vehicle and AL irinotecan group, revealed 11 pathways. Of these pathways, three were upregulated: PTEN Signaling, P53 Signaling and Apoptotic Signaling (Table 2A). The majority of the eight downregulated pathways was involved in inhibition of neurotransmitter signaling. Comparing the fasting groups, 72 pathways were differentially regulated of which 18 were significantly upregulated and one downregulated (Table 2B). Eight overly expressed pathways were involved in cell cycle, cell growth or apoptosis, others mainly regulated cellular growth and the immune response. The tumor AL and tumor fasting groups showed one pathway in common, *Huntington's Disease Signaling*, which was oppositely regulated.

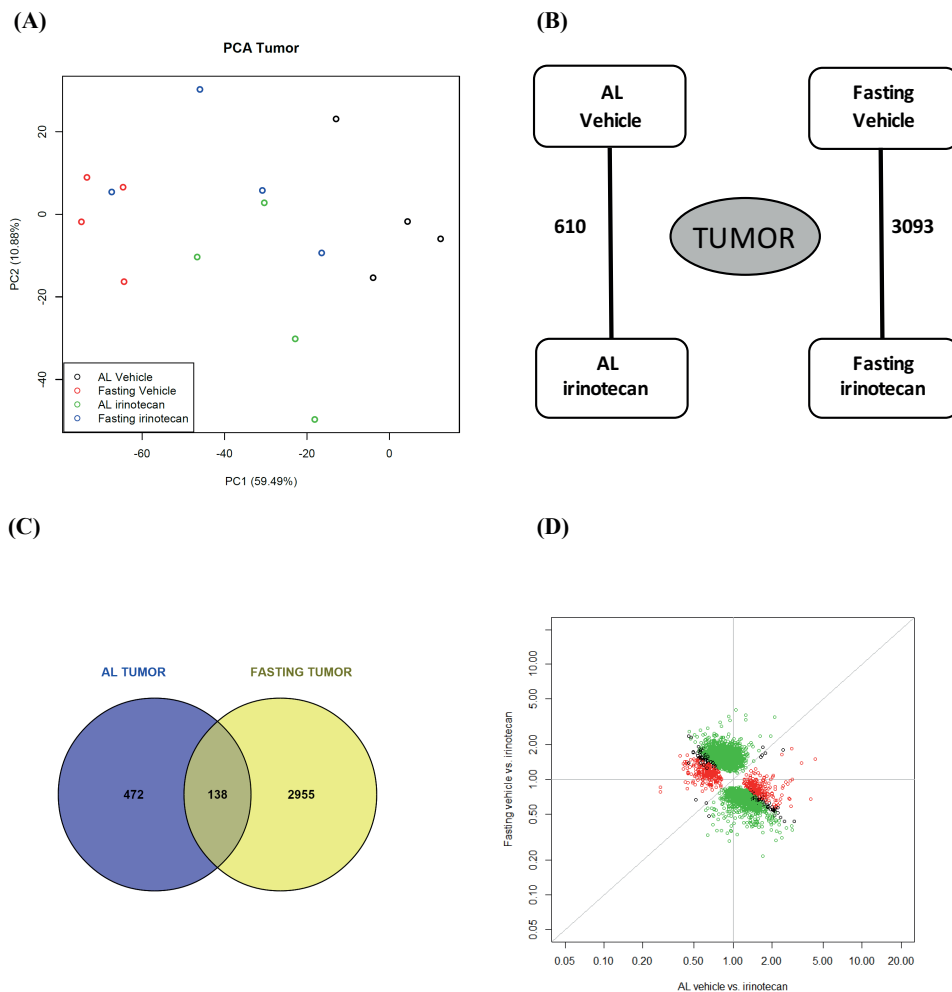


Figure 3. (A) Unbiased principal component analyses (PCA) of tumor samples, based on all probe sets in the microarray. Principal component (PC) 1 is depicted on the x-axis and PC2 is depicted on the y-axis, including the percentage of variance explained by each PC. Each symbol represents one sample of one mouse. Samples of the same group are shown in the same color. AL = ad libitum. **(B)** Number of significantly differentially expressed probe sets (DEPS) in the tumor in AL and fasted groups. **(C)** Venn diagram of overlapping DEPS between the DEPS after the AL tumor groups and the fasting tumor groups, including the unique DEPS of both comparisons. **(D)** Scatterplot of the number of DEPS found in the tumor with false discovery rate of 5%. On the x-axis are the fold changes found in the comparison of AL vehicle vs. AL irinotecan, on the y-axis the fold changes of fasting vehicle vs. fasting irinotecan. Red symbols = AL groups; green symbols = fasting groups; black symbols = overlapping DEPS.

Next, we compared the pathways of liver and tumor tissue of both the AL and fasting groups. The AL groups only had one inhibited pathway in common, involved in neurotransmitter signaling (*i.e. Huntington's Disease Signaling*). In the fasting groups, three pathways downregulated in the liver appeared to be significantly upregulated in the tumor fasting groups: *Colorectal Cancer Metastasis Signaling*, *Aryl Hydrocarbon Receptor Signaling* and *Huntington's Disease Signaling*. Of all 72 pathways regulated in tumor tissue of fasted animals, 17/39 (43%) of the pathways in liver tissue of fasting pathways were oppositely regulated.

Examining genes specifically of interest in tumor tissue, three genes came forward. Heat shock protein 90 (*Hsp90*) is prominently expressed in tumor cells and may play a pivotal role in tumor growth¹¹. *Hsp90* was found to be activated in the tumor AL irinotecan group, whereas the activation in the fasted irinotecan treated tumors was decreased. Two damage response genes either upstream or downstream of P53, *Mdm2* and *Ccng1*, were also activated in both AL and fasting irinotecan groups. *Mdm2* appeared downregulated in the fasting vehicle group, while an activation of *Ccng1* in this group could be detected.

Irinotecan metabolism related gene expression profiles in liver and tumor tissue

We have previously shown that both irinotecan and its active metabolite SN-38 levels are lower in the livers of fasted mice, while plasma levels of irinotecan showed a trend towards higher values compared to AL fed mice¹⁰. Here, we examined expression of genes involved in the metabolism and transportation of irinotecan (Figures 4, S2).

Table 2. Overview of the top overrepresented canonical pathways in tumor ranked by their *P*-value

Canonical Pathway	Pathway classification	<i>P</i> -value	Genes Ratio	Z-score
<i>Tumor – AL vehicle vs. AL irinotecan</i>				
PTEN Signaling	Apoptosis; Cancer	1.57 ^E -02	7/119 (5.9%)	+2.646
P53 Signaling	Cancer	3.51 ^E -02	6/111 (5.4%)	+1.342
Apoptotic Signaling	Apoptosis	4.74 ^E -02	5/90 (5.6%)	+1.000
Glioma Signaling	Cancer	7.94 ^E -04	9/112 (8.0%)	-2.121
Neuropathic Pain Signaling in Dorsal Horn Neurons	Neurotransmitters and Other Nervous System Signaling	3.78 ^E -05	8/115 (7.0%)	-2.121
CREB Signaling in Neurons	Neurotransmitters and Other Nervous System Signaling; Cellular Growth, Proliferation and Development	2.08 ^E -02	9/185 (4.9%)	-2.121
Nitric Oxide Signaling in the Cardiovascular System	Cardiovascular Signaling	3.78 ^E -02	6/113 (5.3%)	-2.000
Huntington's Disease Signaling	Neurotransmitters and Other Nervous System Signaling	4.18 ^E -02	10/243 (4.1%)	-1.890
Synaptic Long Term Potentiation	Neurotransmitters and Other Nervous System Signaling	4.99 ^E -02	6/121 (5.0%)	-1.633
STAT3 Pathway	Cellular Growth, Proliferation and Development; Transcriptional Regulation	2.30 ^E -02	5/74 (6.8%)	-1.342
Synaptic Long Term Depression	Neurotransmitters and Other Nervous System Signaling	4.29 ^E -02	7/147 (4.8%)	-1.134
<i>Tumor – Fasting vehicle vs. Fasting irinotecan</i>				
Signaling by Rho Family GTPases	Intracellular and Second Messenger Signaling	1.10 ^E -03	35/248 (14.1%)	+3.286
Gaq Signaling	Intracellular and Second Messenger Signaling	2.26 ^E -02	21/161 (13.0%)	+2.828
IL-9 Signaling	Apoptosis; Cytokine Signaling; Cellular Immune Response	2.81 ^E -02	8/45 (17.8%)	+2.828
CD40 Signaling	Humoral Immune Response; Cellular Immune Response	1.85 ^E -04	17/79 (21.5%)	+2.668
TNFR2 Signaling	Apoptosis; Cytokine Signaling	9.29 ^E -03	7/30 (23.3%)	+2.646
Type II Diabetes Mellitus Signaling	Cellular Stress and Injury	8.16 ^E -03	19/128 (14.8%)	+2.500
Colorectal Cancer Metastasis Signaling	Cancer	1.31 ^E -04	38/248 (15.3%)	+2.401
ILK Signaling	Cellular Growth, Proliferation and Development	6.47 ^E -04	30/196 (15.3%)	+2.353
Wnt/Ca+ pathway	Cancer; Organismal Growth and Development	1.84 ^E -02	10/58 (17.2%)	+2.333
RANK Signaling in Osteoclasts	Cellular Growth, Proliferation and Development	6.79 ^E -05	21/102 (20.6%)	+2.236
Aryl Hydrocarbon Receptor Signaling	Cell Cycle Regulation; Apoptosis; Xenobiotic Metabolism; Nuclear Receptor Signaling	8.10 ^E -06	28/140 (20.0%)	+2.200
Acute Myeloid Leukemia Signaling	Cancer	4.85 ^E -04	18/93 (19.4%)	+2.183
Huntington's Disease Signaling	Neurotransmitters and Other Nervous System Signaling	4.74 ^E -07	44/243 (18.1%)	+2.132

Table 2. (continued)

Canonical Pathway	Pathway classification	P-value	Genes Ratio	Z-score
B Cell Activating Factor Signaling	Humoral Immune Response; Cellular Growth, Proliferation and Development	7.34 ^E -05	12/41 (29.3%)	+2.111
CD27 Signaling in Lymphocytes	Apoptosis; Cellular Immune Response	2.68 ^E -04	13/53 (24.5%)	+2.111
Pancreatic Adenocarcinoma Signaling	Cancer	3.34 ^E -03	19/118 (16.1%)	+2.111
NF-κB Signaling	Organismal Growth and Development; Humoral Immune Response; Cytokine Signaling; Cellular Immune Response	3.98 ^E -06	34/181 (18.8%)	+2.058
IL-6 Signaling	Cytokine Signaling; Cellular Immune Response	1.03 ^E -04	24/128 (18.8%)	+2.041
PPARα-RXRα Activation	Nuclear Receptor Signaling	1.26 ^E -06	35/180 (19.4%)	-2.121

All canonical pathways with a z-score of ≤ -1.000 or $\geq +1.000$ are listed in table A. Due to the high number of differentially regulated pathways, in table 2B only the canonical pathways with z-score ≤ -2.000 or $\geq +2.000$ are listed. Pathways with a significant z-score of ≤ -2.000 or $\geq +2.000$ are depicted in bold. Genes ratio= the number and percentage of genes differentially expressed in ratio to the total number of genes involved in the pathway.

Using the AL vehicle group as reference, the analysis in the liver revealed activation of mRNA expression of carboxylesterase 1 (*Ces1*) and *Ces2* in both fasting groups, *i.e.* with and without irinotecan, while both genes were inhibited in the AL irinotecan group. *Ces3* expression was activated by fasting alone and significantly inhibited by irinotecan alone. In combination, the net effect of *Ces3* expression by irinotecan and fasting was practically cancelled out. In tumor tissue, regulation of the carboxylesterases was not distinctly present. Carboxylesterases one to three are needed to convert irinotecan in to its active metabolite SN-38 (Figure 4). *Cyp3a16*, the mouse homolog of *Cyp3a4*, was not regulated in any of the groups, while other members of the cytochrome P450 family involved in drug metabolism appeared to be higher expressed in the fasting groups. Both *Ugt1a1* and *Abcc1*, genes involved in the transport of SN-38 out of the cell, were higher expressed in the fasting irinotecan group compared to the AL irinotecan group.

DISCUSSION

In this study, we confirm that three days of fasting prior to treatment with irinotecan is able to reduce liver toxicity as well as bone marrow depression in mice carrying subcutaneous colorectal carcinoma. Previously, we showed that these signs of somatic resistance to irinotecan were accompanied by a reduction in other side effects as body weight reduction and diarrhea without compromising the antitumor effect^{7,10}. Here we set out to retrieve mechanistic insights in the chemoprotective effects of fasting through transcriptomic analyses of healthy liver and tumor tissue after an irinotecan challenge.

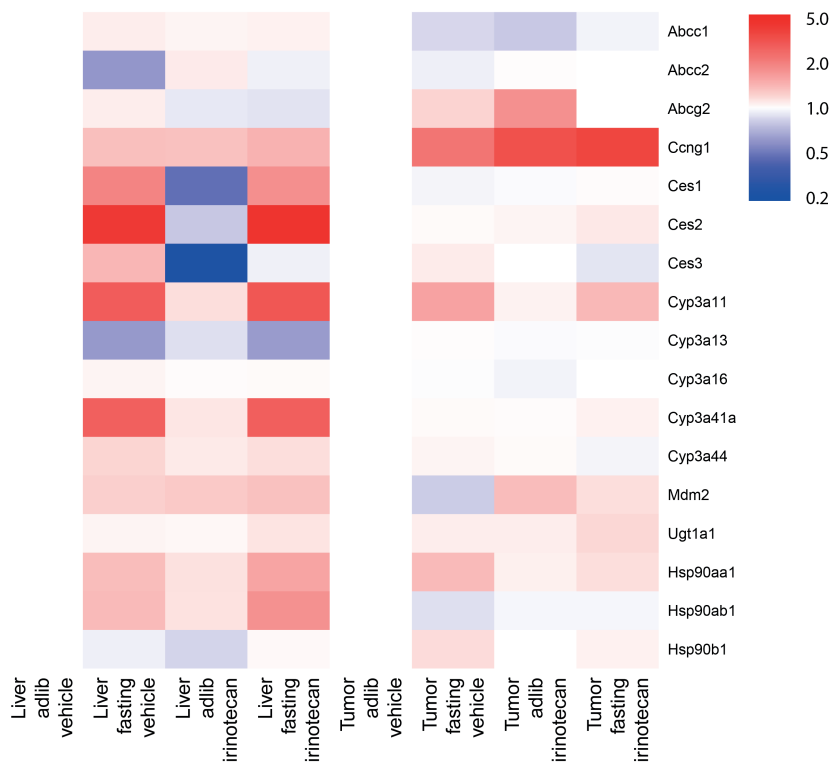


Figure 4. Heatmap of irinotecan-related probe sets in the different treatment groups in liver (left lanes) as well as in tumor tissue (right lanes). Expression profiles were calculated using the ad libitum vehicle group of the corresponding tissue as a reference. In case a multitude of probe sets were related to one gene, the average of the sum of the expression values of all probe sets was calculated. The legend represents the fold ratio of the expression values in a coloring scale, in which a value >1 corresponds to an activation state, and a value <1 to an inhibition state of the gene expression value. Abcc = ATP-binding cassette, subfamily C; Abcg = ATP-binding cassette, subfamily G; Ccng1 = cyclin G1; Ces = carboxylesterase; Cyp = Cytochrome P450; Mdm2 = Mouse double minute 2 homolog; Ugt1a1 = UDP-glucuronosyltransferase 1-1; Hsp = heatshock protein.

Since the most prominent effect of fasting is the reduction of toxic side effects of chemotherapy, its effects should be sought primarily in the healthy tissues including the liver in which the majority of its drug metabolism takes place. In this study, fasting led to a more homogeneous gene expression profile in healthy liver tissue. Together with the 3-fold lower number of genes significantly regulated in the liver upon irinotecan exposure under fasting compared AL conditions, these results point towards a dampened response to

irinotecan in healthy tissue due to fasting. This may be an indication that fasting results in a state that favors maintenance and repair and in which normal cells are protected against toxic stressors during periods of nutrient deprivation^{8,10,12}.

Fasting is able to amend and dampen the genotoxic response in the liver; in AL fed mice treated with irinotecan growth signaling induction and general activation of signaling pathways are prominent adaptations, whereas these pathways are blunted by fasting. Particular of interest is the reduction in cellular injury and cytokine signaling. Cytokines are crucial players in the activation and adaptation to oxidative stress, and therefore the reduction is strong evidence of increased stress resistance induced by fasting¹³. Another marker of cellular stress is RhoA, which is activated by reactive oxygen species (ROS) in fibroblasts and may lead to apoptosis when activated by caspase 3^{14,15}. RhoA signaling was activated in the fasting vehicle group of the liver as indication of a preconditioned state of stress. In the fasting irinotecan group, RhoA activation did not come forward whereas a known inhibitor of RhoA (*i.e.* RhoGDI) was highly activated. An inhibition of RhoA results in a dampening of TGF-beta 1, a transcription factor able to activate ROS and stress-induced injury^{16,17}. These findings are consistent with reduction of cellular stress by fasting, possibly via blunting of cytokine and RhoA signaling, which may play a key role in the protection of DR against adverse side effects of irinotecan.

The mTOR signaling was downregulated as well via inhibition of the p7056 pathway, thereby initiating autophagy^{18,19}. Autophagy is a process initiated for cell survival in healthy tissue, however autophagy in tumor cells also promotes tumorigenesis and tumor progression and therefore has an outcome dependent on the nature of the cells¹³. The effect of mTOR on stress resistance²⁰ also refers to the anti-inflammatory response due to fasting, and the beneficial role for promoting stress resistance after DR therefore holds also true for the side effects of chemotherapy^{9,10}. The activation of the NRF2 stress response might also provide protection against the damage-induced response after irinotecan²¹⁻²³. Posttranscriptional validation is needed to further understand the exact role of cytokine signaling, RhoA, mTOR and NRF2 on stress resistance and prevention of side effects of chemotherapy.

The changes induced by fasting in healthy liver tissue did not come forward in the tumor transcriptome analysis. The PCA plots of the AL and fasting groups revealed a high heterogeneity within all the groups of tumor tissue, which is in contrast with the orchestrated response of the liver. Especially both AL groups (with and without irinotecan treatment) revealed a small number of DEPS. This number was about a 5-fold higher after fasting, however these genes showed only little overlap with the response in liver tissue of fasted irinotecan treated mice. On pathway level, the AL and fasting comparisons with and without irinotecan did not show a common response either; in the AL group

an upregulation of pathways involved in growth inhibition, tumor suppression and cell death was seen. Strikingly, the response of fasted tumor tissue appeared partially oppositely regulated as compared to fasted liver tissue since upregulation of various cell cycle, apoptosis and cytokine pathways in fasted tumor tissue was predominantly found. These results are partially in line with the recently described DSS^{8,10,12}. In addition, the decreased activation of *Hsp90* in tumor tissue of fasted mice after irinotecan administration might point towards an additional inhibitory effect of irinotecan after fasting^{8,11,12}. Thus, although the transcriptomic response of fasted tumor tissue differs significantly from that of AL tumor tissue, this does not affect the antitumor activity of irinotecan^{7,10}. Due to the heterogeneity within the tumor groups, any common pathway responses should be interpreted with care as more studies are needed to fully discern between partly orchestrated -common and heterogenic- individual responses to chemotherapeutic insults in tumor tissue after dietary intervention.

Previously, we found decreased levels of the active metabolite of irinotecan, SN-38, in plasma as well as liver, but not in tumor tissue of fasted mice¹⁰. The relative upregulation of the carboxylesterases in this study would suggest an increased hydrolysis of irinotecan into SN-38^{7,24}. Upregulation of *Ugt1a1* and ABC transporter *Abcc1* is indicative of increased transport of SN-38 out of the cell²⁵⁻²⁷. An increased production of SN-38 in the liver and more efficient excretion by transporters may explain the lowered SN-38 levels in the liver and increased plasma levels we found previously¹⁰. *Ugt1a1* is involved in conversion of SN-38 into its inactive form SN-38G, which reduces the levels of the active drug in the intestine. Since one of the main side effects of irinotecan, diarrhea, is thought to be due to high concentrations of intra-luminal SN-38, this inactivation of SN-38 by *Ugt1a1* could be responsible for the absence of diarrhea in fasted mice²⁸⁻³⁰. Further studies should examine in depth the activity of the enzymes involved in irinotecan drug metabolism and at various time points after exposure in order to understand their role in the reduced side effects induced by fasting. The changes occurring in the drug metabolism of irinotecan as seen in liver tissue were far less prominent in tumor tissue without obvious changes due to fasting. This is consistent with the previous findings that irinotecan and its metabolite levels were not affected by fasting in tumor tissue. The inhibition of mouse double minute 2 homolog (*Mdm2*) in the tumor fasting vehicle group is partially maintained in the fasting irinotecan group, which may point towards an activation of tumor suppressor p53 by fasting³¹. Further research is needed in order to understand the etiology of fasting on the effects of chemotherapy on tumor tissue.

Since pharmacokinetic studies showed that the half-life of SN-38 is approximately 12 hours¹⁰, we choose to explore the transcriptional changes at one time point, using one dosage of irinotecan in the therapeutic window in which the effects of both irinotecan and fasting would be maximal. Analyses of multiple time points and with different dosages of irinotecan

would likely improve our understanding of the results we obtained. In addition, in this experimental model we compare healthy liver tissue and C26 colon cancer cells induced by subcutaneous injection. Other models might provide more information about the effects of fasting on various cancer tissues. Finally, this study only partially explains how fasting changes irinotecan metabolism and how it protects the organism, but not the tumor, against irinotecan exposure. Addressing the impact of fasting on posttranscriptional level will likely improve our understanding of the mechanisms of fasting-induced chemoprotection.

In conclusion, we show that three days of fasting results in protection against the side effects of irinotecan treatment and activates a protective stress response in healthy liver, but not in tumor tissue. Although fasting leads to an increase in differentially regulated pathways following irinotecan treatment in tumor tissue, it does not abrogate its antitumor efficacy. These results further strengthen the oncologic safety of DR in cancer patients, where short-term fasting could improve both efficacy of treatment and quality of life in patients with colorectal cancer treated with irinotecan.

MATERIALS AND METHODS

Animals

Male BALB/c mice of 6-8 weeks old, weighing approximately 25 grams, were obtained from Charles River, Maastricht, the Netherlands. Upon arrival, animals were housed at random in individually ventilated cages (n=4 animals per cage) in a licensed biomedical facility at Erasmus University Medical Center, Rotterdam, the Netherlands. Standard laboratory conditions were maintained, *i.e.* temperature ~22°C, humidity ~50%, and a 12 h light/12 h dark cycle. All mice had free access to water and food (Special Diet Services, Witham, UK) unless mentioned otherwise. Animals were allowed to acclimatize for one week before the start of the experiments. The experimental protocol was approved by the Animal Experiments Committee under the Dutch National Experiments on Animals Act, and complied with the 1986 directive 86/609/EC of the Council of Europe.

C26 colon carcinoma cells

The murine colon carcinoma cell line C26 originally derived from the BALB/c mouse and was cultured in Dulbecco's Modified Eagle's Medium (DMEM) (Sigma Aldrich, St. Louis, MO), supplemented with 10% fetal calf serum (Lonza, Verviers, Belgium), penicillin (100 units/ml) and streptomycin (100 units/ml) (Invitrogen, Auckland, NZ) at 37 degrees Celsius in a 5% carbon dioxide environment. Cells were harvested by brief trypsinization (0.05% trypsin in 0.02% ethylenediamine tetra-acetic acid (EDTA)). For subcutaneous injection,

cells were harvested and after centrifugation, single-cell suspensions were prepared in phosphate buffered saline (PBS) to a final concentration of 2.5×10^5 cells/100 μL . Cell viability was determined by trypan blue staining, and was always $\geq 90\%$.

Experimental setup

Mice ($n=36$) were anesthetized (isoflurane inhalation, 5% isoflurane inhalation initially and then 2% isoflurane with a 1:1 air:oxygen mixture for maintenance of anesthesia) (Figure S1). Both flanks were shaved for precise injection. 2.5×10^5 C26 cells were injected subcutaneously on both sides in a volume of 100 μL , using a 21G needle. Tumors were allowed to grow for 12 days before start of the experiment. Mice were weighed and tumors were measured daily with digital calipers. The mice were randomly divided into four groups ($n=6/\text{group}$). Two groups were fasted for three days and two groups were fed ad libitum (AL). After the fasting period, mice were fed AL again. One AL fed group, and one group of fasted animals, were treated with a single weight-adjusted dose of 133 mg/kg (± 3.3 mg/kg, and ± 2.7 mg/kg respectively) of irinotecan intraperitoneally. The control groups received vehicle treatment (sodium chloride 0.9%). Two hours after injection, all groups received unlimited access to food for 10 hours until the moment of sacrifice. The difference between starting amount and remaining amount of food was used to calculate food consumption per mouse for this 10-hour period. Subsequently, 12 hours after irinotecan administration, the mice were sacrificed by exsanguination.

Fasting protocol

Mice in the AL fed groups were allowed unrestricted access to food, and amount of food eaten per cage was measured daily. Before the start of the fasting period, all mice were transferred to a clean cage and mice in the fasting groups were withheld food for three days starting at 4:00 PM on a Friday until 10:00 AM on a Monday. All animals were given continuous access to water.

Chemotherapy

Irinotecan, HCl-trihydrate 20 mg/mL (Hospira, Benelux) was used for in vivo experiments. Irinotecan was diluted in sodium chloride 0.9% (Braun, Melsungen, Germany) to a final volume of 200 μL per injection, and was given intraperitoneally.

Serum measurements

Mice were killed by exsanguination with cardiac puncture under anesthesia (isoflurane inhalation, 5% isoflurane inhalation initially and then 2% isoflurane with a 1:1 air:oxygen mixture for maintenance of anesthesia). After cardiac puncture, ± 900 μL of blood per mouse was transferred directly into 1 mL tubes (MiniCollect, Greiner Bio-one), containing

EDTA. Samples were directly centrifuged (3,500 rpm; 10 min) after which the serum was transferred to a separate tube. Serum aspartate transaminase (AST), alanine transaminase (ALT), lactate dehydrogenase (LDH), urea, and creatinine levels were analyzed at the Central Clinical Chemical Laboratory of the Erasmus University Medical Center. Fifty μL of blood was used to measure the number of leukocytes with a Z-series Coulter Counter (Beckman Coulter, Woerden, The Netherlands).

Tissue sampling

Livers and tumors were collected and weighed. The median liver lobe was isolated for array analysis and directly stored in RNAlater® Solution (Life Technologies Europe BV, Bleijswijk, the Netherlands) and stored at 4°C until further analysis. Parts of viable tumor border were identified and also directly stored in RNAlater® until further analysis.

RNA isolation

Tumor and liver samples were kept at 4°C in the RNAlater® Solution (Thermo Fisher Scientific™, Breda, the Netherlands) until further analyses. RNA isolation took place between 24 hours and 96 hours after sample collection. Total RNA was extracted via the QIAzol lysis Reagent and miRNAeasy Mini Kits (QIAGEN, Hilden, Germany), according to Qiagen protocol. Concentrated buffers RPE and RWT (QIAGEN) for washing of membrane-bound RNA and purification were added mechanically by using the QIAcube (QIAGEN, Hilden, Germany) via the miRNeasy program. Subsequently, isolated RNA was stored at -80°C. RNA concentrations were measured using the Nanodrop (Thermo Fisher Scientific™, Breda, the Netherlands) and RNA quality was assessed using the 2100 Bio-Analyzer (Agilent Technologies, Amstelveen, the Netherlands), according to manufacturer's instructions. The RNA quality was quantitatively expressed as the RNA Integrity Number (RIN, range 0-10). Out of the six tumor samples and six liver samples per group, the four samples with the highest RIN were used for microarray analyses. RIN-values of the tumor samples ranged between 7.8 and 10, the RIN-values of the liver samples ranged between 7.6 and 8.6.

Array analysis

Microarray hybridization was done at the Microarray Department of the University of Amsterdam (the Netherlands) to Affymetrix HT MG-430 PM Array Plates, according to the Affymetrix protocols. For each group, four biological replicates were used. The output of the hybridization contained raw mean expression data put into CEL files. Subsequent quality control and normalization were done using the pipeline at the www.arrayanalysis.org website (Maastricht University, the Netherlands)³². Normalization was performed via the Robust Multichip Average (RMA) algorithm, and the output of the normalization

consisted of 45,141 probes³³. Both raw and normalized microarray data and their MIAME compliant metadata were deposited at the Gene Expression Omnibus (GEO) database, with number GSE72484 (www.ncbi.nlm.nih.gov/geo).

Statistical analyses

For each set of parameters means and standard errors of the mean were computed. All standard statistical tests were performed using SPSS version 21 for Windows software (Statistical Package for Social Sciences, Chicago, IL) and GraphPad Prism (GraphPad Software Inc., version 5.01). A *P*-value <0.05 was considered to be significant. Microarray analyses were performed using the free software package R (R foundation). Gene expression profiles were compared using the Linear Models for Microarray Data (limma) method with correction for multiple testing using the false discovery rate (FDR) according to Benjamini and Hochberg³⁴. Fold changes were expressed as the geometric mean per diet group against the corresponding AL fed control group, and cutoff values for a significant difference were put at FDR <5%. Functional annotation and analyses were performed using the Ingenuity software (<http://www.ingenuity.com/products/ipa>). Inhibition or activation prediction of the upstream transcription regulators (upstream analysis) was predicted with Ingenuity software by calculating statistical *z*-scores based on the observed gene expression changes in our dataset. Via *z*-scores, the chance of significant prediction based on random data is reduced (http://ingenuity.force.com/ipa/articles/Feature_Description/Upstream-Regulator-Analysis). Cutoff values for a significant activation or inhibition were put at a *z*-score of ≥ 2 or ≤ -2 , respectively.

REFERENCES

1. Torre, L.A., et al. Global cancer statistics, 2012. *CA Cancer J Clin* 65, 87-108 (2015).
2. Adam, R. Colorectal cancer with synchronous liver metastases. *Br J Surg* 94, 129-131 (2007).
3. Cunningham, D., et al. Randomised trial of irinotecan plus supportive care versus supportive care alone after fluorouracil failure for patients with metastatic colorectal cancer. *Lancet* 352, 1413-1418 (1998).
4. Saltz, L.B., et al. Irinotecan plus fluorouracil and leucovorin for metastatic colorectal cancer. Irinotecan Study Group. *N Engl J Med* 343, 905-914 (2000).
5. Rothenberg, M.L. Efficacy and toxicity of irinotecan in patients with colorectal cancer. *Semin Oncol* 25, 39-46 (1998).
6. McCay, C.M., Crowell, M.F. & Maynard, L.A. The effect of retarded growth upon the length of life span and upon the ultimate body size. 1935. *Nutrition* 5, 155-171; discussion 172 (1989).
7. Huisman, S.A., Bijman-Lagcher, W., JN, I.J., Smits, R. & de Bruin, R.W. Fasting protects against the side effects of irinotecan but preserves its anti-tumor effect in *Apc15lox* mutant mice. *Cell Cycle*, 1-7 (2015).
8. Lee, C., et al. Fasting cycles retard growth of tumors and sensitize a range of cancer cell types to chemotherapy. *Sci Transl Med* 4, 124ra127 (2012).
9. Raffaghello, L., et al. Starvation-dependent differential stress resistance protects normal but not cancer cells against high-dose chemotherapy. *Proceedings of the National Academy of Sciences of the United States of America* 105, 8215-8220 (2008).
10. Huisman, S.A., et al. Fasting protects against the side-effects of irinotecan treatment but does not abrogate anti-tumor activity in mice. *Br J Pharmacol* (2015).
11. Wang, B., et al. Hsp90 regulates autophagy and plays a role in cancer therapy. *Tumour Biol* 37, 1-6 (2016).
12. Lee, C., Raffaghello, L. & Longo, V.D. Starvation, detoxification, and multidrug resistance in cancer therapy. *Drug Resist Updat* 15, 114-122 (2012).
13. Sies, H., Berndt, C. & Jones, D.P. Oxidative Stress. *Annu Rev Biochem* 86, 715-748 (2017).
14. Aghajanian, A., Wittchen, E.S., Campbell, S.L. & BurrIDGE, K. Direct activation of RhoA by reactive oxygen species requires a redox-sensitive motif. *PLoS One* 4, e8045 (2009).
15. Bell, M., Sopko, N.A., Matsui, H., Hannan, J.L. & Bivalacqua, T.J. RhoA/ROCK activation in major pelvic ganglion mediates caspase-3 dependent nitrergic neuronal apoptosis following cavernous nerve injury. *Neural Regen Res* 12, 572-573 (2017).
16. Manickam, N., Patel, M., Griendling, K.K., Gorin, Y. & Barnes, J.L. RhoA/Rho kinase mediates TGF-beta1-induced kidney myofibroblast activation through Poldip2/Nox4-derived reactive oxygen species. *Am J Physiol Renal Physiol* 307, F159-171 (2014).
17. Krstic, J., Trivanovic, D., Mojsilovic, S. & Santibanez, J.F. Transforming Growth Factor-Beta and Oxidative Stress Interplay: Implications in Tumorigenesis and Cancer Progression. *Oxid Med Cell Longev* 2015, 654594 (2015).

18. Kim, J., Kundu, M., Viollet, B. & Guan, K.L. AMPK and mTOR regulate autophagy through direct phosphorylation of Ulk1. *Nat-cell Biol* 13, 132-141 (2011).
19. Wang, X.W. & Zhang, Y.J. Targeting mTOR network in colorectal cancer therapy. *World J Gastroenterol* 20, 4178-4188 (2014).
20. Mitchell, J.R., et al. Short-term dietary restriction and fasting precondition against ischemia-reperfusion injury in mice. *Aging Cell* 9, 40-53 (2010).
21. Jaramillo, M.C. & Zhang, D.D. The emerging role of the Nrf2-Keap1 signaling pathway in cancer. *Genes Dev* 27, 2179-2191 (2013).
22. Moon, E.J. & Giaccia, A. Dual roles of NRF2 in tumor prevention and progression: possible implications in cancer treatment. *Free Radic Biol Med* 79, 292-299 (2015).
23. Fontana, L., Partridge, L. & Longo, V.D. Extending healthy life span--from yeast to humans. *Science* 328, 321-326 (2010).
24. Laizure, S.C., Herring, V., Hu, Z., Witbrodt, K. & Parker, R.B. The role of human carboxylesterases in drug metabolism: have we overlooked their importance? *Pharmacotherapy* 33, 210-222 (2013).
25. Etienne-Grimaldi, M.C., et al. UGT1A1 genotype and irinotecan therapy: general review and implementation in routine practice. *Fundam Clin Pharmacol* 29, 219-237 (2015).
26. Cortejoso, L. & Lopez-Fernandez, L.A. Pharmacogenetic markers of toxicity for chemotherapy in colorectal cancer patients. *Pharmacogenomics* 13, 1173-1191 (2012).
27. Innocenti, F., et al. Comprehensive pharmacogenetic analysis of irinotecan neutropenia and pharmacokinetics. *J Clin Oncol* 27, 2604-2614 (2009).
28. de Jong, F.A., Kitzen, J.J., de Bruijn, P., Verweij, J. & Loos, W.J. Hepatic transport, metabolism and biliary excretion of irinotecan in a cancer patient with an external bile drain. *Cancer Biol Ther* 5, 1105-1110 (2006).
29. Li, M., et al. Clinical significance of UGT1A1 gene polymorphisms on irinotecan-based regimens as the treatment in metastatic colorectal cancer. *Onco Targets Ther* 7, 1653-1661 (2014).
30. Cecchin, E., et al. Predictive role of the UGT1A1, UGT1A7, and UGT1A9 genetic variants and their haplotypes on the outcome of metastatic colorectal cancer patients treated with fluorouracil, leucovorin, and irinotecan. *J Clin Oncol* 27, 2457-2465 (2009).
31. Moll, U.M. & Petrenko, O. The MDM2-p53 interaction. *Mol Cancer Res* 1, 1001-1008 (2003).
32. Eijssen, L.M., et al. User-friendly solutions for microarray quality control and pre-processing on ArrayAnalysis.org. *Nucleic Acids Res* 41, W71-76 (2013).
33. Irizarry, R.A., et al. Summaries of Affymetrix GeneChip probe level data. *Nucleic Acids Res* 31, e15 (2003).
34. Green, G.H. & Diggle, P.J. On the operational characteristics of the Benjamini and Hochberg False Discovery Rate procedure. *Stat Appl Genet Mol Biol* 6, Article27 (2007).

SUPPLEMENTARY DATA

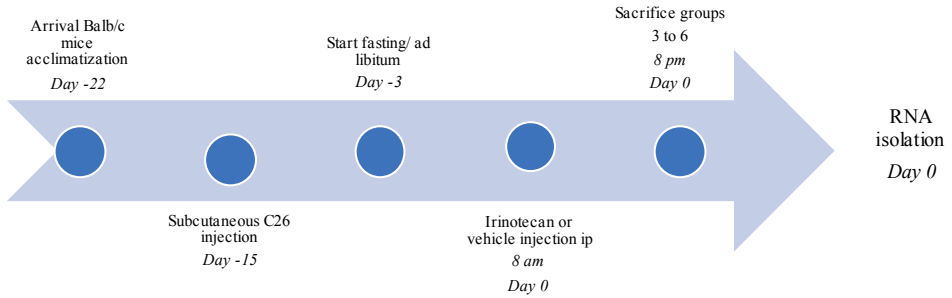


Figure S1. Schematic overview of the experimental set-up, including a timeline from arrival of the mice until sacrifice and subsequent RNA isolation for further analyses. Ip = intraperitoneal.

3

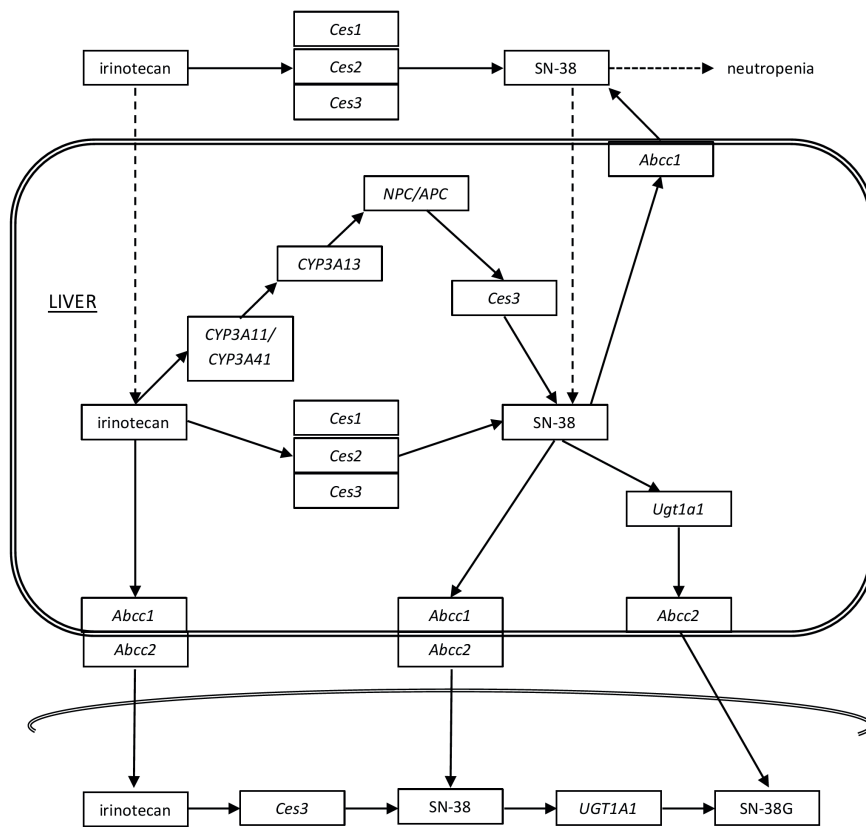
INTESTINE

Figure S2. Overview of the pathway of irinotecan and its metabolism outside and inside the liver cell, including the transportation into the intestine. The main genes and transporters known to be involved in the pathway are depicted. Ces = carboxylesterase; SN-38= active metabolite of irinotecan; SN-38G = SN-38 glucuronide form; Abcc = ATP binding cassette subfamily C; NPC/APC = carbonyloxycamptothecin; Cyp3a = cytochrome P450 3A; Ugt1a1 = Uridine glucuronosyltransferase 1A1.

CHAPTER 4

A SIGNATURE OF RENAL STRESS RESISTANCE INDUCED BY SHORT-TERM DIETARY RESTRICTION, FASTING, AND PROTEIN RESTRICTION

Franny Jongbloed*, Tanja C. Saat*, Mariëlle Verweij, César Payán-Gómez,
Jan H.J. Hoeijmakers, Sandra van den Engel, Conny T. van Oostrom,
Gisela Ambagtsheer, Sandra Imholz, Jeroen L.A. Pennings, Harry van
Steeg, Jan N.M. IJzermans, Martijn E.T. Dollé, Ron W.F. de Bruin

* Authors contributed equally

Scientific Reports. 2017 Jan 19;7:40901

ABSTRACT

During kidney transplantation, ischemia-reperfusion injury (IRI) induces oxidative stress. Short-term preoperative 30% dietary restriction (DR) and 3-day fasting protect against renal IRI. We investigated the contribution of macronutrients to this protection on both phenotypical and transcriptional levels. Male C57BL/6 mice were fed control food ad libitum, underwent two weeks of 30% DR, 3-day fasting, or received a protein-, carbohydrate- or fat-free diet for various periods of time. After completion of each diet, renal gene expression was investigated using microarrays. After induction of renal IRI by clamping the renal pedicles, animals were monitored seven days postoperatively for signs of IRI. In addition to 3-day fasting and two weeks 30% DR, three days of protein-free diet protected against renal IRI as well, whereas the other diets did not. Gene expression patterns significantly overlapped between all diets except the fat-free diet. Detailed meta-analysis showed involvement of nuclear receptor signaling via transcription factors, including FOXO3, HNF4A and HMGA1. In conclusion, three days of a protein-free diet is sufficient to induce protection against renal IRI similar to 3-day fasting and two weeks of 30% DR. The elucidated network of common protective pathways and transcription factors further improves our mechanistic insight into the increased stress resistance induced by short-term DR.

INTRODUCTION

Dietary restriction (DR) is a reduction in food intake without malnutrition¹. Long-term DR is known to extend lifespan, increase overall health and improve resistance to multiple stressors in a wide variety of organisms¹⁻⁵. Although the effect of DR on human lifespan is unknown, studies demonstrate a favorable impact on metabolic parameters associated with long-term health⁶⁻⁸. In addition, DR has been shown to protect against acute stressors including toxic chemotherapy⁹, paracetamol intoxication¹⁰, and oxidative stress induced by ischemia-reperfusion injury (IRI)^{1,11,12}. In clinical kidney transplantation, renal IRI is a major risk factor for organ damage which may result in acute kidney injury¹³, primary non-function¹⁴, delayed graft function¹⁵, and acute and chronic rejection¹⁶ of the graft. After kidney retrieval, cessation of the blood flow (ischemia) leads to hypoxia, nutrient deprivation, and accumulation of metabolic waste products^{15,16}. Reperfusion of the ischemic kidney promotes the generation of reactive oxygen species, triggers apoptotic cell death, and promotes the activation of an inflammatory response resulting in profound tissue injury¹⁷. Prevention or amelioration of renal IRI could increase graft quality, and prolong graft survival. Unfortunately, no effective treatment to reduce or prevent IRI is currently available.

Using renal IRI as a model, we previously demonstrated that the benefits of DR on IRI are induced rapidly: two and four weeks of 30% preoperative DR as well as three days of fasting reduce renal injury and strongly improve survival and kidney function after renal IRI in mice^{1,12}. Hence, DR is a potential intervention for living kidney donors to reduce IRI and improve the transplantation success rate. Whether the protective effect of short- and long-term DR is based on the reduction of calories per se, or specific nutrients, was first investigated in fruit flies, in which long-term protein restriction contributed more to lifespan extension than a reduction in carbohydrates¹⁸. In mice, glucose supplementation did not interfere with fasting-induced protection against renal IRI, which also points towards a role for specific (macro-) nutrients in inducing acute stress resistance¹¹.

In this study, we investigated the role of specific macronutrients in inducing resistance against renal IRI by unrestricted feeding of protein-, carbohydrate-, and fat-free diets. We showed that the absence of protein for three days is sufficient to induce resistance against renal IRI, and revealed common pathways and transcription factors that are implicated in the protective effect of calorie restriction induced by two weeks of 30% DR, three days of fasting, and protein restriction.

RESULTS

Absence of dietary protein induces protection against renal IRI

To determine the effect of short-term macronutrient deficiency on renal IRI, we provided 10-day, 14-day or 3-day regimens of protein-free, carbohydrate (CHO)-free and fat-free diets before inducing renal IRI.

As previously shown, mice that were fed a protein-free diet for six or 14 days tend to voluntarily decrease their food intake as compared to animals that were fed a normal diet¹⁹. We indeed found that mice fed a protein-free diet for 10 days decreased their dietary food intake by approximately 30% (Figure S1A), resulting in significant body weight loss up until 20% on day 10 (Figure S1B). The reduction in food intake and body weight was less substantial in mice fed a carbohydrate (CHO)-free diet for 14 days. A fat-free diet for 14 days led to a small increase in body weight. Only the protein-free diet improved survival (Figure S1C) and kidney function (Figure S1D) following renal IRI. However, due to the reduction in food intake and body weight, the effect of the absence of protein per se could not be disentangled from the effect of calorie restriction.

Subsequently, to separate the effect of the absence of protein from calorie restriction, mice were fed a protein-free diet for three consecutive days. We first showed that survival and kidney function of mice receiving 30% DR for three days did not differ from mice fed ad libitum (Figure 1A, B)¹¹. Mice fed the protein-free diet for three days had significantly improved survival (Figure 1C) and kidney function compared to control mice ($P < 0.05$) (Figure 1D). The energy intake during the 3-day protein-free dietary intervention was decreased, but did not significantly differ from the intake of animals fed the control diet for three days ($P = 0.13$) (Figure 1E). Body weight of mice on the protein free diet decreased by 9%, while body weight of mice that were fed a control diet did not change. Mice receiving 30% DR for three days lost about 8% of their body weight (Figure 1F).

Common gene expression profiles between macronutrient-free diets, fasting and DR

To examine, in an unbiased manner, the transcriptomic response of the kidney, microarray analysis was performed on 45,141 probe sets in kidney samples after three days of fasting, three days and two weeks of 30% DR, and three days of a protein-, fat- or carbohydrate-free diet. Each diet was subsequently compared to its corresponding AL fed control group.

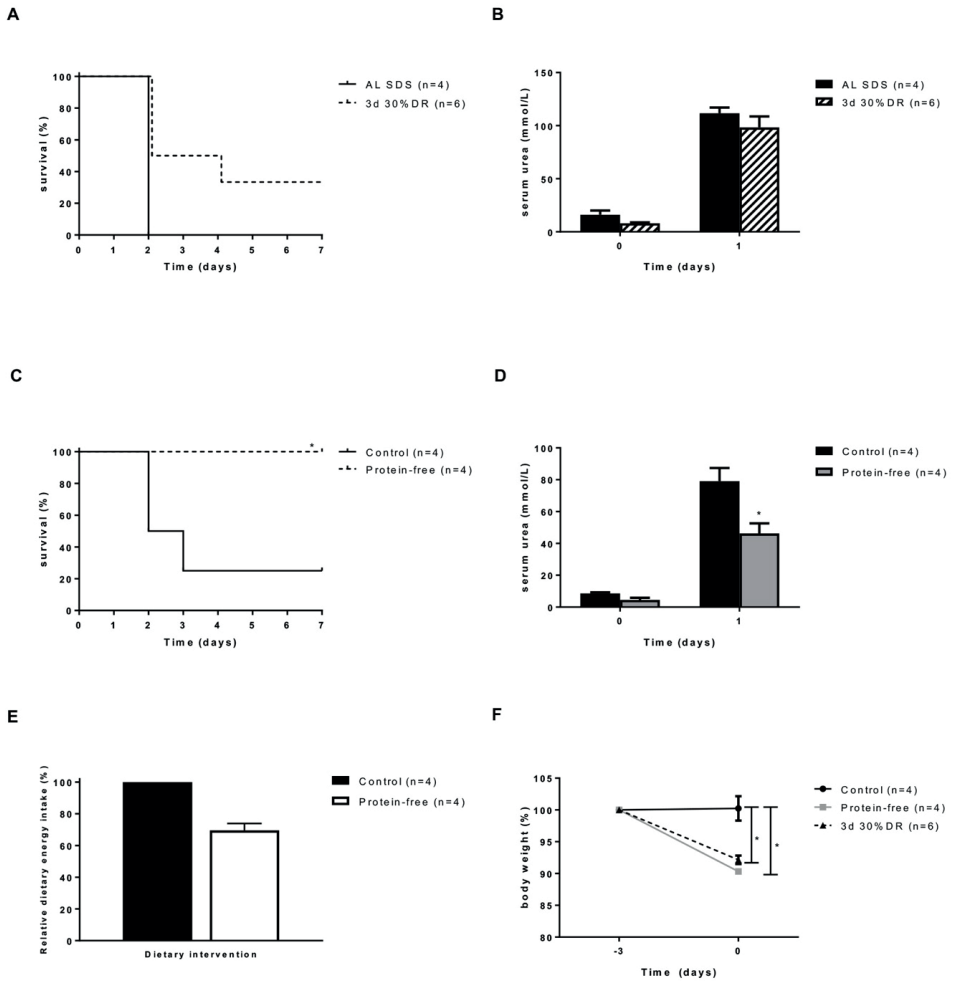


Figure 1. A protein-free diet protects against renal IRI. (A) Three days of 30% DR did not protect against renal IRI. (B) Serum urea levels before and at day one after renal IRI did not differ between mice fed ad libitum (AL) for three days of 30% DR and a control diet. (C) Three days of protein-free diet improved survival compared with AL fed controls. (D) Serum urea levels of AL fed protein-free mice were significantly better compared to AL fed control mice ($P < 0.05$). (E) Three days of protein-free diet resulted in 30% calorie restriction. (F) Mice fed a protein-free diet or a 30% DR diet for three days lost significantly more body weight than mice fed the control diet. Body weight changes did not differ between the protein-free diet and 3-day 30% DR. AL Control= ad libitum fed SDS chow, Control= control diet for the macronutrient diets, protein free= ad libitum fed protein-free diet. *= significance with $P < 0.05$.

4

As the three days of fasting on the one hand and two weeks 30% DR and 3-day 30% DR on the other hand were each performed as individual cohorts using their own control group, we had three different control groups for all interventions combined. No significant differences in gene expression profiles were observed between the different control diets (data not shown). The highest number of significantly differentially expressed probe sets (DEPS) was found after three days of fasting, namely 2,604, of which 1,268 were up- and 1,336 downregulated. Two weeks of 30% DR gave rise to a five times lower number: 492 DEPS, of which 265 were upregulated and 227 were downregulated. Three days of protein-free diet induced 391 DEPS, with 230 probe sets up- and 161 downregulated. Of the non-protective diets, the 3-day fat-free diet did not induce any DEPS when compared to control diet fed mice, while three days of a CHO-free diet induced 1,717 DEPS containing 613 up- and 1,104 downregulated sets. Three days of 30% DR resulted in 454 DEPS, of which 284 up- and 170 downregulated.

Several analytic approaches were performed to compare the transcriptomic response between all diets. First, a comparison was made based on the number of overlapping DEPS and the corresponding significance of the overlap (Table 1). Based on the maximum relative overlap, the 3-day protein-free diet and 3-day fasting demonstrated the most resemblance to each other with 222 DEPS in common, corresponding to 53.3% relative overlap. Two-weeks 30% DR showed 45.9% relative overlap with three days of fasting, with 247 DEPS in common. To compare the significance of these overlapping fractions, the enrichment factors (EF) with corresponding *P*-values were calculated. Comparison of the two identically modified diets differing only in intervention time, namely 3-days 30% DR and two weeks 30% DR, resulted in the highest EF with a 39 times higher number of DEPS in common than would have been expected by chance (Table 1). Comparison of the 3-day protein-free diet with 3-day 30% DR resulted in an EF of 29. All enrichments were significant, with values lower than $8.66E-48$, suggesting a significant common transcriptomic response between dietary interventions with the exception of a 3-day fat-free diet. As directionality of the DEPS was not accounted for in this comparison, we explored dendrographic heat maps. Since the 3-day fasting dataset was hybridized on a different date, the date of hybridization caused a stronger effect than the biological signal (Figure S2). It was therefore not possible to integrate all complete datasets in one informative heat map analysis. As a solution, we assumed 3-day fasting to represent the widest transcriptomic protective response, and all data sets were limited to its highest number of 2,604 DEPS. The resulting heat map (Figure 2A) shows that the majority of the DEPS have similar directionalities, with the lowest expression levels in the fat-free diet. The horizontal dendrogram, based on the (dis)similarity between expression data for probe sets, shows that three days of fasting portrays the largest differences with the other groups, however, this was an assumption, since the heat map is based on the probe sets differentially regulated after three days of fasting.

Compared to 3-days of fasting, a 3-day CHO-free diet is the least clustered with the other dietary groups. The 3-day protein-free diet clusters closely with the non-protective 3-day fat-free diet, based on the number of probe sets as well as the expression levels. Three days 30% DR had a similar cluster pattern as two weeks of 30% DR.

Table 1. Comparison of the overlapping DEPS between the five dietary interventions and their corresponding *P*-value and enrichment factor

Comparison	Overlapping DEPS	Overlap (%)*	Enrichment factor	<i>P</i> -value
Protein-free vs. Fasting	222	53.3	9.8	5.27 ^E -169
2wks 30% DR vs. Fasting	247	45.9	8.7	8.88 ^E -171
3d 30% DR vs. Fasting	208	42.0	8.7	3.12 ^E -156
2wks 30% DR vs. 3d 30% DR	195	28.1	39.4	3.44 ^E -270
Protein-free vs. CHO-free	113	24.9	6.0	5.84 ^E -55
Fasting vs. CHO-free	584	23.7	5.9	3.73 ^E -300
2wks 30% DR vs. CHO-free	122	20.4	8.2	5.71 ^E -76
3d 30% DR vs. CHO-free	107	19.6	5.8	8.66 ^E -48
Protein-free vs. 3d 30% DR	116	18.5	29.5	2.22 ^E -138
Protein-free vs. 2wks 30% DR	95	15.2	22.3	1.15 ^E -99

The highest percentage of relative overlap was found between three days of protein-free diet and three days of fasting. The enrichment factor indicates the number of times the overlapping DEPS is higher than expected by chance. All diets showed a significantly overlapping number of DEPS, as shown by the corresponding *p*-values in the last column. *Relative overlap is calculated by the number of DEPS in common between the two groups, divided by the total number of unique DEPS across both groups, relative to the theoretical maximum overlap according to this formula.

Subsequently, the same set of 2,604 DEPS significantly regulated after fasting compared to AL fed controls, was used for a principal component analysis (PCA) among the macronutrient-free diets, two weeks- and three days 30% DR, and their control diets (Figure 2B). Samples from the control diets and the 3-day fat-free diet clustered together, with high overlap and corresponding directionality between the groups. With a large distance on the principal component (PC) 2 axis, a similar clustering was seen among the 3-day 30% DR and two weeks 30% DR samples. The protein-free diet had its own cluster, separated on both PC axes from the other groups. The 3-day CHO-free diet resembled the DR diets, but showed no overlap with these diets and showed a large dissimilarity to the other groups.

To compare the transcriptomic responses between all dietary interventions, all DEPS were visualized in a Venn diagram (Figure 3A). This revealed a total of 40 overlapping DEPS in the three protective diets, while 30 overlapping DEPS were also present in the non-protective

CHO-free diet. The genes corresponding to the 70 DEPS in common are listed in Table S1. Comparing 3-day 30% DR with the protective diets, a similar pattern was observed; only 15 DEPS overlapped in the three protective diets, while 47 DEPS were also present in the non-protective 3-day 30% DR diet (Figure 3B). However, both numbers of overlapping genes appeared too small to perform pathway analysis with the aim to find a common denominator of protection against renal IRI, and therefore an alternative approximation for analysis was used.

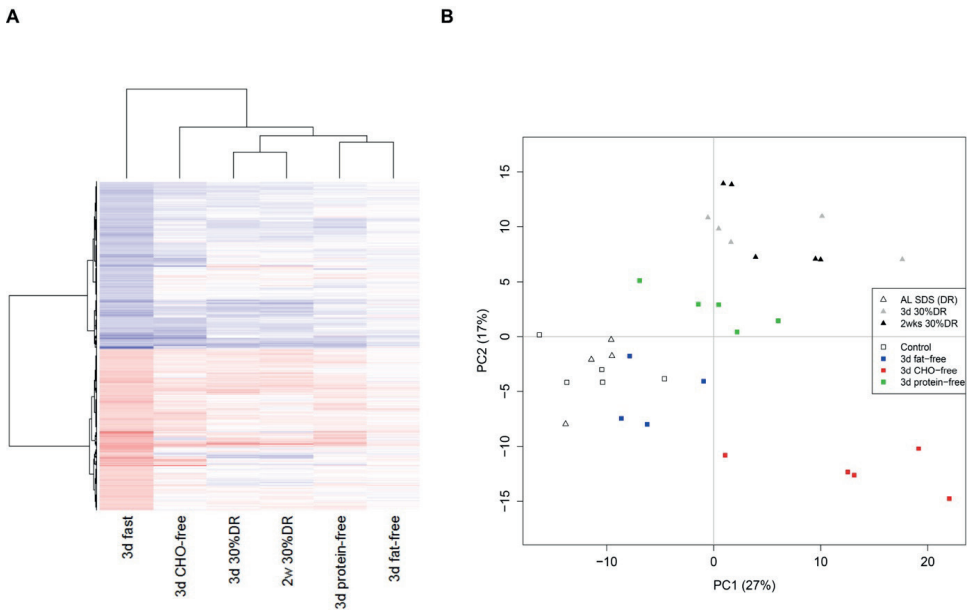


Figure 2. Heat map and PCA plots of directional and cluster patterns in all dietary interventions based on the differentially expressed probe sets (DEPS) after three days of fasting compared to its control group. (A) The majority of the DEPS in the kidney after three days of fasting showed the same directionality in the other dietary interventions. The 3-day CHO-free diet was the least clustered with the other diets, followed by two weeks 30% DR and a 3-day protein-free diet. The fat-free diet, showing no significant DEPS, clustered together with a 3-day protein-free diet. Red= upregulation, blue = downregulation, white = no change. CHO-free = carbohydrate-free. **(B)** Principal component analysis (PCA) plot, based on the 2604 significantly regulated probe sets after three days fasting compared to the control diet fed animals. Both two weeks 30% DR and three days of 30% DR diet clustered close to each other based on the DEPS found after three days of fasting. The two control diets, control and SDS diet, clustered together with the non-protective fat-free diet. Three days of CHO-free diet positioned closely to two weeks and three days of 30% DR, but did not overlap with these diets. The protein-free diet had its own cluster, separated from the other groups on both PC axes.

Pathway analyses and transcription factor analyses

To explore the biological value of these transcriptomic responses, we used an individual approximation to identify significantly enriched pathways. The highest enriched pathways after the different dietary interventions were ranked by their $-\log P$ -value and summarized in Table S2. No clear pattern in overlapping pathways between all diets, or between the protective diets and the non-protective CHO-free diet, was observed. One pathway that emerged was the *NRF2-mediated oxidative stress response pathway*, since this pathway was activated by four out of five dietary interventions (Table S2).

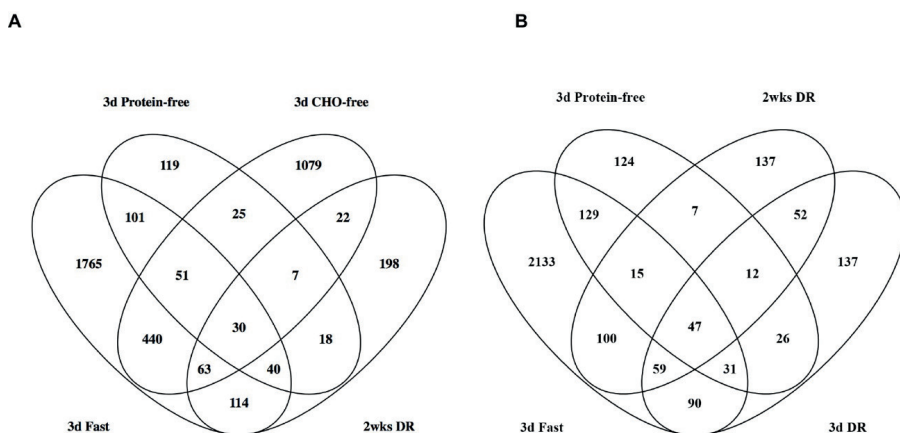


Figure 3. Venn diagram of multiple dietary interventions combined. (A) Venn diagram showing the number of DEPs after three days of fasting, two weeks 30% DR, three days of protein-free diet, three days of CHO-free diet, and their overlap with each diet. Thirty DEPs are differentially regulated in all four diets including the non-protective CHO-free (centre). The protective diets have 70 DEPs in common, of which 40 of those in common with the CHO-free diet are excluded (lower right). (B) Venn diagram showing the number of DEPs after three days of fasting, three days of a protein-free diet, two weeks and three days of 30% DR with their overlap. Forty-seven DEPs are differentially regulated in all four diets (centre). A total of 15 DEPs were overlapping between the three protective diets.

To further identify a common protective response and dissect it from the response of the non-protective CHO-free diet, a more comprehensive meta-analytic approximation was used. A combining rank orders methodology was implemented to prevent bias of the results based on outliers as well as the stronger transcriptomic response after three days of fasting²⁰. By eliminating all significant probe sets induced by the CHO-free diet in this meta-analysis, only 140 DEPs remained. Pathway analysis revealed no significant pathways (data not shown). Theorizing that the protective response might be partially overlapping

with the response of the non-protective CHO-free diet, we repeated the meta-analysis with the three protective diets and the CHO-free diet into the approximation, thus not excluding the 3-day CHO-free diet. This meta-analysis yielded 640 DEPS. The majority of these DEPS in common showed a similar fold change and directionality among the three protective dietary interventions. A pathway analysis of these DEPS demonstrated regulation of nuclear receptor signaling as well as inhibition of cellular stress and injury and biosynthesis pathways amongst the top 10 overrepresented pathway categories (Table 2). Adding the 3-day 30% DR diet in the meta-analysis yielded 279 DEPS. No significant enriched pathways emerged. The 10 highest enriched pathways are depicted in Table S3.

Table 2. Overview of the top 10 overrepresented canonical pathways in the meta-analysis ranked by their *P*-value

Canonical Pathway	Pathway Category	<i>P</i> -value	Genes Ratio	Z-score
LXR/RXR Activation	Nuclear Receptor Signaling	7.24 ^E -09	16/121 (13.2%)	+0.302
FXR/RXR Activation	Nuclear Receptor Signaling	3.63 ^E -06	13/127 (10.2%)	N/A
LPS/IL-1 Mediated Inhibition of RXR Function	Nuclear Receptor Signaling	2.24 ^E -05	16/219 (7.3%)	-2.646
Superpathway of Cholesterol Biosynthesis	Fatty Acids and Lipids Biosynthesis, Sterol Biosynthesis	2.40 ^E -05	6/28 (21.4%)	N/A
NRF2-mediated Oxidative Stress Response	Cellular Stress and Injury	3.72 ^E -05	14/180 (7.8%)	-1.000
Aryl Hydrocarbon Receptor Signaling	Cell Cycle Regulation; Apoptosis; Xenobiotic Metabolism, Nuclear Receptor Signaling	5.13 ^E -05	12/140 (8.6%)	+1.633
PXR/RXR Activation	Nuclear Receptor Signaling	9.12 ^E -05	8/67 (11.9%)	N/A
Intrinsic Prothrombin Activation Pathway	Cardiovascular Signaling; Cellular Stress and Injury	3.47 ^E -03	5/29 (17.2%)	N/A
Superpathway of Geranylgeranyldiphosphate Biosynthesis I	Cofactors, Prosthetic Groups and Electron Carriers Biosynthesis	3.98 ^E -03	4/17 (23.5%)	N/A
Aldosterone Signaling in Epithelial Cells	Cardiovascular Signaling; Nuclear Receptor Signaling	4.57 ^E -03	11/152 (7.2%)	N/A

The top 10 overrepresented pathways derived from the 640 DEPS in common between 3-days of fasting, two weeks 30% DR, three days of a protein-free diet and three days of a carbohydrate-free diet. These pathways are mostly involved in regulation of nuclear receptor signalling (five out of 10), biosynthesis signalling (two out of 10) and cellular stress and injury (two out of 10).

To further explore the regulated DEPS and pathways in relation to the protective response against renal IRI, we examined the involvement of upstream transcription factors (TFs) in the DEPS that emerged from the meta-analysis. In the meta-analysis, 16 TFs were identified of which 12 were predicted to be activated and six inhibited (Table 3). Critical

denominators might be TFs showing the same directionality in the protective diets, but are oppositely directed or not regulated in the non-protective CHO-free diet. The TFs complying with these criteria, in descending order of absolute z-score, were forkhead box O3 (FOXO3), heat shock factor protein 1 (HSF1), and high mobility group AT-hook 1 (HMGA1). Furthermore, hepatocyte nuclear factor 4-alpha (HNF4A) was highly activated in the protective diets, but only minimally in the non-protective CHO-free diet. Also, sterol regulatory element-binding transcription factor 1 (SREBF1) and 2 (SREBF2) were significantly downregulated after three days of fasting and in the protein-free diet, activated in the CHO-free diet but not regulated after two weeks 30% DR. The non-protective three days 30% of DR showed similar results as the protective diets, since all TFs after three days of 30% DR were similarly regulated as after three days of fasting, two weeks 30% DR and the three days of a protein-free diet.

The validity of these findings was further examined by determining mRNA expression levels. The expression levels of *Foxo1* were significantly higher after all diets except the fat-free diet (Figure S4A), while *Foxo3* was significantly upregulated in all diets except after two weeks of 30% DR (Figure S4B). *Foxo4* was only significantly upregulated after three days of protein-free and three days of a carbohydrate-free diet (Figure S4C). *Hnf4a* was not significantly regulated after any of the dietary interventions (Figure S4D). The mRNA expression level of downregulated transcription factor *Srebfl* was only significantly downregulated after three days of fasting (Figure S4E), while *Srebfl2* was significantly downregulated after three days of fasting and three days of a protein-free diet (Figure S4F).

Target pathways possibly involved in the protective effect of renal IRI

Various pathways have been proposed to be involved in the protective response against renal IRI induced by DR and protein restriction. One of these is the eukaryotic translation factor 2 (eIF2 α) signaling pathway, in which eIF2 α is phosphorylated by the general control nonderepressible 2 (Gcn2) kinase, thereby inhibiting initiation of translation¹⁹. The role of Gcn2 and the eIF2 α pathway is subject of debate, and the relevance of this pathway still needs to be elucidated^{19,21}. Our microarray analyses showed a significant upregulation of eIF2 α transcription factor only after three days of fasting, while the *Gcn2* gene and other target genes of the eIF2 α pathway were not significantly differentially regulated after any of the dietary interventions. The mammalian Target of Rapamycin (mTOR) signaling pathway mediates between growth factors, hormones and nutrients to regulate essential cellular functions including survival and protein translation. Inhibition of the mTOR pathway has been demonstrated to increase lifespan in various animal species^{22,23} mTOR is part of mTOR complex 1 (mTORC1), a nutrient sensor complex that is involved in induction of oxidative stress resistance²⁴. We found a downregulation of mTOR after two weeks 30% DR (-0.6;

$P < 0.01$) and 3-days of protein-free diet (-1.7 ; $P < 0.001$) diets, while MTORC1 (-1.6 ; $P < 0.01$) and mTOR (-0.6 ; $P < 0.001$) were downregulated after three days of fasting. Both non-protective diets 3-day CHO-free ($+0.8$; $P < 0.01$) and 3-day 30% DR ($+1.3$; $P < 0.001$) showed an upregulation of mTOR. mTOR activity was examined at protein level by examining ribosomal protein S6 phosphorylation through immunoblotting in kidney extracts from all intervention and control groups. S6 is a down-stream target of mTOR through S6 kinase²⁵.

Table 3. List of upstream transcription factors after meta-analysis with corresponding z-scores in the different dietary interventions

Transcription Factor	Dietary intervention					
	Meta-analysis	3-days fasting	2 weeks 30% DR	Protein-free	CHO-free	3 days 30% DR
SMAD7 – SMAD family member 7	+2.890	+0.718	-0.128	+2.466	N/A	N/A
* FOXO3 - Forkhead box O3	+2.729	+3.303	+1.042	+1.701	-0.314	+1.893
FOXO1 - Forkhead box O1	+2.692	+1.599	-0.109	+0.269	-1.850	+0.360
* HNF4A – Hepatocyte nuclear factor 4 alpha	+2.462	+2.122	+1.179	+2.089	+0.109	+1.327
MYCN – v-myc avian myelocytomatosis viral oncogene	+2.414	+1.982	N/A	+1.245	-2.464	+1.091
CLOCK – Circadian Locomotor Output Cycles Kaput	+2.373	+1.980	+1.119	N/A	+1.940	+1.925
* HMGA1 – High mobility group AT-hook 1	+2.051	+1.432	+2.177	+0.356	N/A	+0.785
MED1 – Mediator complex subunit 1	+2.008	+2.058	N/A	N/A	+0.102	N/A
SPDEF – SAM pointed domain containing ETS transcription factor	+2.000	+2.170	N/A	+1.000	N/A	N/A
LYL1 – Lymphoblastic leukemia associated hematopoiesis regulator 1	+2.000	+2.000	N/A	N/A	N/A	+1.982
SIM1 – Single-minded homolog 1	+2.000	+0.557	N/A	N/A	N/A	N/A
ARNT2 – Aryl hydrocarbon receptor nuclear translocator 2	+2.000	+0.557	N/A	N/A	N/A	N/A
GLI1 – GLI family zinc finger 1	-2.183	N/A	N/A	+0.057	N/A	N/A
* HSF1 – Heat shock factor protein 1	-2.697	-1.659	-2.653	-2.376	+0.462	-0.451
SREBF2 - Sterol regulatory element-binding transcription factor 2	-2.923	-3.420	N/A	-0.243	+0.660	N/A
SREBF1 - Sterol regulatory element-binding transcription factor 1	-3.889	-2.794	N/A	-1.304	+1.229	-0.779

Upstream regulator analysis of the DEPS found in common after 3-days of fasting, two weeks 30% DR and 3-days of protein-free diet (meta-analysis) revealed 16 transcription factors (TFs) significantly regulated, of which 12 were activated and four were inhibited. Highest activated TFs were SMAD7 and FOXO3. *: TFs of interest, that are not or oppositely regulated in the non-protective CHO-free diet.

Compared to the corresponding control group, three days of fasting showed a significant two-fold increase in relative ribosomal protein S6 phosphorylation (Figure 4). In the other dietary interventions, a large variation in phosphorylation levels was observed which did not reach statistical significance.

DISCUSSION

Since the discovery of the beneficial effects of short-term dietary restriction (DR) on stress resistance, optimizing its duration and content to eventually lead to a clinical applicable DR regimen has been an important part of the body of literature about DR^{2,11,19}. Previously we have shown that two and four weeks of 30% DR as well as three days of fasting decreased morbidity and mortality, and improved kidney function in a murine renal IRI model^{1,12}. In the present study, we show that a protein-free diet administered for only three days is sufficient to induce similar protection, whereas fat- and carbohydrate-free diets did not.

Initially, we attempted longer periods of diet interventions, but found that mice fed a protein-free diet during 10 days applied self-restriction of approximately 30% of their normal intake (Figure S1). Therefore, the possible beneficial effects of calorie and protein restriction on kidney function and survival were indistinguishable. In a recent publication, Peng et al. found that mice fed a protein-free diet for six days restricted calorie intake. However, they stated that corrected for body weight, their calorie intake was similar to that of ad libitum fed mice¹⁹. It is unknown whether six days of 30% DR induces protection against IRI, therefore a distinction between protein restriction and calorie restriction is still difficult to make. We showed that three days of 30% DR does not induce protection against renal IRI, and therefore we could disentangle the effects of calorie and protein restriction per se (Figure 1). A protein-free diet, given for three days induced protection, whereas both a CHO-free and fat-free diet given for three or 14 days did not protect against renal IRI (Figure S1). A recent publication by Solon-Biet et al²⁶ showed that the ratio of proteins and carbohydrates rather than DR per se influenced the lifespan of mice as well as metabolic parameters such as insulin and lipids. Since proteins fully substituted the carbohydrates in our CHO-free diet, and carbohydrates fully substituted the proteins in our protein-free diet, these diets further emphasize the importance of the ratio between proteins and carbohydrates (Table S4).

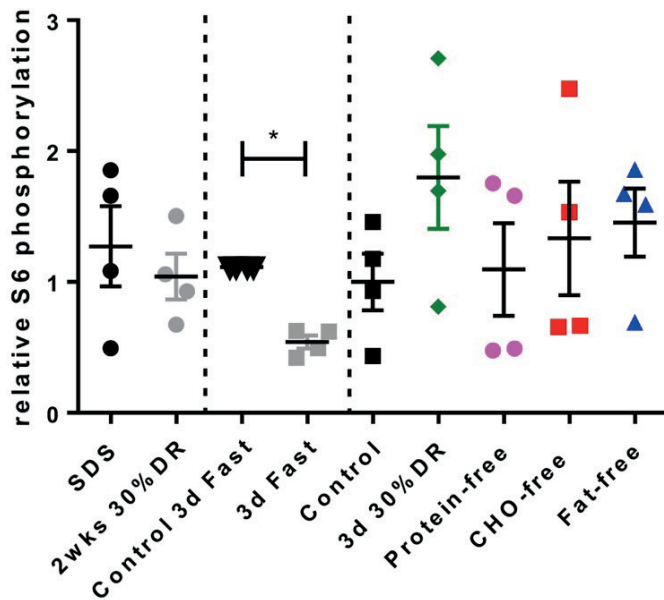


Figure 4. Relative S6 phosphorylation signals in kidney after various diet interventions. The ratio of phosphorylated S6 over total S6 was significantly lower after three days of fasting compared to its control diet. All other dietary interventions showed a large variation in phosphorylation levels that did not reach statistical significance.

Although the beneficial effects of both long-term and short-term DR have been acknowledged, the mechanisms underlying DR are still subject of investigation. Various pathways, factors and genes have been proposed to play a central role in the protective effects²⁷, but attempts to validate these yielded conflicting results²⁸⁻³¹. We produced extensive expression datasets of diets proven to be either protective or not protective against renal IRI. Gene expression profiles of the non-protective CHO-free diet showed a considerable overlap with gene expression profiles of protective diets, namely three days of fasting, two weeks 30% DR and 3-days of protein-free diet (Figure 3). A PCA plot demonstrated the partial different directionality of gene expression in the CHO-free diet compared to the other dietary interventions. The 3-day 30% DR diet also showed considerable overlap with the protective diets, mainly with two weeks 30% DR, and a partially different but also partially overlapping directionality in response. These findings could either indicate that overlapping probe sets and pathways are not involved in the induction of protection against renal IRI, or that they may require additional changes in other probe sets to induce this effect. Particularly, the striking similarity between three days and two weeks 30% DR suggests that three days is sufficient to activate a transcriptomic response which is not yet sufficient to induce phenotypical protection. In addition, the non-protective fat-free diet showed strong

similarity with the protective 3-day protein-free diet, but with gene expression levels that were lower. These results indicate that the directionality, the number of probe sets and the expression levels are of importance in order to induce protection against renal IRI.

To provide structure in the infinite amount of data generated by microarray analysis, we used meta-analytic approximations to specify for overlapping pathways and factors in all diets. A specific meta-analysis in which the DEPS were oppositely regulated in the protective diets versus the non-protective CHO-free diet, resulted in only 160 DEPS and yielded no additional pathways of interest compared to a meta-analysis including the CHO-free diet. In this meta-analysis several TFs, including FOXO3 and HNF4A, remained significantly upregulated in the protective diets whilst not or oppositely regulated in the CHO-free diet (data not shown).

Activation of nuclear receptor signaling pathways dominated the top 10 overrepresented pathways after three days of fasting, two weeks of 30% DR and three days of a protein-free diet (Table 2). Specific retinoid receptors, including the retinoid X receptor (RXR), the pregnane X receptor (PXR) and the peroxisome proliferator-activated receptor (PPAR)³², were also prominently upregulated in our analysis, pointing towards a pivotal role for nuclear receptor signaling. Nuclear receptors are transcription factors that can be activated by steroid hormones and lipid-soluble agents, such as the retinoid acids (RAs)³³. Administration of RAs induces many of the beneficial effects observed after DR. DR is able to ameliorate age-related insulin resistance and degenerative brain diseases, and similar results have been described after treatment with RAs³⁴⁻³⁶. Both DR and administration of RAs are able to protect from ischemic stroke in the brain³⁷⁻³⁹. Signaling pathways activated by the interaction between RAs and nuclear receptors have also been considered to have tumor-, and immune suppressive effects, just as DR^{9,33,40}.

Involvement of nuclear receptor signaling is further supported by the upstream TF analysis (Table 3), since the majority of the activated or inhibited TF could be directly or indirectly linked to the activation of nuclear receptors. The activated TFs in all protective diets that were oppositely or not regulated in the non-protective CHO-free diet are FOXO3, HNF4A, HMGA1 and HSF1. A role for each of these four TFs in increased stress resistance has been previously observed. For example, FOXO3 phosphorylation via the c-Jun N-terminal kinase -pathway results in its nuclear inclusion and activation of various processes involved in cellular stress resistance, biosynthesis, cell cycle regulation as well as apoptosis and autophagy^{41,42}. A fasting-induced interaction, mediated by insulin signaling, with members of the FOXO family and RXR has been described as well⁴³. HMGA1 is a downstream

target of the insulin receptor pathway and could function as an important nuclear factor mediating the binding of FOXO proteins to other nuclear receptors, including the retinoid nuclear receptor family and thereby regulating insulin target genes⁴⁴.

HNF4A is a nuclear TF that is involved in the development as well as in the metabolism of mainly the liver and kidney⁴⁵. Upregulation of HNF4A occurs via co-stimulation of LXR and FXR and usually depends on the presence of low levels of stressors, such as interleukin-1 and tumor necrosis factor alpha. Transcriptional activity of HNF4A is also regulated indirectly by insulin through the action of FOXO1⁴⁵. Activation of HNF4A results in inhibition of the activity of metabolic sensors, including SREBF and the mammalian target of Rapamycin (mTOR)^{46,47}. This leads to downregulation of metabolism, in particular cholesterol metabolism, and may contribute to increased stress resistance via the downregulation of mTOR^{47,48}. We showed that the activity of mTOR, as determined by the phosphorylation of the ribosomal protein S6, was significantly downregulated after three days of fasting. A trend towards lower phosphorylation levels was seen after the other two protective diets: two weeks 30% DR and a 3-day protein-free diet. These data indicate that mTOR may play an important role in the protection against IRI, which may vary according to the type of nutrient deprivation that is offered. Another pathway involved in nutrient sensing is GCN2, of which eIF2 α is an important downstream target. GCN2 becomes transcriptionally activated by deprivation of amino acids and phosphorylates eIF2 α , which leads to the activation of pathways involved in stress resistance. We did not find transcriptional regulation of the *Gcn2* gene in any of the three protective diets. Although our data do not preclude posttranscriptional regulation of this pathway, they corroborate with those of Robertson et al⁴⁹, who observed that GCN2 signaling was not required for protection against renal IRI by protein restriction.

In summary, we demonstrated that three days of a protein-free diet in mice protects against renal IRI, similar to two weeks of 30% DR and three days of fasting. Comparative transcriptional analysis of kidney tissue following these dietary interventions demonstrated a significant overlap in differentially expressed genes and pathways, which are involved in resistance against oxidative damage induced by renal IRI. A meta-analysis of pathways and TFs indicates that DR upregulates at least four TFs that activate a transcriptional response, which, in turn, increases nuclear receptor signaling dependent and independent-cellular stress resistance. However, our attempt to understand the beneficial effects of different dietary restriction regimens on renal IRI by transcriptome analysis suggests that pivotal molecular changes also occur beyond the transcriptional level, and that additional ‘omics’ analyses, including proteomics, are needed to come to a complete understanding.

Therefore, more research is warranted to further elucidate the role of these pathways in the induction of acute stress resistance by short-term DR, which may ultimately lead to “dietary restriction mimetic” therapeutic strategies that exploit the benefits of DR in humans.

MATERIALS AND METHODS

Study design

Sample size calculation of our previous study was based on a 25% decrease of serum urea levels at time point 24 hours after renal IRI, with a standard deviation (SD) of 20% and a power of 0.8^{1,11}. These experiments demonstrated that our renal IRI model was feasible and stable, and we therefore reduced the number of mice to six mice per group in the dietary intervention groups. Primary endpoint of this study was kidney function 24 hours after surgery, measured via serum urea concentrations. Secondary endpoints of this study were mortality rate in the first seven days after surgery and changes in gene expression profiles measured directly after each dietary intervention. Experimental data of two weeks 30% DR and three days of fasting groups were previously obtained¹. Animals were euthanized and excluded from the experiment if their body weight decreased $\geq 20\%$ of their preoperative weight or if they developed a moribund phenotype, including ruffled fur, hunched body posture, hypothermia, and decreased activity^{11,12}.

Animals

C57BL/6 male mice, 10-12 weeks old (20-25 grams), were obtained from Harlan, the Netherlands. Animals were housed in individually ventilated cages (3-4 animals/cage) under standard conditions. All mice had ad libitum (AL) food and water (acidified with HCl to a pH of 2.4-2.7) except where noted. All experiments were performed with the approval of the Animal Experiments Committee of the Erasmus University Medical Center, Rotterdam, the Netherlands under the Dutch National Experiments on Animals Act and according to the ARRIVE Guidelines, Animal Research: Reporting of In Vivo Experiments⁵⁰.

Diets and experimental design

The control chow for the fasting and dietary restriction groups was obtained from Special Diet Services (SDS, Witham, UK). All other diets were purchased from Research Diets, Inc. (New Brunswick, NJ, USA). The macronutrient composition and energy content of all diets are shown in Table S4. The control diet differed from the standard chow given (Special Diet Services, SDS) in the protein source, which consisted of lactic casein protein in case of control diet, while the SDS control consisted of crude protein. These two control diets are designated as “Control” and “SDS” throughout the manuscript.

Long-term dietary intervention

Upon arrival, mice were allowed ad libitum (AL) access to the SDS chow for seven days. At the start of the dietary intervention period, all mice were transferred to clean cages at 4:00 pm. Mice were randomly divided into a group with 30% DR (n=5) or AL access to a carbohydrate-free (CHO-free) diet (n=6) or a fat-free diet (n=6) for 14 days, or a protein-free diet (n=6) for 10 days (Figure S3). Mice in the control group for DR had AL access to the control SDS chow (n=10), the control group for CHO-free and fat-free had AL access to Control diet (n=12). The effect of food intake was measured using pair-fed (PFed) control groups. Pair-feeding of each group was accomplished by giving the PFed groups the identical isocaloric amount of the control diet as the mice on the experimental diet had consumed the day before. The CHO-free, fat-free and protein-free diets were PFed in this manner (n=6/group). Mice with 30% DR were given 70% of the normal daily intake of mice on the control diet, which was administered once daily at 4:00 pm. Since the phenotypical effects of two weeks 30% DR were reported previously, microarray analysis was used as the only outcome for this group¹.

Short-term dietary intervention

Upon arrival, the same procedure was followed as for the long-term experiment. Mice were randomly divided into groups with AL access to control diet (n=4), a protein-free diet (n=6 per group) for three days or 30% DR for three days (n=6), or into groups with AL access to SDS chow or fasting for three days (n=5 per group). Since the phenotypical effects of three days fasting were reported previously, transcriptome analysis was the only parameter for this group¹. For a graphical overview of the experimental setup see Figure S3.

Dietary intake and body weight

Food intake and body weight were measured daily. To determine calorie intake, the daily food intake was corrected for the variation in the energy content (per gram of food) in the diets as follows: food intake per mouse times the number of calories per gram of food. Change in body weight was addressed in percentages calculated by dividing the body weight measurements during the dietary intervention through body weight at onset of the intervention period times 100.

Surgical procedure

Following each dietary intervention, bilateral renal IRI was induced as previously described¹. In brief, mice were anesthetized via inhalation of isoflurane (5% isoflurane initially followed by 2-2.5% with oxygen for maintenance). Via midline abdominal incisions, the renal arteries and veins were exposed followed by occlusion of both renal pedicles for 37 minutes using non-traumatic vascular clamps. Purple discoloration of the

kidneys confirmed ischemia macroscopically, while reperfusion was established when the color of both kidneys normalized after removal of the clamps. The incision was closed with 5/0 sutures in two layers. Following closure, mice received 0.5 ml PBS subcutaneously to compensation for fluid loss. The morning after surgery, another identical dose of PBS was given. Mice intended for microarray analysis were sacrificed immediately after the dietary intervention, without induction of renal IRI.

Kidney function

Kidney function was determined as previously described¹ by measuring serum urea levels in blood samples, collected via retro-orbital puncture while mice were anesthetized, before (T=0) and day 1 (T=1) after induction of renal IRI¹.

Immuno-blotting

Mouse kidney extracts from nine different intervention diets were prepared by sonification with Soniprep 150 (Company, Place, Country) 2-3 times 30 seconds on ice in Laemmli buffer (135 mM Tris-HCl pH 6.8, 4.5% SDS, 22.5% glycerol), supplemented with complete protease inhibitors and PhosSTOP phosphates inhibitors (Roche Diagnostics, Indianapolis, IN, USA) After sonification, lysates were centrifuged at 4 degrees Celsius for 10 minutes. Protein concentrations were measured using the BCA Protein Assay Kit (Pierce Biotechnology, Rockford, USA). 25 µg protein was loaded on a NuPAGE 10% Bis-Tris Gel (Life Technologies LTD, Paisley, UK) and transferred to a PVDF Hybond-P (GE-Healthcare Life Sciences, Uppsala, Sweden) transfer membrane. Immunoblotting was performed with antibodies directed against S6 (#2217S Lot5; 1:1.000) and Phospho-S6 (Ser240/244; #2215 Lot14; 1:500) (Cell Signaling Technology, Danvers, MA, USA). Blotting membranes were incubated with primary antibodies overnight at 4 degrees Celsius, before they were washed and incubated with 1:5000 diluted secondary anti-rabbit-IgG-HRP antibody (GE-Healthcare Life Sciences). Detection was performed by enhanced chemiluminescence using the ECL 2 Western Blotting Substrate (Pierce Biotechnology). Levels of S6 and Phospho-S6 were semi-quantified using the ImageJ software package (<http://rsb.info.nih.gov/ij/index.html>) and S6-phospho/S6-total ratios relative to the control diet were calculated and differences between groups were assessed with a t-test. B-Actin was used as loading control (Sigma; A5441 Lot064M4789V; 1:25.000).

Microarrays

The duration of dietary interventions that were used to study gene expression profiles was three days for all diets with exception of 30% DR, which was given for two weeks. Kidneys were obtained directly after each intervention and were snap frozen in liquid nitrogen until further analyses. An overview of the dietary interventions, the groups of mice and

numbers used for phenotypical and transcriptional endpoints is summarized in Table S5. Total RNA was extracted using QIAzol lysis Reagent and miRNAeasy Mini Kits (QIAGEN, Hilden, Germany), following Qiagen protocol. Addition of wash buffers RPE and RWT (QIAGEN) was done mechanically by using the QIAcube (QIAGEN, Hilden, Germany) via the miRNAeasy program. Isolated RNA was and stored at -80°C. The concentration of RNA was measured by Nanodrop (Thermo Fisher Scientific™, Breda, the Netherlands) and RNA quality was assessed using the 2100 Bio-Analyzer (Agilent Technologies, Amstelveen, the Netherlands) according to manufacturer's instructions. The RNA quality was expressed as the RNA integrity number (RIN, range 0-10). RIN values of included samples ranged between 6.6 and 8.5. Hybridization to Affymetrix HT MG-430 PM Array Plates was performed at the Microarray Department of the University of Amsterdam (the Netherlands), according to Affymetrix protocols. Four to six biological replicates were used for each group. Quality control and normalization were performed using the pipeline at the www.arrayanalysis.org website (Maastricht University, the Netherlands)²⁶. Normalization was done via the Robust Multichip Average (RMA) algorithm⁵¹. Due to a range in hybridization dates between fasting and the other diets (*i.e.* September 2011 versus August 2012), normalization of the data for fasted animals and their controls was done separately. Normalization output consisted of data for 45,141 probes, with several probes corresponding to the same Gene ID. Complete raw and normalized microarray data and their MIAME compliant metadata have been deposited at the Gene expression Omnibus (GEO) database GEO GSE65656 (www.ncbi.nlm.nih.gov/geo). After normalization, outliers were found in the control SDS (control 30% DR), the 3-day fasting and 3-day fat-free diet groups, defined as a deviation in array-array intensity correlations, principal component analysis and cluster dendograms. These outliers were excluded from further analyses (Table S5).

Statistical analysis

Data are expressed as means \pm standard error of the mean (SEM). Statistical analyses were performed using SPSS (version 21.0) and GraphPad Prism (version 5.0). Differences in serum urea concentrations were compared by Mann-Whitney U tests, food intake via the paired t-test and survival rates were analyzed by Log-rank tests. A *P*-value of <0.05 was considered significant. Microarray analyses were performed using the free software package R (R foundation). Gene expression data were compared using the Linear Models for Microarray Data (limma) method with correction for multiple testing using the false discovery rate (FDR) according to Benjamini and Hochberg⁵². Fold changes were expressed as the geometric mean per diet group against the corresponding ad libitum fed control group. Cutoff values for a significant difference were put at FDR <5% with fold change ≥ 1.5 . The enrichment factor (EF) was calculated via the formula: $EF = nA / ((nA \times nB) / nC)$, where *nA* is the number of differentially expressed probe sets (DEPS) in experimental group A, *nB* the

number of DEPS in experimental group B, n_C the number of total genes in the microarray, and n_{AB} the number of common DEPS between n_A and n_B . Data integration of microarrays hybridized in different dates was performed with meta-analysis. The methodology applied was combining rank orders. It is a non-parametric approach based on rank orders. The R package RankProd implemented in INMEX was used²⁰. In summary, for each dataset, the fold changes (FC) were calculated for all possible pairwise comparisons. The ranks of the fold changes within each comparison were used to calculate the rank product for each gene. To assess the null distribution of the rank product within each data set, a permutation test was performed. The process was repeated several times to compute the *P*-value and false discovery rate (FDR) associated with each gene. A gene was selected as differentially expressed if it had an FDR < 5% and an absolute combined FC ≥ 1.5 . Functional annotation and analyses were performed using Ingenuity software (<http://www.ingenuity.com/products/ipa>). The prediction inhibition or activation of the upstream transcription regulators is calculated via de statistical z-score based on the observed gene expression changes in our dataset. Calculating the z-score reduces the chance of significant predictions based on random data (<http://ingenuity.force.com/ipa/articles/FeatureDescription/Upstream-Regulator-Analysis>). Cutoff values for a significant activation or inhibition were met with a z-score of ≥ 2 or ≤ -2 , respectively.

REFERENCES

1. Mitchell, J. R. et al. Short-term dietary restriction and fasting precondition against ischemia-reperfusion injury in mice. *Aging Cell* 9, 40-53, doi:10.1111/j.1474-9726.2009.00532.x (2010).
2. Fontana, L., Partridge, L. & Longo, V. D. Extending healthy life span--from yeast to humans. *Science* 328, 321-326, doi:10.1126/science.1172539 (2010).
3. Robertson, L. T. & Mitchell, J. R. Benefits of short-term dietary restriction in mammals. *Exp Gerontol* 48, 1043-1048, doi:10.1016/j.exger.2013.01.009 (2013).
4. Raffaghello, L. et al. Starvation-dependent differential stress resistance protects normal but not cancer cells against high-dose chemotherapy. *Proc Natl Acad Sci U S A* 105, 8215-8220, doi:10.1073/pnas.0708100105 (2008).
5. Vigne, P., Tauc, M. & Frelin, C. Strong dietary restrictions protect *Drosophila* against anoxia/reoxygenation injuries. *PLoS One* 4, e5422, doi:10.1371/journal.pone.0005422 (2009).
6. Heilbronn, L. K. et al. Effect of 6-month calorie restriction on biomarkers of longevity, metabolic adaptation, and oxidative stress in overweight individuals: a randomized controlled trial. *JAMA* 295, 1539-1548, doi:10.1001/jama.295.13.1539 (2006).
7. Weiss, E. P. et al. Improvements in glucose tolerance and insulin action induced by increasing energy expenditure or decreasing energy intake: a randomized controlled trial. *Am J Clin Nutr* 84, 1033-1042 (2006).
8. Fontana, L. & Klein, S. Aging, adiposity, and calorie restriction. *JAMA* 297, 986-994, doi:10.1001/jama.297.9.986 (2007).
9. Huisman, S. A. et al. Fasting protects against the side-effects of irinotecan treatment but does not abrogate anti-tumor activity in mice. *Br J Pharmacol*, doi:10.1111/bph.13317 (2015).
10. Antoine, D. J., Williams, D. P., Kipar, A., Laverty, H. & Park, B. K. Diet restriction inhibits apoptosis and HMGB1 oxidation and promotes inflammatory cell recruitment during acetaminophen hepatotoxicity. *Mol Med* 16, 479-490, doi:10.2119/molmed.2010.00126 (2010).
11. Verweij, M. et al. Glucose supplementation does not interfere with fasting-induced protection against renal ischemia/reperfusion injury in mice. *Transplantation* 92, 752-758, doi:10.1097/TP.0b013e31822c6ed7 (2011).
12. Jongbloed, F. et al. Preoperative fasting protects against renal ischemia-reperfusion injury in aged and overweight mice. *PLoS One* 9, e100853, doi:10.1371/journal.pone.0100853 (2014).
13. Bonventre, J. V. & Yang, L. Cellular pathophysiology of ischemic acute kidney injury. *J Clin Invest* 121, 4210-4221, doi:10.1172/JCI45161 (2011).
14. Brook, N. R., Waller, J. R. & Nicholson, M. L. Nonheart-beating kidney donation: current practice and future developments. *Kidney Int* 63, 1516-1529, doi:10.1046/j.1523-1755.2003.00854.x (2003).
15. Perico, N., Cattaneo, D., Sayegh, M. H. & Remuzzi, G. Delayed graft function in kidney transplantation. *Lancet* 364, 1814-1827, doi:10.1016/S0140-6736(04)17406-0 (2004).

16. Kosieradzki, M. & Rowinski, W. Ischemia/reperfusion injury in kidney transplantation: mechanisms and prevention. *Transplant Proc* 40, 3279-3288, doi:10.1016/j.transproceed.2008.10.004 (2008).
17. Snoeijis, M. G., van Heurn, L. W. & Buurman, W. A. Biological modulation of renal ischemia-reperfusion injury. *Curr Opin Organ Transplant* 15, 190-199, doi:10.1097/MOT.0b013e32833593eb (2010).
18. Mair, W., Piper, M. D. & Partridge, L. Calories do not explain extension of life span by dietary restriction in *Drosophila*. *PLoS Biol* 3, e223, doi:10.1371/journal.pbio.0030223 (2005).
19. Peng, W. et al. Surgical stress resistance induced by single amino acid deprivation requires *Gcn2* in mice. *Sci Transl Med* 4, 118ra111, doi:10.1126/scitranslmed.3002629 (2012).
20. Xia, J. et al. INMEX--a web-based tool for integrative meta-analysis of expression data. *Nucleic Acids Res* 41, W63-70, doi:10.1093/nar/gkt338 (2013).
21. Gallinetti, J., Harputlugil, E. & Mitchell, J. R. Amino acid sensing in dietary-restriction-mediated longevity: roles of signal-transducing kinases *GCN2* and *TOR*. *Biochem J* 449, 1-10, doi:BJ20121098 [pii] 10.1042/BJ20121098 (2013).
22. Kennedy, B. K. & Lamming, D. W. The Mechanistic Target of Rapamycin: The Grand Conductor of Metabolism and Aging. *Cell Metab* 23, 990-1003, doi:S1550-4131(16)30227-3 [pii] 10.1016/j.cmet.2016.05.009 (2016).
23. Xu, S., Cai, Y. & Wei, Y. mTOR Signaling from Cellular Senescence to Organismal Aging. *Aging Dis* 5, 263-273, doi:10.14336/AD.2014.0500263 ad-5-4-263 [pii] (2014).
24. Hay, N. & Sonenberg, N. Upstream and downstream of mTOR. *Genes Dev* 18, 1926-1945, doi:10.1101/gad.1212704 18/16/1926 [pii] (2004).
25. Wullschleger, S., Loewith, R. & Hall, M. N. TOR signaling in growth and metabolism. *Cell* 124, 471-484, doi:S0092-8674(06)00108-5 [pii] 10.1016/j.cell.2006.01.016 (2006).
26. Solon-Biet, S. M. et al. The ratio of macronutrients, not caloric intake, dictates cardiometabolic health, aging, and longevity in ad libitum-fed mice. *Cell Metab* 19, 418-430, doi:10.1016/j.cmet.2014.02.009 (2014).
27. Longo, V. D. et al. Interventions to Slow Aging in Humans: Are We Ready? *Aging Cell* 14, 497-510, doi:10.1111/accel.12338 (2015).
28. Masoro, E. J. Caloric restriction and aging: controversial issues. *J Gerontol A Biol Sci Med Sci* 61, 14-19 (2006).
29. Cavallini, G., Donati, A., Gori, Z. & Bergamini, E. Towards an understanding of the anti-aging mechanism of caloric restriction. *Curr Aging Sci* 1, 4-9 (2008).
30. Turturro, A., Hass, B. S. & Hart, R. W. Does caloric restriction induce hormesis? *Hum Exp Toxicol* 19, 320-329 (2000).
31. Zhu, Z. et al. PI3K is negatively regulated by PIK3IP1, a novel p110 interacting protein. *Biochem Biophys Res Commun* 358, 66-72, doi:10.1016/j.bbrc.2007.04.096 (2007).

32. Delacroix, L. et al. Cell-specific interaction of retinoic acid receptors with target genes in mouse embryonic fibroblasts and embryonic stem cells. *Mol Cell Biol* 30, 231-244, doi:10.1128/MCB.00756-09 MCB.00756-09 [pii] (2010).
33. Sever, R. & Glass, C. K. Signaling by nuclear receptors. *Cold Spring Harb Perspect Biol* 5, a016709, doi:10.1101/cshperspect.a016709a016709 [pii]5/3/a016709 [pii] (2013).
34. Lee, S. E. et al. Retinoid X receptor alpha overexpression alleviates mitochondrial dysfunction-induced insulin resistance through transcriptional regulation of insulin receptor substrate 1. *Mol Cells* 38, 356-361, doi:10.14348/molcells.2015.2280 molcells.2015.2280 [pii] (2015).
35. Amigo, I. & Kowaltowski, A. J. Dietary restriction in cerebral bioenergetics and redox state. *Redox Biol* 2, 296-304, doi:10.1016/j.redox.2013.12.021 S2213-2317(14)00004-4 [pii] (2014).
36. Chakrabarti, M. et al. Molecular Signaling Mechanisms of Natural and Synthetic Retinoids for Inhibition of Pathogenesis in Alzheimer's Disease. *J Alzheimers Dis* 50, 335-352, doi:JAD150450 [pii] 10.3233/JAD-150450 (2015).
37. Choi, B. K. et al. Reduction of ischemia-induced cerebral injury by all-trans-retinoic acid. *Exp Brain Res* 193, 581-589, doi:10.1007/s00221-008-1660-x (2009).
38. Shen, H. et al. 9-Cis-retinoic acid reduces ischemic brain injury in rodents via bone morphogenetic protein. *J Neurosci Res* 87, 545-555, doi:10.1002/jnr.21865 (2009).
39. Fusco, S. & Pani, G. Brain response to calorie restriction. *Cell Mol Life Sci* 70, 3157-3170, doi:10.1007/s00018-012-1223-y (2013).
40. Meynet, O. & Ricci, J. E. Caloric restriction and cancer: molecular mechanisms and clinical implications. *Trends Mol Med* 20, 419-427, doi:10.1016/j.molmed.2014.05.001 S1471-4914(14)00080-X [pii] (2014).
41. Wu, C. W. & Storey, K. B. FoxO3a-mediated activation of stress responsive genes during early torpor in a mammalian hibernator. *Mol Cell Biochem* 390, 185-195, doi:10.1007/s11010-014-1969-7 (2014).
42. van den Berg, M. C. & Burgering, B. M. Integrating opposing signals toward Forkhead box O. *Antioxid Redox Signal* 14, 607-621, doi:10.1089/ars.2010.3415 (2011).
43. Obrochta, K. M., Krois, C. R., Campos, B. & Napoli, J. L. Insulin regulates retinol dehydrogenase expression and all-trans-retinoic acid biosynthesis through FoxO1. *J Biol Chem* 290, 7259-7268, doi:M114.609313 [pii] 10.1074/jbc.M114.609313 (2015).
44. Chiefari, E. et al. HMGA1 is a novel downstream nuclear target of the insulin receptor signaling pathway. *Sci Rep* 2, 251, doi:10.1038/srep00251 (2012).
45. Araya, N. et al. Cooperative interaction of EWS with CREB-binding protein selectively activates hepatocyte nuclear factor 4-mediated transcription. *J Biol Chem* 278, 5427-5432, doi:10.1074/jbc.M210234200 M210234200 [pii] (2003).
46. Daemen, S., Kutmon, M. & Evelo, C. T. A pathway approach to investigate the function and regulation of SREBPs. *Genes Nutr* 8, 289-300, doi:10.1007/s12263-013-0342-x (2013).

47. Yuan, M., Pino, E., Wu, L., Kacergis, M. & Soukas, A. A. Identification of Akt-independent regulation of hepatic lipogenesis by mammalian target of rapamycin (mTOR) complex 2. *J Biol Chem* 287, 29579-29588, doi:10.1074/jbc.M112.386854 M112.386854 [pii] (2012).
48. van der Vos, K. E. & Coffey, P. J. FOXO-binding partners: it takes two to tango. *Oncogene* 27, 2289-2299, doi:10.1038/onc.2008.22 onc200822 [pii] (2008).
49. Robertson, L. T. et al. Protein and Calorie Restriction Contribute Additively to Protection from Renal Ischemia-reperfusion Injury Partly via Leptin Reduction in Male Mice. *J Nutr* 145, 1717-1727, doi:10.3945/jn.114.199380 jn.114.199380 [pii] (2015).
50. Kilkenny, C., Browne, W. J., Cuthill, I. C., Emerson, M. & Altman, D. G. Improving bioscience research reporting: the ARRIVE guidelines for reporting animal research. *PLoS Biol* 8, e1000412, doi:10.1371/journal.pbio.1000412 (2010).
51. He, X. et al. PIK3IP1, a negative regulator of PI3K, suppresses the development of hepatocellular carcinoma. *Cancer Res* 68, 5591-5598, doi:10.1158/0008-5472.CAN-08-0025 (2008).
52. Green, G. H. & Diggle, P. J. On the operational characteristics of the Benjamini and Hochberg False Discovery Rate procedure. *Stat Appl Genet Mol Biol* 6, Article27, doi:10.2202/1544-6115.1302 (2007).

SUPPLEMENTARY DATA

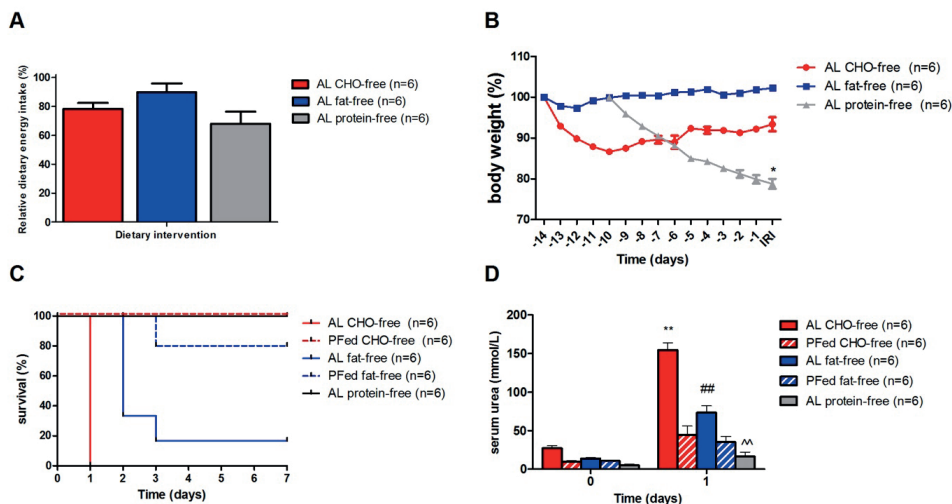


Figure S1. Effects on food intake, body weight and survival by macronutrient free diets and effects on kidney function upon subsequent renal ischemia-reperfusion injury. (A) Relative to their control food intake during the 7-day acclimatization period, mice consumed (cumulatively during the whole intervention period) 21.7% less of the CHO-free diet, 10.1% of the fat-free diet and 32.7% of the protein-free diet. (B) Body weight of mice fed a CHO-free diet decreased during the 14-day period with 6.7%, while mice on a 14-day fat-free diet showed an increase in body weight with 2.3%. Mice fed a protein-free diet for 10 days lost more than 20% of their body weight on day 10. Because of this substantial loss of body weight, the protein-free diet was limited to a period of 10 days or less in the subsequent ischemia-reperfusion experiments. (C) Mouse mortality rates upon renal ischemia-reperfusion injury after both the CHO- and fat-free diet were significantly higher than their PFed controls ($P < 0.05$). Mice fed a protein-free diet for 10 days showed a 100% survival following renal IRI. (D) Kidney function as determined by serum urea levels on day 1 after induction of renal IRI were significantly worsened in both the CHO-free ($P < 0.05$) and fat-free ($P < 0.05$) groups compared to PFed groups. Mice fed a protein-free diet showed lower serum urea levels one day after induction of IRI compared with CHO-free ($P < 0.01$), the PFed CHO-free ($P < 0.05$), the fat-free ($P < 0.01$) and the PFed fat-free group ($P < 0.05$). * = $P < 0.05$ compared to AL CHO-free diet on day 0. ## = $P < 0.05$ compared to AL fat-free diet on day 0. ^^ = $P < 0.05$ compared to AL protein-free diet on day 0.

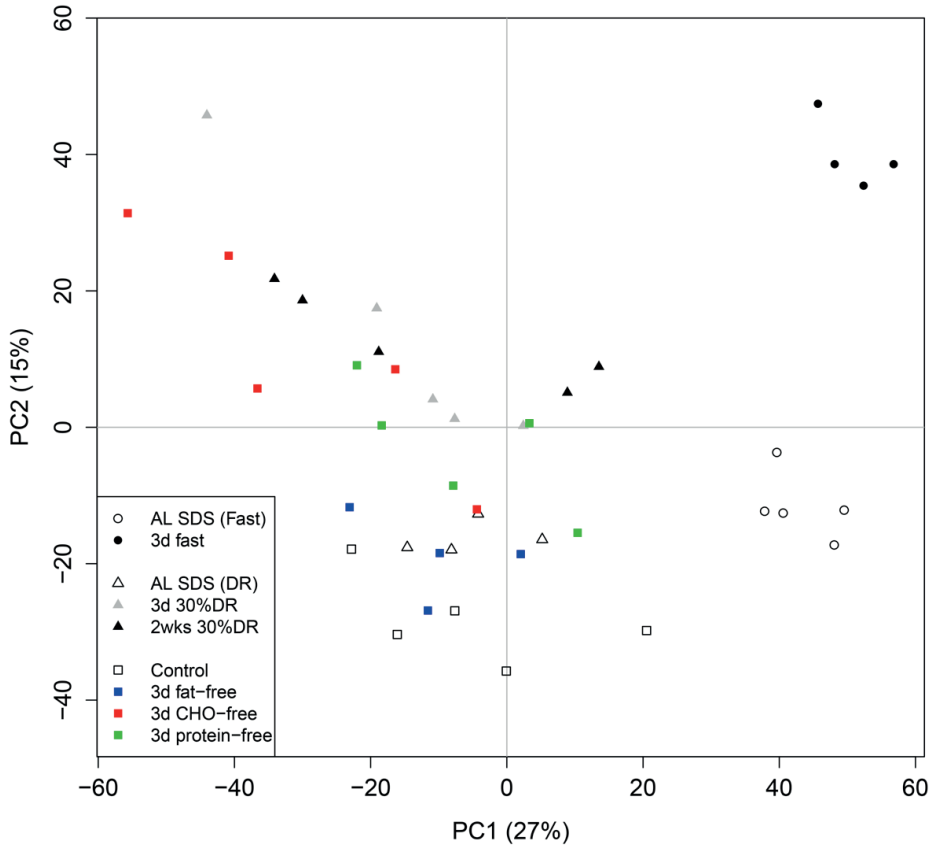


Figure S2. PCA of all probes on the microarray chip. This unbiased analysis shows the largest source of variability, PC1, is related to the date of hybridization. The 3-day fasting group and their corresponding control group were hybridized on a different date than the other groups. This result made the joint analysis of all datasets impracticable. PC2 explains only 15% of the variability, and it is related to the dietary interventions compared to the control samples. AL SDS (Fast)= control group of the 3-day fasting mice. AL SDS (DR) = control group of the 2 weeks 30% DR mice. Control = control group of the macronutrient-free diets.

4

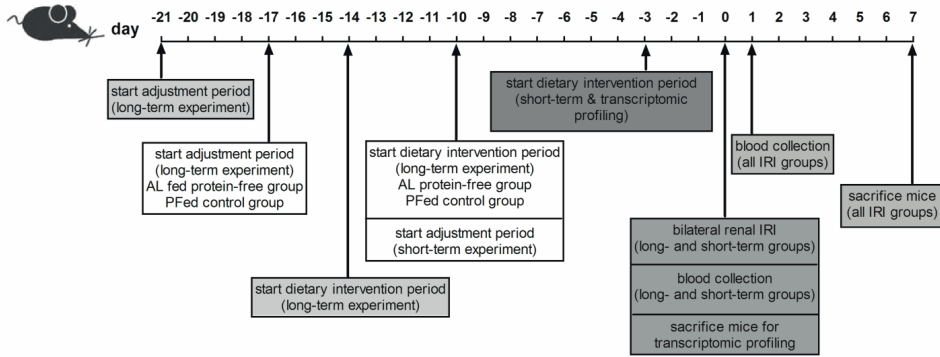


Figure S3. Schematic overview of the experimental design. After an acclimation period for all groups of 7 days on SDS chow, the long-term experiments started with diets given for either 10- or 14 days. At day -3 relative to induction of ischemia-reperfusion injury (IRI) the short-term dietary intervention and gene expression profiling experiments were started. At day 0, animals used for transcriptomic profiling were sacrificed for further analyses. In the other groups, blood collection was followed by induction of bilateral renal IRI for 37 minutes and collection of blood one day later. Mice were followed until day 7 after IRI, after which they were sacrificed.

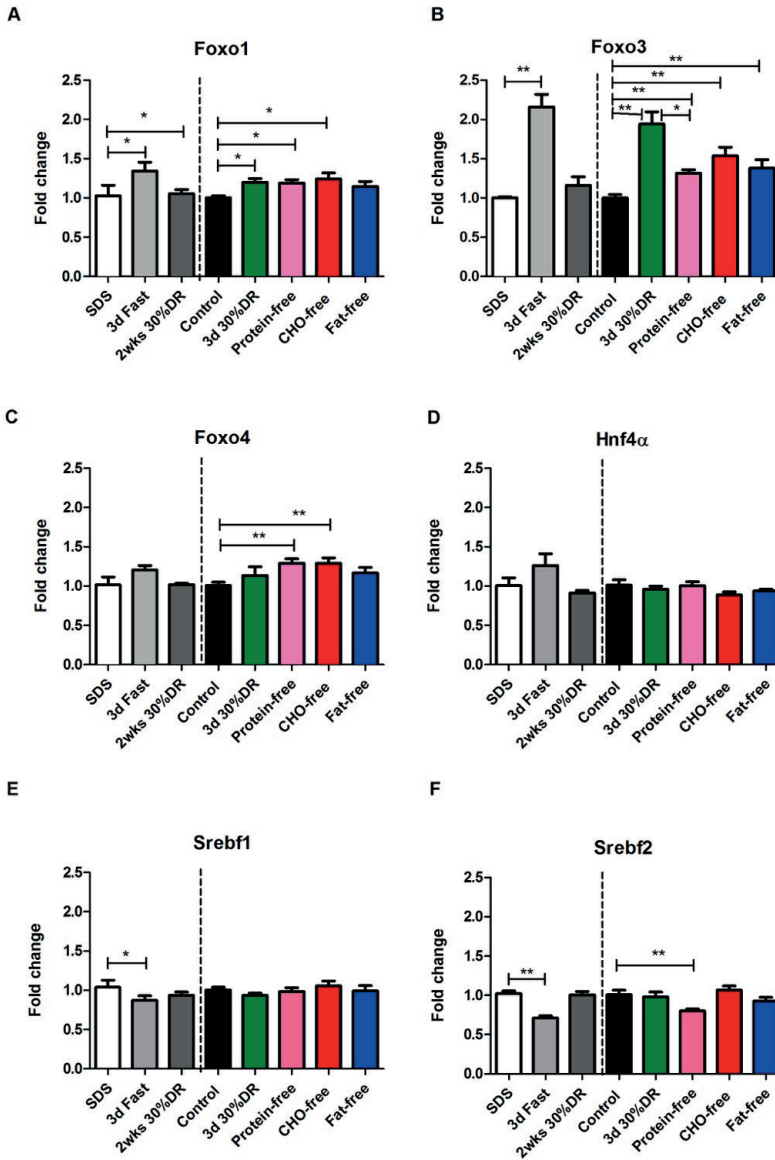


Figure S4. PCR data of mRNA expression levels of genes related to significantly regulated transcription factors. (A) Foxo1 was significantly higher after all diets except the fat-free diet. (B) Foxo3 showed significant upregulation after all diets except the 2 weeks 30% DR. (C) FOXO4 expression levels were significant higher after 3 days of 30% DR and 3-days of a CHO-free diet. (D) Hnf4α was not significantly regulated after any of the dietary interventions. (E) Srebf1 was downregulated after 3 days of fasting, while (F) Srebf2 was significantly downregulated after both 3 days of fasting and a 3-day protein-free diet. FOXO = forkhead box O; Hnf4α = hepatocyte nuclear factor 4-alpha; Srebf = sterol regulatory element-binding transcription factor 1. * = $P < 0.05$; ** = $P < 0.01$.

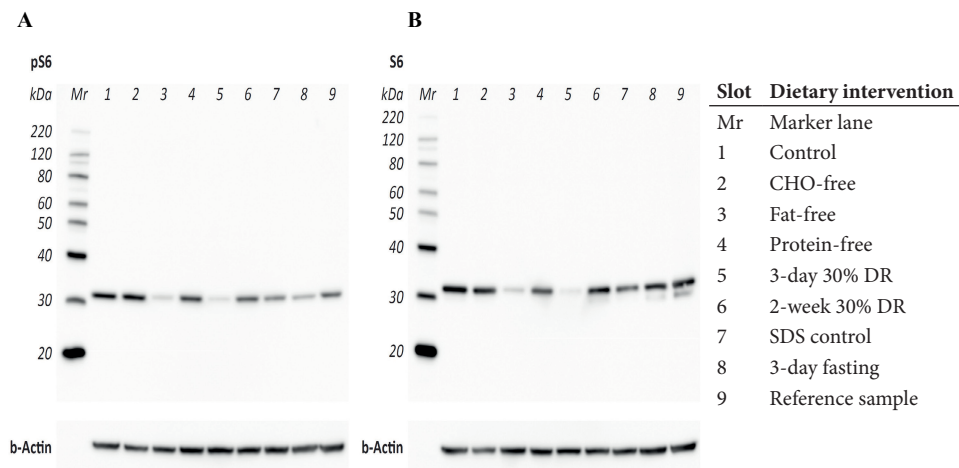


Figure S5. Representative Western blots of kidney extracts for both phosphorylated (A) and total (B) ribosomal protein S6 with β -actin as a loading control used for the relative quantification in Figure 4. The depicted exemplary blots show a full set of kidney extracts from each indicated diet group (lanes 1 – 8) next to a marker lane (lane Mr) and a reference sample (lane 9). In total, four such sets of Western blots were generated, each with four unique complete series for each diet group. For interblot comparison the exact same amount of the reference sample (lane 9) was loaded on each blot. The relative phosphorylation ratios depicted in Figure 4. are derived from the quantified signal of the main band in each lane, subtracted with background and corrected for both the sample dependent β -actin signal and the blot dependent signal of the reference sample.

Table S1. List of genes corresponding to the DEPS found in common between all dietary interventions combined

Affymetrix ID	Entrez Gene ID	Symbol	Gene Name	Log Ratio
1415802_PM_at	20501	SLC16A1	solute carrier family 16 (monocarboxylate transporter), member 1	-0,488
1415828_PM_a_at	28146	SERP1	stress-associated endoplasmic reticulum protein 1	-0,639
1416414_PM_at	100952	EMILIN1	elastin microfibril interfacer 1	-0,623
1416630_PM_at	15903	ID3	inhibitor of DNA binding 3, dominant negative helix-loop-helix protein	1,008
1417150_PM_at	15567	SLC6A4	solute carrier family 6 (neurotransmitter transporter), member 4	0,537
1418591_PM_at	58233	DNAJA4	DnaJ (Hsp40) homolog, subfamily A, member 4	-0,709
1419040_PM_at	56448	Cyp2d22	cytochrome P450, family 2, subfamily d, polypeptide 22	1,033
1422974_PM_at	23959	NT5E	5'-nucleotidase, ecto (CD73)	-1,037
1423392_PM_at	29876	CLIC4	chloride intracellular channel 4	-0,782
1423627_PM_at	18104	NQO1	NAD(P)H dehydrogenase, quinone 1	1,024
1424618_PM_at	15445	HPD	4-hydroxyphenylpyruvate dioxygenase	1,064
1424983_PM_a_at	78832	CACUL1	CDK2-associated, cullin domain 1	-0,746
1426568_PM_at	117591	SLC2A9	solute carrier family 2 (facilitated glucose transporter), member 9	0,684
1426896_PM_at	59057	ZNF24	zinc finger protein 24	-0,495
1427364_PM_a_at	18263	ODC1	ornithine decarboxylase 1	-0,975
1427931_PM_s_at	216134	PDXK	pyridoxal (pyridoxine, vitamin B6) kinase	1,251
1428332_PM_at	216505	PIK3IP1	phosphoinositide-3-kinase interacting protein 1	0,828
1433557_PM_at	52609	CBX7	chromobox homolog 7	0,618
1434437_PM_x_at	20135	RRM2	ribonucleotide reductase M2	-0,128
1434974_PM_at	228026	PDK1	pyruvate dehydrogenase kinase, isozyme 1	0,683
1436893_PM_a_at	57438	MARCH7	membrane-associated ring finger (C3HC4) 7, E3 ubiquitin protein ligase	0,585
1438211_PM_s_at	13170	DBP	D site of albumin promoter (albumin D-box) binding protein	1,768
1439797_PM_at	19015	PPARD	peroxisome proliferator-activated receptor delta	-0,838
1443870_PM_at	239273	ABCC4	ATP-binding cassette, sub-family C (CFTR/MRP), member 4	1,063
1449183_PM_at	12846	COMT	catechol-O-methyltransferase	-0,944
1449460_PM_at	142688	ASB13	ankyrin repeat and SOCS box containing 13	-0,686
1449848_PM_at	14675	GNA14	guanine nucleotide binding protein (G protein), alpha 14	-0,832

Table S1. (continued)

Affymetrix ID	Entrez Gene ID	Symbol	Gene Name	Log Ratio
1451122_PM_at	319554	IDI1	isopentenyl-diphosphate delta isomerase 1	-1,173
1452264_PM_at	209039	TNS2	tensin 2	0,757
1454709_PM_at	100201	TMEM64	transmembrane protein 64	-0,867
1455293_PM_at	235497	LEO1	LEO1 homolog, Paf1/RNA polymerase II complex component	-0,727
1455343_PM_at	233765	PLEKHA7	pleckstrin homology domain containing, family A member 7	0,922
1455393_PM_at	12870	CP	ceruloplasmin (ferroxidase)	1,037
1455490_PM_at	18703	PIGR	polymeric immunoglobulin receptor	0,924
1457689_PM_at	319934	SBF2	SET binding factor 2	0,761
1458176_PM_at	18628	PER3	period circadian clock 3	1,072
1460239_PM_at	66109	TSPAN13	tetraspanin 13	-0,925

The Affymetrix probe sets, their corresponding Entrez Gene ID, symbol, gene name and log ratio are depicted in ascending order of the Affymetrix probe set. Only the probe sets with a corresponding gene ID are listed, therefore probe sets corresponding to the same gene ID are excluded. Log Ratio = log transformed fold change.

Table S2. Top 10 overrepresented canonical pathways after fasting, dietary restriction and macronutrient free diets individually ranked by their $-\log P$ -value

Canonical Pathway	P-value	Genes Ratio
<i>3-day FASTING</i>		
Superpathway Cholesterol Biosynthesis	3.41 ^E -08	14/87 (16.1%)
Cholesterol Biosynthesis I / II / III	2.18 ^E -06	8/40 (20.0%)
LXR / RXR Activation	2.20 ^E -06	27/139 (19.4%)
NRF2-mediated Oxidative Stress Response	6.27 ^E -06	34/195 (17.4%)
LPS/IL-1 Mediated Inhibition of RXR Function	7.46 ^E -06	39/245 (15.9%)
Acute Phase Response Signaling	7.24 ^E -05	30/181 (16.6%)
GADD45 Signaling	1.25 ^E -04	8/24 (33.3%)
AMPK Signaling	1.25 ^E -04	25/180 (13.9%)
VDR/RXR Activation	2.18 ^E -04	17/88 (19.3%)
Xenobiotic Metabolism Signaling	3.00 ^E -04	42/304 (13.8%)
<i>2-week 30% DR</i>		
Circadian Rhythm Signaling	1.41 ^E -05	6/38 (15.8%)
Aldosterone Signaling Epithelial Cells	3.20 ^E -05	11/168 (6.5%)
Guanosine Nucleotides Degradation II	7.85 ^E -04	3/22 (13.6%)
Urate Biosynthesis	1.01 ^E -03	3/22 (13.6%)
Phenylalanine Degradation IV	1.27 ^E -03	3/39 (7.7%)
2-ketoglutarate Dehydrogenase Complex	1.48 ^E -03	2/9 (22.2%)
Adenosine Nucleotides Degradation II	1.57 ^E -03	3/26 (11.5%)
NRF2-mediated Oxidative Stress Response	2.39 ^E -03	9/195 (4.6%)
Protein Ubiquitination Pathway	2.63 ^E -03	11/270 (4.1%)
Purine Nucleotides Degradation II	2.71 ^E -03	3/35 (8.6%)
<i>3-day PROTEIN-FREE</i>		
Intrinsic Prothrombin Activation Pathway	5.18 ^E -04	4/37 (10.8%)
Superpathway Cholesterol Biosynthesis	6.79 ^E -04	4/87 (4.6%)
LPS/IL-1 Mediated Inhibition of RXR Function	8.81 ^E -04	10/245 (4.1%)
Mevalonate Pathway I	9.87 ^E -04	3/29 (10.3%)
Creatine-phosphate Biosynthesis	1.77 ^E -03	2/9 (22.2%)
Superpathway of Geranylgeranyl	2.02 ^E -03	3/37 (8.1%)
PXR/RXR Activation	2.12 ^E -03	5/92 (5.4%)
GADD45 Signaling	2.35 ^E -03	3/24 (12.5%)
Tryptophan Degradation	4.84 ^E -03	2/18 (11.1%)
Nicotine Degradation II	9.33 ^E -03	4/85 (4.7%)

Table S2. (continued)

Canonical Pathway	P-value	Genes Ratio
<i>3-day CARBOHYDRATE-FREE</i>		
Histamine Degradation	9.52 ^E -05	6/29 (20.7%)
Pyrimidine Deoxygenase De Novo Biosynthesis I	1.57 ^E -04	6/34 (17.6%)
Superpathway of Serine and Glycine Biosynthesis I	2.57 ^E -04	4/18 (22.2%)
Glycolysis I	6.98 ^E -04	7/41 (17.1%)
NRF2-mediated Oxidative Stress Response	8.17 ^E -04	24/195 (12.3%)
Cholesterol Biosynthesis I / II / III	1.04 ^E -03	5/40 (12.5%)
Colanic Acid Building Blocks Biosynthesis	1.52 ^E -03	5/36 (13.9%)
Fatty Acid β -oxidation	1.52 ^E -03	5/21 (23.8%)
Protein Ubiquitination Pathway	1.58 ^E -03	30/270 (11.1%)
Folate Transformations I	1.84 ^E -03	4/32 (12.5%)
<i>3-day 30% DR</i>		
Dopamine Degradation	1.08 ^E -04	5/35 (14.3%)
Aryl Hydrocarbon Receptor Signaling	1.37 ^E -04	9/140 (6.4%)
LPS/IL-1 Mediated Inhibition of RXR Function	2.48 ^E -04	11/221 (5.0%)
PXR/RXR Activation	2.63 ^E -04	6/65 (9.2%)
Circadian Rhythm Signaling	1.03 ^E -03	4/33 (12.1%)
NRF2-mediated Oxidative Stress Response	1.42 ^E -03	9/193 (4.7%)
Tyrosine Degradation I	1.82 ^E -03	2/5 (40.0%)
Histamine Degradation	2.09 ^E -03	3/19 (15.8%)
Noradrenaline and Adrenaline Degradation	2.14 ^E -03	4/40 (10.0%)
Adipogenesis Pathway	2.52 ^E -03	7/134 (5.2%)

Top 10 overrepresented pathways after dietary restriction and macronutrient free diets, with the exception of the 3-day fat-free diet that showed no differentially expressed probe sets. Analysis revealed no pathways regulated in common between the three protective diets. Furthermore, no pathways were oppositely regulated in the non-protective CHO-free diet. Genes ratio is the number and percentage of genes differentially expressed in ratio to the total number of genes involved in the pathway.

Table S3. Top 10 overrepresented canonical pathways after the meta-analysis including fasting, dietary restriction and macronutrient free diets ranked by their $-\log P$ -value*Meta-analysis II (including 3-day 30% DR)*

Canonical Pathway	Pathway Category	P-value	Genes Ratio	Z-score
LPS/IL-1 Mediated Inhibition of RXR Function	Nuclear Receptor Signaling	4.68 ^E -05	10/221 (4.5%)	N/A
NRF2-mediated Oxidative Stress Response	Cellular Stress and Injury	8.92 ^E -05	9/193 (4.7%)	N/A
PXR/RXR Activation	Nuclear Receptor Signaling	3.59 ^E -04	5/65 (7.7%)	N/A
Noradrenaline and Adrenaline Degradation	Degradation/Utilization/ Assimilation; Hormones	5.25 ^E -04	4/40 (10.0%)	N/A
Aryl Hydrocarbon Receptor Signaling	Cell Cycle Regulation; Apoptosis; Xenobiotic Metabolism, Nuclear Receptor Signaling	2.08 ^E -03	6/140 (4.3%)	N/A
Superpathway of Cholesterol Biosynthesis	Fatty Acids and Lipids Biosynthesis, Sterol Biosynthesis	2.23 ^E -03	3/28 (10.7%)	N/A
Glutathione-mediated Detoxification	Degradation/Utilization/ Assimilation; Detoxification	2.47 ^E -03	3/29 (10.3%)	N/A
Circadian Rhythm Signaling	Neurotransmitters and Other Nervous System Signaling	3.59 ^E -03	3/33 (9.1%)	N/A
Retinoate Biosynthesis I	Vitamin (A) Biosynthesis; Cofactors, Prosthetic Groups and Electron Carriers Biosynthesis	3.91 ^E -03	3/34 (8.8%)	N/A
Dopamine Degradation	Degradation/Utilization/ Assimilation; Amines and Polyamines Degradation	4.25 ^E -03	3/35 (8.6%)	N/A

The top 10 overrepresented pathways derived from the 279 DEPS in common between 3-days of fasting, 2 weeks 30% DR, 3 days of a protein-free and 3 days of a 30% DR diet. These pathways are mostly involved in regulation of nuclear receptor signalling (5 out of 10), biosynthesis signalling (2 out of 10) and cellular stress and injury (2 out of 10).

Table S4. Composition and energy content of the individual diets

Ingredient	Control	SDS-CRMP	Carbohydrate-free	Fat-free	Protein-free
Crude protein* (%/g)		16.4			
Casein, lactic (%/g)	20.0		99.2	31.3	0
Total kcal/g	3.8	3.3	3.4	3.5	3.8
Protein (g/kg)	179.0	183.5	887.9	280.1	0.0
Carbohydrate (g/kg)	710.0	574.0	1.0	710.0	889.0
Fat (g/kg)	45.0	33.6	45.0	0.0	45.0
Fiber (g/kg)	50.0	24.8	50.0	50.0	50.0
Protein (g%)	17.0	22.0	77.2	24.9	0
Carbohydrate (g%)	67.3	68.9	0.1	63.1	86.2
Fat (g%)	4.3	9.1	3.9	0.0	4.4
Fiber (g%)	4.7	4.2	4.3	4.4	4.8
Protein (kcal/kg)	716	734	3551	1121	0
Carbohydrate (kcal/kg)	2840	2296	4	2840	3556
Fat (kcal/kg)	405	303	405	0	405
Protein (kcal%)	18	22	90	28	0
Carbohydrate (kcal%)	72	69	0	72	90
Fat (kcal%)	10	9	10	0	10

*protein sources: wheat, barley, soya, maize, potato protein

Table S5. Overview of the dietary interventions, the groups and numbers of mice used for phenotypical and transcriptional endpoints

Dietary Intervention	Model	Duration (days)	Number of mice	Follow-up (days)	Parameters measured
<i>(A) Overview IRI long-term experiments</i>					
Control SDS	C57BL/6	14	10	7	Survival, body weight, kidney function
Control	C57BL/6	14	12	7	Survival, body weight, kidney function
Fat-free	C57BL/6	14	6	7	Survival, body weight, kidney function
Pair-fed fat-free	C57BL/6	14	6	7	Survival, body weight, kidney function
Carbohydrate-free	C57BL/6	14	6	1	Survival, body weight, kidney function
Pair-fed carbohydrate-free	C57BL/6	14	6	7	Survival, body weight, kidney function
Protein-free	C57BL/6	10	6	7	Survival, body weight, kidney function
<i>(B) Overview IRI short-term experiments</i>					
Control	C57BL/6	3	4	7	Survival, body weight, kidney function
Protein-free	C57BL/6	3	4	7	Survival, body weight, kidney function
AL Control (control to 3-day 30% DR)	C57BL/6	3	4	7	Survival, body weight, kidney function
3 days 30% DR	C57BL/6	3	6	7	Survival, body weight, kidney function
<i>(C) Overview of gene transcription experiments</i>					
Control SDS (control 2-week 30% DR)	C57BL/6	14	4	0	Gene expression profiling in kidney tissue
2-week 30% DR	C57BL/6	14	5	0	Gene expression profiling in kidney tissue
Control SDS (control 3-day fasting)	C57BL/6	3	5	0	Gene expression profiling in kidney tissue
3-day fasting	C57BL/6	3	4	0	Gene expression profiling in kidney tissue
Control	C57BL/6	3	5	0	Gene expression profiling in kidney tissue
Protein-free	C57BL/6	3	5	0	Gene expression profiling in kidney tissue
Fat-free	C57BL/6	3	4	0	Gene expression profiling in kidney tissue
Carbohydrate-free	C57BL/6	3	5	0	Gene expression profiling in kidney tissue

CHAPTER 5

THE ROLE OF PROTEIN AND ESSENTIAL AMINO ACIDS IN THE PROTECTION AGAINST HEPATIC ISCHEMIA-REPERFUSION INJURY IN MICE

Franny Jongbloed*, Tanja C. Saat*, Sandra van den Engel, Jeroen L.A. Pennings, Conny T. van Oostrom, Jan N.M. IJzermans, Harry van Steeg, Martijn E.T. Dollé, Ron W.F. de Bruin

* Authors contributed equally

Manuscript

ABSTRACT

Ischemia-reperfusion injury (IRI) is inevitable during major liver surgery and liver transplantation leading to oxidative stress. Preoperative short-term 30% dietary restriction (DR), 3-days of fasting and 3-days of a protein-free diet protect against IRI. Here, we further disentangled the role of essential amino acids on the effects of DR on liver IRI. Male C57BL/6 mice were randomized to preoperative ad libitum control food or 3 days of 30% DR, methionine-free, leucine-free or tryptophan-free diet for three days. Liver IRI was induced by partial occlusion of the blood flow (70%) of the liver for 75 minutes. Food intake and body weight were monitored until postoperative day 1. Hepatic damage was measured biochemically and histologically at six and 24 hours after IRI. After completing each diet, liver gene expression profiles were determined by microarray analysis. All amino acid free diets resulted in body weight loss prior to IRI. Liver IRI was already significantly decreased by both the leucine- and tryptophan-free diets at six hours after IRI, and by the methionine-free diet at 24 hours. Microarray analysis showed similar transcriptomic responses in all amino acid-free diets, yet with a lower magnitude in the methionine-free diet. Detailed analysis of overlapping genes suggested a role for pathways involved in nuclear receptor signaling, stress resistance and cell cycle regulation via transcription factors NRF2, FOXM1, SREBF2 and SMARCB1. A short-term preoperative tryptophan-free, leucine-free and methionine-free diet protect against hepatic IRI similar to a protein-free diet, through a network of pathways potentially activated by NRF2, FOXM1, SREBF2 and SMARCB1.

INTRODUCTION

Dietary restriction (DR) is defined as a reduction in food intake without malnutrition¹. Long-term DR is known to extend lifespan¹, increase health span² and improve resistance to multiple stressors^{1,3} in a wide variety of organisms⁴⁻⁶. Although the effect of DR on lifespan in humans is not known, studies show a favorable impact on metabolic parameters associated with long-term health⁷⁻⁹. In addition, previous studies showed that two weeks of 30% DR and three days of fasting increase stress resistance and protect against oxidative stress induced by ischemia-reperfusion injury (IRI) in mice^{1,10}.

During major liver surgery and liver transplantation IRI is inevitable and a risk factor for complications including primary graft dysfunction and primary non-function, thereby causing morbidity and mortality¹¹⁻¹³. Cessation of the blood flow (ischemia) leads to hypoxia, nutrient deprivation and activation of anaerobic metabolic system¹³. Reperfusion of the liver promotes the activation of an inflammatory response, causing further cellular damage and the generation of reactive oxygen species (ROS)¹³. Therefore, counteracting the adverse effects of IRI could improve the outcome after liver transplantation and liver resection. Unfortunately, at this moment no effective treatment for IRI is available.

Whether the protection by short-term DR is based on a reduction of calories or based on the reduction of specific nutrients is not yet completely unraveled. Also, the search for the underlying mechanisms of DR is still ongoing. In mice, liquid glucose supplementation did not interfere with the protective effect of three days of fasting against renal IRI¹⁴. In fruit flies, long-term protein restriction contributed more to extension of the life span compared to the reduction of carbohydrates or fat^{15, 16}. We previously investigated the role of specific macronutrients by unrestricted feeding of protein-, carbohydrate-, and fat-free diets in inducing resistance against renal IRI. We showed that three days of a protein- but not a carbohydrate- or a fat-free diet, before the induction of renal IRI improved survival and kidney function similarly as DR and fasting¹⁷. These results point towards a role for specific nutrients in the protective effect against renal IRI.

In the present study, we investigated the role of preoperative essential amino acid (EAA)-free diets by unrestricted feeding of methionine (Met)-free, leucine (Leu)-free and tryptophan (Trp)-free diets in reducing oxidative damage in the liver, and analyzed the transcriptomic response of the liver to these diets.

RESULTS

Single EAA deprivation protects against hepatic IRI

To disentangle the role of single EAA in the protection against hepatic IRI, mice were administered a Met-free, Leu-free or Trp-free diet for three days. The results were compared with a control diet and diets that are known to either protect or not protect against IRI¹⁷. We have demonstrated that three days of a protein-free diet induces protection against renal IRI, while others also showed these results in other IRI models, including hepatic IRI¹. On the contrary, three days of 30% DR does not induce resistance against renal IRI¹⁷, which makes it a control group for reduced calorie intake and concomitant body weight loss observed during feeding of EAA free diets.

Mice fed a protein- or EAA-free diet during three days restricted themselves on calorie intake (Figure 1A). Mice fed the Met-free diet restricted food intake by 44%, while the Leu-free diet resulted in a restriction of 45%. A Trp-diet resulted in the smallest decrease in calorie intake, namely an average of 9% fewer calories than mice fed a control diet.

Mice fed three days of a protein-free diet lost on average 9.8% of their body weight, while mice fed the non-protective 3-days of 30% DR showed a similar pattern in body weight loss (Figure 1B). Mice fed a single EAA-free diet also lost body weight: a Met-free diet resulted in 9.5% body weight loss, a Leu-free diet 6.2% and a Trp-free diet 8.5% (Figure 1C). After induction of hepatic IRI, mice on a protein-free diet resumed intake of the control food within 24 hours and showed no further weight loss, while ad libitum fed mice or mice restricted for 30% during three days lost weight after surgery. Mice fed the EAA-free diet resumed food intake postoperatively and stabilized their body weight (Figure 1C).

Serum levels of liver enzymes ALT (Figure 2A) and LDH (Figure 2B) were significantly lower in the Leu-free and Trp-free groups than in the control group at six and 24 hours postoperatively. At 24 hours after hepatic IRI, all EAA-free diets showed significantly lower liver enzymes (Figure 2A/B). Histological analysis of the livers supports these findings. At six hours after reperfusion, the percentage of hemorrhagic necrosis was significantly lower in the Leu-free and Trp-free diets than in the control group (Figure 2C). At 24 hours postoperatively, the percentage of necrosis was increased compared to six hours, but still a significant lower percentage of necrosis was seen in the Leu-free and Met-free diet, while the reduction did not reach significance in the Trp-free diet. The number of neutrophils, as a marker for the acute inflammatory response in the liver, was significantly higher in the Leu-free and Trp-free diets than in the control group at six hours (Figure 2D), despite the lower percentage of hemorrhagic necrosis.

Livers from animals fed the non-protective 3-days of 30% DR showed a significantly increased number of neutrophils, suggesting an ongoing inflammatory response after IRI in this group (Figure 2D).

Taken together, deprivation of essential amino acids methionine, leucine and tryptophan for three days induces protection against liver IRI similar to a 3-day protein-free diet independent of preoperative body weight loss and voluntary DR. The beneficial effects of Leu and Trp are more pronounced at six hours after IRI while the effects of all EAA-free diets are seen at 24 hours postoperatively.

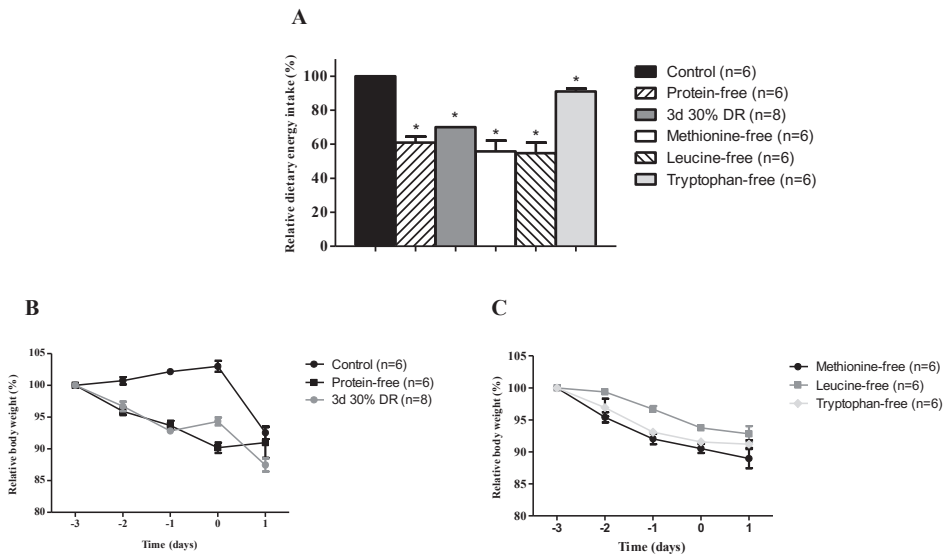


Figure 1. Food intake and body weight. (A) Relative dietary energy intake during the 3-day intervention. Mice fed a tryptophan-free consumed on average 9% fewer calories than mice fed the control diet. Mice fed a methionine-free diet had 44.2% fewer calories, while mice on a leucine-free diet consumed 45.2% fewer calories than mice fed the control diet. In comparison, mice fed a protein-free diet ate 39.1% fewer calories. (B+C). The 3-day nutritional interventions started at day -3 and hepatic IRI was induced at day 0, after which all mice received control chow. During the dietary intervention all mice, except the control chow fed group, showed a decrease in body weight. Postoperative day 1, mice that had been fed an essential amino acid (EAA)-free diet lost less body weight compared to the control mice. Besides that, the protein-free mice gained weight.

5

Transcriptional responses after a methionine-, leucine- and tryptophan-free diet are highly overlapping

To examine transcriptome responses amongst the different EAA-free diets and their controls, a principal component analysis (PCA) was made based on all probe sets in the microarray data (Figure 3A).

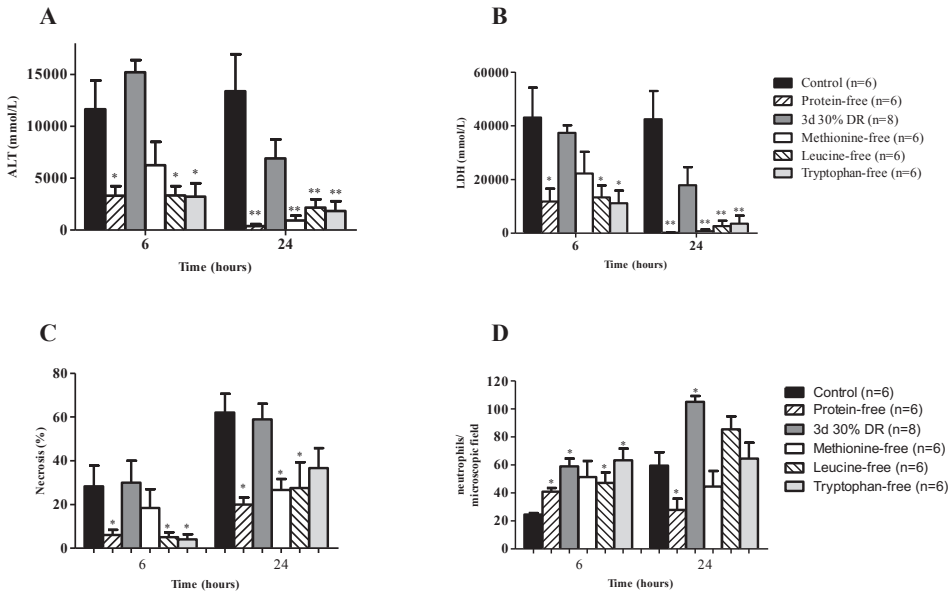


Figure 2. Essential amino acid free diets reduce liver injury. (A) Serum concentration of the liver-specific enzyme alanine aminotransferase (ALT), indicative of liver damage, were significantly lower levels at six and 24 hours after IRI in mice fed a protein-free or amino acid-free diet. * $P < 0.05$, ** $P < 0.01$ versus the control group at the same time point. (B) Twenty-four hours after IRI, serum concentration of lactate dehydrogenase (LDH), indicative of tissue breakdown, was significant lower in mice on a protein-free or amino acid-free diet. * $P < 0.05$, ** $P < 0.01$ versus the control group at the same time point. (C) Six hours after reperfusion, livers from mice fed leucine-free and tryptophan-free diets showed less hemorrhagic necrosis compared to the control group. Twenty-four hours after reperfusion the protein-, leucine- and methionine-free diets induced significantly less damage compared to the control group. * $P < 0.05$, ** $P < 0.01$ versus the control group. (D) At 24 hours post-reperfusion, the protein-free diet had a lower number of neutrophils than the control group, while the 30% DR remained with a significantly higher neutrophil count. * $P < 0.05$, versus the control group.

In this unbiased PCA plot, PC1 explains 15% and PC2 explains 13% of the total variance of the probe sets. Examination of the PCA showed distinct separation of the mice in the control group and in the Met-free group, with uniformity within these groups along PC2. However, the Met-free cluster was grouped closely on PC1 with the cluster of control mice. In contrast, the Leu-free and Trp-free groups showed a high degree of overlap, differentiating as a whole from the former two groups on PC1 and with an intermediate response on PC2 (Figure 3A). A dendrogram, based on the unbiased hierarchical clustering of all mice, showed two distinct clusters of the control group and the Met-free group, which were connected higher up the dendrogram (Figure 3B). The Leu-free and Trp-free groups had a similar hierarchy, with no distinctive clustering between the two groups.

The transcriptomic response was further analyzed by determining the differentially expressed probe sets (DEPS) after each dietary intervention compared to the control group. The Met-free diet induced the smallest number of DEPS, namely 572 with 348 upregulated and 224 downregulated DEPS. The Leu-free diet resulted in 933 DEPS, of which 476 were upregulated and 457 downregulated. The Trp-free diet induced 1,155 DEPS of which 579 were upregulated and 576 were downregulated. To analyze the overlap between the groups, a Venn diagram was made with these DEPS, and 137 genes overlapped between all three diets (Figure 3C). The DEPS of the Leu-free and Trp-free diets showed the most similarity, with 603 genes present in both diets, comprising 65% of the DEPS induced by the Leu-free diet and 52% by the Trp-free diet. Of all differentially regulated genes in common between the Leu-free and Trp-free diets, 99% had the same directionality (results not shown). The Met-free induced the highest percentage of unique DEPS, namely 334 out of the 573 (58%). However, the directionality pattern of all differentially regulated genes reached an 84% agreement between Met-free and Leu-free diet and an 86% agreement between Met-free and Trp-free. Despite the stronger response induced by the Leu-free and Trp-free diets, there is a high overlap in transcriptional responses between all three EAA-free diets.

Essential amino acid-free diets regulate the cellular stress response, nuclear signaling and cell cycle

Subsequent unbiased analysis of the gene expression profiles was performed via pathway analysis and upstream transcription factor analysis. Analyses of differentially regulated pathways by the EAA-free diets focused on canonical pathways with a positive or negative z-score, which indicates a significant activation or inhibition of the pathway, respectively. Three days of Met-free diet resulted in 11 regulated pathways, of which eight activated and three inhibited. The most prominent activated pathways were involved in cellular stress and injury, cell cycle regulation and growth signaling. Inhibition occurred mainly of the nuclear receptor signaling pathway (Table 1A). The Leu-free diet induced 29 differentially regulated pathways, of which 21 activated and eight inhibited (Table 1B). These pathways

represented mainly an activation of the cellular immune response and intracellular and second messenger signaling, in combination with an inhibition of nuclear receptor signaling and cellular stress and injury. Analysis of the Trp-free diet revealed 15 pathways, including eight activated and seven inhibited pathways. The activated pathways were mostly involved in cellular immune responses and cell cycle regulation, while inhibited pathways included nuclear receptor signaling and cancer pathways (Table 1C).

Comparison of overlapping pathways revealed that five out of the 11 pathways regulated by the Met-free diet were also regulated by the Leu-free diet, and four out of the 11 pathways by the Trp-free diet, all with similar directionalities. These overlapping pathways were amongst the highest regulated pathways including activation of NRF2-mediated stress response and G2/M Checkpoint Regulation pathways, and inhibition of the LPS/IL-1 mediated inhibition of RXR Function as well as the LXR/RXR activation pathway. In addition to the pathways in common between the three EAA-free diets, the Leu-free and Trp-free diets had another four pathways in common of which two had the same directionality, namely *Calcium-induced T-lymphocyte apoptosis* and *Sphingosine-1-phosphate signaling*.

Analysis of the upstream transcription factors (TFs) activated or inhibited by the EAA-free diets resulted in a list of factors depicted in Table S1. The highest activated TF by the Met-free diet was NFE2L2, *i.e.* NRF2, followed by ATF4 and SMARCB1. NFE2L2 and SMARCB1 were also significantly activated by the Leu-free and Trp-free diets, while ATF4 met a significant z-score in the Trp-free diet and showed a trend towards significance in the Leu-free diet (1.838). The strongest inhibited TF by the Met-free diet was SREBF2, followed by FOXM1 and MYBL2. Both SREBF2 and FOXM1 were also significantly inhibited by the Leu- and Trp-free diets, while MYBL2 only reached significance in the after the Leu-free (-2.000) and not in the Trp-free diet (-1.633) (Table 2). Of the 18 significantly regulated TFs by the Met-free diet, 14 and 13 TFs were also regulated by the Leu-free and Trp-free diet, respectively. All of these TFs showed the same directionality in all three EAA-free diets.

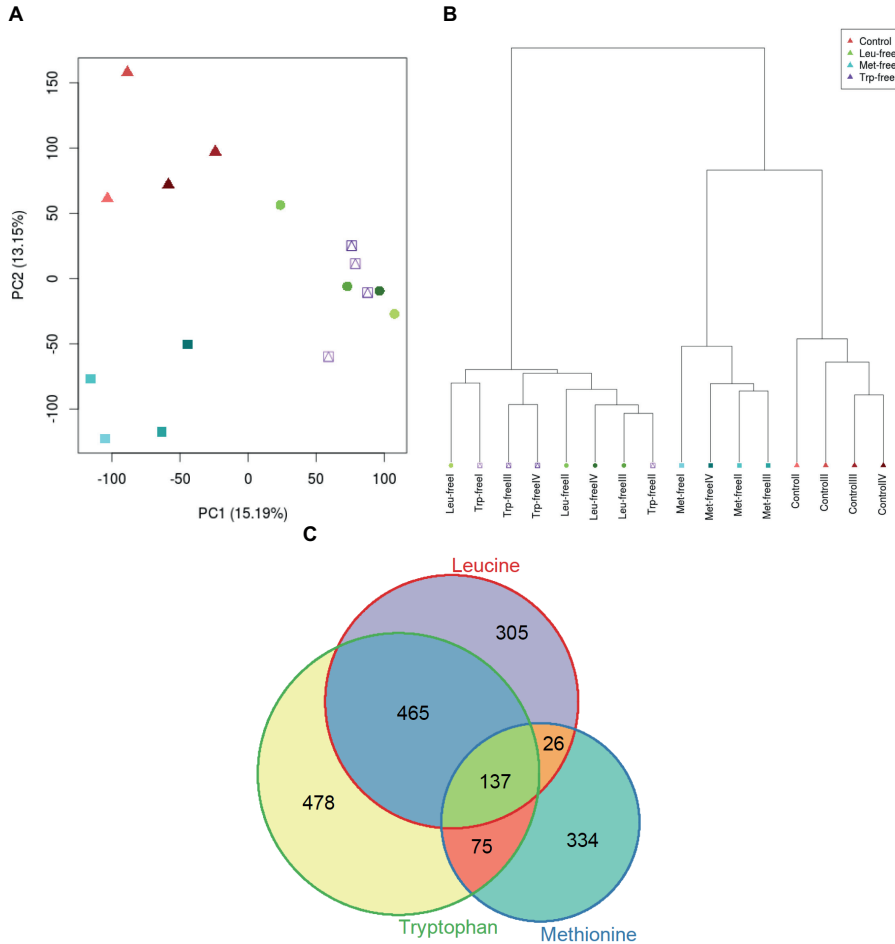


Figure 3. Principal component analysis and overlapping probe sets. (A) Unbiased principal component analysis (PCA) after normalization of all genes in the dataset. A distinct clustering of the control group and the methionine-free group is seen, with a clear separation of the groups on the principal component (PC) 2 but not on the PC1. The leucine-group and tryptophan-free have a highly overlapping clustering, with small intergroup variability. Their combined cluster is mainly separated from the control group and the methionine-free group on the PC1. (B) Dendrogram based on the unbiased hierarchical clustering of all mice. The control group and methionine-free group have individual branches, but are connected higher up in the dendrogram. The leucine-free and tryptophan-free group overlap and are intertwined in the dendrogram. (C) Venn diagram of the differentially expressed probe sets (DEPS) overlapping between the methionine-free, leucine-free and tryptophan-free diets. A total of 137 genes overlapped between all diets. Of all genes in the leucine-free diet, 64% overlapped with the tryptophan-free diet. The methionine-free diet had the highest percentage of unique DEPS, namely 334 out of the 573 (58%).

5

Table 1. Overview of the top overrepresented activated and inhibited canonical pathways after each amino acid-free diet ranked by their $-\log P$ -value

Canonical Pathway	Pathway Classification	P-value	Genes Ratio	Z-score
<i>Methionine-free</i>				
LXR/RXR Activation	Nuclear Receptor Signaling	3.24 ^{E-02}	6/121 (5%)	-2.236
LPS/IL-1 Mediated Inhibition of RXR Function	Nuclear Receptor Signaling	5.61 ^{E-10}	22/222 (10.0%)	-1.897
Antioxidant Action of Vitamin C	Cellular Stress and Injury	1.61 ^{E-02}	6/103 (5.8%)	-1.000
PPARa/RXRa Activation	Nuclear Receptor Signaling	8.78 ^{E-03}	9/178 (5.1%)	+0.378
eNOS Signaling	Cardiovascular Signaling	3.37 ^{E-02}	7/155 (4.5%)	+0.447
ERK5 Signaling	Intracellular and Second Messenger Signaling	3.53 ^{E-02}	4/63 (6.3%)	+1.000
CNTF Signaling	Cytokine Signaling/ Neurotransmitters and Other Nervous System Signaling/ Cellular Growth	3.53 ^{E-02}	4/63 (6.3%)	+1.000
UVA-Induced MAPK Signaling	Cellular Stress and Injury	1.54 ^{E-02}	6/102 (5.9%)	+1.000
Cell Cycle: G2/M DNA Damage Checkpoint Regulation	Cell Cycle Regulation	2.68 ^{E-03}	5/49 (10.2%)	+1.342
Melanocyte Development and Pigmentation Signaling	Growth Factor Signaling	3.94 ^{E-02}	5/95 (5.3%)	+2.000
NRF2-mediated Oxidative Stress Response	Cellular Stress and Injury	1.54 ^{E-07}	18/193 (9.3%)	+2.646
<i>Leucine-Free</i>				
NRF2-mediated Oxidative Stress Response	Cellular Stress and Injury	3.46 ^{E-05}	18/193 (9.3%)	+2.309
Calcium-induced T-lymphocyte Apoptosis	Apoptosis/Cellular Immune Response	1.94 ^{E-04}	9/66 (13.6%)	+1.000
LPS/IL-1 Mediated Inhibition of RXR Function	Nuclear Receptor Signaling	2.09 ^{E-04}	18/222 (8.1%)	-0.816
Role of NFAT in Regulation of the Immune Response	Intracellular and Second Messenger Signaling	6.87 ^{E-04}	15/185 (8.1%)	+1.069
Cholecystokinin/Gastrin-mediated Signaling	Neurotransmitters and Other Nervous System Signaling	1.18 ^{E-03}	10/101 (9.9%)	+1.265
CD28 Signaling in T Helper Cells	Cellular Immune Response	2.61 ^{E-03}	11/131 (8.4%)	+0.447
PKCo Signaling in T Lymphocytes	Cellular Immune Response	2.77 ^{E-03}	11/132 (8.3%)	+1.508
Tec Kinase Signaling	Intracellular and Second Messenger Signaling	6.95 ^{E-03}	12/170 (7.1%)	+0.333
Phospholipase C Signaling	Intracellular and Second Messenger Signaling	7.42 ^{E-03}	15/237 (6.3%)	+1.291

Table 1. (continued)

Canonical Pathway	Pathway Classification	P-value	Genes Ratio	Z-score
Thrombin Signaling	Cardiovascular Signaling	1.11 ^E -02	13/203 (6.4%)	+0.905
LXR/RXR Activation	Nuclear Receptor Signaling	1.31 ^E -02	9/121 (7.4%)	-1.000
CXCR4 Signaling	Cellular Immune Response / Cytokine Signaling	1.42 ^E -02	11/165 (6.7%)	+0.378
Cell Cycle: G2/M DNA Damage Checkpoint Regulation	Cell Cycle Regulation	1.76 ^E -02	5/49 (10.2%)	+1.000
Production of Nitric Oxide and Reactive Oxygen Species in Macrophages	Cellular Immune Response	1.77 ^E -02	12/193 (6.2%)	-0.302
PI3K Signaling in B Lymphocytes	Cellular Immune Response	1.85 ^E -02	9/128 (7.0%)	-0.333
G Beta Gamma Signaling	Intracellular and Second Messenger Signaling	1.96 ^E -02	7/88 (8.0%)	+0.378
Relaxin Signaling	Organismal Growth and Development / Growth Factor Signaling	2.05 ^E -02	10/152 (6.6%)	-0.447
Colorectal Cancer Metastasis Signaling	Cancer	2.27 ^E -02	14/247 (5.7%)	+0.577
Actin Nucleation by ARP-WASP Complex	Intracellular and Second Messenger Signaling	2.96 ^E -02	5/56 (8.9%)	+1.342
Synaptic Long Term Potentiation	Neurotransmitters and Other Nervous System Signaling	3.36 ^E -02	8/120 (6.7%)	+0.707
Dendritic Cell Maturation	Cytokine Signaling/ Cellular Immune Response	3.55 ^E -02	11/190 (5.8%)	+1.897
ICOS-ICOSL Signaling in T Helper Cells	Cellular Immune Response	3.65 ^E -02	8/122 (6.6%)	+1.890
Sphingosine-1-phosphate Signaling	Intracellular and Second Messenger Signaling	3.81 ^E -02	8/123 (6.5%)	+1.414
Macropinocytosis Signaling	Cellular Immune Response	4.01 ^E -02	6/81 (7.4%)	+1.000
UV-Induced MAPK Signaling	Cellular Stress and Injury	4.07 ^E -02	4/42 (9.5%)	-1.000
Antioxidant Action of Vitamin C	Cellular Stress and Injury	4.14 ^E -02	7/103 (6.8%)	-1.000
RhoGDI Signaling	Intracellular and Second Messenger Signaling	4.40 ^E -02	10/173 (5.8%)	-0.378
IL-8 Signaling	Cytokine Signaling	4.42 ^E -02	11/197 (5.6%)	+1.508
ERK5 Signaling	Intracellular and Second Messenger Signaling	4.58 ^E -02	5/63 (7.9%)	+0.447
<i>Tryptophan-free</i>				
LPS/IL-1 Mediated Inhibition of RXR Function	Nuclear Receptor Signaling	1.25 ^E -05	23/222 (10.4%)	-1.667

Table 1. (continued)

Canonical Pathway	Pathway Classification	P-value	Genes Ratio	Z-score
NRF2-mediated Oxidative Stress Response	Cellular Stress and Injury	1.40 ^E -05	21/193 (10.9%)	+1.941
Colorectal Cancer Metastasis Signaling	Cancer	4.77 ^E -04	21/247 (8.5%)	-0.447
Sumoylation Pathway	Cellular Stress and Injury/ Transcriptional Regulation	9.90 ^E -04	11/96 (11.5%)	+0.333
Calcium-induced T Lymphocyte Apoptosis	Apoptosis/Cellular Immune Response	3.32 ^E -03	8/66 (12.1%)	+1.134
LXR/RXR Activation	Nuclear Receptor Signaling	2.11 ^E -03	12/121 (9.9%)	-0.447
Wnt/B-catenin Signaling	Cancer / Organismal Growth and Development	1.20 ^E -02	13/169 (7.7%)	-0.333
Cholecystokinin/Gastrin-mediated Signaling	Neurotransmitters and Other Nervous System Signaling	1.42 ^E -02	9/101 (8.9%)	-0.333
MIF Regulation of Innate Immunity	Cellular Immune Response	1.85 ^E -02	5/41 (12.2%)	+1.342
IGF-1 Signaling	Growth Factor Signaling	1.90 ^E -02	9/106 (8.5%)	+0.447
UVC-Induced MAPK Signaling	Cellular Stress Injury	2.04 ^E -02	5/42 (11.9%)	-1.342
MIF-mediated Glucocorticoid Regulation	Cellular Immune Response / Nuclear Receptor Signaling	3.47 ^E -02	4/33 (12.1%)	+2.000
Cell Cycle: G2/M DNA Damage Checkpoint Regulation	Cell Cycle Regulation	3.69 ^E -02	5/49 (10.2%)	+2.000
Mitotic Roles of Polo-Like Kinase	Cell Cycle Regulation	3.81 ^E -02	6/66 (9.1%)	-2.000
TWEAK Signaling	Apoptosis / Cytokine Signaling	3.82 ^E -02	4/34 (11.8%)	-1.000
Sphingosine-1-phosphate Signaling	Intracellular and Second Messenger Signaling	4.36 ^E -02	9/123 (7.3%)	+0.707

Pathways are defined via the canonical pathways and pathway classification. Only pathways with a z-score were included. Analyses are based on the analyses done in Ingenuity and Ingenuity Target Explorer. Genes ratio = the number and percentage of probe sets differentially expressed in ratio to the total number of genes involved in the pathway. Z-score = based on the observed gene expression changes in the specific array datasets.

Table 2. List of significantly up- or downregulated upstream transcription factors in the liver with corresponding z-scores regulated by all three amino-acid-free diets

Upstream Regulator	State	Methionine-free		Tryptophan-free		Leucine-free	
		Z-score	P-value	Z-score	P-value	Z-score	P-value
NFE2L2	Activated	4.545	6.28 ^E -13	2.975	3.12 ^E -11	2.919	3.92 ^E -07
SMARCB1	Activated	2.026	9.12 ^E -06	2.436	9.74 ^E -04	2.465	2.14 ^E -06
SREBF2	Inhibited	-2.804	1.26 ^E -04	-5.540	8.96 ^E -26	-5.159	1.87 ^E -28
FOXM1	Inhibited	-2.671	1.66 ^E -04	-3.096	1.76 ^E -05	-2.391	6.91 ^E -06

Upstream regulator analysis of the differentially regulated genes found in common after 3-day methionine-free, tryptophan-free and leucine-free diet revealed four significantly regulated transcription factors, of which two were activated and two were inhibited.

DISCUSSION

In this study we demonstrated that, in addition to a protein-free diet, a Met-free, a Leu-free and a Trp-free diet for three days induce a similar protection against hepatic IRI. We show that cellular stress-, nuclear receptor-, and cell cycle regulation pathways are regulated by all three EAA-free diets, and that transcription factors NRF2, FOXM1, SREBF2 and SMARCB1 may be implicated in orchestrating this response.

Previously, we have shown that two weeks of 30% DR as well as three days of fasting are sufficient to induce resistance against hepatic and renal IRI^{1,10,18}. Recently, we and others showed that absence of protein is the main contributor to these effects^{17,19}. Here, we further dissected the role of essential amino acids, and demonstrated that the absence of one single essential amino acid is sufficient to induce the increased stress resistance associated with DR leading to protection against hepatic IRI. Mice fed EAA-free diets voluntarily restricted food intake by approximately 30%. Since we showed that three days of 30% DR without deprivation of EAA is insufficient to induce protection against hepatic IRI, the restricted food intake due to EAA-free diets is ruled out as a factor and the absence of EAA during three days is therefore responsible for inducing these beneficial effects.

All three EAA-free diets induced a similar protective effect, indicative of a common denominator of induction of the beneficial response. To extract this denominator, we determined mRNA expression profiles of liver tissue following administration of the EAA-free diets and performed microarray analyses. These data show that EAA deprivation modifies the transcriptome at three different pathway levels.

First, cell metabolism is altered as indicated by the nuclear receptor signaling response via the activation of the retinol pathway. Nuclear receptors are transcription factors that are known to be activated by steroid hormones and lipi-soluble agents, such as the retinoid acids (RAs)²⁰. As previously shown, RAs are able to induce many of the beneficial effects observed after DR. RAs are able to protect from ischemic stroke in the brain and have a positive effect on insulin resistance²¹⁻²⁴. This activation is in line with our previous results, where nuclear receptor signaling activation was proposed as one of the main contributors to the beneficial effects of DR against renal IRI¹⁷. In our renal IRI model, upstream transcription factor FOXO3 was identified as a main player of the activation of the nuclear receptor response. FOXO3 was upregulated after all three EAA-free diets, however only reached statistical significance after the Trp-free diet. Besides cell metabolism, FOXO3 phosphorylation and activation is at the basis of many processes, most importantly stress resistance and autophagy^{25,26}. These data strengthen the role of nuclear receptor signaling mediated by FOXO3, however excludes FOXO3 as the only contributor for the beneficial effects. For instance, the LXR/RXR pathway has been implicated in the response as well²⁷. The liver X receptor (LXR) is mainly expressed in the liver and is an important factor of its lipid metabolism²⁸. However, we found an inhibition of this pathway in our EAA-free analysis. The downregulation of the LXR/RXR pathway might in part be a response to the massive downregulation of SREBF2 by all EAA-free diets, which is a main regulator of the pathway²⁹. Blocking SREBF2 in a mouse model showed to be effective in preventing the development of hepatic steatosis and insulin resistance, and might be more important than the activation of the LXR/RXR pathway itself²⁷. Our results suggest that inhibition of SREBF2 might play a role in the protective effect on hepatic IRI. Future studies with for instance SREBF2 *-/-* mouse models could highlight the effects of SREBF-2 deficiency on IRI.

Second, we found two transcription factors involved with inhibition of cellular proliferation. FOXM1, which increases G2/M DNA damage checkpoint activity³⁰, and SMARCB1 which inhibits cellular proliferation by mediating between various signaling pathways as part of the SWI/SNF complex. In recent work, SMARCB1 has been named often as a tumor suppressor via inhibition of cell growth^{31,32}. Inhibition of cell growth is a common feature induced by DR regimens. We propose that the evolutionary adaptive response to DR that shifts resources from growth (metabolism and temporary withdrawal from the cell cycle) to maintenance occurs already after three days of essential amino acid deprivation³³. The associated increase in stress resistance is rapidly induced and offers robust protection against hepatic IRI.

Third, all three EAA-free diets induced a strong activation of the *NRF2-mediated oxidative stress response*, both on transcription factor and pathway level. NRF2 increases stress resistance³⁰, and we have already implicated NRF2 in the protection against renal IRI after three days of fasting^{1,17,18}. In response to environmental stress, including protein deprivation, NRF2 is activated by phosphorylation of eIF2 α via *Gcn2*^{30,34,35} and results in the transcription of genes involved in antioxidant defense, reduction of inflammation and cell survival. In NRF2 knock-out models, similar effects of DR on cellular stress injury as in NRF2 proficient models could not be induced^{30,36}. This indicates that NRF2 is indeed a major player yet not the only player in the protection against IRI. Our results demonstrate that activation of nuclear receptors signaling, inhibition of cellular proliferation and activation of the NRF2-pathway might be the essential package required to induce the beneficial effects of hepatic IRI. Validation studies should further emphasize on how these regulators induce protection against oxidative stress induced by IRI.

Taken together, we report that three essential amino acid-free diets given for three days protect against hepatic IRI in a mouse model possibly mediated via transcription factors NRF2, FOXM1, SREBF2 and SMARCB1. Further in depth analysis through functional and pharmacological modulation of these factors may provide mimetics for treatment against ROS-related injury.

MATERIAL AND METHODS

Animals

Male C57BL/6 (approximately 25 grams) were obtained from Harlan (Horst, the Netherlands). Animals were kept under standard laboratory conditions, and were housed in individually ventilated cages (n = 3 animals/cage). All mice had ad libitum (AL) access to food and water (acidified with HCl). All experiments were performed with the approval of the appropriate local ethical board.

Diets

Before dietary intervention, all mice were acclimatized during seven days and fed the standard Special Diet Services (SDS) chow. All other diets used for dietary intervention were purchased from Research Diets, Inc. (New Brunswick, NJ, USA). The SDS chow was used as a control diet for the fasted and 30% dietary restricted mice¹. As a control for the protein-free and EAA-free diet, a specific control diet was used since this diet has the same protein source as the EAA-free diets, including all EAA (Table S2). The protein source of the EAA-free diets is derived from a crystalline L-amino acid mixture leaving out one of the specific amino acids (Met-free, Leu-free or Trp-free). During the experiment, 3-day 30%

DR was used as a negative control group while previous studies showed that this dietary intervention did not protect against IRI¹⁷. Mice on three days of 30% DR were given 70% of their normal daily intake of the SDS chow. Three days of protein-free diet was used as a positive control since this diet protects against IRI¹². Mice on protein-, Trp-free, Met-free and Leu-free diets were transferred to clean cages with the specific diet given at 4:00 pm. Mice on the control diet were used as the control group. Body weight of the mice was recorded daily. An overview of the composition of the diets used is shown in Table S2.

Hepatic ischemia-reperfusion model

Mice were anesthetized by isoflurane/N₂/O₂ inhalation. To maintain their body temperature mice, were placed on a heating pad. All surgeries were performed between 9:00 am and 1:00 pm. Partial (70%) hepatic IRI was induced by occlusion of the blood flow of the left lateral and median liver lobes with a non-traumatic microvascular clamp for 75 minutes, which causes ischemia of the liver tissue. After clamp removal, the restoration of blood flow in the liver leads to reperfusion. No mortality was observed associated with this amount of damage to the liver. After surgery, all mice received 0.5 mL of phosphate-buffered saline subcutaneously and were placed under a heating lamp until they recovered from anesthesia. Directly after, all mice had free access to SDS chow and water.

Hepatocellular injury

Preoperatively fed and fasted mice were euthanized before surgery (baseline), six hours and 24 hours after reperfusion (n = 5-6 per time point). Serum levels of hepatic damage markers alanine aminotransferase (ALT), aspartate aminotransferase (AST) and lactate dehydrogenase (LDH) at the Central Clinical Chemical Laboratory of the Erasmus University Medical Center. Hemorrhagic necrosis was scored before, and at six and 24 hours after reperfusion (n = 5-6 per time point) in 3µm thick Hematoxylin and Eosin stained liver sections at a magnification of 100x by two observers blinded to the treatment. Hemorrhagic necrosis was characterized by the loss of the cellular architecture and the presence of erythrocytes in necrotic areas. The percentage of hemorrhagic necrosis per microscopic field was determined using the following scoring system: 0% (absent), 0% to 20% (<20% necrosis per microscopic field), 20% to 40% (20% to <40% necrosis per microscopic field) etcetera until 100% necrosis.

Immunohistochemistry

Frozen liver sections (5 μm) from different time points (baseline, six and 24 hours after reperfusion) were stained with a monoclonal antibody against neutrophils and visualized with an alkaline phosphatase secondary antibody. Per section two observers blinded to the treatment counted the number of neutrophils in 10 microscopic fields at magnifications of 400x.

Microarray analysis

For microarray analysis, mice were either fed the control diet or put on either a protein-, Leu-free, Trp-free or Met-free diet for three consecutive days, after which the mice were sacrificed. Directly after each intervention, liver samples were taken and snap frozen in liquid nitrogen for further analyses. RNA isolation of the liver samples was performed as described previously^{17,18}. RNA quality was tested via the RNA integrity number (RIN, range 0-10). All samples used scored a RIN between 7.7 and 9.5. Hybridization to Affymetrix HT MG-430 PM Array Plates was performed at the Microarray Department of the University of Amsterdam (the Netherlands), according to Affymetrix protocols and as described previously^{17,18}. The procedure for all samples was performed on the same batch. Normalization was done using the Robust Multichip Average (RMA) algorithm at the website www.arrayanalysis.org. Data output consisted of 45,141 probes, whereby more probes could present the same Gene ID.

Statistical analysis

Data were expressed as mean \pm standard error of the mean. Differences in groups were analyzed by Mann-Whitney U tests with SPSS (version 21). Differences were considered significant at $P < 0.05$. Microarray analyses were performed using the free software package R (R foundation), using the Linear Models for Microarray Data (limma) method with correction for multiple testing using the false discovery rate (FDR) according to Benjamini and Hochberg. Fold changes were expressed as the geometric mean per diet group against the corresponding ad libitum fed control group. An FDR $< 5\%$ with fold change ≥ 1.5 were used as cut-off values for significance. The enrichment factor (EF), defined as the number of times an observation was higher than expected by chance, was calculated via the formula: $EF = nAB / ((nA \times nB) / nC)$, where nA is the number of differentially expressed probe sets (DEPS) in experimental group A, nB the number of DEPS in experimental group B, nC the number of total genes in the microarray, and nAB the number of common DEPS between nA and nB. Functional annotation and analyses were performed QIAGEN's Ingenuity® Pathway Analysis (IPA®, QIAGEN Redwood City, www.qiagen.com/ingenuity). Subsequent pathway and target categories were generated using the QIAGEN's Ingenuity Target Explorer (QIAGEN's, <https://targetexplorer.ingenuity.com/>). The prediction inhibition or

activation of the upstream transcription regulators are calculated via de statistical z-score based on the observed gene expression changes in our dataset. Calculating the z-score reduces the chance of significant predictions based on random data (http://ingenuity.force.com/ipa/articles/Feature_Description/Upstream-Regulator-Analysis). A z-score ≥ 2 or ≤ -2 was set as significant.

REFERENCES

1. Mitchell, J.R., et al., Short-term dietary restriction and fasting precondition against ischemia-reperfusion injury in mice. *Aging Cell*, 2010. 9(1): p. 40-53.
2. Robertson, L.T. and J.R. Mitchell, Benefits of short-term dietary restriction in mammals. *Exp Gerontol*, 2013. 48(10): p. 1043-8.
3. Yamagishi, T., et al., Severe, short-term food restriction improves cardiac function following ischemia/reperfusion in perfused rat hearts. *Heart Vessels*, 2010. 25(5): p. 417-25.
4. McCay, C.M., M.F. Crowell, and L.A. Maynard, The effect of retarded growth upon the length of life span and upon the ultimate body size. 1935. *Nutrition*, 1989. 5(3): p. 155-71; discussion 172.
5. Mair, W., et al., Demography of dietary restriction and death in *Drosophila*. *Science*, 2003. 301(5640): p. 1731-3.
6. Colman, R.J., et al., Caloric restriction delays disease onset and mortality in rhesus monkeys. *Science*, 2009. 325(5937): p. 201-4.
7. Ravussin, E., et al., A 2-Year Randomized Controlled Trial of Human Caloric Restriction: Feasibility and Effects on Predictors of Health Span and Longevity. *J Gerontol A Biol Sci Med Sci*, 2015. 70(9): p. 1097-104.
8. Fontana, L., L. Partridge, and V.D. Longo, Extending healthy life span--from yeast to humans. *Science*, 2010. 328(5976): p. 321-6.
9. Heilbronn, L.K., et al., Effect of 6-month calorie restriction on biomarkers of longevity, metabolic adaptation, and oxidative stress in overweight individuals: a randomized controlled trial. *JAMA*, 2006. 295(13): p. 1539-48.
10. Verweij, M., et al., Preoperative fasting protects mice against hepatic ischemia/reperfusion injury: mechanisms and effects on liver regeneration. *Liver Transpl*, 2011. 17(6): p. 695-704.
11. Uemura, T., et al., Liver retransplantation for primary nonfunction: analysis of a 20-year single-center experience. *Liver Transpl*, 2007. 13(2): p. 227-33.
12. Ben-Ari, Z., et al., Induction of heme oxygenase-1 protects mouse liver from apoptotic ischemia/reperfusion injury. *Apoptosis*, 2013. 18(5): p. 547-55.
13. Datta, G., B.J. Fuller, and B.R. Davidson, Molecular mechanisms of liver ischemia-reperfusion injury: insights from transgenic knockout models. *World J Gastroenterol*, 2013. 19(11): p. 1683-98.
14. Verweij, M., et al., Glucose supplementation does not interfere with fasting-induced protection against renal ischemia/reperfusion injury in mice. *Transplantation*, 2011. 92(7): p. 752-8.
15. Jensen, K., et al., Sex-specific effects of protein and carbohydrate intake on reproduction but not lifespan in *Drosophila melanogaster*. *Aging Cell*, 2015. 14(4): p. 605-15.
16. Bruce, K.D., et al., High carbohydrate-low protein consumption maximizes *Drosophila* lifespan. *Exp Gerontol*, 2013. 48(10): p. 1129-35.

17. Jongbloed, F., et al., A signature of renal stress resistance induced by short-term dietary restriction, fasting, and protein restriction. *Sci Rep*, 2017. 7: p. 40901.
18. Jongbloed, F., et al., Preoperative fasting protects against renal ischemia-reperfusion injury in aged and overweight mice. *PLoS One*, 2014. 9(6): p. e100853.
19. Solon-Biet, S.M., et al., The ratio of macronutrients, not caloric intake, dictates cardiometabolic health, aging, and longevity in ad libitum-fed mice. *Cell Metab*, 2014. 19(3): p. 418-30.
20. Sever, R. and C.K. Glass, Signaling by nuclear receptors. *Cold Spring Harb Perspect Biol*, 2013. 5(3): p. a016709.
21. Lee, S.E., et al., Retinoid X receptor alpha overexpression alleviates mitochondrial dysfunction-induced insulin resistance through transcriptional regulation of insulin receptor substrate 1. *Mol Cells*, 2015. 38(4): p. 356-61.
22. Chakrabarti, M., et al., Molecular Signaling Mechanisms of Natural and Synthetic Retinoids for Inhibition of Pathogenesis in Alzheimer's Disease. *J Alzheimers Dis*, 2016. 50(2): p. 335-52.
23. Choi, B.K., et al., Reduction of ischemia-induced cerebral injury by all-trans-retinoic acid. *Exp Brain Res*, 2009. 193(4): p. 581-9.
24. Shen, H., et al., 9-Cis-retinoic acid reduces ischemic brain injury in rodents via bone morphogenetic protein. *J Neurosci Res*, 2009. 87(2): p. 545-55.
25. Wu, C.W. and K.B. Storey, FoxO3a-mediated activation of stress responsive genes during early torpor in a mammalian hibernator. *Mol Cell Biochem*, 2014. 390(1-2): p. 185-95.
26. van den Berg, M.C. and B.M. Burgering, Integrating opposing signals toward Forkhead box O. *Antioxid Redox Signal*, 2011. 14(4): p. 607-21.
27. Rong, X., et al., LXRs regulate ER stress and inflammation through dynamic modulation of membrane phospholipid composition. *Cell Metab*, 2013. 18(5): p. 685-97.
28. Edwards, P.A., M.A. Kennedy, and P.A. Mak, LXRs; oxysterol-activated nuclear receptors that regulate genes controlling lipid homeostasis. *Vascul Pharmacol*, 2002. 38(4): p. 249-56.
29. Bensinger, S.J., et al., LXR signaling couples sterol metabolism to proliferation in the acquired immune response. *Cell*, 2008. 134(1): p. 97-111.
30. Hine, C.M. and J.R. Mitchell, NRF2 and the Phase II Response in Acute Stress Resistance Induced by Dietary Restriction. *J Clin Exp Pathol*, 2012. S4(4).
31. Kalimuthu, S.N. and R. Chetty, Gene of the month: SMARCB1. *J Clin Pathol*, 2016. 69(6): p. 484-9.
32. Kohashi, K. and Y. Oda, Oncogenic roles of SMARCB1/INI1 and its deficient tumors. *Cancer Sci*, 2017.
33. Shanley, D.P. and T.B. Kirkwood, Calorie restriction and aging: a life-history analysis. *Evolution*, 2000. 54(3): p. 740-50.
34. Peng, W., et al., Surgical stress resistance induced by single amino acid deprivation requires Gcn2 in mice. *Sci Transl Med*, 2012. 4(118): p. 118ra11.

35. Lageix, S., et al., Enhanced interaction between pseudokinase and kinase domains in Gcn2 stimulates eIF2alpha phosphorylation in starved cells. *PLoS Genet*, 2014. 10(5): p. e1004326.
36. Martin-Montalvo, A., et al., NRF2, cancer and calorie restriction. *Oncogene*, 2011. 30(5): p. 505-20.

SUPPLEMENTARY DATA

Table S1. List of significantly up- or downregulated upstream transcription factors in the liver by a methionine-free, leucine-free or tryptophan-free diet with the corresponding z-scores

Upstream Regulator	Gene ratio (Log2)	Z-score	P-value	Z-score	P-value	Z-score	P-value
<i>Methionine-free</i>		<i>Tryptophan</i>				<i>Leucine</i>	
NFE2L2	0.297	4.545	6.28 ^E -13	2.975	3.12 ^E -11	2.919	3.92 ^E -07
ATF4	0.393	2.911	7.45 ^E -05	2.686	7.60 ^E -09	1.838	2.41 ^E -06
NUPR1	1.593	2.558	8.47 ^E -04	2.846	2.92 ^E -05	1.667	1.06 ^E -05
KMT2D	0.180	2.449	1.15 ^E -01	N/A	N/A	N/A	N/A
CEBPD	0.390	2.194	8.83 ^E -04	1.994	3.42 ^E -01	1.104	1.39 ^E -02
NFKB1	0.007	2.182	1.37 ^E -01	N/A	N/A	0.344	7.05 ^E -03
KLF4	0.782	2.110	7.47 ^E -02	1.994	4.08 ^E -01	3.101	3.00 ^E -01
SMARCB1	-0.164	2.026	9.12 ^E -06	2.436	9.74 ^E -04	2.465	2.14 ^E -06
TAF4	0.393	2.000	2.57 ^E -03	N/A	N/A	N/A	N/A
MAFF	1.398	2.000	3.37 ^E -05	N/A	N/A	N/A	N/A
TBX2	0.047	-2.000	6.89 ^E -02	-2.530	7.43 ^E -04	-1.890	1.11 ^E -02
Esrra	0.327	-2.000	4.14 ^E -02	N/A	N/A	N/A	N/A
ATF6	0.216	-2.000	7.27 ^E -03	-0.553	1.78 ^E -05	-1.161	1.15 ^E -04
FOXO1	-0.167	-2.139	9.30 ^E -07	-0.465	1.51 ^E -09	-1.269	6.53 ^E -11
STAT5B	0.123	-2.157	2.12 ^E -02	-0.901	3.17 ^E -04	-1.463	4.42 ^E -02
MYBL2	0.157	-2.236	1.79 ^E -04	-1.633	1.79 ^E -04	-2.000	1.03 ^E -02
FOXM1	-0.080	-2.671	1.66 ^E -04	-3.096	1.76 ^E -5	-2.391	6.91 ^E -06
SREBF2	0.086	-2.804	1.26 ^E -04	-5.540	8.96 ^E -26	-5.159	1.87 ^E -28
<i>Leucine-free</i>		<i>Tryptophan-free</i>				<i>Methionine-free</i>	
KLF4	0.907	3.101	3.00 ^E -01	1.994	4.08 ^E -01	2.110	7.47 ^E -02
NFE2L2	0.397	2.919	3.92 ^E -07	2.975	3.12 ^E -11	4.545	6.28 ^E -13
KDM5B	-0.376	2.739	8.34 ^E -08	2.999	3.88 ^E -07	1.615	1.13 ^E -04
TRIM24	-0.415	2.714	3.19 ^E -04	3.043	1.20 ^E -04	N/A	N/A
SMARCB1	-0.126	2.465	2.14 ^E -06	2.436	9.74 ^E -04	2.026	9.12 ^E -06
POU5F1	-0.120	2.234	4.60 ^E -01	-1.103	9.75 ^E -04	N/A	N/A
ETS1	0.829	2.198	2.28 ^E -02	N/A	N/A	N/A	N/A
NOTCH1	-0.165	2.137	8.04 ^E -02	0.309	4.59 ^E -02	0.727	9.18 ^E -03
MYBL2	0.097	-2.000	1.03 ^E -02	-1.633	1.79 ^E -04	-2.236	1.79 ^E -04
NFYA	-0.197	-2.007	1.27 ^E -11	-0.840	5.51 ^E -12	-0.128	7.02 ^E -06
ARNTL	0.217	-2.180	2.56 ^E -03	-1.539	1.41 ^E -03	N/A	N/A
E2F2	-0.287	-2.236	5.13 ^E -03	N/A	N/A	N/A	N/A
PDX1	0.029	-2.321	1.75 ^E -05	-0.739	6.55 ^E -06	N/A	N/A
FOXM1	-0.309	-2.391	6.91 ^E -06	-3.096	1.76 ^E -05	-2.671	1.66 ^E -04

Table S1. (continued)

Upstream Regulator	Gene ratio (Log2)	Z-score	P-value	Z-score	P-value	Z-score	P-value
E2F1	-0.217	-2.480	1.50 ^E -05	-1.068	6.08 ^E -06	-1.564	8.48 ^E -04
MLXIPL	-0.039	-2.510	1.27 ^E -09	-2.345	1.35 ^E -07	-0.927	3.18 ^E -03
IRF7	-0.338	-2.599	2.83 ^E -01	-3.088	1.15 ^E -01	N/A	N/A
SIRT2	0.113	-2.646	8.82 ^E -07	-2.646	3.30 ^E -06	N/A	N/A
PPARGC1B	-0.681	-3.396	1.96 ^E -07	-3.248	1.06 ^E -05	-1.980	2.81 ^E -02
SREBF1	-0.534	-4.605	2.68 ^E -24	-4.998	1.55 ^E -23	-1.020	6.88 ^E -05
SREBF2	-0.453	-5.159	1.87 ^E -28	-5.540	9.96 ^E -26	-2.804	1.26 ^E -04
<i>Tryptophan-free</i>				<i>Leucine-free</i>		<i>Methionine-free</i>	
TRIM24	0.241	3.043	1.20 ^E 04	2.714	3.19 ^E -04	N/A	N/A
KDM5B	-0.602	2.999	3.88 ^E -07	2.739	8.34 ^E -08	1.615	1.13 ^E -04
NFE2L2	0.198	2.975	3.12 ^E -11	2.919	3.92 ^E -07	4.545	6.28 ^E -13
NUPR1	0.772	2.846	2.92 ^E -05	1.667	1.06 ^E -05	2.558	8.47 ^E -04
HTT	-0.347	2.784	1.12 ^E -03	N/A	N/A	N/A	3.16 ^E -04
ATF4	0.317	2.686	7.60 ^E -09	1.838	2.41 ^E -06	2.911	7.54 ^E -05
SMARCB1	0.188	2.436	9.74 ^E -04	2.465	2.14 ^E -06	2.026	9.12 ^E -06
HAND2	0.931	2.224	4.42 ^E -02	N/A	N/A	N/A	N/A
FLI1	0.635	2.150	5.36 ^E -05	1.364	6.55 ^E -05	N/A	N/A
FOXO3	-0.209	2.095	2.00 ^E -10	0.448	9.73 ^E -08	0.588	1.75 ^E -06
GATA4	-0.378	2.071	1.12 ^E -01	N/A	N/A	N/A	N/A
TCF3	0.171	2.032	7.48 ^E -05	1.265	9.72 ^E -04	1.890	1.66 ^E -02
IRF5	-0.327	-2.138	5.91 ^E -03	N/A	N/A	N/A	N/A
STAT1	-0.661	-2.145	5.93 ^E -05	-0.540	1.73 ^E -06	-1.706	1.34 ^E -03
MLX	-0.124	-2.181	1.20 ^E -09	-1.977	1.09 ^E -07	N/A	7.61 ^E -03
MLXIPL	0.054	-2.345	1.35 ^E -07	-2.510	1.27 ^E -09	-0.927	3.18 ^E -03
MYOD1	0.108	-2.465	1.20 ^E -01	-1.242	1.85 ^E -02	-1.657	5.12 ^E -03
EGR1	-0.180	-2.520	2.14 ^E -03	-1.925	7.99 ^E -04	-1.344	3.23 ^E -02
TBX2	-0.001	-2.530	7.43-04	-1.890	1.11 ^E -02	-2.000	6.89 ^E -02
SIRT2	0.170	-2.646	3.30 ^E -06	-2.646	8.82 ^E -07	N/A	N/A
IRF7	-0.349	-3.088	1.15 ^E -01	-2.599	2.83 ^E -01	N/A	N/A
FOXM1	-0.181	-3.096	1.76 ^E -05	-2.391	6.91 ^E -06	-2.671	1.66 ^E -04
IRF3	0.254	-3.128	4.08 ^E -03	-1.359	5.45 ^E -04	N/A	N/A
PPARGC1B	-0.755	-3.248	1.06 ^E -05	-3.396	1.96 ^E -07	-1.980	2.81 ^E -02
SREBF1	-0.247	-4.998	1.55 ^E -23	-4.605	2.68 ^E -04	-1.020	6.88 ^E -05
SREBF2	-0.474	-5.540	8.96 ^E -26	-5.159	1.87 ^E -28	-2.804	1.26 ^E -04

All significantly up- or downregulated transcription factors (TF) after completion of each diet are shown, together with their log-ratio of the gene corresponding to the TF. Of all TF, the z-scores of the other two diets are compared and shown in the same table. N/A = not available.



Table S2. Composition and energy content of the restricted and control diets.

Diet	Control SDS	Control	Protein-free	Methionine-free	Leucine-free	Tryptophan-free
<i>Ingredient</i>	<i>g</i>	<i>g</i>	<i>g</i>	<i>g</i>	<i>g</i>	<i>g</i>
Casein, Lactic	0	200	0	0	0	0
L-Cystine	0	3	0	4.2	4.2	4.2
L-Isoleucine	0.77	0	0	7.6	7.6	7.6
L-Leucine	1.46	0	0	15.8	0	15.8
L-Lysine	1.04	0	0	13.2	13.2	13.2
L-Methionine	0.28	0	0	0	5.1	5.1
L-Phenylalanine	0.96	0	0	8.4	8.4	8.4
L-Threonine	0.69	0	0	7.2	7.2	7.2
L-Tryptophan	0.22	0	0	2.1	2.1	0
L-Valine	0.91	0	0	9.3	9.3	9.3
L-Histidine-HCl-H ₂ O	0	0	0	4.6	4.6	4.6
L-Alanine	1.19	0	0	5.1	5.1	5.1
L-Arginine	0	0	0	6	6	6
L-Aspartic Acid	1.00	0	0	12.1	12.1	12.1
L-Glutamic Acid	3.72	0	0	38.2	38.2	38.2
Glycine	1.55	0	0	3	3	3
L-Proline	1.34	0	0	17.8	17.8	17.8
L-Serine	0.78	0	0	10	10	10
L-Tyrosine	0.69	0	0	9.2	9.2	9.2
Total L-Amino Acids		3	0	173.8	163.1	176.8
Corn Starch	42.37%	315	344	320.1	330.8	317.1
Maltodextrin 10		35	35	35	35	35
Sucrose		350	500	350	350	350
Cellulose, BW200	3.89%	50	50	50	50	50
Soybean Oil		25	25	25	25	25
Lard		20	20	20	20	20
Mineral Mix S10026		10	10	10	10	10
DiCalcium Phosphate		13	13	13	13	13
Calcium Carbonate		5.5	5.5	5.5	5.5	5.5
Potassium Citrate, 1 H ₂ O		16.5	16.5	16.5	16.5	16.5
Vitamin Mix V10001		10	10	10	10	10

Table S2. (continued)

Diet	Control SDS	Control	Protein-free	Methionine-free	Leucine-free	Tryptophan-free
<i>Ingredient</i>	<i>g</i>	<i>g</i>	<i>g</i>	<i>g</i>	<i>g</i>	<i>g</i>
Vitamin Mix V10001C		0	0	0	0	0
Choline Bitartrate		2	2	2	2	2
Sodium Bicarbonate		0	0	7.5	7.5	7.5
FD&C Blue Dye #1		0	0	0.025	0.025	0
FD&C Yellow Dye #5		0.05	0	0	0.025	0.025
FD&C Red Dye #40		0	0.05	0.025	0	0.025
Total		1055.05	1031.05	1038.45	1038.45	1038.45
kcal/g	3.59	3.8	3.8	3.8	3.8	3.8
Protein	200.3	179.0	0.0	173.8	163.1	176.8
Carbohydrate	627.5	710.0	889.0	715.1	725.8	712.1
Fat	36.2	45.0	45.0	45.0	45.0	45.0
Fiber		50.0	50.0	50.0	50.0	50.0
g%						
Protein	22.3	17.0	0	16.7	15.7	17.0
Carbohydrate	68.9	67.3	86.2	68.9	69.9	68.6
Fat	9.08	4.3	4.4	4.3	4.3	4.3
Fiber	4.23	4.7	4.8	4.8	4.8	4.8
kcal						
Protein	801	716	0	695	652	707
Carbohydrate	2510	2840	3556	2860	2903	2848
Fat	326	405	405	405	405	405
kcal%						
Protein	22	18	0	18	16	18
Carbohydrate	69	72	90	72	73	72
Fat	9.0	10	10	10	10	10

Control SDS = control diet given during acclimatization period and the diet of which the 3-days 30% DR diet is based; Control = control diet for the protein-free, methionine-free, leucine-free and tryptophan-free diet.



PART III

CLINICAL APPLICATIONS OF DIETARY RESTRICTION

Chapter 6

The effects of morbid obesity, metabolic syndrome and bariatric surgery on aging of the T-cell immune system

Submitted

Chapter 7

Preoperative calorie and protein restriction is feasible and safe in healthy kidney donors and morbidly obese patients: a pilot study

Nutrients. 2016 May 20;8(5):306

Chapter 8

Combined calorie and protein restriction improves outcome in living kidney donors and kidney transplant recipients

Submitted

CHAPTER 6

THE EFFECTS OF MORBID OBESITY, METABOLIC SYNDROME AND BARIATRIC SURGERY ON AGING OF THE T-CELL IMMUNE SYSTEM

Franny Jongbloed, Ruud W.J. Meijers, Jan N.M. IJzermans, René
A. Klaassen, Martijn E.T. Dollé, Michiel G.H. Betjes, Ron W.F.
de Bruin*, Erwin van der Harst*, Nicolle H.R. Litjens*

*Authors contributed equally

Submitted

ABSTRACT

Morbid obesity adversely affects health and is associated with subclinical systemic inflammation and features of accelerated aging, including the T-cell immune system. The presence of metabolic syndrome (MetS) may potentiate these phenomena. Bariatric surgery might delay or reverse accelerated aging in morbidly obese patients. To examine the effects of bariatric surgery on accelerated immune aging, we measured telomere length and phenotypic characteristics of circulating T-cells in morbidly obese patients before and after bariatric surgery. Ten healthy controls (HC) and 108 morbidly obese patients scheduled for bariatric surgery were included: 41 without MetS and 67 with MetS. Relative telomere length (RTL) and differentiation status were measured in circulating CD4⁺ and CD8⁺ T-cells via flowcytometry. T-cell characteristics were compared for age, MetS, cytomegalovirus (CMV)-serostatus and gender prior to, and at three, six and 12 months after bariatric surgery. Data were compared with those of age-matched HC. Thymic output, represented by numbers of CD31-expressing naive T-cells, was significantly higher in patients ≤ 50 years of age without MetS. MetS, CMV-seropositivity, older age and male gender significantly enhanced T-cell differentiation. Patients with MetS had significant lower CD4⁺ RTL than patients without MetS and HC, which was most pronounced in patients ≤ 50 years of age and CMV-seropositive. Within the first year after bariatric surgery, telomere attrition was increased in CD4⁺ T-cells. Interestingly, T-cells were less differentiated following bariatric surgery, which was most pronounced in the MetS group. Especially in morbidly obese patients ≤ 50 years of age, MetS significantly decreased the RTL of CD4⁺ and enhanced T-cell differentiation. This was only partially reversed following bariatric surgery. These data suggest that obese patients with MetS are at risk for accelerated aging of the T-cell immune system and might benefit from bariatric surgery at an earlier stage.

INTRODUCTION

Obesity (BMI >30) is a risk factor for a wide variety of diseases including hypertension, liver steatosis and cancer¹. The metabolic syndrome (MetS), characterized by biochemical dysregulation of triglycerides, high-density lipoprotein (HDL) cholesterol, glucose, blood pressure and increase in abdominal waist circumference increases this risk². MetS in the context of obesity is associated with the development of a chronic subclinical systemic inflammatory state³. Major players in the development of this inflammatory milieu are adipocytokines, adipokines and cytokines produced by white adipocytes that closely regulate lipid metabolism and the inflammatory response⁴. Adipocytokines contribute to the development of insulin resistance and production of reactive oxygen species^{3,5,6}.

Immunological changes also have been linked to the reduced lifespan seen in morbidly obese patients⁷. The link between chronic (sub)clinical inflammation and advancing age, a phenomenon called ‘inflammaging’, leads to accelerated aging and frailty⁸. This inflammaging might present itself via a decrease in circulating naive T-cells as well as an increase in more mature T-cells, such as terminally differentiated effector memory RA (EMRA) T-cells. The pro-inflammatory state in morbid obese patients resembles that of inflammaging seen in older people, as the production of adipocytokines leads to impairment of the T-cell system³. Total T-cell numbers as well as cytotoxic CD8⁺ and CD4⁺ T-cells are reported to be positively associated with BMI and the prevalence of MetS by some authors⁹⁻¹¹, but not by others^{12,13}. Studies investigating the full T-cell differentiation status in obesity in relation to obesity with or without MetS are currently lacking.

Cytomegalovirus (CMV) prevalence ranges from 30-100% and depends on socio-economic and ethnic background¹⁴. CMV leaves a clear fingerprint on circulating T-cells, which resembles T-cell aging. A decreased CD4⁺/CD8⁺ ratio, a more differentiated memory T-cell compartment and expansion of T-cells lacking expression of the costimulatory molecule CD28 have been associated with CMV-seropositivity and attrition of telomeres in T-cells¹⁵⁻¹⁹. Therefore, we considered CMV-seropositivity as a separate entity in our study.

Validated biomarkers for human T-cell aging are reduced numbers of circulating recent thymic emigrants (RTE) as representatives of thymic involution, an enhanced T-cell differentiation status, and attrition of telomeres^{15,20,21}. Telomeres are small DNA repeats located at the end of chromosomes that protect from fusion but shorten with each cell division²². Several studies find that BMI is inversely correlated with telomere length in T-cells^{22,23}. However, this has not been established in all studies^{22,24}. The effect of MetS on T-cell aging has not yet been investigated.

Bariatric surgery may be indicated as a treatment for morbidly obese patients²⁵. Besides rapid loss of body weight, bariatric surgery has been reported to reverse obesity-related diseases including diabetes mellitus and dyslipidemia²⁵. Whether this procedure also induces reversal of aging, in particular premature T-cell aging, is unclear.

Therefore, we aimed to determine the effects of morbid obesity and MetS on aging of circulating T-cell subsets as well as the potential reversal of T-cell aging by bariatric surgery. We show that the presence of MetS is an individual risk factor for premature aging of the T-cell immune system of morbidly obese patients and a partial reversal of the aging process may be established by bariatric surgery. These data show that MetS predisposes to accelerated T-cell aging and may be a biomarker identifying patients that benefit from bariatric surgery.

RESULTS

Baseline characteristics

A total of 118 participants were included in this study, consisting of 10 HC and 108 morbidly obese patients. Of the latter, 41 persons with a BMI of ≥ 35 did not have MetS and 67 had MetS. Table 1 summarizes the baseline characteristics of the included participants. Patients without MetS were more often female than patients with MetS. When dividing the groups in patients ≤ 50 and > 50 years, patients with MetS were significantly older in the group ≤ 50 years. No significant differences were observed with respect to distribution of CMV-seropositivity amongst the study groups.

Lower numbers of recent thymic emigrants due to MetS and age

In both CD4⁺ and CD8⁺ T-cell compartments, no significant differences were induced by obesity and MetS (Table 2). No age-related decline in CD4⁺ RTE in the total group was observed, however the group without MetS did show a significant decline. The effects were stronger in the CD8⁺ T-cell population, which showed an age-related decline in RTE for morbidly obese patients as well as for patients with and without MetS (Table 2). These data suggest an age-related decline in RTE which is most significant in the CD8⁺ T-cell compartment and intensified by the presence of MetS. CMV-seropositivity had no effect on RTE. Female patients had a significantly higher number of CD4⁺ RTE compared to male patients, whereas no significant differences were observed for CD8⁺ RTE (Table 2).

Table 1. Baseline characteristics of the three different patient cohorts

Characteristics/ Subjects	BMI \geq 35 no MetS	BMI \geq 35 with MetS	Healthy Individuals
N	41	67	10
Gender (male/female)*	5/36*	21/44*	2/8
BMI (Kg/m2)*	43 (35-66)*	43 (35-65)	25 \pm 1.5*
Age (yrs)	39 (18-62)	43 (22-60)	45 (27-59)
<i>AGE \leq50/ >50 YEARS</i>			
N	28/13	41/26	6/4
Age (yrs)*	31(18-49)*/54(51-62)	36(22-48)*/55(50-60)	36(27-48)/57(55-59)
<i>CMV-/CMV+</i>			
N	27/14	30/29	5/5
Age (yrs)	39(18-62)/38(25-56)	42(22-60)/45(25-60)	42(27-54)/56(28-59)

MetS = metabolic syndrome; BMI = Body Mass Index; CMV = cytomegalovirus. Significance between two groups are highlighted with an asterisk at the groups within the significant comparisons. * = $P < 0.05$

Obesity and metabolic syndrome enhance T-cell differentiation status

Obesity resulted in a significant higher number of CD4⁺ central memory (CM; CD45R0⁺/CCR7⁺) cells compared to HC (Table 2). This significance remained in both MetS and no MetS groups. The presence of MetS resulted in an advanced T-cell differentiation, with significant increased numbers of CD4⁺ CD28null T-cells. In the CD8⁺ compartment, obesity led to a higher number of more differentiated effector memory RA (EMRA; CD45R0⁺/CCR7⁻) cells. Upon dissection into the presence or absence of MetS, this higher number of EMRA CD8⁺ T-cells only remained significant in the MetS group. The presence of MetS also induced a significantly higher number of total memory, central memory, differentiated EMRA and CD28null cells in the CD8⁺ compartment. (Table 2). Advanced age led to a significant lower number of CD8⁺ naive T-cells (CD45RO⁻/CCR7⁺). In patients \leq 50 years, the presence of MetS gave rise to a higher number of CD4⁺CD28null T-cells. In the CD8⁺ compartment, the younger age resulted in significantly more mature CD8⁺ EMRA T-cells, while patients >50 years having MetS showed higher total number of CD8⁺ cells, central memory cells and total number of memory T-cells, including EMRA and CD28null T-cells. Taken together, in both age groups MetS resulted in a shift towards a more mature T-cell differentiation status, which was most pronounced in the older age group. CMV-seropositivity resulted in more differentiated (EMRA and CD28null) T-cells in both CD4⁺ and CD8⁺ T-cells. Gender differences were reflected by the higher number of CD4⁺ CD31 naive and EMRA T-cells in female patients compared to males (Table 3). A multivariate analysis including MetS,

age, CMV-seropositivity and gender revealed that CMV-seropositivity was an independent factor for the enhanced CD4⁺ T-cell differentiation status. For the CD8⁺ T-cell markers, independent factors were age, CMV-seropositivity as well as gender (Table S1).

Table 2. *P*-values of the different T-cell differentiation markers of the different patient cohorts prior to bariatric surgery

Parameter	Obesity	MetS	Age	MetS x Age	CMV	Gender
CD4 T-cells	0.73	0.37	0.97	0.25	0.54	0.38
CD4 naive T-cells	0.58	0.76	0.67	0.17	0.15	0.17
CD4 CD31 naive T-cells	0.82	0.84	0.32	0.97	0.19	0.02 (↑)
CD4 memory T-cells	0.26	0.26	0.69	0.65	0.70	0.92
CD4 central-memory T-cells	0.003 (↑)	0.23	0.98	0.74	0.39	0.34
CD4 effector-memory T-cells	0.20	0.99	0.42	0.84	0.02 (↑)	0.07
CD4 EMRA T-cells	0.11	0.19	0.24	0.22	0.02 (↑)	0.008 (↑)
CD4 CD28null memory T-cells	0.16	0.01 (↑)	0.64	0.03 (↑)	<0.001 (↑)	0.35
CD8 T-cells	0.86	0.11	0.60	0.009 (↓)	0.006 (↓)	0.15
CD8 naive T-cells	0.75	0.85	0.008 (↓)	0.46	0.34	0.46
CD8 CD31 naive T-cells	0.41	0.92	<0.0001 (↓)	0.002 (↓)	0.82	0.36
CD8 memory T-cells	0.01 (↑)	0.004 (↑)	0.35	0.02 (↑)	0.002 (↑)	0.07
CD8 central-memory T-cells	0.39	0.004 (↑)	0.93	0.002 (↑)	0.15	0.03 (↑)
CD8 effector-memory T-cells	0.14	0.47	0.50	0.38	0.11	0.80
CD8 EMRA T-cells	0.002 (↑)	0.005 (↑)	0.27	0.03 (↑)	0.001 (↑)	0.12
CD8 CD28null memory T-cells	0.57	0.01 (↑)	0.15	0.01 (↑)	<0.001 (↑)	0.17

Explanation of group comparisons: Obesity = total obesity group vs. healthy controls; MetS = MetS vs. no MetS; Age = total group >50 years vs. ≤50 years; MetS x Age = MetS group >50 years vs. ≤50 years; CMV = total group CMV vs. no CMV; Gender = total group female vs. male patients. MetS = metabolic syndrome. CMV = cytomegalovirus. Significant comparisons are depicted in bold. Arrows indicate direction of significance.

Metabolic syndrome and age affect relative telomere length of T-cells prior to bariatric surgery

One-way analysis of variance showed a significant decline in the RTL of CD4⁺ T-cells in the MetS group ($P=0.046$) (Figure 1A). Individual comparisons revealed that this difference was based on the significant decline in RTL in the MetS group compared to the no MetS group ($P=0.03$). Age did not influence RTL (Figure 1B). In patients ≤50 years, MetS significantly shortened RTL in CD4⁺ T-cells ($P=0.04$) (Figure 1C). No significance was seen in the group

>50 years with or without MetS, however a large dispersion in interquartile ranges was seen in both groups. No significant differences were seen in CD8⁺ RTL in either the different MetS (Figure 1D), age (Figure 1E) or combined MetS and age (Figure 1F) groups. These results demonstrate that MetS enhances telomere attrition in the CD4⁺ compartment, with most pronounced changes in the younger patients. CMV-related attrition of telomeres was only observed within the CD4⁺, but not the CD8⁺ T-cell compartment of morbidly obese patients without MetS ($P=0.03$). In a multivariate analysis including MetS, age, CMV-seropositivity and gender none of these were independent factors for RTL in both CD4⁺ and CD8⁺ T-cells (Table S1).

T-cell aging is partially reversed following bariatric surgery

Up to 12 months after surgery, a significant decrease in CD4⁺ RTE was observed, which was most significant between time points zero and six months (Table 3). No differences were seen for these RTE within the CD8⁺ T-cell compartment for the total obesity, no MetS and the MetS groups (Table 3).

A decrease in both EM and CD28null differentiated T-cells was noted for in CD4⁺ T-cells in the total obesity group (Table 3). Pairwise comparisons revealed the most significant decrease in the period between zero to six months postoperatively. Comparison of the groups with and without MetS, the decrease in CD28null CD4⁺ T-cells remained significant in the MetS group only. A decrease in CD8⁺ T-cell differentiation was reflected by a significant increase in CM and a decrease in EM T-cells. A trend towards decrease was seen for both EMRA and CD28null CD8⁺ T-cells. Upon dissection of the morbidly obese patients into the no MetS and MetS group, a trend towards lower numbers of CD8⁺ EMRA T-cells was observed for the MetS group (Table 3).

Relative telomere length restores in the first months after bariatric surgery

Telomere attrition seemed to restore following bariatric surgery in morbidly obese patients with MetS up to six months after surgery, with a significant increase in RTL between zero and three months postoperatively. However, a shortening was observed at 12 months postoperatively with an overall significant effect between zero and 12 months ($P=0.02$) (Figure 2A). Comparison between individual time points showed a significant increased directionality in CD4⁺ RTL within the first three months after surgery, however a decline in RTL was shown at the later time points, of which the decrease between three and 12 months remained significant after adjusting ($P=0.04$).

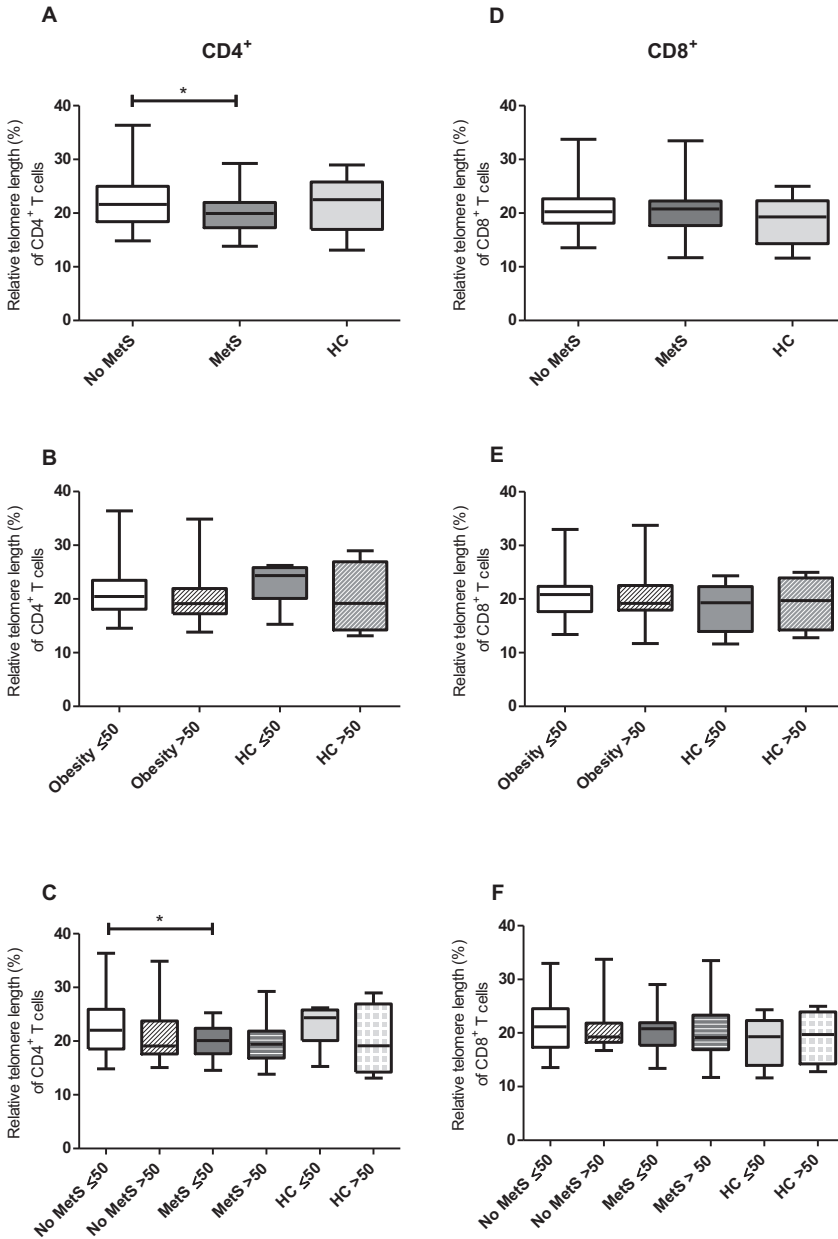


Figure 1. Relative telomere length (RTL) prior to bariatric surgery. (A) RTL of CD4⁺ T-cells was significantly lower in the MetS group compared to no MetS. (B) Age did not have an effect on RTL of CD4⁺ T-cells. (C) In patients ≤50 years, MetS resulted in lower CD4⁺ RTL than in the absence of MetS. In patients >50 years, a large spread in interquartile range was seen in both groups. (D) No changes were seen in the CD8⁺ RTL due to MetS, (E) due to age or (F) due to both MetS and age. MetS = metabolic syndrome. HC = healthy controls. * = $P < 0.05$.

These significances were lost after dividing the group into a no MetS (Figure 2B) and a MetS (Figure 2C) group. The CD8⁺ RTL showed no significant changes over time in either the total obesity (Figure 2D), the no MetS (Figure 2E) or the MetS (Figure 2F) group.

Table 3. *P*-values of the different T-cell differentiation markers of both CD4⁺ and CD8⁺ of the different patient cohorts between 0 and 12 months after bariatric surgery

Parameter	Obesity	No MetS	MetS
CD4 T-cells	0.18	0.24	0.24
CD4 Naive T-cells	0.11	0.15	0.33
CD4 CD31 naive T-cells	0.03 (↓)	0.15	0.12
CD4 Memory T-cells	0.27	0.24	0.62
CD4 Central-memory T-cells	0.39	0.24	0.80
CD4 Effector-memory T-cells	0.02 (↓)	0.07	0.07
CD4 EMRA T-cells	0.19	0.83	0.20
CD4 CD28null memory T-cells	0.01 (↓)	0.15	0.048 (↓)
CD8 T-cells	0.47	0.80	0.15
CD8 Naive T-cells	0.78	0.90	0.53
CD8 CD31 naive T-cells	0.32	0.24	0.80
CD8 Memory T-cells	0.06	0.15	0.12
CD8 Central-memory T-cells	0.03 (↑)	0.31	0.12
CD8 Effector-memory T-cells	0.045 (↓)	0.31	0.15
CD8 EMRA T-cells	0.07	0.19	0.07
CD8CD28null memory T-cells	0.07	0.11	0.15

Obesity = total group of patients. No MetS = all patients without MetS. MetS = all patients with MetS. Significant comparisons are depicted in bold. Arrows indicate direction of significance.

DISCUSSION

In present study, we show that prior to bariatric surgery morbidly obese patients with metabolic syndrome (MetS) have shorter telomeres than morbidly obese patients without MetS, which is most pronounced in the younger age group. This attrition of telomeres is accompanied by a more differentiated T-cell compartment, indicating that MetS results in accelerated aging of T-cells. After surgery, this more differentiated T-cell status was ameliorated including a partial restoration of telomeres in the first six months

postoperatively. Our results suggest that bariatric surgery may facilitate partial restoration of this accelerated T-cell aging and thus may help to ameliorate morbidity in morbidly obese patients.

The underlying chronic inflammatory state in obesity resembles the consequences of inflammaging as seen in older healthy individuals. Inflammaging affects the immune system, causing a release of cytokines which eventually leads in a vicious circle to increased damage on cells and tissues²⁸. Also, the thymus involutes with age resulting in remodeling of the CD4/CD8 T-cell ratio and an enhanced T-cell differentiation state^{8,26}. T-cells are part of the adaptive immune system and are derived from lymphoid precursor cells in bone marrow, migrating towards the thymus to further differentiate. In response to infectious agents, either T-helper (CD4⁺) or T-cytotoxic (CD8⁺) cells differentiate from naive to into memory cells to generate a potent second response to the same stimuli. Within the memory T-cell pool, central (CM) and effector memory (EM) T-cells can be distinguished, both with different phenotypical and functional characteristics. CM and EM T-cells are predominant within circulating CD4⁺ and CD8⁺ T-cells, respectively²⁷. Changes to the T-cell mediated adaptive immunity due to obesity has been shown before, for instance obesity increases both the total numbers of CD4⁺ and CD8⁺ T-cells²⁸ while causing a decrease in CD4⁺ regulatory T-cells^{11,29,30}. The effects of obesity on maturation of the T-cell system has only been investigated in children, where obesity led to an increase in differentiated EM and EMRA T-cells³¹. In patients with renal failure, uremia causes a chronic inflammatory environment inducing a severe depletion of naive T-cells and a shift to more differentiated T-cells, reflected by a decrease in CM and increase in EM and EMRA^{15,32,33}. In this study, we show that obesity causes a shift towards fully differentiated T-cell effector memory cells (EMRA) with a much stronger effect in older patients with MetS. Presumably, the number of differentiated T-cells increases with age while the number of naive cells decreases³⁴. We confirm the latter, however after correcting for age and the presence of MetS we showed a strikingly different T-cell compartment with a decrease in naive T-cells and a marked increase in EMRA and CD28null T-cells. These results were much more pronounced in the CD8⁺ T-cell compartment, which is in line with the latest literature showing that the immunological changes due to obesity affect mostly CD8⁺ T-cells¹³. This pronounced effect of MetS on T-cell immunity and telomere length is of clinical interest, since it enables us to identify patients within the morbidly obese patients who have a potentially increased risk of morbidity and therefore a higher need for surgical intervention.

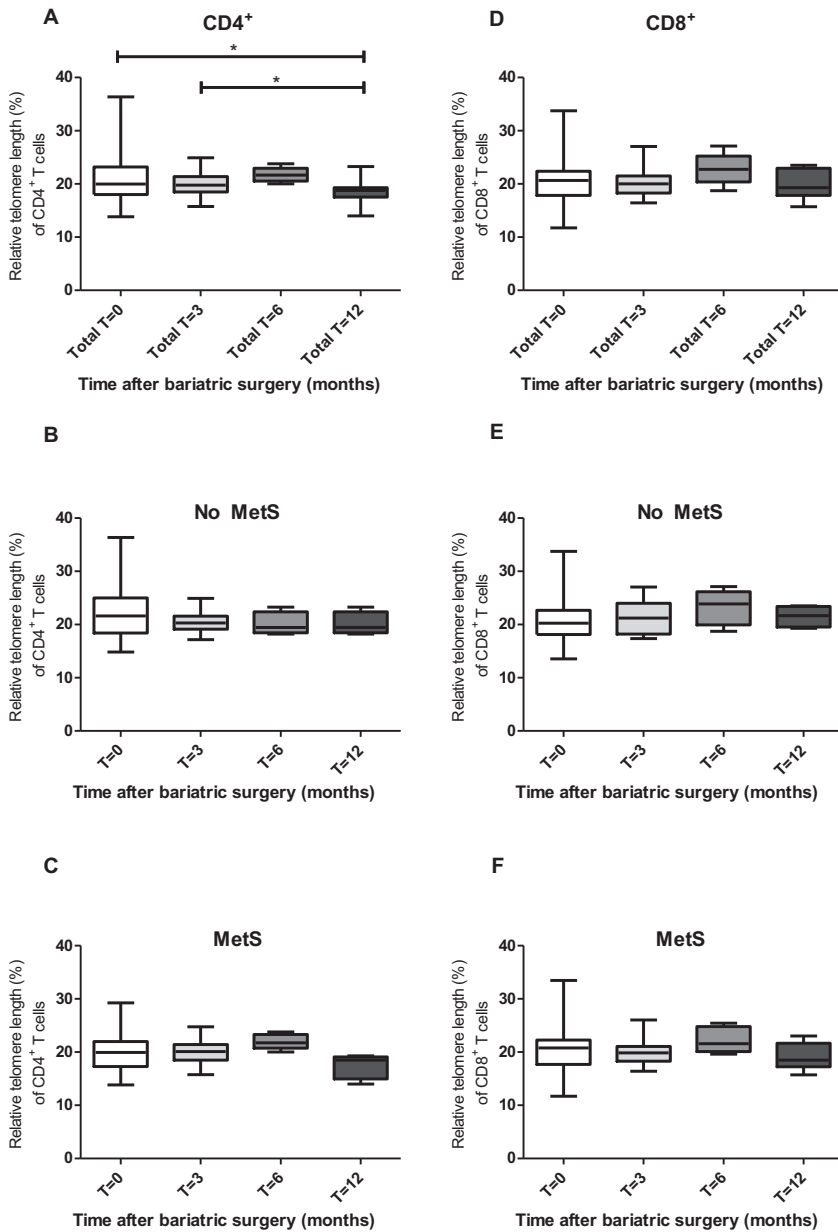


Figure 2. Relative telomere length (RTL) after bariatric surgery. (A) CD4⁺ RTL of the total obesity group significantly increased up to six months postoperatively, after which RTL significantly declined again. (B) No CD4⁺ RTL differences were seen in the group without MetS, or (C) in the group with MetS. (D) No changes were seen in the CD8⁺ RTL due to obesity, or (E) in the group without MetS or (F) with MetS. A paired samples test was used; missing values were excluded from the analysis. MetS = metabolic syndrome. * = $P < 0.05$.

T-cell aging is associated with attrition of telomeres, which can be easily measured in circulating T-cells via flowcytometry^{22,35}. A relationship between obesity and telomere attrition in circulating leukocytes and T-cells has been previously described, however the results are ambiguous^{11,24,36,37}. One study also investigated the importance of MetS but could not find a deleterious role of MetS on telomere shortening in leukocytes³⁹. In addition to obesity itself, we show that enhanced telomere attrition occurs when MetS as a comorbidity is present in morbidly obese patients, most notable in patients of ≤ 50 years. Differences in the methods used to measure telomere length might contribute to the discrepancies with other studies. Namely, the other groups used a quantitative PCR assay technique to measure relative telomere length and our flowcytometry assay might be more sensitive to pick up differences within a particular population of T-cells³⁶.

The hypothesis that bariatric surgery ameliorates attrition of telomeres in addition to resolving the obesity-associated diseases such as diabetes mellitus, has been investigated previously but results are inconclusive^{36,37}. These studies are not directly comparable since the follow-up period after bariatric surgery differs between one and 10 years. Formichi et al.³⁷ showed a significant decline at three, six and 12 months postoperatively, while we showed a trend towards increase in RTL in the first three months postoperatively until a decline was seen only at 12 months postoperatively. This improvement induced earlier on after surgery is in line with the rapid weight loss and reversal of diabetes mellitus as seen after bariatric surgery²⁵. As Formichi et al. mentioned, the decline in RTL could be induced by the acute catabolic state induced by bariatric surgery³⁷. Further research and larger cohort studies are warranted in order to investigate whether RTL might be further restored after bariatric surgery and at which time point this might be visible. In addition to the effects on RTL, bariatric surgery also induced subtle changes in the T-cell differentiation state, a link that has not been investigated previously. Especially in the total obesity group a decrease in more matured T-cells was shown, while MetS revealed to be an independent factor for the decrease in CD4⁺ CD28null T-cells. These results underscore that bariatric surgery may restore the premature immunological T-cell aging seen in morbidly obese patients. Since the eligibility of bariatric surgery is still largely dependent on general indicators such as BMI, this study justifies the need for clarification of the criteria for bariatric surgery based on individual patient characteristics.

Telomere attrition and T-cell differentiation status are influenced by various, mostly non-adjustable factors such as age and CMV-seropositivity²². While we show no differences in RTL due to these factors, we do demonstrate that CMV and age are both independent factors for enhanced T-cell differentiation status. These results were most prominent in the CD8⁺ T-cell population, which is in line with previous findings³⁴. We also identified the effect of gender on RTL as well as T-cell differentiation, since the restoration of RTL

and T-cell differentiation was more pronounced in the female patients. This suggests a dominant effect of gender on T-cell aging. These effects could be mitigated since female patients undergoing bariatric surgery are usually younger than males. Whether female patients might benefit more from bariatric surgery concerning T-cell aging remains unclear. Further studies should fortify the role of gender on premature aging of morbidly obese patients.

There are several limitations attached to this study. The sample size of morbidly obese patients and the healthy control group is relatively small which could conceal effects on different subpopulations within our cohort. Especially the selected group of patients investigated after surgery is small as well as the short follow-up period of one year. Further inclusions would increase the likelihood of revealing differences in the studied cohort. Also, a longer follow-up period gives additional information about the long-term effects of bariatric surgery on T-cell differentiation. In addition, since we measured RTL in the total circulating CD4⁺ and CD8⁺ T-cell compartments the effects seen in RTL might be the result of shifts in specific T-cell subsets as seen for the significant increase in CD28null T-cells due to obesity and MetS. Further studies should identify the changes in RTL within these specific subsets to correlate these findings. Finally, not all effects of obesity are reflected in the circulation and therefore investigating the effects on the corner stone of obesity, the fat tissue itself, will allow the association between the effect of excess of fat tissue and changes seen in the immune system.

In conclusion, we show that the metabolic syndrome induced by morbid obesity causes telomere attrition in combination with enhanced T-cell differentiation in both circulating CD4⁺ and CD8⁺ T-cells, indicative of accelerated aging of the T-cell compartment. This shortening of telomeres and enhanced T-cell differentiation state are ameliorated shortly after bariatric surgery. These data suggest that obese patients with MetS are at risk for accelerated aging of the T-cell immune system and might benefit from bariatric surgery at an earlier stage.

SUBJECTS AND METHODS

Study design

This study was designed as a non-randomized prospective cohort-study. The study was approved by the general Medical Ethical Committee (METC) with MEC identification number 2012-134 of the Erasmus University Medical Center, Rotterdam, the Netherlands. Approval of the inclusion center occurred via the Board of Directors of the Maasstad Hospital, Rotterdam, the Netherlands, with local identification number 2012-51. The

study is performed in accordance with the local METC guidelines. The trial is registered as part of the PROTECT trial in the Dutch trial registry database using trial code 3663 (www.trialregister.nl). This study was performed in accordance with the CONSORT 2010 statement, according to the Declaration of Helsinki³⁸.

Healthy living kidney donors and healthy volunteers that gave written informed consent served as age-matched healthy controls (HC) (n=10) and the study was approved by the Medical Ethical Committee of the Erasmus MC (Biobank of the METC, METC number 2012-022).

Study population

Patients with obesity and morbid obesity scheduled to undergo bariatric surgery whom visited the outpatient clinic at the Maastad Hospital between March 2014 and August 2015 were invited to participate in the study. All participating patients gave written informed consent before inclusion. A patient flowchart showing all inclusions and exclusions is depicted in Figure S1. To be eligible for bariatric surgery, patients had to have a body mass index (BMI, kg/m² ≥ 35 with or without the presence of the metabolic syndrome (MetS). MetS was defined in accordance to the National Cholesterol Education Program ATP III Guidelines, as fulfilling 3 out of 5 criteria³⁹. Exclusion criteria were a BMI < 35, other comorbidities than MetS, patients without basic understanding of the Dutch or English language, or patients undergoing another form of bariatric surgery than a laparoscopic gastric bypass procedure (LGBP).

Bariatric surgery

The LGBP was used in all patients. In short, the jejunum is divided at 50 cm from the ligament of Treitz into a biliopancreatic limb and a 150-cm alimentary Roux-limb. The proximal segment of the stomach is made into a small pouch with stapling devices. A side-to-side anastomosis is created between the pouch and the Roux-limb. The biliopancreatic limb is connected to the Roux limb, 150 cm distally.

Blood collection

After providing written informed consent, a venous blood sample was obtained prior to surgery. The duration until scheduled surgery was between several days and five months after first blood sample. At time points prior to bariatric surgery, venous samples of 108 patients were collected for analysis. A selection of patients was asked to donate another venous blood sample at time points three (n=48), six (n=10) and 12 (n=11) months after surgery (Figure S1). The selection was made since not all patients showed up in the outpatient clinic during their scheduled follow-up clinics, or patients decided to be followed-up elsewhere

(for example by their general practitioner). All blood samples were collected in 10.0 mL BD Lithium-Heparin tubes (Franklin Lakes, NJ, USA), with a maximum of two tubes per time point.

CMV serology

Cytomegalovirus (CMV) serology was assessed of all participants included in the study at the diagnostic Department of Virology of Erasmus University Medical Center, by determining the presence of plasma IgG antibodies to CMV with an enzyme immune assay (Biomérieux, VIDAS, Lyon, France). The results were expressed as arbitrary units/mL (AU/mL), and an outcome of ≥ 6 AU/mL was considered positive.

T-cell phenotyping and PBMC isolation

A whole blood staining was performed and analyzed on the BD FACSCanto II (BD (Erembodegem, Belgium) using FACSDiva software version 6.1.2 (BD) in order to determine percentages and absolute numbers of T-cell subsets (Table 1). The analysis procedure as well as further characterization of the T-cells has been described previously⁴⁰. Peripheral blood mononuclear cells (PBMC) were isolated from heparinized blood samples by Ficoll gradient centrifugation as described in detail before⁴¹. PBMC were stored at -150°C at 10×10^6 per vial until further experiments.

Table 1. T-cell subsets and their corresponding staining markers

T-cell subset	Marker
Recent thymic emigrants (RTE)	CD31+ naive
Naive T-cells	CD45RO- / CCR7+
Central memory T-cells (CM)	CD45RO+ / CCR7+
Effector memory T cecls (EM)	CD45RO+ / CCR7-
Terminally differentiated effector memory T-cells (EMRA)	CD45RO - / CCR7-
Total memory T-cells (MEM)	Sum of CM, EM & EMRA
Advanced differentiated T-cells	CD28null

Relative telomere length

The relative telomere length of peripheral blood T-cells was determined by flow fluorescent in situ hybridization (flowFISH) technique, as described previously¹⁵. By using the subcell line 1301 of CCRF-CEM (known for its long telomeres) as a reference, a relative telomere length was calculated using the following formula:

$$RTL = \frac{(\text{median FL1 sample cells with probe} - \text{median FL1 sample cells without probe}) \times \text{DNA index of control (=2)cells}}{(\text{median FL1 control cells with probe} - \text{median FL1 control cells without probe}) \times \text{DNA index of sample (=1)cells}} \times 100$$

Statistical analysis

Statistics were computed with use of SPSS version 23 (IBM Corp, released 2015, IBM SPSS Statistics for Mac, Version 23.0, Armonk, NY: IBM Corp), and GraphPad Prism (GraphPad Software Inc., version 5.01). For all individual parameters, median and interquartile ranges were computed. Comparison of more than two parameters was done via One-Way ANOVA, considering normal distribution as tested by the Gaussian approximation. Related samples from the same patient were analyzed via the related-samples Friedman's test. Prior to bariatric surgery a multivariate analysis was computed via general linear models option in SPSS, considering the Wilks' Lambda test to evaluate which variables contributed to T-cell characteristics measured in the circulation. Figures were made in Graphpad. For all parameters, $P < 0.05$ was considered significant.

REFERENCES

1. Follow-up to the Political Declaration of the High-level Meeting of the General Assembly on the Prevention and Control of Non-Communicable Diseases 2013 [Available from: http://apps.who.int/eur.idm.oclc.org/gb/ebwha/pdf_files/WHA66/A66_R10-en.pdf].
2. Grundy SM. Metabolic syndrome update. *Trends Cardiovasc Med*. 2016;26(4):364-73.
3. Cao H. Adipocytokines in obesity and metabolic disease. *J Endocrinol*. 2014;220(2):T47-59.
4. Ouchi N. Adipocytokines in Cardiovascular and Metabolic Diseases. *J Atheroscler Thromb*. 2016;23(6):645-54.
5. Daniele G, Guardado Mendoza R, Winnier D, Fiorentino TV, Pengou Z, Cornell J, et al. The inflammatory status score including IL-6, TNF-alpha, osteopontin, fractalkine, MCP-1 and adiponectin underlies whole-body insulin resistance and hyperglycemia in type 2 diabetes mellitus. *Acta Diabetol*. 2014;51(1):123-31.
6. Han CY. Roles of Reactive Oxygen Species on Insulin Resistance in Adipose Tissue. *Diabetes Metab J*. 2016;40(4):272-9.
7. Jura M, Kozak LP. Obesity and related consequences to ageing. *Age (Dordr)*. 2016;38(1):23.
8. Xia S, Zhang X, Zheng S, Khanabdali R, Kalionis B, Wu J, et al. An Update on Inflamm-Aging: Mechanisms, Prevention, and Treatment. *J Immunol Res*. 2016;2016:8426874.
9. Boi SK, Buchta CM, Pearson NA, Francis MB, Meyerholz DK, Grobe JL, et al. Obesity alters immune and metabolic profiles: New insight from obese-resistant mice on high-fat diet. *Obesity (Silver Spring)*. 2016;24(10):2140-9.
10. Maioli TU, Goncalves JL, Miranda MC, Martins VD, Horta LS, Moreira TG, et al. High sugar and butter (HSB) diet induces obesity and metabolic syndrome with decrease in regulatory T-cells in adipose tissue of mice. *Inflamm Res*. 2016;65(2):169-78.
11. Wagner NM, Brandhorst G, Czepluch F, Lankeit M, Eberle C, Herzberg S, et al. Circulating regulatory T-cells are reduced in obesity and may identify subjects at increased metabolic and cardiovascular risk. *Obesity (Silver Spring)*. 2013;21(3):461-8.
12. Sultan A, Strodthoff D, Robertson AK, Paulsson-Berne G, Fauconnier J, Parini P, et al. T-cell-mediated inflammation in adipose tissue does not cause insulin resistance in hyperlipidemic mice. *Circ Res*. 2009;104(8):961-8.
13. Apostolopoulos V, de Courten MP, Stojanovska L, Blatch GL, Tangalakis K, de Courten B. The complex immunological and inflammatory network of adipose tissue in obesity. *Mol Nutr Food Res*. 2016;60(1):43-57.
14. Betjes MG, Litjens NH, Zietse R. Seropositivity for cytomegalovirus in patients with end-stage renal disease is strongly associated with atherosclerotic disease. *Nephrol Dial Transplant*. 2007;22(11):3298-303.
15. Betjes MG, Langerak AW, van der Spek A, de Wit EA, Litjens NH. Premature aging of circulating T-cells in patients with end-stage renal disease. *Kidney Int*. 2011;80(2):208-17.

16. Derhovanessian E, Larbi A, Pawelec G. Biomarkers of human immunosenescence: impact of Cytomegalovirus infection. *Curr Opin Immunol.* 2009;21(4):440-5.
17. Litjens NH, de Wit EA, Betjes MG. Differential effects of age, cytomegalovirus-seropositivity and end-stage renal disease (ESRD) on circulating T lymphocyte subsets. *Immun Ageing.* 2011;8(1):2.
18. Wikby A, Johansson B, Olsson J, Lofgren S, Nilsson BO, Ferguson F. Expansions of peripheral blood CD8 T-lymphocyte subpopulations and an association with cytomegalovirus seropositivity in the elderly: the Swedish NONA immune study. *Exp Gerontol.* 2002;37(2-3):445-53.
19. van de Berg PJ, Griffiths SJ, Yong SL, Macaulay R, Bemelman FJ, Jackson S, et al. Cytomegalovirus infection reduces telomere length of the circulating T-cell pool. *J Immunol.* 2010;184(7):3417-23.
20. Naylor K, Li G, Vallejo AN, Lee WW, Koetz K, Bryl E, et al. The influence of age on T-cell generation and TCR diversity. *J Immunol.* 2005;174(11):7446-52.
21. Zubakov D, Liu F, van Zelm MC, Vermeulen J, Oostra BA, van Duijn CM, et al. Estimating human age from T-cell DNA rearrangements. *Curr Biol.* 2010;20(22):R970-1.
22. Aubert G, Lansdorp PM. Telomeres and aging. *Physiol Rev.* 2008;88(2):557-79.
23. Huzen J, Wong LS, van Veldhuisen DJ, Samani NJ, Zwinderman AH, Codd V, et al. Telomere length loss due to smoking and metabolic traits. *J Intern Med.* 2014;275(2):155-63.
24. Weischer M, Bojesen SE, Nordestgaard BG. Telomere shortening unrelated to smoking, body weight, physical activity, and alcohol intake: 4,576 general population individuals with repeat measurements 10 years apart. *PLoS Genet.* 2014;10(3):e1004191.
25. Nguyen NT, Varela JE. Bariatric surgery for obesity and metabolic disorders: state of the art. *Nat Rev Gastroenterol Hepatol.* 2016.
26. Baylis D, Bartlett DB, Patel HP, Roberts HC. Understanding how we age: insights into inflammaging. *Longev Healthspan.* 2013;2(1):8.
27. Sallusto F, Geginat J, Lanzavecchia A. Central memory and effector memory T-cell subsets: function, generation, and maintenance. *Annu Rev Immunol.* 2004;22:745-63.
28. Duffaut C, Zakaroff-Girard A, Bourlier V, Decaunes P, Maumus M, Chiotasso P, et al. Interplay between human adipocytes and T lymphocytes in obesity: CCL20 as an adipochemokine and T lymphocytes as lipogenic modulators. *Arterioscler Thromb Vasc Biol.* 2009;29(10):1608-14.
29. Feuerer M, Herrero L, Cippolletta D, Naaz A, Wong J, Nayer A, et al. Lean, but not obese, fat is enriched for a unique population of regulatory T-cells that affect metabolic parameters. *Nat Med.* 2009;15(8):930-9.
30. Deiluiis J, Shah Z, Shah N, Needleman B, Mikami D, Narula V, et al. Visceral adipose inflammation in obesity is associated with critical alterations in tregulatory cell numbers. *PLoS One.* 2011;6(1):e16376.

31. Spielmann G, Johnston CA, O'Connor DP, Foreyt JP, Simpson RJ. Excess body mass is associated with T-cell differentiation indicative of immune ageing in children. *Clin Exp Immunol.* 2014;176(2):246-54.
32. Meijers RW, Betjes MG, Baan CC, Litjens NH. T-cell ageing in end-stage renal disease patients: Assessment and clinical relevance. *World J Nephrol.* 2014;3(4):268-76.
33. Meijers RW, Litjens NH, de Wit EA, Langerak AW, van der Spek A, Baan CC, et al. Cytomegalovirus contributes partly to uraemia-associated premature immunological ageing of the T-cell compartment. *Clin Exp Immunol.* 2013;174(3):424-32.
34. Tzanetakou IP, Katsilambros NL, Benetos A, Mikhailidis DP, Perrea DN. "Is obesity linked to aging?": adipose tissue and the role of telomeres. *Ageing Res Rev.* 2012;11(2):220-9.
35. Laimer M, Melmer A, Lamina C, Raschenberger J, Adamovski P, Engl J, et al. Telomere length increase after weight loss induced by bariatric surgery: results from a 10 year prospective study. *Int J Obes (Lond).* 2016;40(5):773-8.
36. Formichi C, Cantara S, Ciuoli C, Neri O, Chiofalo F, Selmi F, et al. Weight loss associated with bariatric surgery does not restore short telomere length of severe obese patients after 1 year. *Obes Surg.* 2014;24(12):2089-93.
37. Schulz KF, Altman DG, Moher D, Group C. CONSORT 2010 statement: updated guidelines for reporting parallel group randomised trials. *BMJ.* 2010;340:c332.
38. National Cholesterol Education Program Expert Panel on Detection E, Treatment of High Blood Cholesterol in A. Third Report of the National Cholesterol Education Program (NCEP) Expert Panel on Detection, Evaluation, and Treatment of High Blood Cholesterol in Adults (Adult Treatment Panel III) final report. *Circulation.* 2002;106(25):3143-421.
39. Meijers RW, Litjens NH, de Wit EA, Langerak AW, Baan CC, Betjes MG. Uremia-associated immunological aging is stably imprinted in the T-cell system and not reversed by kidney transplantation. *Transpl Int.* 2014;27(12):1272-84.
40. Litjens NH, Huisman M, Baan CC, van Druningen CJ, Betjes MG. Hepatitis B vaccine-specific CD4(+) T-cells can be detected and characterised at the single cell level: limited usefulness of dendritic cells as signal enhancers. *J Immunol Methods.* 2008;330(1-2):1-11.

SUPPLEMENTARY DATA

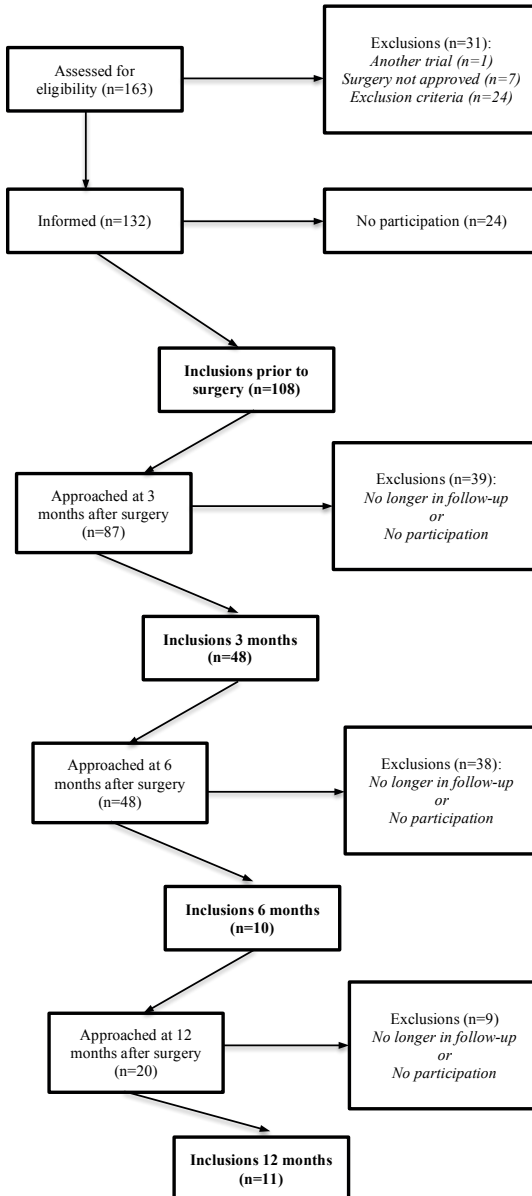


Figure S1. Flowchart showing patient inclusion and exclusion criteria. Exclusion criteria were based on the preset exclusion criteria, mainly based on the criteria for the presence of metabolic syndrome as set by the National Cholesterol Education Program ATPIII Guidelines. Eligible patients set for undergoing bariatric surgery were approached at the outpatient clinic at the Maasstad Hospital, Rotterdam, the Netherlands.

Table S1. Multivariate analysis of the factors MetS, age, CMV-status and gender on relative telomere length and T-cell differentiation status prior to bariatric surgery

Model	Factors			
	MetS	Age	CMV-status	Gender
Model 1:				
RTL: CD4 ⁺ & CD8 ⁺	0.13	0.64	0.47	0.98
Model 2				
T-cell phenotype: CD4 ⁺	0.36	0.57	<0.001	0.29
Model 3				
T-cell phenotype: CD8 ⁺	0.77	0.03	0.005	0.01

Significant *P*-values (*P*<0.05) are depicted in bold. Model = the generalized linear model based on mentioned variables. MetS: MetS vs. no MetS; Age: >50 vs. ≤50 years; CMV-status: CMV+ vs. CMV-; Gender: female vs. male. T-cell phenotype included the following T-cell subsets: naive, CD31 naive, central memory, effector memory, effector memory RA, memory, CD28null and absolute T-cell numbers. MetS = metabolic syndrome; CMV = cytomegalovirus; RTL = relative telomere length.

CHAPTER 7

PREOPERATIVE CALORIE AND PROTEIN RESTRICTION IS FEASIBLE AND SAFE IN HEALTHY KIDNEY DONORS AND MORBIDLY OBESE PATIENTS: A PILOT STUDY

Franny Jongbloed, Ron W.F. de Bruin, René A. Klaassen,
Piet Beekhof, Harry van Steeg, Frank J.M.F. Dor, Erwin van
der Harst, Martijn E.T. Dollé, Jan N.M. IJzermans

Nutrients. 2016 May 20;8(5):306

ABSTRACT

Surgery-induced oxidative stress increases the risk of perioperative complications and delay in postoperative recovery. In mice, short-term preoperative dietary and protein restriction protect against oxidative stress. We investigated the feasibility of a calorie- and protein-restricted diet in two patient populations. In this pilot study, 30 living kidney donors and 38 morbidly obese patients awaiting surgery were randomized into three groups: a restricted diet group, who received a synthetic liquid diet with 30% fewer calories and 80% less protein for five consecutive days; a group who received a synthetic diet containing the daily energy requirements (DER); and a control group. Feasibility was assessed using self-reported discomfort, body weight changes, and metabolic parameters in blood samples. Twenty patients (71%) complied with the restricted and 13 (65%) with the DER-diet. In total, 68% of the patients reported minor discomfort that resolved after normal eating resumed. The mean weight loss on the restricted diet was significantly greater (2.4 kg) than in the control group (0 kg, $P=0.002$), but not in the DER-diet (1.5 kg). The restricted diet significantly reduced levels of serum urea and plasma prealbumin (PAB) and retinol binding protein (RBP). A short-term preoperative calorie- and protein-restricted diet is feasible in kidney donors and morbidly obese patients. Compliance is high and can be objectively measured via changes in urea, PAB, and RBP levels. These results demonstrate that this diet can be used to study the effects of dietary restriction on surgery-induced oxidative stress in a clinical setting.

INTRODUCTION

Reactive oxygen species (ROS) that the body produces during surgical procedures induce oxidative stress and lead to imbalances in homeostasis^{1,2}. The subsequent stress response elicits hormonal, metabolic, and immunological changes that increase the risk of perioperative complications and may hamper postoperative recovery^{1,3}. This risk is increased by pre-existing factors such as obesity⁴, and by perioperative factors such as ischemia-reperfusion injury (IRI) during organ transplantation^{5,6}. Although treatments that decrease ROS production could reduce perioperative and postoperative complications, no effective clinical therapy is currently available.

In animal studies, dietary restriction (DR) protects against ROS-induced damage. We demonstrated previously that short-term preoperative 30% DR protects against the oxidative damage induced by renal IRI in mice and improves postoperative survival and kidney function⁷⁻⁹, and similarly protects against liver IRI¹⁰. The beneficial effects of fasting on renal IRI are also observed in aged obese mice of both genders, suggesting that DR induces protection against ROS independent of age and gender¹¹.

Translating DR to humans in a clinical setting is difficult, because of the effort required by patients to voluntarily restrict their calorie intake. In addition, DR goes against the generally held beliefs that patients should be well fed before surgery to prevent malnutrition. Finally, the diet composition and duration that induce similar benefits in humans as observed in rodents is not known¹². Studies examining the effects of a very low-calorie diet prior to bariatric surgery report contradictory effects on perioperative and postoperative outcomes, and adherence to the diet in these studies was not measured objectively^{13,14}. In our previous pilot study in living kidney donors, we showed that three days of 30% DR followed by 24 h of fasting prior to kidney donation was feasible and safe, but had limited effects on outcome^{15,16}. Subsequent results from murine experiments suggested that the beneficial effects were mainly due to restriction in protein intake¹⁷. The effect of protein restriction (PR) has not yet been investigated in a clinical setting.

Therefore, our current pilot study investigated the feasibility of a preoperative diet combining DR and PR in two patient populations: living kidney donors and morbidly obese patients scheduled for laparoscopic donor nephrectomy or laparoscopic bariatric surgery, respectively. To identify objective markers of diet adherence, we measured both standard and experimental metabolic markers. Our results showed that short-term DR is feasible and represents a promising next step in investigating the effects of preoperative DR on surgery-related outcome in a clinical setting.

RESULTS

Study population

Of the 45 living kidney donors that were included initially and who underwent randomization, 30 were equally distributed ($n = 10$) in the three groups and completed the study. Of the 54 morbidly obese patients that were included initially, 38 were distributed in the three groups with 18 patients in the restricted diet group, 10 in the DER-diet group, and 10 in the control group (Figure S1). At baseline, the morbidly obese patients group had significantly higher average body weight and BMI and was significantly more often female (Table 1). There were no differences in the baseline characteristics after randomization between dropouts and patients who completed the study.

Table 1. Baseline characteristics of the study population

Parameter	Living Kidney Donors ($n = 30$)	Morbidly Obese Patients ($n = 38$)	<i>P</i> -Value
Age, years	47 ± 13	43 ± 9	0.17
Gender, F/M	12/18	31/7	0.003
Body weight, kg	82.8 ± 17.3	129.1 ± 24.6	<0.001
BMI, kg/m ²	26.6 ± 4.6	44.5 ± 5.4	<0.001

Baseline characteristics of the study population; Values are depicted as mean ± standard deviation; Significant *P*-values are depicted in bold; At baseline, the morbidly obese patients group had a significantly higher average body weight and BMI and were significantly more often female. F=female; M=male; BMI= body mass index.

Compliance with the diets by kidney donors and morbidly obese patients

A total of 10 living kidney donors and 18 morbidly obese patients were randomized into the restricted diet group. This group received a synthetic diet with a mean calorie restriction of 30% and a mean protein restriction of 80% relative to each patient's DER. Twenty individuals (71%) reported completing the five-day diet (Figure S2). Eight out of 10 kidney donors (80%), and 12 out of 18 morbidly obese patients (67%) reported completing the restricted diet.

Ten donors and 10 morbidly obese patients were randomized into the DER-diet. This group received a synthetic diet which resulted in a mean DR of 4% without PR. Thirteen out of 20 (65%) individuals receiving this diet reported completing the diet. Of the kidney donors, four out of 10 (40%) completed the diet; nine out of 10 (90%) morbidly obese patients completed the diet (Figure S2).

Twenty patients were randomized into the control group. Nine out of 10 donors (90%) filled in the diary for five consecutive days, while seven out of 10 (70%) morbidly obese patients filled in the diary. An analysis of the dietary diaries was performed to calculate average percentages of protein, carbohydrate and fat-intake. Nine patients in the control group had complete filled-in diaries and were included in the analysis. Average nutrient content consisted of 18% protein, 48% carbohydrates and 34% fat.

DISCOMFORT DURING THE DIETARY INTERVENTIONS

No major side effects were reported during or after the dietary interventions.

Twenty out of 28 individuals (71%) receiving the restricted diet reported 35 instances of minor discomfort that resolved during or directly after finishing the diet (Figure 1). In general, the shake drinks were well tolerated and were reported to be palatable. A higher percentage of kidney donors (40%) than morbidly obese patients (20%) reported discomfort related to nutritional intake, e.g., hunger and appetite. In contrast, a higher percentage of morbidly obese patients (90%) than kidney donors (20%) reported gastrointestinal discomfort, e.g., stool change, nausea, stomachache and dyspepsia. Three out of eight patients whom did not complete the diet mentioned gastrointestinal discomfort as the main reason.

Of patients on the DER-diet, 13 out of 20 (65%) reported 26 instances of minor discomfort during the diet. Kidney donors reported mostly gastrointestinal discomfort (90%), while the morbidly obese reported gastrointestinal discomfort (50%) and discomfort related to nutritional intake, such as distaste and appetite (50%).

Discomfort was scored semi-quantitatively using the VAS questionnaires at time points before, during, and after the diet. Patients that completed the restricted diet had significantly higher levels of nausea ($P=0.009$) and decreased wellbeing ($P=0.02$) during the diet than before the diet (Figure 2). These scores returned to baseline on day 1 after finishing the diet. There were no differences in pain scores at the three time points. Those on the DER-diet also reported higher nausea scores during the intervention ($P=0.04$). No differences were seen for the pain scores before, during, and after the diet for either dietary intervention, no changes were reported in the control group.

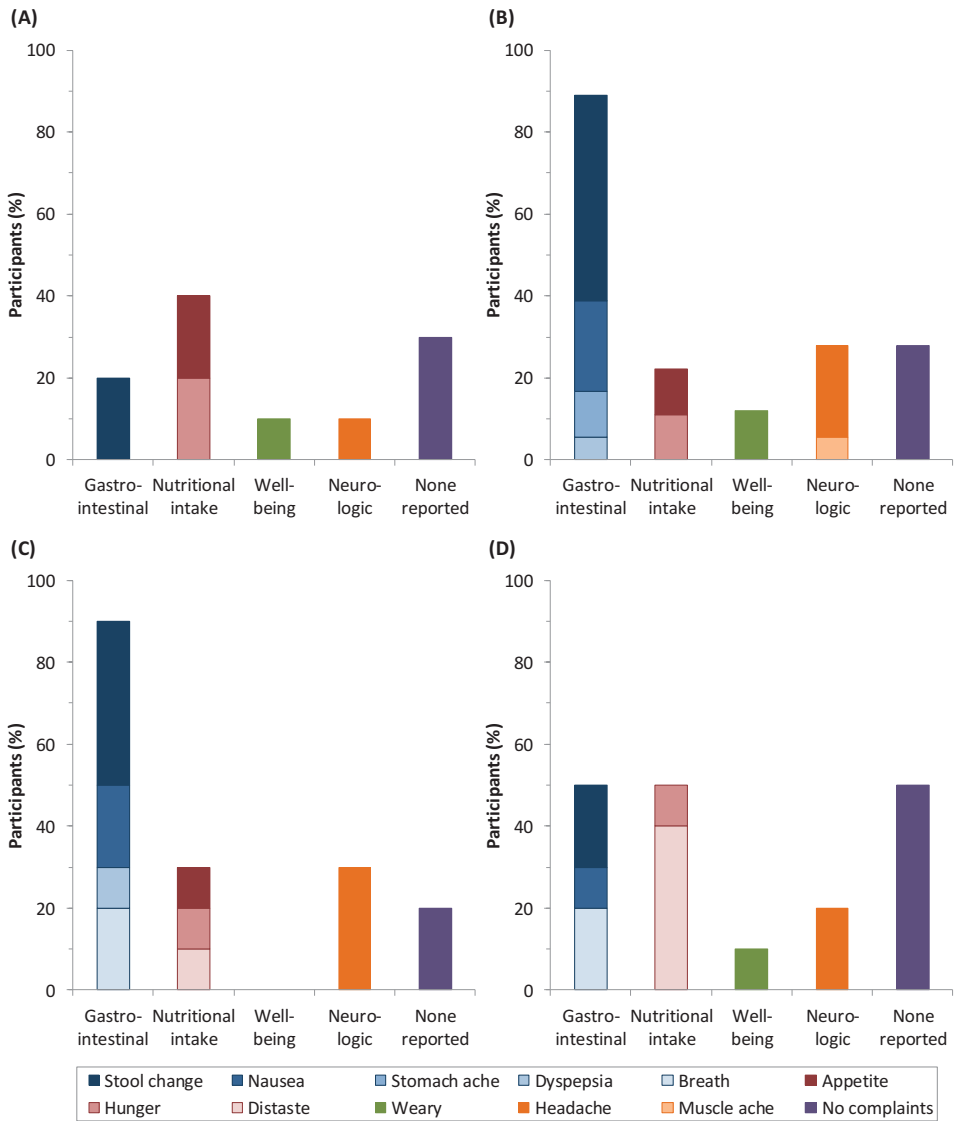


Figure 1. The number of side effects as percentages of participants in groups consuming a restricted diet and a daily energy requirements diet (DER-diet). (A) Side effects of the dietary restriction and protein restriction diet in the kidney donors were mostly related to nutritional intake and to the gastrointestinal tract; **(B)** Morbidly obese patients showed relatively more gastrointestinal discomfort; **(C)** A total of 90% of the kidney donors reported gastrointestinal discomfort during the DER-diet; **(D)** This percentage was lower in the morbidly obese patients and was the same as discomfort related to nutritional intake. Effects are clustered based on the origin of the symptoms. Within each cluster, each side effect is depicted in a different shade of color.

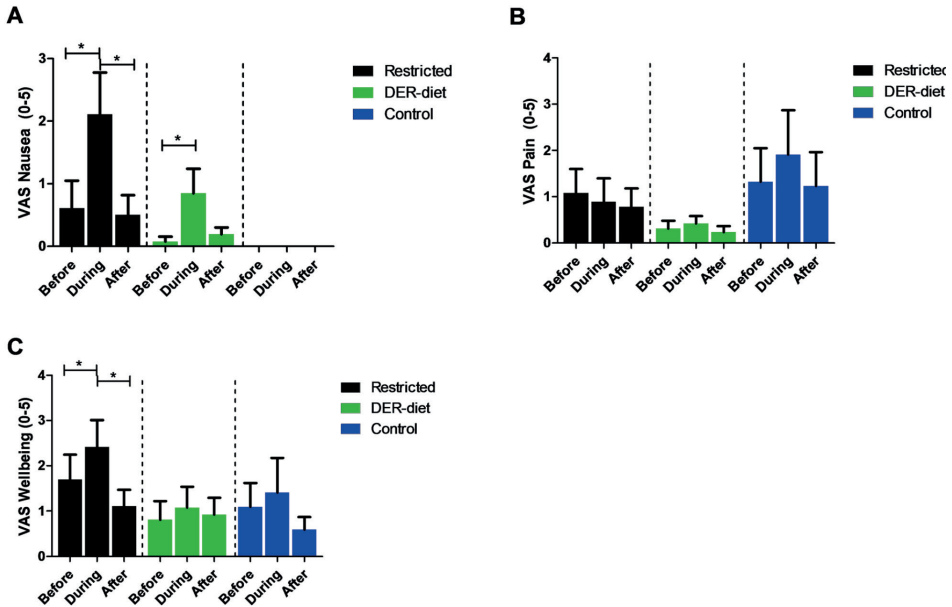


Figure 2. Visual Analogue Scores (VAS) for nausea, pain, and wellbeing before, during, and after each dietary intervention. (A) The nausea scores increased significantly for patients on the restricted diet and the DER-diet but normalized to baseline levels directly after the intervention period was over; (B) The pain scores did not change significantly during the dietary interventions; (C) The restricted diet resulted in significant decreased VAS wellbeing scores during the diet compared to before, but normalized again directly after the intervention period was over; * $P < 0.05$. Bars represent the standard error of the mean; DER = daily energy requirements.

Body weight

Individuals who adhered to the restricted diet lost on average 2.5% of their total body weight, corresponding to 2.4 ± 1.4 kg, based on the body weight measurements at the outpatient clinic before the start of the dietary restriction and on the day after its completion (Figure 3). This body weight loss was significantly greater ($P=0.002$) than in individuals without dietary restriction ($n=6$), who did not lose weight (0.2% of their total body weight). The body weight changes were not significantly different between the kidney donors and bariatric surgery patients. The DER-diet ($n=3$) resulted in an average loss of 1.5 ± 1.4 kg (1.7%), which was not significantly different from either the restricted diet group or the control group.

Markers of metabolism and compliance

Before and after all dietary interventions, blood samples were collected and serum and plasma was stored for further analyses. Only samples taken from fasted patients were used for these analyses. Due to the exclusion of samples from patients who did not fast, too few samples were available from the kidney donors for statistical analysis within this group. Therefore, the data from both kidney donors and morbidly obese patients were pooled. Due to a variation in baseline levels between the different patient groups, relative differences were compared between groups using the change in values before and after the intervention.

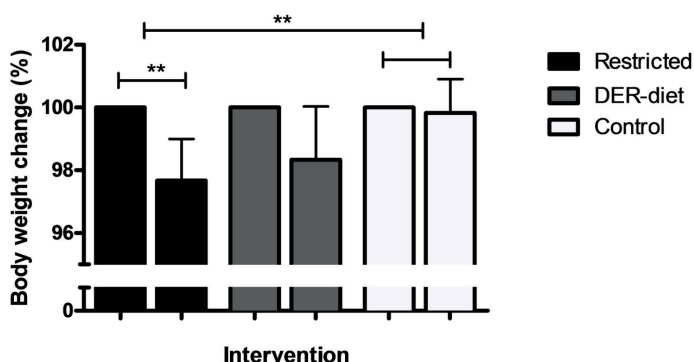


Figure 3. Body weight changes in the three dietary intervention groups. Patients on the restricted diet lost an average of 2.5% of their body weight, corresponding to 2.4 ± 1.4 kg; This body weight loss was significantly greater than in the control group, which showed no change; The DER-diet resulted in a 1.7% loss in body weight (1.5 ± 1.4 kg), which was not significantly different than the two other groups; Changes are shown as percentages compared to the body weight at baseline; ** $P < 0.01$. Bars represent the standard error of the mean. DER = daily energy requirements.

Metabolic changes due to the dietary interventions as well as intragroup variations were extensively assessed via a panel of 147 metabolic parameters (Table S1). The impact of the two diets on protein metabolism was measured using serum albumin, urea and amino acids levels. The restricted diet did not significantly change serum albumin (Figure 4A). Serum albumin was increased by 7% after the DER-diet, but did not reach significance ($P=0.006$). The increase after the DER-diet showed a trend towards higher levels compared to the relative change in the restricted diet ($P=0.006$) and the control group ($P=0.003$) (Table 2). No significant changes were seen in the control group. Serum urea was on average 37.5% lower after the restricted diet than before the diet ($P=0.002$), which was also significantly different from the DER-diet ($P < 0.001$) and the control group ($P < 0.001$) (Figure 4B). There were no significant changes in serum urea in the DER-diet group or in the control group.

Of the serum amino acids measured, none differed significantly between the groups (Figure 4C/D). The relative decrease of 18% in valine levels was significant compared to the relative difference of the DER-diet and the control group (Table 2). The cumulative sum of BCAAs, namely isoleucine, leucine and valine, showed a trend towards a decrease after the restricted diet ($P=0.005$), but not after the DER-diet or in the control group. The relative decrease of 16% in the combined BCAAs also showed a trend compared to the relative change after the DER-diet ($P=0.004$) and the control group ($P=0.004$). Other amino acid levels were not significantly changed after any of the diets.

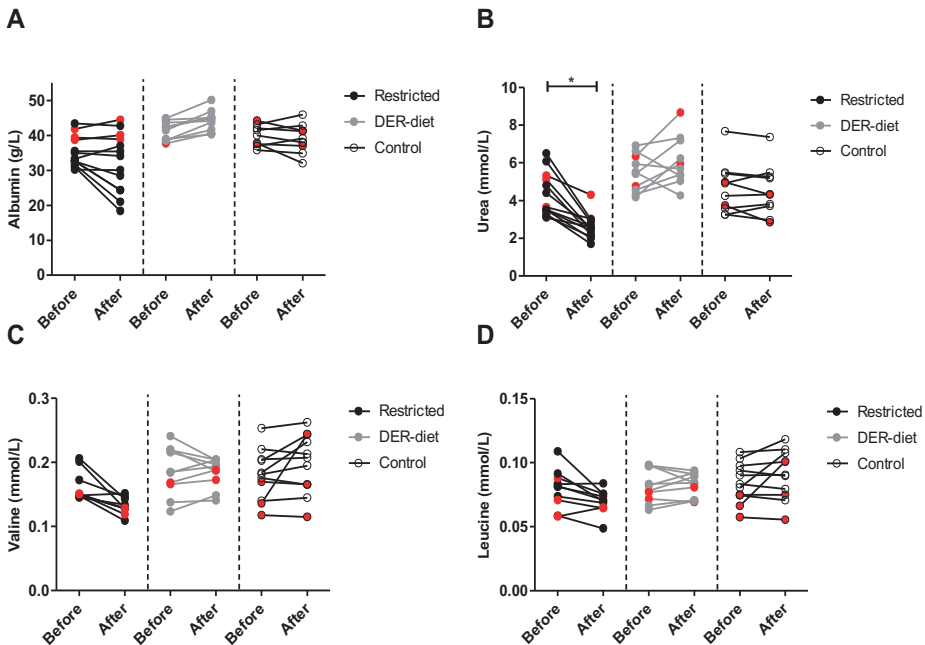


Figure 4. Serum levels of albumin, urea, valine and leucine after the three dietary interventions. (A) Serum albumin did not significantly change in any of the groups. (B) Serum urea was decreased significantly after the restricted diet, while it did not change after the DER diet or in the control group; both serum valine (C) and leucine (D) did not differ between groups, but did show a trend towards a decrease after the restricted diet; red symbols = kidney donors, as opposed to morbidly obese individuals (black or gray symbols); DER = daily energy requirements.

Neither serum markers glucose nor insulin changed significantly before *versus* after the intervention in three diet groups (Table 3). After the restricted diet, high-density-lipoprotein (HDL) was significantly decreased ($P=0.006$), but did not remain significant after the Bonferroni correction for multiple testing.

Table 2. Relative changes in metabolic parameters, amino acids and compliance markers after the dietary interventions with their corresponding *P*-value of intragroup differences

Parameter	Intervention			<i>P</i> -Value Restricted- DER	<i>P</i> -Value Restricted- Control	<i>P</i> -Value DER- Control
	Restricted Diet (% Change)	DER-Diet (% Change)	Control (% Change)			
<i>Metabolic</i>						
Albumin (g/L)	-9	+7.2	-1.9	<i>0.006</i>	0.212	<i>0.003</i>
Urea (mmol/L)	-37.5	+13.8	-2.6	<0.0001	<0.0001	0.067
Creatinine (mmol/L)	+15.1	12.2	-2.0	0.51	<i>0.009</i>	<i>0.03</i>
Glucose (mmol/L)	-1.8	-0.6	+6.2	0.76	0.10	0.20
Ferritin	+17.5	+21.2	+20.2	0.73	0.89	0.95
Insulin (pmol/L)	+27.2	+13.7	+52.2	0.70	0.68	0.34
<i>Amino Acids</i>						
Alanine (mmol/L)	-3.6	+3.1	-5.8	0.37	0.74	0.20
Glutamine (mmol/L)	+2.1	+0.1	+2.9	0.72	0.90	0.51
Glycine (mmol/L)	+7.8	+3.3	+5.0	0.37	0.61	0.73
Histidine (mmol/L)	-11.0	-8.6	-0.2	0.72	0.15	0.12
Isoleucine (mmol/L)	-12.8	-2.7	+11.0	0.15	<i>0.03</i>	0.15
Leucine (mmol/L)	-11.1	+2.1	+8.0	<i>0.01</i>	<i>0.01</i>	0.37
Phenylalanine (mmol/L)	-4.9	+5.3	+6.4	0.06	<i>0.03</i>	0.81
Tyrosine (mmol/L)	-10.0	+5.0	0.6	0.09	0.19	0.56
Valine (mmol/L)	-17.9	+0.7	+11.6	0.002	<i>0.003</i>	0.22
BCAA * (mmol/L)	-16.4	-1.3%	+8.8%	<i>0.004</i>	<i>0.004</i>	0.22
<i>Miscellaneous</i>						
Prealbumin (mg/L)	-17.2	+1.0	-1.2	0.002	0.0001	0.77
Retinol Binding Protein (mg/L)	-20.5	+5.6	-0.9	0.0002	0.0001	0.26

Relative changes in metabolic parameters, amino acids and compliance markers after the dietary interventions with their corresponding *p*-value of intragroup differences. Values are depicted as mean \pm standard error of the mean. Significant *p*-values are depicted in Italics. Significant *p*-values after the Bonferroni correction for multiple testing are depicted in bold and Italics. * BCAA = branched chain amino acids; cumulative sum of isoleucine, leucine and valine.

Table 3. Changes in metabolic parameters after the dietary intervention groups

Parameter	Intervention								
	Restricted Diet			DER-Diet			Control		
	Before	After	P-Value	Before	After	P-Value	Before	After	P-Value
<i>Metabolic</i>									
Albumin (g/L) *	35.2 ± 1.2	32.3 ± 2.4	0.09	41.3 ± 0.8	44.2 ± 0.9	0.006	39.9 ± 1.0	39.0 ± 1.3	0.57
Urea (mmol/L)	4.3 ± 0.3	2.6 ± 0.2	0.0002	5.5 ± 0.3	6.1 ± 0.4	0.19	4.7 ± 0.4	4.5 ± 0.4	0.36
Creatinine (mmol/L)	72.6 ± 3.3	83.4 ± 4.4	0.002	69.5 ± 3.7	78.5 ± 5.6	0.01	66.4 ± 6.4	63.5 ± 5.5	0.92
Glucose (mmol/L)	4.9 ± 0.2	4.8 ± 0.2	0.53	5.7 ± 0.2	5.6 ± 0.2	0.85	5.2 ± 0.3	5.8 ± 0.3	0.13
Insulin (pmol/L) **	62.4 ± 18.6	60.9 ± 18.9	1.00	98.4 ± 18.1	106.1 ± 23.2	0.28	157.6 ± 46.3	195.5 ± 65.1	0.46
Cholesterol (mmol/L)	5.1 ± 0.5	4.5 ± 0.6	0.03	4.7 ± 0.3	4.5 ± 0.3	0.13	4.4 ± 0.3	4.8 ± 0.3	0.19
Free fatty acids (mmol/L)	0.52 ± 0.03	0.72 ± 0.09	0.09	0.55 ± 0.05	0.67 ± 0.04	0.01	0.48 ± 0.05	0.56 ± 0.09	0.49
Saturated fatty acids (mmol/L)	4.18 ± 0.25	4.01 ± 0.21	0.11	3.46 ± 0.25	3.03 ± 0.19	0.002	3.59 ± 0.17	3.60 ± 0.17	0.27
Triglycerides (mmol/L)	1.31 ± 0.19	1.37 ± 0.25	0.97	1.60 ± 0.42	1.51 ± 0.28	0.92	1.57 ± 0.27	1.66 ± 0.31	0.70
HDL (mmol/L)	1.32 ± 0.09	1.12 ± 0.12	0.006	1.27 ± 0.09	1.24 ± 0.10	0.30	1.18 ± 0.11	1.28 ± 0.11	0.59
LDL (mmol/L)	3.9 ± 0.7	4.0 ± 0.7	0.69	2.9 ± 0.3	2.7 ± 0.3	0.06	2.6 ± 0.3	2.9 ± 0.3	0.32
<i>Amino Acids</i>									
Alanine (mmol/L)	0.45 ± 0.02	0.43 ± 0.4	0.49	0.44 ± 0.02	0.45 ± 0.02	0.77	0.45 ± 0.02	0.42 ± 0.02	0.37
Glutamine (mmol/L)	0.47 ± 0.02	0.47 ± 0.02	0.63	0.49 ± 0.02	0.49 ± 0.02	1.00	0.45 ± 0.02	0.46 ± 0.02	0.35
Glycine (mmol/L)	0.26 ± 0.007	0.28 ± 0.01	0.08	0.28 ± 0.009	0.29 ± 0.01	0.85	0.25 ± 0.006	0.26 ± 0.009	0.18
Histidine (mmol/L)	0.06 ± 0.003	0.06 ± 0.004	0.08	0.07 ± 0.003	0.06 ± 0.002	0.01	0.07 ± 0.003	0.07 ± 0.004	0.83
Isoleucine (mmol/L)	0.06 ± 0.004	0.05 ± 0.002	0.06	0.05 ± 0.005	0.05 ± 0.003	0.43	0.06 ± 0.004	0.06 ± 0.005	0.40
Leucine (mmol/L)	0.08 ± 0.005	0.07 ± 0.003	0.02	0.08 ± 0.004	0.08 ± 0.003	0.63	0.08 ± 0.005	0.09 ± 0.006	0.50
Phenylalanine (mmol/L)	0.08 ± 0.005	0.08 ± 0.003	0.23	0.08 ± 0.003	0.09 ± 0.003	0.08	0.08 ± 0.004	0.09 ± 0.005	0.03

Table 3. (continued)

Parameter	Intervention								
	Restricted Diet			DER-Diet			Control		
	Before	After	<i>P-Value</i>	Before	After	<i>P-Value</i>	Before	After	<i>P-Value</i>
Tyrosine (mmol/L)	0.05 ± 0.003	0.05 ± 0.002	0.08	0.06 ± 0.003	0.06 ± 0.004	0.70	0.06 ± 0.004	0.06 ± 0.003	0.58
Valine (mmol/L)	0.16 ± 0.007	0.13 ± 0.004	<i>0.004</i>	0.19 ± 0.01	0.18 ± 0.007	1.00	0.18 ± 0.01	0.20 ± 0.01	0.17

Changes in metabolic parameters after the dietary intervention groups. Values are depicted as mean ± standard error of the mean. Significant *P*-values are depicted *Italics*, while significant *p*-values after the Bonferroni correction for multiple testing are depicted in bold and *Italics*. * baseline levels in the restricted diet group are significantly lower than in the DER-diet and control group. This is due to a high percentage of patients with serum albumin levels which lay below the normal values of 35–55 g/L. ** baseline levels in the control group are higher, due to patients with levels of serum insulin of >180 pmol/L.

Detailed analysis of HDL-subclasses showed a trend towards a decrease in the medium HDL-particles, while other HDL-subclasses were not affected (data not shown). The DER-diet group had higher free fatty acids after the intervention ($P=0.01$), based on an increase of saturated fatty acids (SFA) ($P=0.002$). Furthermore, the DER-diet resulted in a significant decrease in serum cholesterol ($P=0.03$) Lipoprotein subclasses very small very-low-density-lipoprotein (XS-VLDL), intermediate-density-lipoprotein (IDL) and large low-density-lipoprotein (L-LDL) showed a trend towards a decrease due to the DER-diet, but this did not reach significance (data not shown).

Both plasma prealbumin (PAB) (Figure 5A) and plasma retinol binding protein (RBP) (Figure 5B) were significantly lower after the restricted diet compared to levels before starting the diet, decreasing on average 27% ($P=0.0002$) and 22% ($P=0.001$), respectively. All except one patient in the restricted diet group showed a decrease in serum PAB and RBP. The eight patients who did not complete the restricted diet showed an average increase of 10% in PAB (Figure 5C) and 7% in RBP (Figure 5D), which was significantly different than the measures of those who completed the diet. No significant changes were seen in the DER-diet and in the control group in both PAB (Figure 5A) and RBP (Figure 5B).

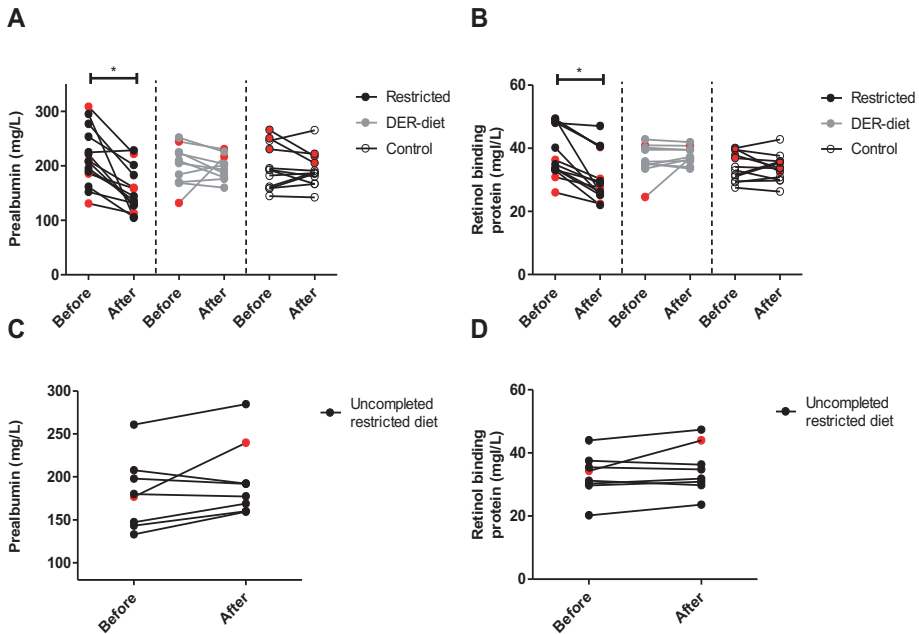


Figure 5. Plasma levels of prealbumin (PAB) and retinol binding protein (RBP) after the three dietary interventions. (A) Prealbumin (PAB) and (B) retinol binding protein (RBP) both decreased significantly after the restricted diet, with no changes seen in the DER-diet group or in the control group. (C) PAB and (D) RBP did not change in patients who did not complete the restricted diet. The two corresponding values for the individual patients are connected with a line. * $P \leq 0.002$. Red symbols = kidney donors in the restricted diet group. DER = daily energy requirements.

DISCUSSION

In this study, we showed that both kidney donors and morbidly obese patients are able to adhere to a synthetic calorie- and protein-restricted diet for five consecutive days with only minor discomfort. The metabolic markers PAB and RBP showed the strongest correlation with adherence to the diet, and together with serum urea could form a potential objective marker set to validate compliance to a diet comprising 30% DR and 80% PR.

The rationale for combining DR and PR in this clinical diet was based on the known beneficial effects of short-term DR and short-term PR¹⁷⁻¹⁸. We showed previously that several DR regimens protect against renal IRI in mice and result in upregulation of anti-oxidants,

reduction of pro-inflammatory cytokines, improved kidney function, and increased survival^{7,19}. DR also protects against IRI in aged-obese mice of both sexes, suggesting that the DR-induced effects on the stress response could be broadly applied¹¹.

It is not clear how the benefits of DR should be translated to humans in a clinical setting. Longer-term DR (e.g., for weeks) is considered undesirable, since feelings of hunger and fatigue and the risk of malnutrition could alter the wellbeing of patients prior to surgery. However, a shorter period could be insufficient to confer the same beneficial effects as in animal studies. Most clinical studies of preoperative DR have been performed in bariatric surgery patients and were designed to evaluate the effects of DR on weight loss and liver size reduction^{13,14}. One study showed reduction in steatosis and steatohepatitis after liver resection due to preoperative dietary and fat restriction²⁰. We previously used a DR regimen of three days of 30% DR followed by 24 hours of fasting in living kidney donors, which proved to be feasible; unfortunately, this did not induce a beneficial response similar to that seen in mice^{15,16}. This could be because the DR duration or restriction level was insufficient, or because the diet did not include PR. Based on this experience^{15,16}, we extended the number of days of the diet, and restricted protein intake by 80% in addition to the 30% DR.

A total adherence rate of 71% was reached, which was comparable between kidney donors and morbidly obese patients. Many factors influence adherence, such as the duration of the intervention as well as the frequency of daily doses. Osterberg et al. showed that the average adherence rate in clinical trials ranges between 43 and 78%²¹. They also reported an average adherence rate between 30 and 80% in patients who took three to four medication doses a day²¹, which is comparable to the three to four shakes per day in the restricted diet group of our study. In light of these results, our compliance rate is acceptable considering the fact that these patients did not receive the diet immediately prior to surgery, and therefore did not expect a beneficial effect. Further studies investigating the potential beneficial effects of this dietary regimen might further increase the compliance rate in these patient populations.

Safety and discomfort of a preoperative diet are important factors to consider in terms of compliance and applicability. We found that serum albumin, insulin and ferritin measures did not change as a result of the restricted diet, indicating that malnutrition was not induced. As a measurement of discomfort, the VAS nausea scores were significantly increased in patients following the restricted diet, but since the scores did not exceed 2.5 points out of 10, nausea cannot be considered highly clinically relevant. The patients that withdrew early from the diet reported discomfort, mostly gastrointestinal tract-related, as the reason for withdrawal. This discomfort could be due to the liquid composition of the diet, since the change from normal food to liquid meal replacements has a direct effect on defecation. Offering patients more solid nutrition could reduce this discomfort and

increase compliance. Interestingly, the morbidly obese patients more often complained about gastrointestinal symptoms during the restricted diet than the kidney donors did. A possible explanation is provided by the link between obesity and functional gastrointestinal disorders (FGIDS), such as irritable bowel syndrome and diarrhea²². FGIDS could make obese people more vulnerable to gastrointestinal symptoms when nutritional intake changes. During the DER-diet, both serum albumin and free saturated fatty acids increased. Together with the complaints related to gastrointestinal tract and nutritional intake, these results indicate that the patients on the DER-diet received relatively more fat than during normal food consumption. This could be the cause of nausea and stool change reported by the DER-diet groups. Based on the incidence and severity of the discomfort, together with the percentage of withdrawals from the DER-diet group and metabolic changes, we do not consider the DER-diet an appropriate control diet for future studies.

Ideally, determination of adherence to the diet would be based on objective measures. It has been shown that higher intake of calories and protein significantly increases PAB and RBP in patients at risk for malnutrition²³⁻²⁵. Both PAB and RBP significantly decreased in patients receiving the restricted diet in this study, while no changes were seen in the DER-diet group, in the control group, or in individuals who did not complete the diet. With only small interpatient variability, both markers therefore have great value in terms of objectively measuring compliance to a restricted diet. In addition, serum levels of BCAAs valine and leucine as well as the combination of all three BCAAs decreased in the restricted diet, with no changes in the DER-diet and the control group. This decrease with lowered protein intake is in line with a recent study by Solon-Biet et al. who showed that higher levels of circulating BCAAs were correlated with the percentage of protein intake¹⁷. Patients who received the restricted diet also showed a significant decrease in serum urea. Previous studies have shown a relationship between dietary protein intake and serum urea²⁶. Interestingly, one patient provided the restricted diet showed no decrease in four of these five markers, raising doubts regarding diet compliance by this individual. Hence, a combination of these markers may very well distinguish between compliance and non-compliance to a diet comprising DR and PR. Further research is needed to validate these markers in larger cohorts of different patient populations in order to establish their independent value as compliance markers.

This pilot study has some limitations, including a high percentage of dropouts, a small sample size, and the exclusion of some blood samples that were obtained from non-fasted patients. The high number of dropouts was mostly due to logistical reasons; in some cases, the surgery date was moved up, and in others the patients did not undergo surgery. Some of the included patients declined to participate after providing written informed consent due to the stressful period prior to surgery; these patients were subsequently excluded. These logistical problems are difficult to solve, and further studies should anticipate a relatively

high percentage of dropouts. Ensuring that the patients fast overnight before blood is drawn will increase the sample size and the potential value of the study. Finally, a larger sample size is needed in order to validate the results of this study and to investigate the effects of a diet comprising DR and PR on perioperative and postoperative responses.

Although safety was not an outcome measure, we have carefully monitored the patients' peri- and postoperative course in the present study, and have observed no differences in type and rate of complications and length of hospital stay between the three study groups.

In conclusion, our results show that a diet comprising DR and PR is feasible in both living kidney donors and in morbidly obese patients awaiting surgery. This restricted diet was easily instituted and adherence to the diet could be measured objectively using a combination of laboratory parameters. Minor adaptations to the diet, such as increasing the amount of non-liquid food during the diet, could lead to an even higher compliance rate and to decreased discomfort. This short-term dietary intervention is feasible and ready for further investigation of the effects of DR on perioperative and postoperative responses in a clinical setting.

SUBJECTS AND METHODS

Study design

This pilot study was designed as a prospective multicenter pilot study. The study was approved by the Medical Ethics Committee (METC, MEC number 2012-134) of the Erasmus University Medical Center, Rotterdam, The Netherlands, and by the Board of Directors of the Maastad Hospital, Rotterdam, The Netherlands. The study procedures were in accordance with the METC guidelines. The trial is registered as the PROTECT trial in the Dutch trial registry database using trial code 3663 (www.trialregister.nl). This manuscript was prepared in accordance with the CONSORT 2010 statement²⁷, according to the Declaration of Helsinki.

Inclusion and exclusion criteria

The coordinating investigator approached patients at the hospitals' outpatient clinic during their scheduled doctor appointments. All patients included in the study gave written informed consent to participate. Patients were informed that this study only aimed to establish the feasibility of the diet in surgical patients. A patient flowchart showing inclusions/exclusions and randomization procedures is depicted in Figure S3.

Kidney donors

Kidney donors visited the outpatient clinic at the Erasmus MC, University Medical Center Rotterdam between February 2013 and May 2014. To be eligible for the study, patients had to be between 18 and 70 years old, have a BMI ≥ 19 , could not participate in another clinical trial in the 30 days prior to the day they were approached, and could have no known allergies to any of the ingredients in the diets. An additional exclusion criterion was a surgery performed outside the Erasmus MC due to participation in the cross-over kidney donation program²⁸. Out of 124 kidney donors, 90 were eligible to participate in the study and were approached. Initially, 45 donors gave informed consent. After the outpatient clinic visit and before the scheduled surgery, 15 donors withdrew from the study for personal or logistical reasons (Figure S3). Included dropouts after randomization were replaced until the desired number of inclusions was reached. Thirty donors were equally ($n = 10$) randomized into each of the three intervention groups.

Bariatric surgery patients

The morbidly obese patients visited the outpatient clinic at the Maasstad Hospital between March 2013 and August 2014. To participate in the study, patients had to be between 18 and 60 years of age with a BMI ≥ 40 , could not have participated in another clinical study in the 30 days prior to the day they were approached, and could have no known allergies to any of the ingredients in the diets. Additional exclusion criteria were the presence of diabetes mellitus or morbid obesity caused by a known genetic syndrome or genetic defect. Diabetic patients were excluded to eliminate this confounding variable between the two surgery groups, as diabetic patients are not admitted to the living kidney donor program. Diabetes mellitus was defined as a fasted plasma glucose level ≥ 7 mmol/L as measured on two different days, or as either a fasted plasma glucose level ≥ 7 mmol/L or a non-fasted plasma glucose level ≥ 11.1 mmol/L with symptoms of hyperglycemia (such as thirst and polyuria). Out of 143 morbidly obese patients, 84 were eligible to participate and were therefore approached; 54 provided written informed consent. Sixteen patients dropped out of the study for various reasons (Figure S3). Included dropouts after randomization were replaced until the desired number of inclusions was reached. Since a high number of dropouts after randomization and start of the restricted occurred due to logistical reasons, additional patients were included in the restricted diet group. Eventually, 18 patients were randomized to the restricted diet, 10 patients to the DER-diet and 10 patients to the control group.

Dietary intervention

All dietary interventions lasted for five consecutive days and were given in an outpatient setting. For the kidney donors, the diet was initiated six days prior to surgery. For the morbidly obese patients, the diet started between several weeks to five days prior to the surgery date. After providing written informed consent, patients were randomized into one of three groups. During the study, patients were offered a contact person whom they were able to approach with an accessibility of 24 hours per day with questions regarding the diet, which they frequently did. Directly after completion of the diet, patients visited the outpatient clinic to evaluate their experience, and to donate a venous blood sample. The first group received a 30% DR and 80% PR restricted diet. This synthetic liquid diet containing an estimated 70% of the individual's required calories and 20% of the individual's protein, based on the basal metabolic rates and on the daily energy requirements (DER) as calculated with the Harris–Benedict formula²⁹. The Harris–Benedict formula takes into account gender, height, age, body weight and estimated activity level. This formula is validated up to a BMI of 40. Whenever an individual had a BMI >40, the body weight corresponding to a BMI of 40 was used to calculate the DER. Normal protein intake was set at 15% of the total calories based on the DER. Participants received calorie- and protein-restricted powder shakes (Scandishake® Mix, Nutricia Advanced Medical Nutrition, The Netherlands) as the main component of the diet. The shake was provided as a powder consisting of 4% protein, 53% carbohydrates and 43% fat, and was diluted with water. The main protein source was casein with a limited amount of whey protein (Table S2). The shakes were combined with a limited number of protein-restricted products (mainly fruits and vegetables) until the desired individual diet was reached. These protein-restricted products included: all fruits except bananas, all vegetables in a limited amount of 200 g per day with the exception of asparagus, and a maximum of one piece of gingerbread per day. The second group received a synthetic diet that was isocaloric to each individual's DER (termed the DER-diet), which was also calculated using the Harris–Benedict formula²⁰. The DER-diet was offered as a shake (Nutridrink® Compact, Nutricia Advanced Medical Nutrition, The Netherlands) and was consumed without further dilution. This shake consisted of 16% protein, 49% carbohydrates and 35% fat (Table S2). A limited number of protein-restricted products as offered to the restricted diet group, was added until the individual's DER was reached and average protein intake was an estimated 15% of all calories. All participants, randomized to either the restricted diet or the DER-diet, were blinded to which diet they received. The third group did not receive a synthetic diet or a dietary intervention. This group continued their usual daily eating pattern. Patients were asked to keep a diet diary during the period in which patients in the other two groups received the synthetic diet. Using this diary, their daily nutritional intake was measured and calculated for five days, resulting in mean overall

daily nutritional intake values. Experienced dieticians analyzed the diaries and calculated the DER, the average kilocalorie intake, and the average protein, fat and carbohydrate intake.

Outcome parameters

Subjective measurements

To analyze subjective health outcomes, all patients were asked to fill in a standardized questionnaire, the Visual Analogue Score (VAS), for evaluation of nausea, pain and general wellbeing³⁰. The VAS questionnaire uses a scale ranging from zero to 10, with zero representing no pain, nausea or decrease in wellbeing and 10 corresponding to the worst pain, nausea or decrease in wellbeing. The questionnaires were completed at three different time points: one day prior to starting the dietary intervention, on day three of the intervention and one day after completion of the 5-day intervention period when normal food intake was resumed. Side effects and discomfort were defined as any secondary effect related to the intervention. A distinction was made between major side effects and minor discomfort. Major side effects were defined as symptoms related to the intervention that remained days or weeks after the intervention or that required hospitalization. Minor discomfort included symptoms that caused discomfort during the intervention, but immediately disappeared after the dietary intervention.

Objective measurements

Before and after the dietary intervention, the following data were obtained from all patients: body weight, age, gender, length, and estimated physical activity level and duration. During the outpatient clinic visit and one day after the dietary intervention, two tubes of blood were collected: a 5.0 mL BD Vacutainer CPT tube (Franklin Lakes, NJ, USA) and a 5.0 mL BD Vacutainer® SST™ II Advance serum tube. After centrifuging for 20 min at 1500× g or for 10 min at 2300× g, respectively, both the plasma and serum were collected and stored at –80 °C until further analysis. Only blood samples from patients that had fasted overnight were used for the analysis. “Fasted” was defined as no food intake overnight, *i.e.* for at least eight hours prior to blood withdrawal. In serum samples the metabolic parameters albumin, urea, creatinine, glucose, ferritin, cholesterol, free fatty acids, triglycerides and high-density lipoprotein (HDL), and in plasma samples parameters prealbumin (PAB) and retinol binding protein (RBP) were measured and processed on the UniCel D×C 800 Synchron (R) Chemistry System (Beckman, Poway, CA, USA). Insulin was analyzed using the Access 2 ImmunoAssay System (Beckman) (Table S2). In addition, 143 metabolic markers were measured in serum samples by Brainshake (Brainshake Ltd., Helsinki, Finland), as summed

up in a list of the service deliverables provided by Brainshake (http://www.brainshake.fi/service-deliverables-web-v1_0)³¹. A schematic overview of all of the parameters and measurements, as well as the experimental timeline, is shown in Figure S2.

Randomization

Randomization was performed using computer-generated lists, which were printed out and put into opaque envelopes by an employee not involved in the study. The first 30 sequential numbers of each group (*i.e.*, kidney donors and morbidly obese patients) were generated at once. Sequential numbers for the two groups were distinguishable. After these blocks, the total number of dropouts was randomized in one block by the same procedure. The coordinating investigator approached patients eligible for the study at the hospitals' outpatient clinic during their scheduled doctor appointments. Allocation occurred after informed consent was given. All participants randomized to either the restricted diet or the DER-diet were blinded to which diet they received.

Statistical analysis

Categorical data are presented as numbers (percentage) and continuous variables as mean (SD/normal distribution) or median (interquartile distance/no normal distribution). The data were tested for normality using the Shapiro–Wilks test and visual assessment. Continuous data were compared using either the non-parametric Mann-Whitney test or the t-test for parametric data. Related samples were analyzed using the non-parametric Wilcoxon signed rank test. Semi-quantitative scoring of the questionnaires was performed via the paired t-test. Significance was set at $P < 0.05$. A Bonferroni correction for multiple testing was performed on the metabolic parameters. A P -value of ≤ 0.002 was considered significant. The analyses were performed using Statistical Packages for Social Sciences 21.0 (SPSS Inc., Chicago, IL, USA), GraphPad Prism (GraphPad Software Inc., La Jolla, CA, USA, version 5.01), and Office Excel (2010). This study was designed as a pilot study and therefore no power calculations were performed.

REFERENCES

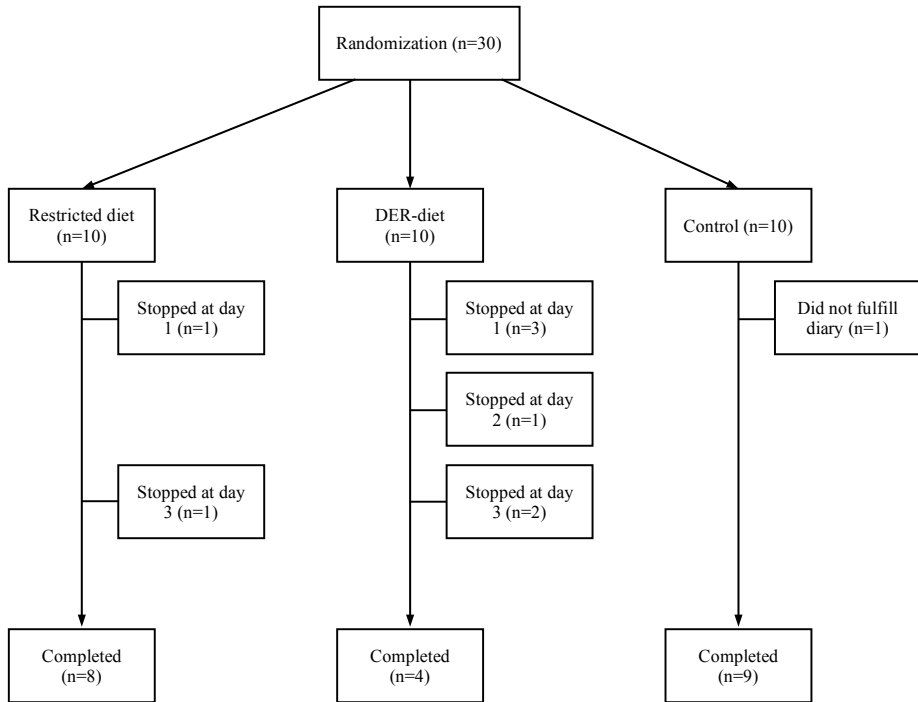
1. Blackburn, G.L. Metabolic considerations in management of surgical patients. *Surg. Clin N. Am.* 2011, 91, 467–480.
2. Lushchak, V.I. Free radicals, reactive oxygen species, oxidative stress and its classification. *Chem. Biol. Interact.* 2014, 224C, 164–175.
3. Kucukakin, B.; Gogenur, I.; Reiter, R.J.; Rosenberg, J. Oxidative stress in relation to surgery: Is there a role for the antioxidant melatonin? *J. Surg. Res.* 2009, 152, 338–347.
4. Calder, P.C.; Ahluwalia, N.; Brouns, F.; Buetler, T.; Clement, K.; Cunningham, K.; Esposito, K.; Jonsson, L.S.; Kolb, H.; Lansink, M.; et al. Dietary factors and low-grade inflammation in relation to overweight and obesity. *Br. J. Nutr.* 2011, 106 (Suppl. S3), S5–S78.
5. Snoeijis, M.G.; van Heurn, L.W.; Buurman, W.A. Biological modulation of renal ischemia-reperfusion injury. *Curr. Opin. Organ Transplant.* 2010, 15, 190–199.
6. Bonventre, J.V.; Yang, L. Cellular pathophysiology of ischemic acute kidney injury. *J. Clin. Investig.* 2011, 121, 4210–4221.
7. Mitchell, J.R.; Verweij, M.; Brand, K.; van de Ven, M.; Goemaere, N.; van den Engel, S.; Chu, T.; Forrer, F.; Muller, C.; de Jong, M.; et al. Short-term dietary restriction and fasting precondition against ischemia-reperfusion injury in mice. *Aging Cell* 2010, 9, 40–53.
8. Van Ginhoven, T.M.; Huisman, T.M.; van den Berg, J.W.; Ijzermans, J.N.; Delhanty, P.J.; de Bruin, R.W. Preoperative fasting induced protection against renal ischemia/reperfusion injury is independent of ghrelin in mice. *Nutr. Res.* 2010, 30, 865–869.
9. Van Ginhoven, T.M.; van den Berg, J.W.; Dik, W.A.; Ijzermans, J.N.; de Bruin, R.W. Preoperative fasting induces protection against renal ischemia/reperfusion injury by a corticosterone-independent mechanism. *Transpl. Int.* 2010, 23, 1171–1178.
10. Verweij, M.; van Ginhoven, T.M.; Mitchell, J.R.; Sluiter, W.; van den Engel, S.; Roest, H.P.; Torabi, E.; Ijzermans, J.N.; Hoeijmakers, J.H.; de Bruin, R.W. Preoperative fasting protects mice against hepatic ischemia/reperfusion injury: Mechanisms and effects on liver regeneration. *Liver Transpl.* 2011, 17, 695–704.
11. Jongbloed, F.; de Bruin, R.W.; Pennings, J.L.; Payan-Gomez, C.; van den Engel, S.; van Oostrom, C.T.; de Bruin, A.; Hoeijmakers, J.H.; van Steeg, H.; Ijzermans, J.N.; et al. Preoperative fasting protects against renal ischemia-reperfusion injury in aged and overweight mice. *PLoS ONE* 2014, 9, e100853.
12. Mitchell, J.R.; Beckman, J.A.; Nguyen, L.L.; Ozaki, C.K. Reducing elective vascular surgery perioperative risk with brief preoperative dietary restriction. *Surgery* 2013, 153, 594–598.
13. Van Nieuwenhove, Y.; Dambrauskas, Z.; Campillo-Soto, A.; van Dielen, F.; Wiezer, R.; Janssen, I.; Kramer, M.; Thorell, A. Preoperative very low-calorie diet and operative outcome after laparoscopic gastric bypass: A randomized multicenter study. *Arch. Surg.* 2011, 146, 1300–1305.

14. Carbajo, M.A.; Castro, M.J.; Kleinfinger, S.; Gomez-Arenas, S.; Ortiz-Solorzano, J.; Wellman, R.; Garcia-Ianza, C.; Luque, E. Effects of a balanced energy and high protein formula diet (vegstart complet(r)) vs. Low-calorie regular diet in morbid obese patients prior to bariatric surgery (laparoscopic single anastomosis gastric bypass): A prospective, double-blind randomized study. *Nutr. Hosp.* 2010, 25, 939–948.
15. Van Ginhoven, T.M.; de Bruin, R.W.; Timmermans, M.; Mitchell, J.R.; Hoeijmakers, J.H.; IJzermans, J.N. Pre-operative dietary restriction is feasible in live-kidney donors. *Clin. Transplant.* 2011, 25, 486–494.
16. Van Ginhoven, T.M.; Dik, W.A.; Mitchell, J.R.; Smits-te Nijenhuis, M.A.; van Holten-Neelen, C.; Hooijkaas, H.; Hoeijmakers, J.H.; de Bruin, R.W.; IJzermans, J.N. Dietary restriction modifies certain aspects of the postoperative acute phase response. *J. Surg. Res.* 2011, 171, 582–589.
17. Solon-Biet, S.M.; McMahon, A.C.; Ballard, J.W.; Ruohonen, K.; Wu, L.E.; Cogger, V.C.; Warren, A.; Huang, X.; Pichaud, N.; Melvin, R.G.; et al. The ratio of macronutrients, not caloric intake, dictates cardiometabolic health, aging, and longevity in ad libitum-fed mice. *Cell Metab.* 2014, 19, 418–430.
18. Harputlugil, E.; Hine, C.; Vargas, D.; Robertson, L.; Manning, B.D.; Mitchell, J.R. The tsc complex is required for the benefits of dietary protein restriction on stress resistance in vivo. *Cell Rep.* 2014, 8, 1160–1170.
19. Pamplona, R.; Barja, G. Mitochondrial oxidative stress, aging and caloric restriction: The protein and methionine connection. *Biochim. Biophys. Acta* 2006, 1757, 496–508.
20. Verweij, M.; Sluiter, W.; van den Engel, S.; Jansen, E.; IJzermans, J.N.; de Bruin, R.W. Altered mitochondrial functioning induced by preoperative fasting may underlie protection against renal ischemia/reperfusion injury. *J. Cell Biochem.* 2013, 114, 230–237.
21. Reeves, J.G.; Suriawinata, A.A.; Ng, D.P.; Holubar, S.D.; Mills, J.B.; Barth, R.J., Jr. Short-term preoperative diet modification reduces steatosis and blood loss in patients undergoing liver resection. *Surgery* 2013, 154, 1031–1037.
22. Osterberg, L.; Blaschke, T. Adherence to medication. *N. Engl. J. Med.* 2005, 353, 487–497.
23. Ho, W.; Spiegel, B.M.R. The relationship between obesity and functional gastrointestinal disorders: Causation, association, or neither? *Gastroenterol. Hepatol.* 2008, 4, 572–578.
24. Bauer, P.; Charpentier, C.; Bouchet, C.; Nace, L.; Raffy, F.; Gaconnet, N. Parenteral with enteral nutrition in the critically ill. *Intensive Care Med.* 2000, 26, 893–900.
25. Tempel, Z.; Grandhi, R.; Maserati, M.; Panczykowski, D.; Ochoa, J.; Russavage, J.; Okonkwo, D. Prealbumin as a serum biomarker of impaired perioperative nutritional status and risk for surgical site infection after spine surgery. *J. Neurol. Surg. A Cent. Eur. Neurosurg.* 2015, 76, 139–143.
26. Addis, T.; Barrett, E.; Poo, L.J.; Yuen, D.W. The relation between the serum urea concentration and the protein consumption of normal individuals. *J. Clin. Investig.* 1947, 26, 869–874.
27. Schulz, K.F.; Altman, D.G.; Moher, D.; Group, C. Consort 2010 statement: Updated guidelines for reporting parallel group randomised trials. *BMJ* 2010, 340, c332.

28. De Klerk, M.; Kal-van Gestel, J.A.; Haase-Kromwijk, B.J.; Claas, F.H.; Weimar, W.; Living Donor Kidney Exchange, P. Eight years of outcomes of the dutch living donor kidney exchange program. *Clin. Transpl.* 2011, 287–290.
29. Roza, A.M.; Shizgal, H.M. The harris benedict equation reevaluated: Resting energy requirements and the body cell mass. *Am. J. Clin. Nutr.* 1984, 40, 168–182.
30. Wewers, M.E.; Lowe, N.K. A critical review of visual analogue scales in the measurement of clinical phenomena. *Res. Nurs. Health* 1990, 13, 227–236.

SUPPLEMENTARY DATA

(A) LIVING KIDNEY DONORS



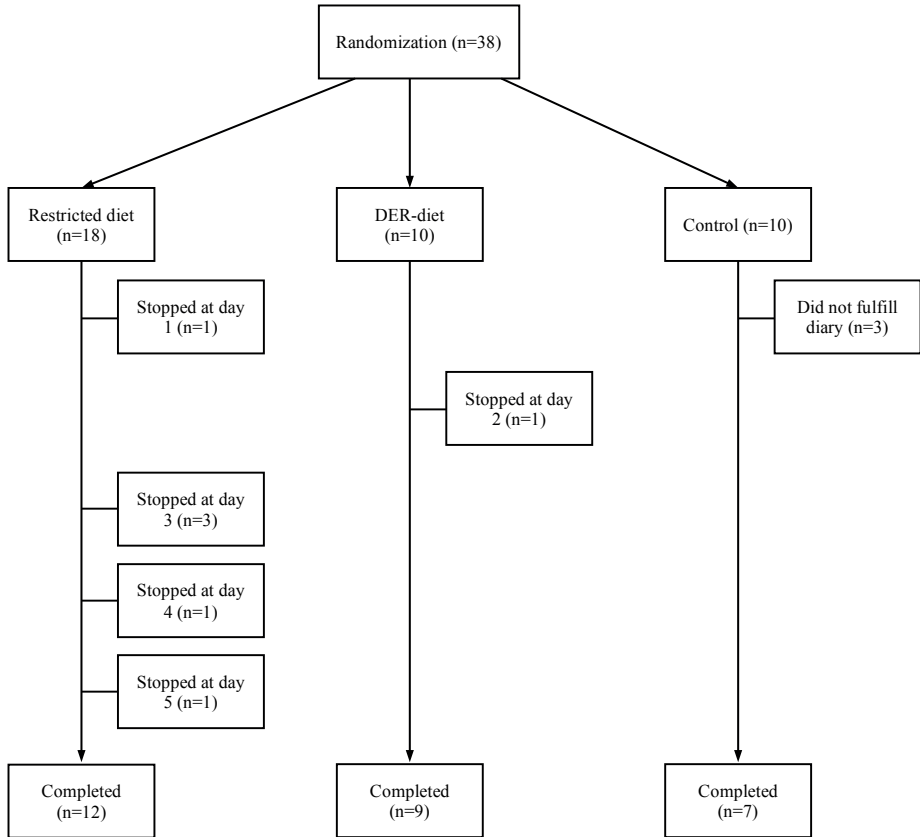
(B) MORBIDLY OBESE PATIENTS

Figure S1. Flowchart of the randomization and follow-up of the inclusions. (A) Thirty kidney donors were equally randomized into each of the three intervention groups. Eight out of 10 kidney donors completed the diet; 1 stopped at day 1 and 1 at day 3. The DER-diet was completed by 4 donors; 3 stopped at day 1, 1 at day 2 and 2 at day 3. One donor did not complete the diet diary. **(B)** Twelve out of 18 morbidly obese patients completed the diet; 1 stopped at day 1, 3 at day 3, 1 at day 4 and 1 at day 5. Nine out of 10 completed the DER-diet, with only one patient who stopped at day 2. Three out of 10 patients did not complete the diet diary. DER = daily energy requirements.

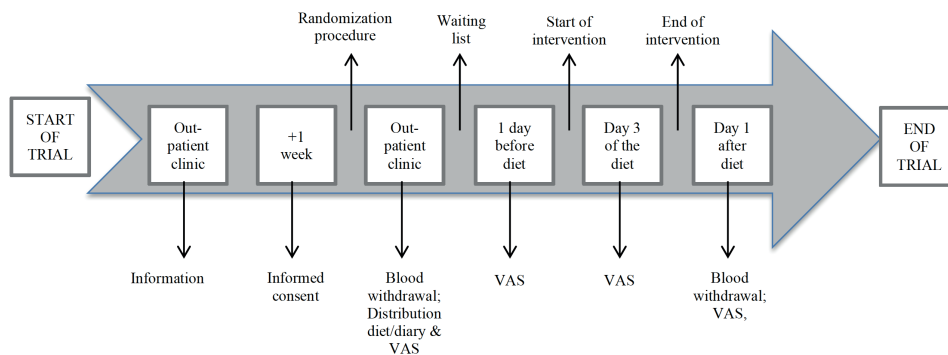
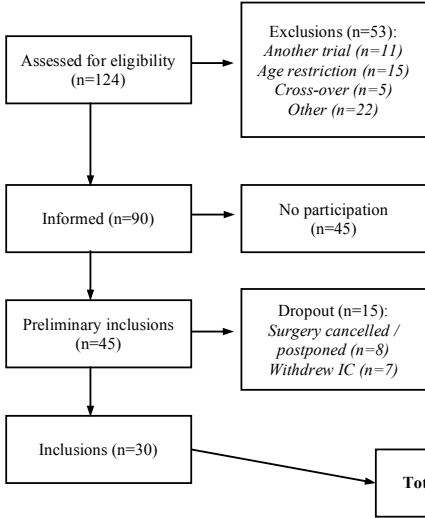


Figure S2. Timeline of the study from the first outpatient clinic visit until the end of the trial.

Each patient was approached at the first outpatient clinic appointment, and informed consent was signed a week later. Subsequently, the randomization procedure was performed and pre-study blood samples were taken. The diets were consumed or, for the control group, the dietary diary was kept, for five consecutive days. The day after the diet ended, blood samples were taken again, and the trial ended. VAS = Visual Analogue Score.

LIVING KIDNEY DONORS



MORBIDLY OBESE PATIENTS

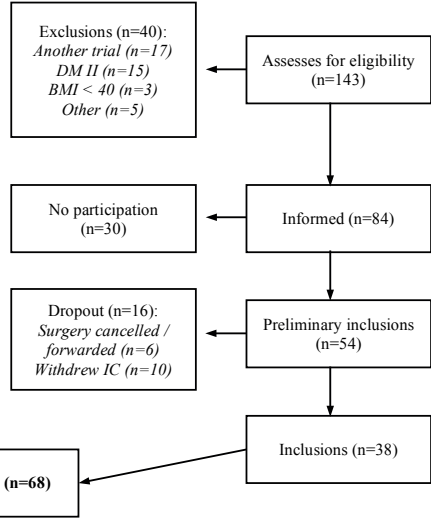


Figure S3. Flowchart showing patient inclusions and exclusions. Exclusions were based on preset exclusion criteria. Eligible kidney donors were approached at the outpatient clinic at the Erasmus MC, University Medical Center Rotterdam, and eligible morbidly obese patients were approached at the Maastad Hospital, Rotterdam, The Netherlands. Additional morbidly obese patients were included after many were withdrawn due to logistical reasons. BMI = body mass index. Cross-over = cross-over program at which the surgery takes place outside of the Erasmus MC, University Medical Center Rotterdam. DM II = diabetes mellitus type II. IC = informed consent.



Table S1. List of all parameters measured and the material and method of analysis

Biomarker	Abbreviation	Matrix	Method of analysis	Company of assay	Assay product number
Albumin	ALB	Serum	Autoanal	Beckman	442765
Cholesterol	CHOL	Serum	Autoanal	Beckman	467825
Creatinine	CREA	Serum	Autoanal	Beckman	442760
Ferritin	FER	Serum	Immunoanal	Beckman	33020
Free fatty acids	FFA	Serum	Autoanal	Wako	NEFA-HR2
Glucose	GLU	Serum	Autoanal	Beckman	442640
High-density lipoprotein	HDL	Serum	Autoanal	Beckman	650207
Insulin	INS	Serum	Immunoanal	Beckman	33410
Prealbumin	PAB	Plasma	Immunoturbi	Beckman	475106
Retinol binding protein	RBP	Plasma	Immunoturbi	Diazyme	DZ187A-K
Triglycerides	TG	Serum	Autoanal	Beckman	445850
Urea	UREA	Serum	Autoanal	Beckman	442820

Abbreviations: Autoanal = autoanalyzer; immunoanal: immunoanalyzer; immunoturbi = immunoturbidimetry

Table S2. The composition and energy content of the restricted diet and DER-diet

Diet Average content per 100 gram/mL	Restricted diet	DER-diet
Energy (kcal)	507	240
(kJ)	2120	1010
Protein (g)	4.98	9.6
Protein (% of energy intake)	4.0	16.0
Casein (g)	4.3	8.8
Whey protein (g)	0.4	0.8
Carbohydrates (g)	67.0	29.7
Carbohydrates (% of energy intake)	53.0	49.0
Glucose (g)	0.8	0.3
Fructose (g)	0.0	0.0
Lactose (g)	3.2	<0.5
Maltose (g)	2.5	14.6
Sucrose (g)	14.0	0.0
Polysaccharides (g)	46.3	14.3
Other (g)	0.2	0.4
Fat (g)	24.5	9.3
Fat (% of energy intake)	43	35.0
Saturated fat (g)	7.7	0.9
Monounsaturated fat (g)	7.3	5.7
Polyunsaturated fat (g)	9.4	2.7
Linoleic acid (g)	8.1	2.1
A-linoleic acid (g)	0.9	0.4
Fibres	0.0	0.0
Sodium (mg)	128	96
Potassium (mg)	272	236
Chloride (mg)	163	91
Calcium (mg)	85	174
Phosphor (mg)	147	174
Magnesium (mg)	30	33
Ferritin (mg)	0.0	3.8
Zinc (mg)	0.0	2.9
Copper (mg)	0.0	0.43
Manganic (mg)	0.0	0.8
Fluoride (mg)	0.0	0.2

Table S3. (continued)

Diet Average content per 100 gram/mL	Restricted diet	DER-diet
Molybdenum (µg)	0.0	24.0
Selenium (µg)	0.0	14
Chrome (µg)	0.0	16
Iodine (µg)	0.0	32
Vitamin A (µg-RE)	0.0	240
Carotenoids (mg)	0.0	0.0
Vitamin D (µg)	0.0	1.8
Vitamin E (mg α-TE)	0.0	3.0
Vitamin K (µg)	0.0	13.0
Thiamin (mg)	0.0	0.4
Riboflavin (mg)	0.0	0.4
Niacin (mg NE)	0.0	4.3
Panθοtheenzuur (mg)	0.0	1.3
Vitamin B6 (mg)	0.0	0.4
Foliumzuur (µg)	0.0	64
B12 (µg)	0.0	0.7
Biotin (µg)	0.0	9.6
Vitamin C (mg)	0.0	224
Choline (mg)	0.0	88

Kcal=kilocalories; kJ=kilojoule; g= grams; mg=milligrams; µg=micrograms; DER=daily energy requirements

CHAPTER 8

COMBINED CALORIE AND PROTEIN RESTRICTION IMPROVES OUTCOME IN LIVING KIDNEY DONORS AND KIDNEY TRANSPLANT RECIPIENTS

Franny Jongbloed, Ron W.F. de Bruin, Piet Beekhof, Paul
Wäckers, Dennis A. Hesselink, Harry van Steeg, Jan H.J.
Hoeijmakers, Martijn E.T. Dollé, Jan N.M. IJzermans

Submitted

ABSTRACT

Dietary restriction prolongs life- and health span and increases stress resistance in numerous species. A previous clinical study showed that five days of combined calorie and protein restriction (CCPR) before invasive surgery was safe in kidney donors and that adherence to the diet was high. In the present study, the effects of preoperative CCPR in living kidney donors and their transplanted kidneys was investigated. Thirty-five living kidney donors were randomized into either the CCPR (n=15) or control (n=20) group. The CCPR diet reduced calorie intake by 30% and protein intake by 80% during the five days immediately prior to organ donation. Donors in the control group had no restrictions and ate their own regular diet. All patients adhered to the diet. From postoperative day (POD) 2 up until month 1, kidney function of the donors was significantly better in the CCPR group compared with control donors. Recipients of CCPR donors also showed significantly improved kidney function compared with their control group. In addition, the recipients of CCPR kidneys showed a significantly lower incidence of slow graft function and acute rejection. CCPR inhibited cellular immune response pathways and activated stress-resistance signaling. Thus, short-term preoperative CCPR significantly improves recovery of kidney function in donors and the function of the transplanted kidney in recipients. These observations are the first to show that the benefits of CCPR can be induced rapidly in humans and that CCPR may be used clinically to improve outcomes in clinical settings involving ischemia-reperfusion damage.

INTRODUCTION

Dietary restriction (DR) increases resistance to reactive oxygen species (ROS) during both acute and chronic stress, and recently we found that DR at the level of genome function reduces transcriptional stress by attenuating DNA damage accumulation¹⁻⁴. Consequently, DR enhances defense and maintenance mechanisms including cellular programs, enabling resistance to a variety of stressors including ischemia-reperfusion injury (IRI). IRI arises from acute oxidative stress that inevitably occurs during organ (e.g. kidney) transplantation and many other surgical procedures. The phase of ischemia after kidney retrieval leads to hypoxia and an increase in metabolic waste products, while reperfusion after restoration of renal blood flow results in the production of ROS and an inflammatory response⁵⁻⁷. Living donor kidney transplantation (LDKT) greatly improves function and survival of the kidney allograft compared to kidneys from deceased donors⁸. Nonetheless, and despite the markedly shorter ischemia times following LDKT, IRI remains a risk factor for poor outcome^{9,10}. Amelioration of renal IRI could therefore greatly improve both graft and thereby transplant recipient survival¹¹.

Previously, we showed that short-term DR counteracts perioperative stress and protects against both renal and hepatic IRI in mice, irrespective of gender, age, body weight and genetic background^{12,13}. Subsequently, we demonstrated that this protection could also be induced by dietary deprivation of protein alone for three days prior to renal IRI, indicating that the effects of calorie and protein restriction might act synergistically¹⁴.

Translation of the beneficial effects of short-term DR to humans has mostly proven difficult and unsuccessful¹⁵. Recently, we reported the results of a randomized, controlled clinical trial which demonstrated that prescription of a combined calorie and protein restricted (CCPR) diet is feasible and safe in living kidney donors, as well as in patients undergoing bariatric surgery¹⁶. Here, we demonstrate that a CCPR diet has beneficial effects on the postoperative outcomes of both living kidney donors and their kidney transplant recipients.

RESULTS

Baseline characteristics

Thirty-five living kidney donors were randomized into either the CCPR (n=15) or the control group (n=20) between May 2, 2014 and November 18, 2015 (Figure S1). The difference in patient numbers between the groups is due to the additional inclusions to replace dropouts. The baseline characteristics of these 35 donors are listed in Table 1A. Donors in the CCPR group were more often female ($P=0.024$) and consequently had a

lower serum creatinine concentration at the outpatient clinic visit ($P=0.018$). Baseline characteristics of all transplant recipients (Table 1B) and the donors of whom biopsies were used for transcriptomic profiling (Table S1) showed no differences between the two groups.

Table 1A. Baseline characteristics of living kidney donors

Parameter	CCPR (n=15)	Control (n=20)	P-value
Age (years)	55 (51-55)	54 (46-59)	0.395
Gender (Male/Female)	4/11	13/7	0.028
BMI (kg/m ²)	23.7 (22.4-27.6)	26.0 (26.6-29.1)	0.157
Systolic blood pressure (mm/Hg)	128 (123-137)	128 (122-137)	1.000
Creatinine (mmol/L)	71 (66-78)	80 (71-91)	0.021
CKD-EPI eGFR (mL/min)	86 (72-90)	80 (73-89)	0.672
Urea (mmol/L)	5.3 (4.4-5.8)	5.3 (4.2-6.1)	0.986
Glucose (mmol/L)	5.3 (5.0-5.7)	5.0 (4.8-5.9)	0.217
Albumin (g/L)	47 (44-48)	46 (45-47)	0.398
Triglycerides (mmol/L)	1.22 (0.85-1.50)	1.31 (1.00-1.68)	0.488
Hemoglobin (mmol/L)	8.8 (8.4-9.0)	9.2 (8.7-9.6)	0.031
Trombocytes (10 ⁹ /L)	234 (213-294)	253 (206-289)	0.972
CRP (mg/L)	1.1 (0.7-1.9)	1.5 (0.6-2.4)	0.259
Leukocytes (10 ⁹ /L)	6.6 (5.5-7.4)	6.6 (5.5-7.8)	0.652
Bilirubin (μmol/L)	6 (5-10)	7 (5-12)	0.467
Potassium (mmol/L)	4.4 (4.2-4.6)	4.3 (4.1-4.7)	0.444
Type of donation (R/U/A)	3/3/9	4/12/4	0.083
Side of nephrectomy (Left/Right)	8/7	12/8	0.712
Method used (Laparoscopic/HARP)	12/3	14/6	0.523

Table 1B. Baseline characteristics of kidney transplant recipients

Parameter	CCPR (n=15)	Control (n=20)	P-value
Age (years)	56 (44-67)	54 (45-58)	0.250
Gender (Male/Female)	8/7	10/10	0.863
Kreatinine (mmol/L)	495 (442-637)	449 (321-902)	0.351
CKD-EPI eGFR (mL/min)	9 (7-11)	11 (5-14)	0.471
Urea (mmol/L)	19.9 (16.2-31.4)	22.6 (15.0-27.1)	0.881
Potassium (mmol/L)	5.4 (4.7-5.8)	4.7 (4.4-5.3)	0.092
Hemoglobin (mmol/L)	6.6 (6.2-7.5)	7.3 (6.6-8.3)	0.166

Table 1B. (continued)

Parameter	CCPR (n=15)	Control (n=20)	P-value
CRP (mg/L)	2.7 (1.5-4.7)	2.1 (0.6-5.2)	0.205
Leukocytes (10 ⁹ /L)	7.8 (6.8-9.7)	6.1 (5.5-8.2)	0.106
Type of donation (R/U/A)	3/3/9	4/12/4	0.083
Immunosuppressive therapy prior to transplantation (Yes/No)	4/11	5/15	1.000
Dialysis prior to transplantation (Yes/No)	6/9	9/11	0.687
Side of transplantation (Left/Right)	4/11	7/12	0.549

Values are depicted as median \pm interquartile range. Significant values are depicted in bold. BMI = body mass index; CKD-EPI eGFR = estimated glomerular filtration rate using the CKD-EPI formula; CRP = C-reactive protein. Type of donation: R = related; U = unrelated; A = anonymous. HARP = hand-assisted retroperitoneal nephrectomy. † = both creatinine and hemoglobin levels of the living kidney donors were lower in the CCPR than the control group as a consequence of the gender differences in both groups. * = all kidney transplant recipients met the criteria for end-stage renal disease with a CKD-EPI eGFR <15 mL/min. Significance = $P < 0.05$.

Compliance to the diet and surgical outcome

All 15 donors in the CCPR group indicated they had adhered to the diet. This was in line with a number of independent parameters investigated. Serum levels of the adherence markers prealbumin (PAB), retinol binding protein (RBP), and the branched-chain amino acids valine and leucine were all significantly decreased after the CCPR diet (Figure S2). All donors in the CCPR group showed a decline in adherence markers, and they lost an average of 2.0 kilograms (range -4;0 kilograms) of body weight during the diet, which differed significantly from the slight average weight gain of 0.4 kilograms (range -4; +1 kilograms) observed in the control group ($P=0.006$). Perioperative outcomes did not significantly differ between the two arms in both donors and recipients (Table S2).

Postoperative outcome

Comparison of kidney donors receiving a control or CCPR diet

Prior to the dietary intervention, serum creatinine levels significantly differed between donors in the CCPR and the control group (Figure 1A, POD-pre). One day before surgery (*i.e.* at day 5 of dietary intervention), serum creatinine levels were similar (Figure 1A, POD-1). To assess postoperative changes in kidney function, a linear mixed-effects model analysis correlating with repeated follow-up measurements in each patient was used with random intercepts per patient. The donors on CCPR showed a significantly better clearance of absolute serum creatinine levels than the control group on postoperative day (POD) 2, POD3 and on postoperative month (POMo) 1, with a mean difference of 14.5 $\mu\text{mol/L}$ (Table 2A). Absolute CKD-EPI eGFR (eGFR) values did not significantly differ in both groups. To correct for baseline interpatient variability, the relative values of both creatinine

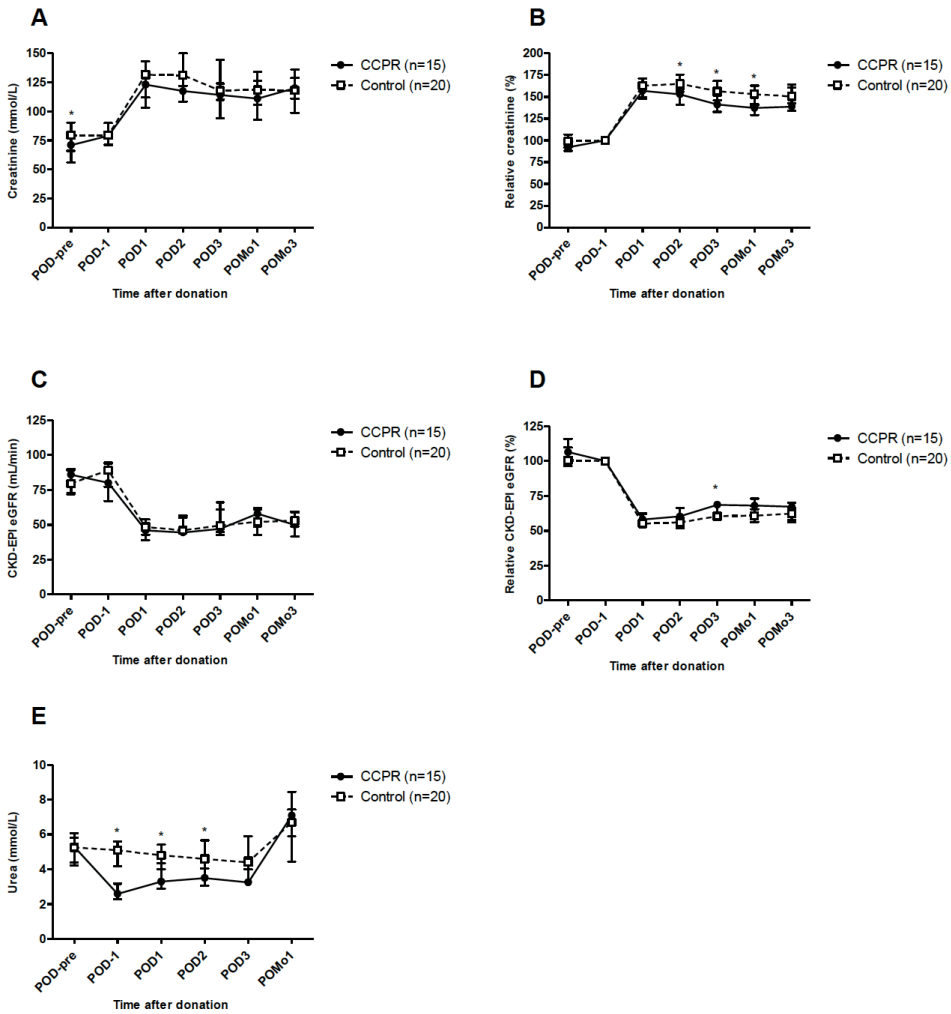


Figure 1. Kidney function of living kidney donors before and after kidney donation. (A) At start of the study (POD-pre), creatinine levels were significantly higher in the control group. Postoperatively, a trend towards lower levels of creatinine were observed in the CCPR-group. (B) Taking POD-1 as cut-off value, relative creatinine clearance was significantly improved in the CCPR-group at POD2, POD3 and POMo1. (C) Absolute glomerular filtration rate did not significantly differ between the groups. (D) Relative eGFR showed significant improvement in the CCPR group at POD3. (E) Serum urea levels were significantly lower in the CPPR-group on POD1 and remained so in the first two postoperative days. Values are depicted as median \pm interquartile range. CCPR = combined calorie and protein restriction; POD = postoperative day; POMo = postoperative month; eGFR = estimated glomerular filtration rate using the CKD-EPI formula. *=significant values.

and eGFR clearance were calculated and analyzed. Again, relative creatinine clearance was significantly improved in the CCPR donors compared to the control group on POD2, POD3 and POMo1 with a difference of 14,6% on average. In addition, relative eGFR was significantly better in the CCPR group as well, both on POD2, POD3 and POMo1 with an improvement difference of 6% on average (Table 2A). Subsequently, changes per time point were assessed. The CCPR donors showed a trend towards better clearance of absolute creatinine compared to the control group (Figure 1A). During the first three postoperative days, relative creatinine clearance was significantly better in the CCPR donors on POD2 ($P=0.030$) and POD3 ($P=0.042$). These values remained significantly different at month 1 after surgery ($P=0.040$, Figure 1B), indicating long-term improvement. Absolute eGFR values did not differ between the groups (Figure 1C). In the first postoperative days, relative eGFR was significantly better in the CCPR donors on POD3 ($P=0.033$) (Figure 1D). Serum urea levels were significantly lower in the CCPR group on POD-1 ($P<0.001$), suggesting effects of the CCPR diet on kidney function per se. This difference persisted after surgery on POD1 ($P=0.003$), POD2 ($P=0.005$) and lower on POD3 ($P=0.09$) (Figure 1E).

Table 2A. Random intercept mixed-effects differences, standard errors (Std. Error) and P -values for kidney function outcome of the living kidney donors

Time point	Parameter					
	Creatinine ($\mu\text{mol/L}$)			CKD-EPI eGFR (mL/min)		
	<i>Absolute values</i>					
	Difference	Std. Error	P -value	Difference	Std. Error	P -value
POD-pre	- 1,83	6,09	0.765	- 6,68	3,66	0.074
POD1	- 6,57	6,09	0.286	- 2,82	3,66	0.445
POD2	- 14,02	6,13	0.027	+ 0,38	3,67	0.918
POD3	- 15,35	6,29	0.018	+ 1,22	3,78	0.748
POMo1	- 14,52	6,19	0.023	+ 1,73	3,70	0.643
POMo3	- 10,23	6,13	0.102	- 1,42	3,68	0.701
	<i>Relative values</i>					
	Difference	Std. Error	P -value	Difference	Std. Error	P -value
POD1	- 4,38	72,44	0.399	+ 1,30	2,34	0.579
POD2	- 13,95	76,15	0.010	+ 5,36	2,38	0.027
POD3	- 15,53	88,28	0.006	+ 5,78	2,51	0.024
POMo1	- 14,35	80,27	0.009	+ 7,14	2,42	0.004
POMo3	- 9,28	77,61	0.084	+ 3,04	2,39	0.208

Although the postoperative C-reactive protein (CRP) concentrations tended to be lower in the CCPR donors, no statistically significant difference was observed with control donors (Figure 2A). No differences in leukocyte numbers were seen (Figure 2B). Thus, the CCPR diet induced a specific nephroprotection postoperatively, but had no significant effect on systemic inflammatory markers.

Comparison of kidney recipients receiving a control or CCPR diet

Ideally, urine production in kidney transplant recipients starts directly after revascularization of the graft. In the CCPR group, urine production was delayed in 1/15 (7%) patients compared with 5/20 (25%) in the control group ($P=0.135$) (Table 3 and S2B). On POD1, a trend towards lower incidence of partial acute tubular necrosis (ATN) as indicated on a MAG3 scan, was found in the CCPR group (Table 3). As expected in a living kidney donor setting, delayed graft function (DGF) did not occur. Slow graft function (SGF) occurred significantly more often in the control group: 5/20 (25%) *versus* 0/15 (0%) ($P=0.020$). The incidence of biopsy-proven acute rejection (BPAR) was significantly higher in the control group than in the CCPR group: 8/20 (40%) *versus* 1/15 (7%) ($P=0.013$). Two kidney transplant recipients (both in the control group) developed severe acute rejection and subsequently underwent a transplant nephrectomy on days 6 and 12 after transplantation, respectively. Data from these patients were censored from the day of transplant removal. The postoperative immunosuppressive drug regimen was similar in both groups (tacrolimus (Tac), mycophenolate mofetil (MMF) and prednisolone), except for two patients in the control group who received belatacept instead of Tac. These two patients experienced BPAR and were switched from belatacept to Tac. The Tac pre-dose concentrations showed a trend towards higher concentrations in the CCPR group on POD3 ($P=0.065$) and POD5 ($P=0.094$). No significant differences were seen in the duration of hospital stay nor in the incidence or severity of the other postoperative complications during hospital stay (Table 3).

Linear mixed-effects model analysis showed a significant improved absolute creatinine clearance in the CCPR recipients as from POD1 until POD5, with on average an improvement of 200 $\mu\text{mol/L}$ per day in the CCPR group. No significant differences in absolute eGFR values were observed (Table 2B).

Again, relative values of both creatinine and eGFR clearance showed significantly improved creatinine values in the CCPR group as from POD1 until POD5, correlating with a difference of 25% improved values compared to the control group (Table 2B). Assessment per time point showed no significant differences of absolute serum creatinine concentrations between groups throughout the postoperative follow-up (Figure 3A). Relative creatinine concentrations showed a trend towards improvement in the CCPR group on POD4

($P=0.057$), POD6 ($P=0.037$), and POD14 ($P=0.020$), with an average decrease of 70% in the CCPR group compared with 40% in the control group (Figure 3B). Absolute eGFR values did not differ between groups throughout the postoperative period (Figure 3C), while relative eGFR showed a trend towards better values in the CCPR group on POD 6 ($P=0.032$) (Figure 3D).

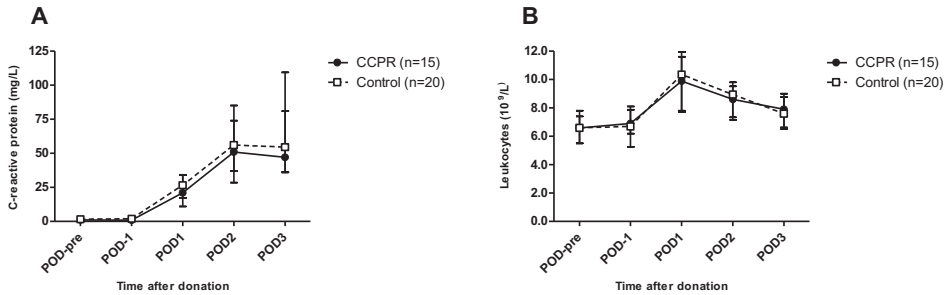


Figure 2. Systemic inflammatory markers in living kidney donors before and after kidney donation. (A) Levels of systemic inflammatory marker C-reactive protein before and after live kidney donation were not significantly different between the CCPR and the control group. (B) Levels of leukocytes did not significantly differ between both groups either, and only reached high-normal levels on POD1 after surgery. Values are depicted as median \pm interquartile range. CCPR = combined calorie and protein restriction; POD = postoperative day.

Table 2B. Random intercept mixed-effects differences, standard errors (Std. Error) and *P*-value for kidney function outcome of the kidney transplant recipients

Time point	Parameter					
	Creatinine ($\mu\text{mol/L}$)			CKD-EPI eGFR (mL/min)		
	<i>Absolute values</i>					
	Difference	Std. Error	<i>P</i> -value	Difference	Std. Error	<i>P</i> -value
POD-pre	- 23,43	85,23	0.784	- 1,15	5,969	0.848
POD1	- 161,60	85,23	0.062	+ 1,10	5,969	0.854
POD2	- 188,02	85,23	0.031	+ 2,37	5,969	0.693
POD3	- 199,73	85,23	0.022	+ 6,50	5,969	0.280
POD4	- 202,02	85,23	0.021	+ 8,82	5,969	0.144
POD5	- 185,74	85,60	0.033	+ 11,28	5,969	0.063
POD6	- 140,75	85,23	0.103	+ 7,46	5,995	0.218
POD7	- 142,53	85,62	0.100	+ 5,98	5,996	0.322
POD14	- 84,16	86,04	0.331	+ 7,94	6,027	0.192
POD21	- 52,44	86,50	0.546	+ 3,46	6,027	0.568
POMo1	- 59,44	86,50	0.494	+ 8,44	6,027	0.166
POMo2	- 50,75	86,50	0.559	+ 7,16	6,027	0.239
POMo3	- 50,74	86,50	0.559	+ 5,05	6,027	0.405
POMo6	- 53,36	86,04	0.537	+ 2,85	6,027	0.638
	<i>Relative values</i>					
	Difference	Std. Error	<i>P</i> -value	Difference	Std. Error	<i>P</i> -value
POD1	- 21,82	10,46	0.040	+ 29,25	121,47	0.810
POD2	- 28,63	10,46	0.007	+ 43,05	121,47	0.724
POD3	- 28,82	10,46	0.007	+ 89,63	121,47	0.463
POD4	- 28,47	10,46	0.008	+ 123,00	121,47	0.315
POD5	- 21,33	10,46	0.044	+ 166,78	121,47	0.174
POD6	- 15,90	10,46	0.132	+ 180,70	121,47	0.141
POD7	- 16,71	10,52	0.116	+ 119,54	122,05	0.331
POD14	- 12,13	10,59	0.255	+ 107,60	122,67	0.383
POD21	- 8,50	10,67	0.428	+ 19,12	122,67	0.877
POMo1	- 9,94	10,67	0.354	+ 82,78	122,67	0.502
POMo2	- 9,52	10,67	0.374	+ 7,67	122,67	0.950
POMo3	- 9,20	10,67	0.391	- 23,77	122,67	0.847
POMo6	- 6,10	10,67	0.569	- 55,09	122,67	0.655

CCPR= Combined Calorie and Protein Restriction; CKD-EPI eGFR = Chronic Kidney Disease Epidemiology Collaboration estimated Glomerular Filtration Rate. Differences are based on the outcomes of the CCPR group versus the control group. Relative values are set with POD-pre as baseline value, and therefore this time point was not included in the analysis of the relative differences. Significant *P*-values are depicted in bold.

Table 3. Postoperative outcome and complications in kidney transplant recipients in the first 14 days after surgery

Parameter	CCPR (n=15)	Control (n=20)	P-value
Urine production during surgery (yes/no (%))	1/15 (7%)	5/20 (25%)	0.135
ATN on MAG3 scan (yes/no)	2/15 (7%)	6/20 (30%)	0.209
Delayed graft function (yes/no)	0/15 (0%)	0/20 (0%)	1.000
Slow graft function (yes/no)	0/15 (0%)	5/20 (25%)	0.020
Acute rejection, biopsy-proven (yes/no)	1/15 (7%)	8/20 (40%)	0.013
Hospital stay (days)	13 ± 1	14 ± 1	0.556
Any complication (yes/no)	10/5 (73%)	16/4 (75%)	0.445
Clavien-Dindo score (0-4)	1.5 ± 0.3	1.5 ± 0.2	0.986
Tacrolimus level POD3	15.0 ± 1.8	10.6 ± 1.4	0.065
Tacrolimus level POD5	14.5 ± 1.8	10.8 ± 1.2	0.094
Tacrolimus level POD10 (µg/L)	12.7 ± 1.5	10.6 ± 1.0	0.251

Values are depicted as median ± interquartile range. ATN = acute tubular necrosis; MAG3 = renal scintigraphy scan; POD = postoperative day; Clavien-Dindo = official classification score for postoperative surgical complications. CCPR = combined caloric and protein restriction. Significance is considered at $P < 0.05$ and is depicted in bold.

Gender based differences

Since baseline characteristics between the two study groups differed concerning gender, a subgroup analysis stratified by gender was performed. In the female donors, a consistent trend in improved relative creatinine clearance and eGFR was observed for prolonged periods after POD1 (Figure S3). In male donors, relative creatinine concentrations were significantly improved in the CCPR group at POMo1 ($P=0.009$) and POMo3 ($P=0.022$) (Figure S4). Division based on gender of the donors showed for female CCPR kidneys a consistent trend for improved relative creatinine and eGFR that did not reach statistical significance (Figure S3F and S3H). The most pronounced CCPR-related differences in the kidney transplant recipients were observed in kidneys of the male donors; absolute and relative creatinine clearance was improved in the recipients of the male CCPR donors as from POD1 until POD7 (Figure S4E-H).

Comparison of the transcriptome in kidneys from control or CCPR diet

To get a more detailed insight into the main differences between both groups of donors that might help to explain the clinical impact of the CCPR diet, we performed a full genome expression profile analysis of the kidneys using renal biopsies from all 20 donors taken during transplantation before implantation and directly after cold-ischemia. Moreover, several other gene expression profiling studies have been published, providing an interesting basis

for comparison. A principal component analysis (PCA) showed that gender represented the largest discriminator (Figure S5). Therefore, we decided to separately analyze male (n=3-5) and female (n=5-7) kidneys.

The PCA of the female kidney transcriptome showed the largest differentiation between the control and CCPR groups on the PC axis 1 (Figure 4A). For male donors, some differentiation was seen on PC axis 2 (Figure 4B). Since one sample had to be excluded due to a low RNA yield, only 3 male patients in the CCPR group remained. In view of the statistics, the analysis was restricted to the females and later, the data of the males were compared to search for similarities. Results of the analysis of these male kidney tissues are given in Table S3.

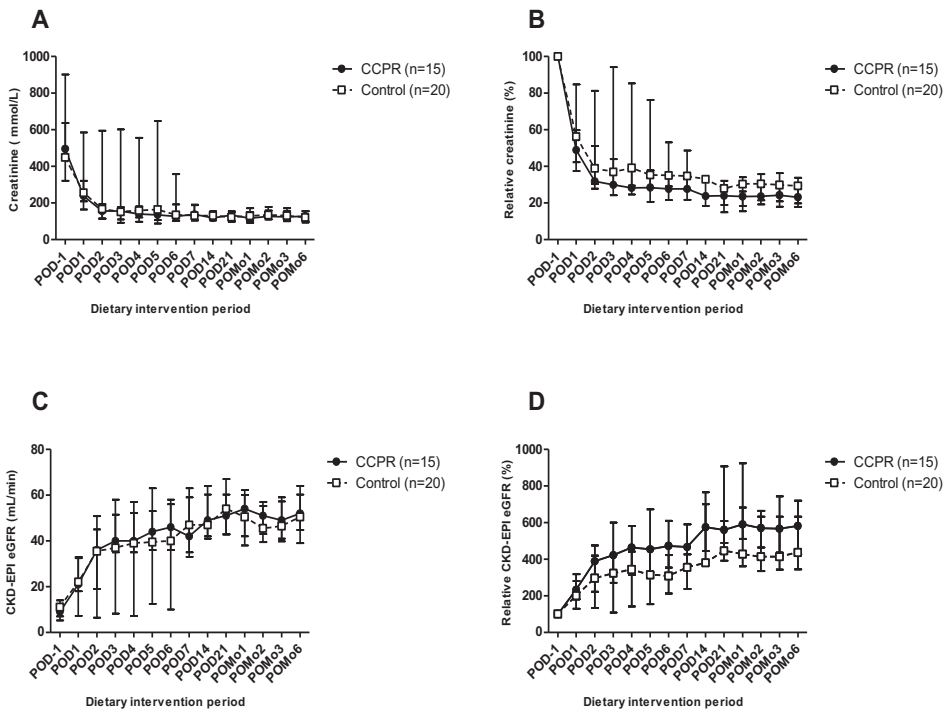


Figure 3. Kidney function of transplant recipients before and after surgery. (A) Serum creatinine showed a trend towards absolute lower levels in the CCPR-group throughout the first 14 days after surgery. (B) Relative creatinine levels, calculated using POD-1 as cutoff value, showed a down sloping trend as from POD4 up to POD14. (C) Following the creatinine clearance, eGFR also showed a trend towards improvement in the CCPR-group throughout the first days after surgery. (D) Relative eGFR showed an improvement in the CCPR-group as well. Values are depicted as median \pm interquartile range. CCPR = combined calorie and protein restriction; POD = postoperative day; POMo = postoperative month; eGFR = estimated glomerular filtration rate using the CKD-EPI formula.

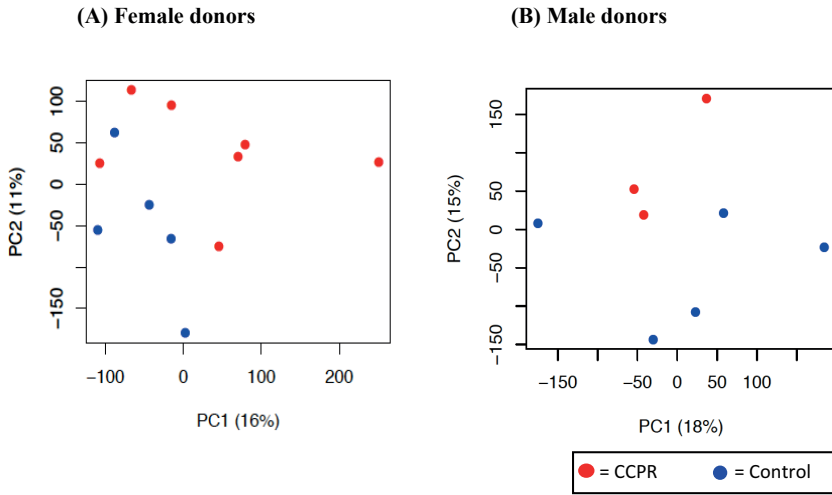


Figure 4. Principal component analysis of kidney tissue in female and male donors. (A) The unbiased principal component analysis (PCA) of all female donors showed the most variation of genes on the principal component (PC) axis 1 and some clustering of the two intervention groups is shown. (B) The PCA of the male donors was based on only three kidneys in the CCPR group, and showed little variation on PC axis 2. Principal component (PC) 1 is depicted on the x-axis and PC2 is depicted on the y-axis, followed by the percentage of variance explained by each axis. Each symbol represents one sample of one donor. Samples of the same group are shown in the same color. CCPR = combined calorie and protein restriction.

The CCPR group of female donors showed 480 differentially expressed transcripts (DET), of which 239 were downregulated and 241 upregulated. Pathway analysis showed a trend towards downregulation of pathways as shown by the more pronounced presence of downregulated genes in these pathways. However, the inhibitory directionality of these pathways was not statistically significant as evidenced by the absence of a z-score. One pathway was significantly upregulated with a z-score >2 , namely *EIF2 Signaling* (Table 4A). Other, not significantly activated pathways included the *NRF2-mediated Oxidative Stress Response*, cell cycle regulator *Cell Cycle: G2/M DNA Damage Checkpoint Regulation* and amino acid metabolism. Analysis of upstream transcription factors (TFs) in female donors revealed three significantly activated TFs, namely MYCN, MYC and NKX2-3. In addition, two TFs were significantly inhibited, namely PRDM1 and SMARCB1 (Table 3B).

Table 4A. Pathway analysis in female kidney tissue

Inguenuity Canonical Pathways	Ratio	Up/ Down	P-value	Z-score
eIF2 Signaling	9/221 (4.1%)	9/0	6.50 ^E -04	2,449
Primary Immunodeficiency Signaling	4/48 (8.3%)	0/4	1.72 ^E -03	N/A
Interferon Signaling	3/36 (8.3%)	0/3	6.65 ^E -03	N/A
Complement System	3/37 (8.1%)	0/3	7.18 ^E -03	N/A
Aldosterone Signaling in Epithelial Cells	6/166 (3.6%)	5/1	9.03 ^E -03	N/A
Autoimmune Thyroid Disease Signaling	3/47 (6.4%)	0/3	1.39 ^E -02	N/A
Hematopoiesis from Pluripotent Stem Cells	3/47 (6.4%)	0/3	1.39 ^E -02	N/A
Communication between Innate and Adaptive Immune Cells	4/89 (4.5%)	0/4	1.53 ^E -02	N/A
Cell Cycle: G2/M DNA Damage Checkpoint Regulation	3/49 (6.1%)	2/1	1.55 ^E -02	N/A
NRF2-mediated Oxidative Stress Response	6/193 (3.1%)	6/0	1.79 ^E -02	N/A
Asparagine Degradation I	1/2 (50.0%)	0/1	2.13 ^E -02	N/A
β-alanine Degradation I	1/2 (50.0%)	0/1	2.13 ^E -02	N/A
Proline Degradation	1/2 (50.0%)	0/1	2.13 ^E -02	N/A
Alanine Degradation III	1/2 (50.0%)	0/1	2.13 ^E -02	N/A
Alanine Biosynthesis II	1/2 (50.0%)	0/1	2.13 ^E -02	N/A

A. The top 15 overrepresented pathways derived from the differentially expressed transcripts (DET) in the CCPR diet compared to the control group in kidney tissue of female donors. The pathways show their corresponding ratio of regulated genes as percentage of total genes in the pathway, the ^E-value and the Z-score for predicted activation or inhibition of the pathways. Significantly activated pathway is depicted in bold.

Table 4B. Upstream transcription factor analysis in female kidney tissue

Upstream regulator	Description	Z-score	P-value	Gene log ratio
MYCN	MYCN proto-oncogene, bHLH transcription factor	+2.985	8.83 ^E -04	-0.102
MYC	MYCN proto-oncogene, bHLH transcription factor	+2.191	1.00 ^E -00	-0.325
NKX2-3	NK2 homeobox 3	+2.000	2.07 ^E -01	0.197
NKFBIA	NFκB inhibitor alpha	+1.492	4.64 ^E -02	-0.349
SMARCA4	SWI/SNF related, matrix associated, actin dependent regulator of chromatin, subfamily a, member 4	+0.600	1.44 ^E -02	-0.387
MITF	Melanogenesis associated transcription factor	+ 0.447	4.31 ^E -02	0.322
STAT3	Signal transducer and activator of transcription 3	+ 0.391	7.60 ^E -04	-0.433
PITX2	Paired like homeodomain 2	+ 1.065	2.23 ^E -03	-0.065
SATB1	SATB homeobox 1	+0.128	8.67 ^E -03	0.365
WT1	Wilms tumor 1	+ 0.101	4.24 ^E -02	0.265
HNF4A	Hepatocyte nuclear factor 4 alpha	-0.315	7.41 ^E -03	-0.239

Table 4B. (continued)

Upstream regulator	Description	Z-score	P-value	Gene log ratio
HSF1	Heat shock transcription factor 1	-0.251	4.50 ^E -02	-0.271
GATA3	GATA binding protein 3	-0.425	2.77 ^E -02	-0.360
KMT2D	Lysine methyltransferase 2D	-0.447	3.99 ^E -02	-0.251
EGR1	Early growth response 1	-0.600	4.68 ^E -02	0.130
TCF7L2	Transcription factor 7 like 2	-0.632	2.99 ^E -03	-0.329
PML	Promyelocytic leukemia	-0.785	4.28 ^E -04	-0.558
SMAD4	SMAD family member 4	-1.067	1.21 ^E -02	-0.361
STAT1	Signal transducer and activator of transcription 1	-1.534	1.23 ^E -02	-0.431
CREB1	cAMP responsive element binding protein 1	-1.591	1.97 ^E -02	0.295
IRF7	Interferon regulatory factor 7	-1.671	8.91 ^E -03	-0.374
BRCA1	BRCA1, DNA repair associated	-1.719	1.24 ^E -04	0.228
POU2AF1	POU class 2 associating factor 1	-1.987	2.87 ^E -03	+0.287
PRDM1	PR/SET domain 1	-2.121	2.75 ^E -03	-0.429
SMARCB1	SWI/SNF related, matrix associated, actin dependent regulator of chromatin, subfamily b, member 1	-2.236	9.96 ^E -03	0.351

B. Differentially regulated upstream transcription factors (TFs) derived from the DET in the CCPR diet compared to the control group in kidney tissue of female donors, with their corresponding Z-score, P-value and gene log ratio. Significantly activated or inhibited TFs are depicted in bold.

DISCUSSION

Extensive animal studies have unequivocally established the beneficial effects of various short-term DR regimens on stress resistance, including renal and hepatic IRI, with the largest protection seen by fasting, calorie and protein restriction^{10,12,14,17}. However, translation to clinical interventions has proven difficult because of concerns about the possible side effects of preoperative restrictive diets, lack of voluntary adherence and uncertainty regarding the DR strategy to be used¹⁵. Our randomized, controlled clinical trial demonstrates that five days of CCPR before live kidney donation is feasible, safe and significantly improves renal recovery in both donors and their recipients. These findings have wide clinical impact.

DR was feasible as evidenced by the fact that all 15 donors adhered to the diet. Next to the self-reported adherence, we independently confirmed compliance to the diet based on significant weight loss and altered adherence markers prealbumin and retinol binding protein in the CCPR group. Levels of systemic postoperative inflammation markers were similar in both groups, which suggests that CCPR diet does not affect the postoperative

inflammatory response¹⁵. The incidence of perioperative and postoperative complications in the kidney donors did not differ between groups either, which shows that concerns regarding a compromised immune response and wound healing following DR in a surgical setting are unwarranted and which underscores the safety of a CCPR diet¹⁵.

The beneficial protective effects of the CCRP diet on the kidney were shown by significantly improved renal function: creatinine clearance and glomerular filtration rate in the first postoperative days until hospital discharge of the donors, as well as the significant decrease of serum urea concentrations both preoperatively and postoperatively. The improved postoperative kidney function in donors due to the CCPR diet in a setting of only marginal decrease in creatinine clearance due to kidney removal itself¹⁸, further underscores the powerful effects of the CCPR diet. Subgroup analyses showed a common improved renal outcome in both male and female donors, albeit this improvement seemed to occur earlier after surgery in females.

The ameliorated outcome in the kidney donors is further strengthened by the significantly, clinically highly relevant improvement of creatinine clearance in the kidney transplant recipients from CCPR donors. Interestingly, male recipients appeared to show better serum creatinine clearance compared to female recipients. To determine whether females have a different susceptibility to IRI or response to DR, these results need to be validated in larger cohorts. Transplant recipients of CCPR donors showed a trend towards higher Tacrolimus pre-dose concentrations which suggests CCPR alters the metabolism of Tac. Despite higher exposure to Tac, which is correlated with increased nephrotoxicity¹⁹, the creatinine clearance was superior in the CCPR recipients. Together with the significantly lower incidence of acute rejection and SGF, these data indicate that short-term CCPR induces increased stress resistance in humans resulting in protecting the transplanted kidney from ischemic damage and from acute rejection. Two recipients in the control group developed uncontrollable acute rejection which necessitated transplant nephrectomy²⁰. However, these patients received belatacept rather than Tac-based immunosuppression. Although non-nephrotoxic, belatacept is a less potent immunosuppressant than Tac, we feel that these two severe cases of rejection are explained by the type of immunosuppressive therapy²¹. Excluding both patients from the statistical analysis did not impact the creatinine clearance and eGFR results in the recipients (data not shown).

Transcriptome analysis in kidney tissue obtained during surgery revealed changes in cell cycle and stress resistance pathways due to the CCPR diet. In particular, the suggested inhibition of cell cycle G2M phase regulation and upregulation of NRF2-mediated stress response and eIF2 signaling revealed a strong overlap with our preclinical data in kidneys of mice subjected to protein-free, calorie-restricted or fasting diets^{12,14,22}. Activation of

eIF2 reduces global translation, allowing cells to switch from growth to maintenance and inducing stress resistance²³. These similarities highlight the evolutionary conservation of the response to DR, which is already present in humans after five days of CCPR. In addition, a trend towards inhibition of the immune response was seen. However, this did not reach statistical significance, presumably due to the small sample size and the heterogeneity of the human tissue. Other studies using DR in heart, skeletal muscle and liver tissue in animal models showed similar inhibition of cell cycle regulation and immune system signaling as well as an upregulation of stress response pathways, including the NRF2 pathway²⁴⁻²⁷. Transcriptome profiles of aged rat kidneys revealed an opposite image of our results induced by CCPR, such as the upregulation of immune pathways, including cytokine and T-cell signaling as well as NF- κ B activation²⁸, and are in agreement with our current results as long term diet restriction delays aging². Recently, the transcription factor *Myc* was found as an important signaling molecule activated by protein restriction in *Drosophila*, potentiating innate immunity and increasing stress resistance²⁹. We found MYC as one of the highest activated transcription factors following CCPR. Since pharmacological overexpression of *Myc* mimicked the effect of DR, MYC might well be a target to develop a dietary restriction mimetic²⁹. No transcriptome analysis studies have been performed in human kidneys following DR. However, several reports on transcriptome profiling in human kidneys after transplantation were published recently. One of those performed gene expression analysis on biopsies three months after transplantation and identified 13 genes of interest that were correlated to worse allograft outcome at 12-months post-transplantation. Ankyrin repeat and SOCS Box containing 15 (*ASB15*), was significantly decreased in their analysis and this downregulation was associated with worse kidney function at 12 months³⁰. This gene was upregulated in the CCPR diet group in our unbiased profiling and might have a potential role in the protection against acute and chronic rejection³⁰. *Asb15* was discovered in 2002 as a member of the suppressor of cytokine box superfamily (SOCS) and is expressed mainly in the heart and kidney³¹. Not much is known about the function of the gene. The SOCS family, however, has been identified as a regulator of protein turnover and protein degradation, especially degradation of cytokines³². Another study, examining the link between interstitial fibrosis and gene expression profiles at 12 months after transplantation, revealed no similarities with our results³³ but found a relationship between increased serum levels of RBP and worse creatinine clearance. We showed that RBP levels decrease due to the diet, and it is worth looking into the functional role of RBP in relation to renal outcome³³. Taken together, our transcriptome analysis shows hints towards increased stress resistance and possible downregulation of the immune response by DR. In addition, *ASB15* revealed to be a gene of interest to investigate in future studies.

This study has several limitations. It was designed as a pilot study in a single transplantation center, therefore only a small cohort of patients was included and no power calculations were performed. Replacement of donor-recipient pairs that were excluded from the waiting list for various reasons (Figure S1) was performed until the desired number of 15 donors in the CCPR group was reached. As a result, the number of donors included in the control group was higher. In addition, expression analysis was only performed at mRNA level. Investigating the effects of CCPR in a larger cohort, in a different surgical population, and on a posttranscriptional level might underscore its clinical potential as well as reveal the mechanisms by which short-term DR acts in humans. Two patients received the immunosuppressive agent belatacept rather than Tac after inclusion and randomization. These patients developed acute rejection, and were excluded from the study after their rejected kidney was removed. A significantly higher number of female than male donors was included due to the difference in willingness to donate between men and women that has been described earlier³⁴. Future studies should strive for inclusion of equal numbers of both sexes.

In conclusion, we show that a CCPR diet given during five days immediately before kidney donation accelerates adaptation of kidney function of the remaining kidney and increases resistance to IRI in human kidney transplantation as evidenced by a more rapid recovery of kidney transplant function. On a transcriptional level, hints towards a switch from growth to maintenance and increased stress resistance were found. Given its non-invasive character and safety, our CCPR diet may have great impact on increasing resistance to surgical-related stress in humans.

SUBJECTS AND METHODS

Study design

This pilot study was designed as a randomized, controlled trial and was approved by the Medical Ethics Committee (METC, MEC number 2012-134) of the Erasmus MC, University Medical Center Rotterdam, The Netherlands. The study procedures were in accordance with the local METC guidelines. All subjects provided written informed consent before inclusion. The trial was registered on October 12, 2012 in the Dutch trial registry under trial code 3663 (www.trialregister.nl). This manuscript was prepared in accordance with the CONSORT 2010 statement³⁵.

Subjects

Living kidney donors were approached by the trial coordinator (FJ) and then included during the work up for donation at the outpatient clinic of the department of Surgery of the Erasmus MC, University Medical Center Rotterdam, between May 2, 2014 and November 18, 2015. To be eligible for participation in the study, donors had to be between 18 and 70 years old, had to have a BMI ≥ 19 kg/m², were not allowed to participate in another clinical trial in the 30 days prior to the day they were approached, and could have no known allergies to any of the ingredients in the diets. Figure S1. Randomization was performed using computer-generated lists as described previously¹⁶. No statistical power calculation for sample size was performed due to the pilot design of the study. In addition, since the detrimental effects of laparoscopic surgery on healthy living kidney donors was expected to be marginal, the inclusion of a substantially large number of donors was to be expected to reveal a significance based on a power calculation. With only a limited number of procedures per year, this inclusion rate would not have been feasible.

Dietary intervention

Patients in the CCPR group received a diet containing 30% fewer calories and 80% fewer protein. Dietary needs were calculated using the Harris–Benedict formula³⁶ as described previously¹⁶. The diet was given for five consecutive days and was initiated five days prior to surgery. The diet was based on a synthetic liquid diet as described previously¹⁶, and was supplemented with a limited number of low-protein and protein-free products (mainly fruits and vegetables) until the desired preset individual needs were met (Table S3). The calorie- and protein-restricted powder Scandishake® Mix shakes were kindly provided by Nutricia Advanced Medical Nutrition, The Netherlands. As described previously, the shake was provided as powder which was diluted with water. The powder consisted of 4% protein, 53% carbohydrate and 43% fat, respectively¹⁶ (Table S3). The control group had no dietary restrictions and continued their normal diet.

Surgical procedures

Preoperative, perioperative, and postoperative anesthetic care concerning drug administration, ventilation and fluid regimens was carried out according to our local protocol for the kidney donors and kidney recipients. Donor kidneys were obtained via either a laparoscopic nephrectomy or a hand-assisted retroperitoneal nephrectomy (HARP)³⁷. Kidney transplantation was performed via an open approach, and the kidney was positioned supra-inguinally on the external iliac artery and the external iliac vein. Additional informed consent was asked from the transplant recipients to obtain kidney

biopsies. Biopsies of the renal cortex were taken at the end of the cold ischemia time (kidney off ice), just before implantation in the recipient was started using a punch biopsy with a diameter of 4 mm.

Immunosuppressive therapy

Kidney transplant recipients received the same initial immunosuppressive therapy, except for two patients in the control group who received betalcept (Bristol-Myers Squib, NYC, NY) instead of tacrolimus. The initial immunosuppressive treatment consisted of tacrolimus (Prograf®; Astellas Pharma, Leiden, The Netherlands), mycophenolate mofetil (MMF; CellCept®; Roche Pharmaceuticals, Woerden, The Netherlands) and prednisolone treatment. All patients received induction therapy with basiliximab (Simulect®, Novartis Pharma, Arnhem, the Netherlands). The doses, target whole blood or plasma concentrations, and phasing of immunosuppressive therapy has been described elsewhere in detail³⁸.

Outcome parameters

Living kidney donors

Before and after the dietary intervention, the following data were obtained from all donors: body weight, age, gender, length, and systolic blood pressure. The time point before dietary intervention was set at the moment of inclusion in the trial during a visit at the outpatient clinic. The time point of first blood withdrawal before start of the dietary intervention, POD-pre, varied from one day up to over a year. Therefore, we used POD-1 values after the dietary intervention as cutoff levels for the calculation of relative values. Before and at various time points after surgery, serum levels of parameters shown in Table S4 were determined. Since kidney function is dependent on various factors, including gender and age, relative values for serum creatinine and CKD-EPI eGFR were calculated. A schematic overview of the experimental timeline of the study is shown in Figure S2. Processing of the blood samples was done as described previously¹⁶.

Kidney transplant recipients

Before and after the dietary intervention, the following data were obtained from all transplant recipients: body weight, age, gender, length, and systolic blood pressure. Before and at various time points after surgery, serum values of parameters shown in Table S4 were determined. For assessment of standard laboratory values of transplant recipients without informed consent for the kidney biopsies, a non-WMO study addendum was handed in to the local METC of the Erasmus MC, Rotterdam, the Netherlands. In our center, all patients routinely undergo a mercaptoacetyl triglycine (MAG3) renal scintigraphy on postoperative day (POD) 1 to assess renal perfusion. In case of a gradual increase of activity in the parenchyma of the transplanted kidney without evidence of cortical excretion, acute

tubular necrosis (ATN) was suspected and recorded. Delayed graft function (DGF) was defined as the need for dialysis in the first postoperative week³⁹. Slow graft function (SGF) was defined as an estimated glomerular filtration rate (eGFR) ≤ 10 ml/min per 1.73 m² at day 6 after transplantation³⁹. Classification of surgical complications was done using the Clavien-Dindo classification of surgical complications⁴⁰.

mRNA-sequence analysis

For gene expression analysis, 10 donors were included in the CCPR group and 10 donors in the control group. Biopsies were taken at the end of the cold preservation period (kidney off ice), directly before implantation. Biopsies were put in 2 mL Eppendorf tubes (Eppendorf Group, New York, USA) containing 1 mL of RNAlater RNA Stabilization Reagent (QIAGEN Benelux B.V., Venlo, the Netherlands), and were kept at 4°C for at least 48 hours. Total RNA extraction and measurement of RNA concentration was done as described previously^{13,14}. The RNA quality was expressed as the RNA integrity number (RIN, range 0-10), and values ranged between 6.1 and 8.2. Handling, analysis and visualization of the data was performed in R. Principal component analysis (PCA) and density plots of the raw counts revealed an outlying sample that had a very low RNA concentration. This sample was omitted from further analysis. A filtering step was performed to remove low count transcripts: transcripts had to be sequenced at least three times per sample and two times per experimental group within gender. The filtering step resulted in 175,756 transcripts for analysis. Differentially expressed transcripts between diet type within gender were calculated using DESeq2. False Discovery Rate correction was performed as described by Storey and Tibshirani^{41,42}. Complete raw and normalized microarray data and their MIAME compliant metadata have been deposited at the Gene expression Omnibus (GEO) database GSE103532 (www.ncbi.nlm.nih.gov/geo).

End points

The primary end point was the postoperative kidney function in the kidney donors as measured by serum creatinine and CKD-EPI eGFR⁴³. The main secondary end point was the transcriptional changes induced by the CCPR diet as measured by gene expression analysis in kidney biopsies. Additional secondary end points of the donors included: compliance to the CCPR diet, metabolic changes induced by the CCPR diet, and perioperative outcome. Secondary end points of the recipients were postoperative kidney transplant function, perioperative outcome (including blood loss, urine production), and the incidence of DGF, SGF and ATN defined as described previously³⁹.

Statistical analysis

Categorical data are presented as numbers (percentage) and continuous variables as median \pm interquartile range (IQR). The data were tested for normality using the Shapiro–Wilks test and subsequent visual assessment. Continuous data were compared using the non-parametric Mann–Whitney U test. A Bonferroni correction for multiple testing was performed on the postoperative kidney function parameters. In the living kidney donors, this correction was done separately for the short-term outcome until POD3 and the long-term outcome until POMo3. In the transplant recipients, the cutoff for short-term outcome was set at POD7, and the cutoff for the long-term outcome on POMo6. To assess changes in GFR and creatinine levels over time for both donors and recipients, lme4 (Bates, Maechler & Bolker, 2012) for R 3.3.3 was used to perform a linear mixed effects analysis of the relationship between the outcomes of interest and treatment category. Random intercepts per patient were modelled. Visual inspection of residual plots did not reveal any obvious deviations from homoscedasticity or normality. Significance for the linear mixed-effects model analysis was set at $P < 0.05$ with t-tests using Satterthwaite approximations to degrees of freedom. The analyses were performed using Statistical Packages for Social Sciences 23.0 (IBM Inc., Chicago, IL, USA), R (R foundation), GraphPad Prism (GraphPad Software Inc., version 5.01), and Office Excel (Microsoft (Office) 2016).

REFERENCES

1. Luo, H., Chiang, H.H., Louw, M., Susanto, A. & Chen, D. Nutrient Sensing and the Oxidative Stress Response. *Trends Endocrinol Metab* 28, 449-460 (2017).
2. Vermeij, W.P., et al. Restricted diet delays accelerated ageing and genomic stress in DNA-repair-deficient mice. *Nature* 537, 427-431 (2016).
3. Fontana, L., Partridge, L. & Longo, V.D. Extending healthy life span--from yeast to humans. *Science* 328, 321-326 (2010).
4. Antoine, D.J., Williams, D.P., Kipar, A., Laverty, H. & Park, B.K. Diet restriction inhibits apoptosis and HMGB1 oxidation and promotes inflammatory cell recruitment during acetaminophen hepatotoxicity. *Mol Med* 16, 479-490 (2010).
5. Perico, N., Cattaneo, D., Sayegh, M.H. & Remuzzi, G. Delayed graft function in kidney transplantation. *Lancet* 364, 1814-1827 (2004).
6. Kosieradzki, M. & Rowinski, W. Ischemia/reperfusion injury in kidney transplantation: mechanisms and prevention. *Transplant Proc* 40, 3279-3288 (2008).
7. Snoeijs, M.G., van Heurn, L.W. & Buurman, W.A. Biological modulation of renal ischemia-reperfusion injury. *Curr Opin Organ Transplant* 15, 190-199 (2010).
8. Moore, D.R., et al. Living Donor Kidney Transplantation: Improving Efficiencies in Live Kidney Donor Evaluation--Recommendations from a Consensus Conference. *Clin J Am Soc Nephrol* 10, 1678-1686 (2015).
9. Nashan, B., Abbud-Filho, M. & Citterio, F. Prediction, prevention, and management of delayed graft function: where are we now? *Clin Transplant* 30, 1198-1208 (2016).
10. Saat, T.C., van den Akker, E.K., JN, I.J., Dor, F.J. & de Bruin, R.W. Improving the outcome of kidney transplantation by ameliorating renal ischemia-reperfusion injury: lost in translation? *J Transl Med* 14, 20 (2016).
11. Salvadori, M., Rosso, G. & Bertoni, E. Update on ischemia-reperfusion injury in kidney transplantation: Pathogenesis and treatment. *World J Transplant* 5, 52-67 (2015).
12. Mitchell, J.R., et al. Short-term dietary restriction and fasting precondition against ischemia-reperfusion injury in mice. *Aging Cell* 9, 40-53 (2010).
13. Jongbloed, F., et al. Preoperative fasting protects against renal ischemia-reperfusion injury in aged and overweight mice. *PLoS One* 9, e100853 (2014).
14. Jongbloed, F., et al. A signature of renal stress resistance induced by short-term dietary restriction, fasting, and protein restriction. *Sci Rep* 7, 40901 (2017).
15. Brandhorst, S., Harputlugil, E., Mitchell, J.R. & Longo, V.D. Protective effects of short-term dietary restriction in surgical stress and chemotherapy. *Ageing Res Rev* (2017).
16. Jongbloed, F., et al. Short-Term Preoperative Calorie and Protein Restriction Is Feasible in Healthy Kidney Donors and Morbidly Obese Patients Scheduled for Surgery. *Nutrients* 8 (2016).

17. Verweij, M., et al. Glucose supplementation does not interfere with fasting-induced protection against renal ischemia/reperfusion injury in mice. *Transplantation* 92, 752-758 (2011).
18. Fehrman-Ekholm, I., Elinder, C.G., Stenbeck, M., Tyden, G. & Groth, C.G. Kidney donors live longer. *Transplantation* 64, 976-978 (1997).
19. Arreola-Guerra, J.M., Serrano, M., Morales-Buenrostro, L.E., Vilatoba, M. & Alberu, J. Tacrolimus Trough Levels as a Risk Factor for Acute Rejection in Renal Transplant Patients. *Ann Transplant* 21, 105-114 (2016).
20. de Graav, G., et al. A Randomized Controlled Clinical Trial Comparing Belatacept With Tacrolimus After De Novo Kidney Transplantation. *Transplantation* 101, 2571-2581 (2017).
21. de Graav, G.N., et al. An Acute Cellular Rejection With Detrimental Outcome Occurring Under Belatacept-Based Immunosuppressive Therapy: An Immunological Analysis. *Transplantation* 100, 1111-1119 (2016).
22. Brandhorst, S. & Longo, V.D. Fasting and Caloric Restriction in Cancer Prevention and Treatment. *Recent Results Cancer Res* 207, 241-266 (2016).
23. Wek, R.C., Jiang, H.Y. & Anthony, T.G. Coping with stress: eIF2 kinases and translational control. *Biochem Soc Trans* 34, 7-11 (2006).
24. Keogh, K., et al. Effect of Dietary Restriction and Subsequent Re-Alimentation on the Transcriptional Profile of Bovine Skeletal Muscle. *PLoS One* 11, e0149373 (2016).
25. Swindell, W.R. Genes regulated by caloric restriction have unique roles within transcriptional networks. *Mech Ageing Dev* 129, 580-592 (2008).
26. Swindell, W.R. Comparative analysis of microarray data identifies common responses to caloric restriction among mouse tissues. *Mech Ageing Dev* 129, 138-153 (2008).
27. Noyan, H., et al. Cardioprotective Signature of Short-Term Caloric Restriction. *PLoS One* 10, e0130658 (2015).
28. Park, D., et al. RNA-Seq analysis reveals new evidence for inflammation-related changes in aged kidney. *Oncotarget* 7, 30037-30048 (2016).
29. Lee, J.E., Rayyan, M., Liao, A., Edery, I. & Pletcher, S.D. Acute Dietary Restriction Acts via TOR, PP2A, and Myc Signaling to Boost Innate Immunity in *Drosophila*. *Cell Rep* 20, 479-490 (2017).
30. O'Connell, P.J., et al. Biopsy transcriptome expression profiling to identify kidney transplants at risk of chronic injury: a multicentre, prospective study. *Lancet* 388, 983-993 (2016).
31. Kile, B.T., et al. The SOCS box: a tale of destruction and degradation. *Trends Biochem Sci* 27, 235-241 (2002).
32. Andresen, C.A., et al. Protein interaction screening for the ankyrin repeats and suppressor of cytokine signaling (SOCS) box (ASB) family identify Asb11 as a novel endoplasmic reticulum resident ubiquitin ligase. *J Biol Chem* 289, 2043-2054 (2014).
33. Azevedo, H., et al. Intra-graft transcriptional profiling of renal transplant patients with tubular dysfunction reveals mechanisms underlying graft injury and recovery. *Hum Genomics* 10, 2 (2016).

34. Oien, C.M., et al. Gender imbalance among donors in living kidney transplantation: the Norwegian experience. *Nephrol Dial Transplant* 20, 783-789 (2005).
35. Schulz, K.F., Altman, D.G. & Moher, D. CONSORT 2010 statement: updated guidelines for reporting parallel group randomised trials. *BMJ* 340, c332 (2010).
36. Roza, A.M. & Shizgal, H.M. The Harris Benedict equation reevaluated: resting energy requirements and the body cell mass. *Am J Clin Nutr* 40, 168-182 (1984).
37. Dols, L.F., et al. Randomized controlled trial comparing hand-assisted retroperitoneoscopic versus standard laparoscopic donor nephrectomy. *Transplantation* 97, 161-167 (2014).
38. Shuker, N., et al. A Randomized Controlled Trial Comparing the Efficacy of Cyp3a5 Genotype-Based With Body-Weight-Based Tacrolimus Dosing After Living Donor Kidney Transplantation. *Am J Transplant* 16, 2085-2096 (2016).
39. Yarlagadda, S.G., et al. Marked variation in the definition and diagnosis of delayed graft function: a systematic review. *Nephrol Dial Transplant* 23, 2995-3003 (2008).
40. Dindo, D., Demartines, N. & Clavien, P.A. Classification of surgical complications: a new proposal with evaluation in a cohort of 6336 patients and results of a survey. *Ann Surg* 240, 205-213 (2004).
41. Storey, J.D. & Tibshirani, R. Statistical significance for genomewide studies. *Proc Natl Acad Sci U S A* 100, 9440-9445 (2003).
42. Storey, J.D. & Tibshirani, R. Statistical methods for identifying differentially expressed genes in DNA microarrays. *Methods Mol Biol* 224, 149-157 (2003).
43. Levey, A.S., et al. A new equation to estimate glomerular filtration rate. *Ann Intern Med* 150, 604-612 (2009).

SUPPLEMENTARY DATA

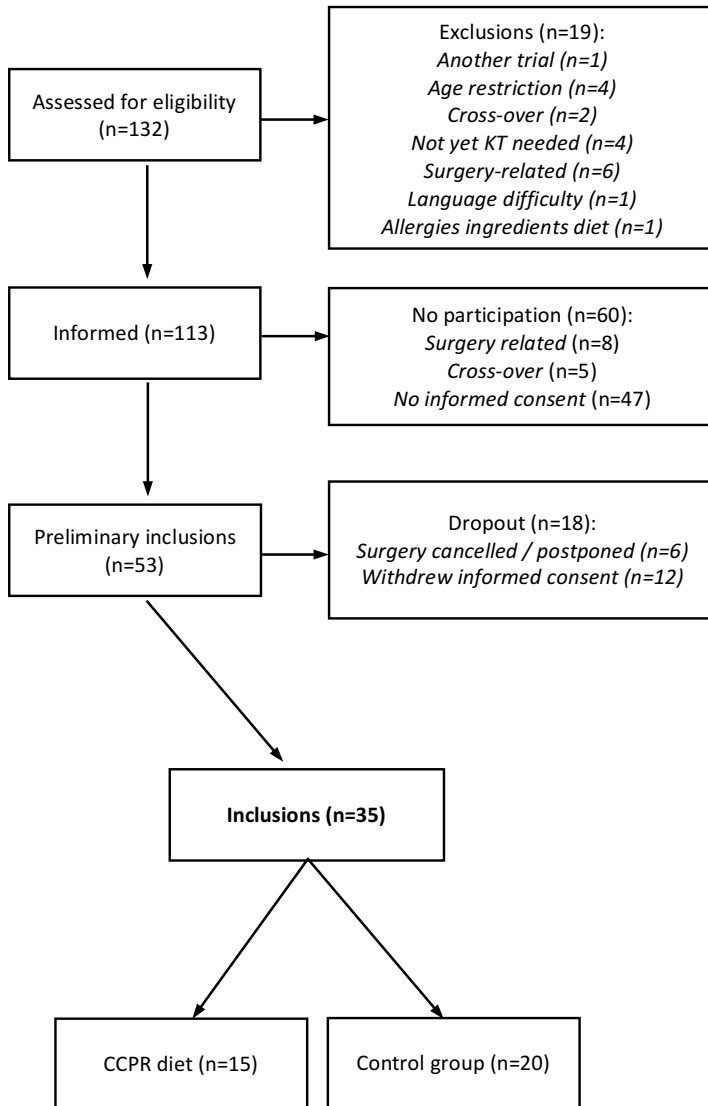


Figure S1. Flowchart of the inclusions and exclusions of the living kidney donors. Exclusions were based on preset exclusion criteria. Eligible kidney donors were approached at the outpatient clinic at the Erasmus MC, University Medical Center Rotterdam, the Netherlands. After information about the study was given, 57% of eligible donors refrained from participating in the study. Cross-over = cross-over program at which the surgery takes place outside of the Erasmus MC. KT = kidney transplantation. CCPR = combined calorie and protein restriction.

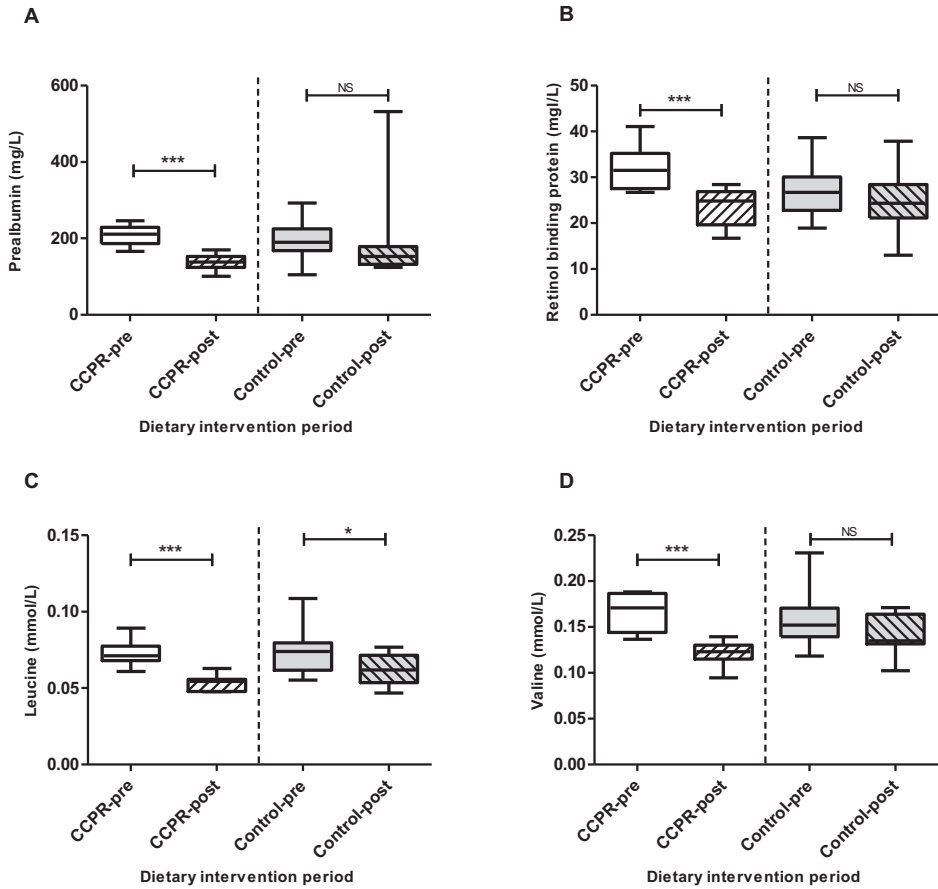


Figure S2. Compliance markers in living kidney donors before and after the CCPR diet compared to the control group. (A) Levels of prealbumin were significantly decreased after the CCPR diet compared to the control group. (B) Retinol binding protein levels were also significantly decreased after the CCPR diet. (C) Absolute levels of the branched-chain amino acid leucine were decreased after the CCPR diet. (D) The absolute numbers of valine were also significantly decreased after the CCPR diet. Values are depicted as mean \pm 95% confidence interval. * = $P < 0.05$; *** = $P < 0.001$; NS = not significant. CCPR = combined calorie and protein restriction.

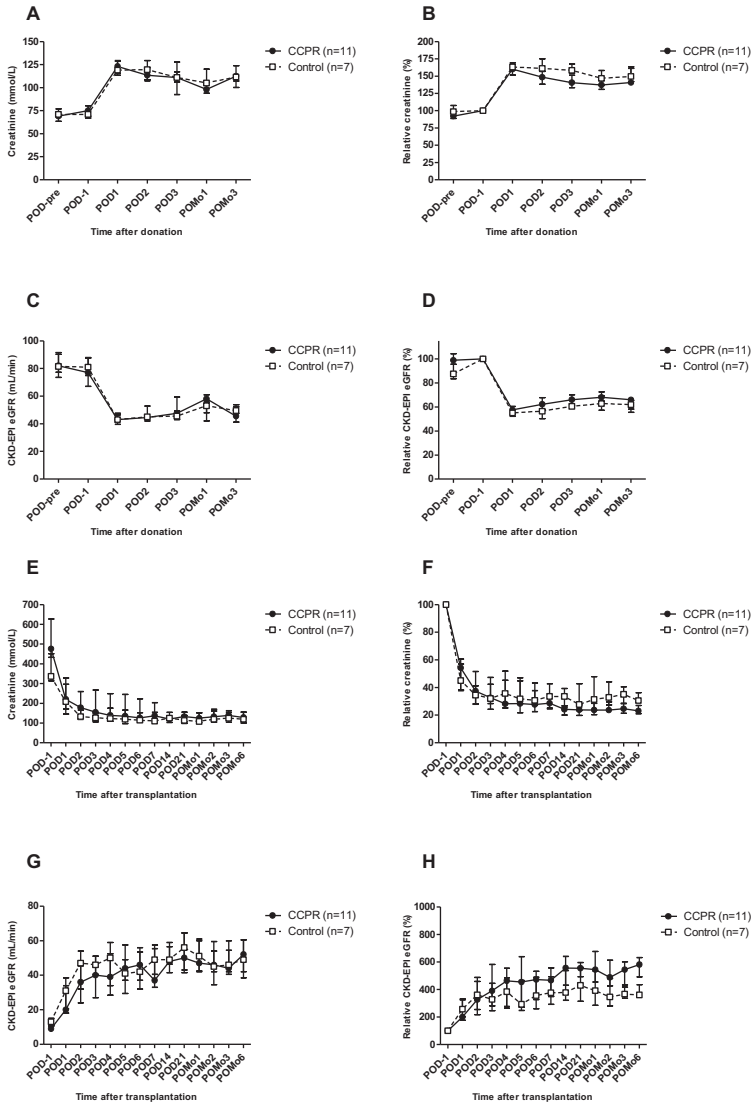


Figure S3. Kidney function of female living kidney donors before and after live kidney donation.

(A) Absolute levels of serum creatinine of the female kidney donors did not differ between the two intervention groups, while the (B) Relative creatinine levels showed a trend towards improvement in the CCPR diet group in the first postoperative days. (C) Estimated glomerular filtration rate (eGFR) showed a similar result, with no changes in absolute eGFR levels and a (D) trend towards improvement in the first postoperative days. In the kidney transplant recipients of female living kidney donors, no significant changes were seen in the (E) absolute creatinine level, the (F) relative creatinine levels, the (G) absolute eGFR and the (H) relative eGFR postoperatively. Values are depicted as median \pm interquartile range. CCPR = combined calorie and protein restriction; POD = postoperative day; POMo = postoperative month; eGFR = estimated glomerular filtration rate. * = $P < 0.05$.

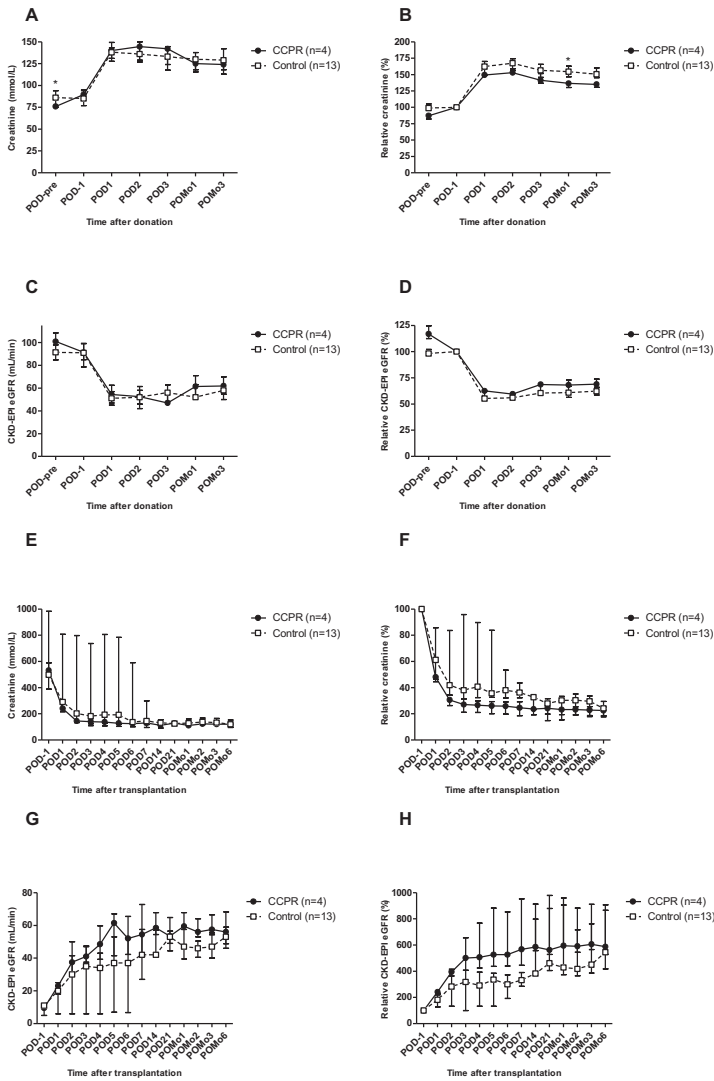


Figure S4. Kidney function of male living kidney donors before and after live kidney donation.

(A) Absolute levels of serum creatinine of the male kidney donors were significantly higher prior to start of the CCPR diet, while no differences between the two intervention groups were seen postoperatively. (B) Relative creatinine levels were significantly improved in the CCPR diet on postoperative month (POMo)1. (C) Estimated glomerular filtration rate (eGFR) showed a lower eGFR in the CCPR prior to start intervention and no differences postoperatively, with similar changes (D) in relative eGFR levels. In the kidney transplant recipients of male kidney donors, (E) absolute creatinine levels were improved as from POD1 until POD7, while (F) relative creatinine levels were better as from POD3 until POD14. (G) Absolute eGFR and the (H) relative eGFR showed a trend towards improvement postoperatively. Values are depicted as median \pm interquartile range. CCPR = combined calorie and protein restriction; POD = postoperative day; POMo = postoperative month; eGFR = estimated glomerular filtration rate. * = $P < 0.05$.

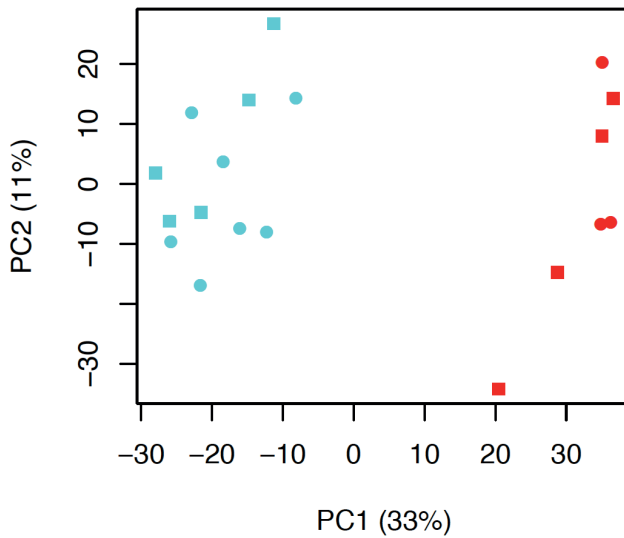


Figure S5. Principal component analysis plot of female and male kidney tissue. An unbiased principal component analysis of all kidney tissue samples obtained during kidney transplantation revealed a strong separation based on gender on both the principal component axis (PC) 1 and 2. Principal component axis 1 is depicted on the x-axis, while component axis 2 is depicted on the y-axis. Biopsies from the combined calorie and protein restriction diet kidneys are depicted with squares, while biopsies from control kidneys are depicted with circles. F = female; M = male.

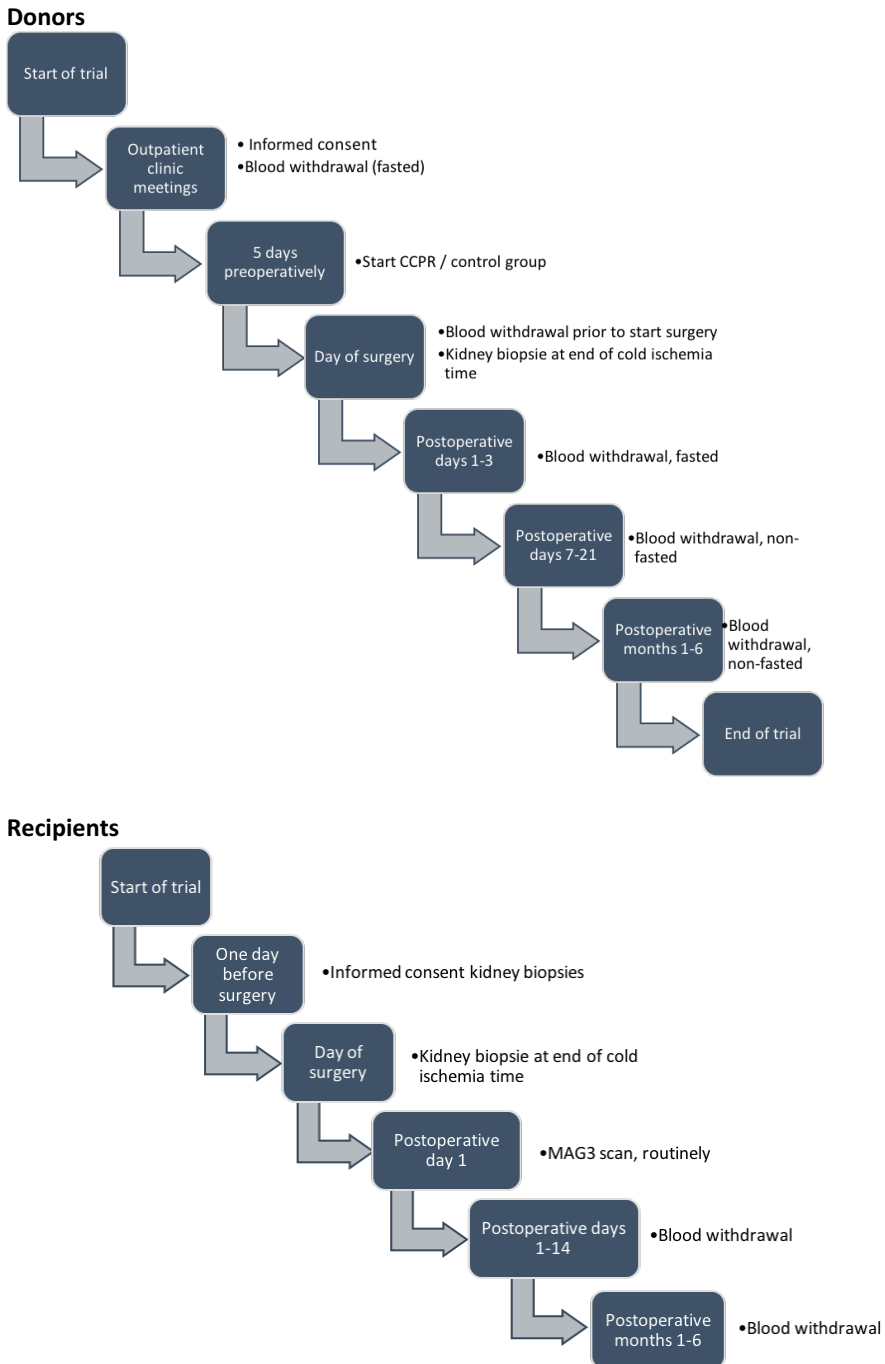


Figure S6. Timeline of living kidney donors and recipients participating in the study, from start until the end of the trial.

Table S1. Baseline characteristics of living kidney donors included in the transcriptome analysis

Parameter	CCPR (n=10)	Control (n=10)	P-value
<i>Donors</i>			
Age (years)	59 (53-61)	51 (44-64)	0.19
Gender (Male/Female)	3/7	5/5	0.39
BMI (kg/m ²)	25.6 (23.3-28.0)	25.4 (23.4-26.0)	0.59
Systolic blood pressure (mm/Hg)	130 (124-136)	128 (124-136)	0.89
Creatinine (mmol/L)	74 (68-82)	78 (71-90)	0.15
eGFR (mL/min)	83 (66-90)	75 (72-83)	0.68
Urea (mmol/L)	5.2 (4.8-5.6)	5.2 (4.0-5.4)	0.46
Glucose (mmol/L)	5.3 (5.1-5.7)	5.1 (4.8-5.8)	0.56
Albumin (g/L)	47 (45-48)	45 (45-47)	0.85
Triglycerides (mmol/L)	1.2 (0.9-1.8)	1.3 (1.2-1.5)	0.62
Hemoglobin (mmol/L)	8.7 (8.4-9.1)	8.9 (8.6-9.2)	0.63
Trombocytes (10 ⁹ /L)	241 (222-302)	223 (206-289)	0.48
CRP (mg/L)	1.4 (1.0-2.0)	1.3 (0.8-2.4)	0.30
Leukocytes (10 ⁹ /L)	6.5 (5.6-7.6)	5.9 (5.5-6.9)	1.00
Bilirubin (μmol/L)	8.0 (5.3-10.0)	6.0 (5.0-7.3)	0.31
Potassium (mmol/L)	4.5 (4.3-4.6)1	4.4 (4.1-4.8)	0.86
Type of donation (R/U/A)	3/1/6	1/6/3	0.79
Side of nephrectomy (Left/Right)	6/4	6.4	1.00
Method used (Laparoscopic/HARP)	7/3	7/3	1.00

No significant differences ($P < 0.05$) were seen in the baseline characteristics of both groups. BMI = body mass index; eGFR = estimated glomerular filtration rate using the CKD-EPI formula; CRP = C-reactive protein. Type of donation: R = related; U = unrelated; A = anonymous. HARP = hand-assisted retroperitoneal nephrectomy.

Table S2. Perioperative outcome of donors and recipients

Parameter	CCPR (n=15)	Control (n=20)	P-value
<i>Donors</i>			
Duration of surgery (HH:MM)	03:29 ± 00:10	03:53 ± 00:10	0.11
Start surgery (HH:MM)	08:11 ± 00:05	08:18 ± 00:07	0.43
Blood loss (milliliters)	47 ± 17	82 ± 24	0.24
Duration warm ischemia time 1 (MM:SS)	03:20 ± 00:18	03:23 ± 00:17	0.90
Duration cold ischemia time (HH:MM)	02:37 ± 00:10	02:45 ± 00:12	0.65
Duration of warm ischemia time 2 (MM:SS)	18:47 ± 01:12	20:00 ± 00:48	0.45
Complications during surgery (yes/no)	1/15	0/20	0.33
<i>Recipients</i>			
Duration of surgery (HH:MM)	03:08 ± 00:11	03:06 ± 00:13	0.92
Start of surgery (HH:MM)	11:54 ± 00:13	12:18 ± 00:10	0.17
Time of kidney perfusion (HH:MM)	13:41 ± 00:16	14:06 ± 00:15	0.31
Time of biopsy (HH:MM)	13:20 ± 00:17	13:28 ± 00:11	0.77
Blood loss (milliliters)	180 ± 30	231 ± 41	0.33
Urine production during surgery (yes/no)	1/15	5/20	0.14
Complications during surgery (yes/no)	1/15	0/20	0.33

Parameters are depicted as mean ± standard error of the mean. CCPR=combined calorie and protein restriction diet. HH:MM=hours:minutes; MM:SS=minutes:seconds. P-value<0.05 is considered significant.

Table S3. Pathway and upstream transcription factor analysis in renal tissue of male donors

Ingenuity Canonical Pathways	Ratio	Up/Down	P-value	Z-score
Xenobiotic Metabolism Signaling	10/287 (3.5%)	4/6	4.80 ^E -06	N/A
Antigen Presentation Pathway	4/38 (10.5%)	1/3	5.83 ^E -05	N/A
Serotonin Degradation	5/75 (6.7%)	0/5	6.23 ^E -05	N/A
LPS/IL-1-Mediated Inhibition of RXR Function	7/221 (3.2%)	2/5	2.42 ^E -04	N/A
Nicotine Degradation II	4/63 (6.3%)	1/3	4.23 ^E -04	N/A
Superpathway of Melatonin Degradation	4/68 (5.9%)	0/4	5.66 ^E -04	N/A
Allograft Rejection Signaling	4/84 (4.8%)	1/3	1.25 ^E -03	N/A
Thyroid Hormone Metabolism II	3/41 (7.3%)	0/3	1.54 ^E -03	N/A
OX40 Signaling Pathway	4/91 (4.4%)	1/3	1.68 ^E -03	N/A
Autoimmune Thyroid Disease Signaling	3/47 (6.4%)	1/2	2.28 ^E -03	N/A
Graft-versus-Host Disease Signaling	3/48 (6.2%)	1/2	2.43 ^E -03	N/A
Phenylalanine Degradation IV	2/14 (14.3%)	0/2	2.68 ^E -03	N/A
Nicotine Degradation III	3/54 (5.6%)	0/3	3.40 ^E -03	N/A
Type I Diabetes Mellitus Signaling	4/111 (3.6%)	2/2	3.46 ^E -03	N/A
Melatonin Degradation I	3/63 (4.8%)	0/3	5.25 ^E -03	N/A

The top 15 overrepresented pathways derived from the differentially expressed transcripts (DET) in the CCPR diet compared to the control group in kidney biopsies of male donors. The pathways show their corresponding ratio of regulated genes as percentage of total genes in the pathway, the *P*-value and the Z-score for predicted activation of inhibition of the pathways.

Table 3. (continued)

Upstream regulator	Description	Z-score	P-value	Gene log ratio
KLF4	Kruppel like factor 4	+2.198	7.17 ^E -04	-0.304
NUPR1	Nuclear protein 1, transcription regulator	+2.000	3.39 ^E -01	+0.081
RELA	RELA proto-oncogene, NF-κB subunit	+1.970	2.53 ^E -03	-0.513
KLF5	Kruppel like factor 5	+1.957	2.78 ^E -04	+0.803
CCND1	Cyclin D1	+1.387	1.37 ^E -02	+0.294
JUN	Jun proto-oncogene, AP-1 transcription factor subunit	+1.296	4.75 ^E -02	-0.129
HIF1A	Hypoxia inducible factor 1 alpha subunit	+1.250	5.40 ^E -04	+0.763
MYC	MYCN proto-oncogene, bHLH transcription factor	+1.224	1.97 ^E -04	+0.537
NOTCH1	Notch 1	+1.188	1.49 ^E -02	+0.357
TWIST1	Twist family bHLH transcription factor 1	+1.000	2.04 ^E -03	-0.152
TP73	Tumor protein 73	+0.639	7.73 ^E -04	+0.170
NKX2-3	NK2 homeobox 3	+0.447	9.09 ^E -03	+0.039
SMARCA4	SWI/SNF related, matrix associated, actin dependent regulator of chromatin, subfamily a, member 4	+0.378	2.59 ^E -02	-0.350
NFKBIA	NFκB inhibitor alpha	+0.295	4.07 ^E -03	+0.163
GATA3	GATA binding protein 3	+0.152	3.62 ^E -02	-0.181
TP53	Tumor protein 53	+0.128	1.99 ^E -06	-0.259
TP63	Tumor protein 63	+0.101	7.14 ^E -03	+0.116
SP1	Sp1 transcription factor	-0.063	1.50 ^E -03	-0.240
ATF3	Activating transcription factor 3	-0.106	1.8e ^E -03	-0.182
NFE2L2	Nuclear factor, erythroid 2 like 2	-0.562	3.28 ^E -02	+0.331
CEBPA	CCAAT/enhancer binding protein alpha	-0.727	3.54 ^E -03	+0.441
MYCN	MYCN proto-oncogene, bHLH transcription factor	-0.923	2.36 ^E -02	-0.030
HMG1	High mobility group AT-hook 1	-1.000	1.13 ^E -02	+0.945
CREBBP	CREB binding protein	-1.004	8.07 ^E -03	+0.409
KLF3	Kruppel like factor 3	-1.134	3.35 ^E -03	-0.302
CEBPB	CCAAT/enhancer binding protein beta	-1.353	2.65 ^E -03	-0.186
HNF4A	Hepatocyte nuclear factor 4 alpha	-3.331	7.37 ^E -04	-0.470

Differentially regulated upstream transcription factors (TFs) derived from the DET in the CCPR diet compared to the control group in kidney biopsies of male donors, with their corresponding Z-score and gene log ratio. Significantly activated or inhibited TFs are depicted in bold.

Table S4. Composition and energy content of the combined calorie and restricted (CCPR) diet

Diet	CCPR diet
Average content per 100 gram/mL	
Energy (kcal)	507
(kJ)	2120
Protein (g)	4.98
Protein (% of energy intake)	4.0
Casein (g)	4.3
Whey protein (g)	0.4
Carbohydrates (g)	67.0
Carbohydrates (% of energy intake)	53.0
Glucose (g)	0.8
Fructose (g)	0.0
Lactose (g)	3.2
Maltose (g)	2.5
Sucrose (g)	14.0
Polysaccharides (g)	46.3
Other (g)	0.2
Fat (g)	24.5
Fat (% of energy intake)	43
Saturated fat (g)	7.7
Monounsaturated fat (g)	7.3
Polyunsaturated fat (g)	9.4
Linoleic acid (g)	8.1
A-linoleic acid (g)	0.9
Fibres	0.0
Sodium (mg)	128
Potassium (mg)	272
Chloride (mg)	163
Calcium (mg)	85
Phosphor (mg)	147
Magnesium (mg)	30

Table S4. (continued)

Diet Average content per 100 gram/mL	CCPR diet
Ferritin (mg)	0.0
Zinc (mg)	0.0
Copper (mg)	0.0
Manganic (mg)	0.0
Fluoride (mg)	0.0
Molybdenum (µg)	0.0
Selenium (µg)	0.0
Chrome (µg)	0.0
Iodine (µg)	0.0
Vitamin A (µg-RE)	0.0
Carotenoids (mg)	0.0
Vitamin D (µg)	0.0
Vitamin E (mg α-TE)	0.0
Vitamin K (µg)	0.0
Thiamin (mg)	0.0
Riboflavin (mg)	0.0
Niacin (mg NE)	0.0
Pantheothenzuur (mg)	0.0
Vitamin B6 (mg)	0.0
Foliumzuur (µg)	0.0
B12 (µg)	0.0
Biotin (µg)	0.0
Vitamin C (mg)	0.0
Choline (mg)	0.0

Table S5. Serum parameters measured in living kidney donors at various time points during the study

Parameter	Assay performed at	Time points of measurements
Creatinine (mmol/L)	Hospital laboratory	Outpatient clinic, daily during hospital admission, POMo 1, 3 & 6
eGFR (mL/min)	Hospital laboratory	Outpatient clinic, daily during hospital admission, POMo 1, 3 & 6
Urea (mmol/L)	Hospital laboratory	Outpatient clinic, daily during hospital admission, POMo 3 & 6
Glucose (mmol/L)	Hospital laboratory	Outpatient clinic, daily during hospital admission, POMo 1, 3 & 6
Albumin (g/L)	Hospital laboratory	Outpatient clinic, daily during hospital admission, POMo 1, 3 & 6
Triglycerides (mmol/L)	Hospital laboratory	Outpatient clinic, daily during hospital admission, POMo 1, 3 & 6
Hemoglobin (mmol/L)	Hospital laboratory	Outpatient clinic, daily during hospital admission, POMo 1, 3 & 6
Trombocytes ($10^9/L$)	Hospital laboratory	Outpatient clinic, daily during hospital admission, POMo 1, 3 & 6
CRP (mg/L)	Hospital laboratory	Outpatient clinic, daily during hospital admission
Leukocytes ($10^9/L$)	Hospital laboratory	Outpatient clinic, daily during hospital admission, POMo 1, 3 & 6
Bilirubin ($\mu\text{mol/L}$)	Hospital laboratory	Outpatient clinic, daily during hospital admission
Potassium (mmol/L)	Hospital laboratory	Outpatient clinic, daily during hospital admission, POMo 1, 3 & 6
Prealbumin (mg/L)	Beckman	Outpatient clinic, peroperatively
Retinol binding protein (mmol/L)	Diazyme	Outpatient clinic, peroperatively
Leucine (mmol/L)	Nightingale	Outpatient clinic, peroperatively, POD 1 & 2
Valine (mmol/L)	Nightingale	Outpatient clinic, peroperatively, POD 1 & 2

eGFR = estimated glomerular filtration rate using the CKD-EPI formula; PoMo = postoperative month; POD = postoperative day; CRP = C-reactive protein.

PART IV

SUMMARY AND DISCUSSION

Chapter 9

Summary and discussion

Chapter 10

Nederlandse samenvatting

CHAPTER 9

SUMMARY AND DISCUSSION

SUMMARY AND DISCUSSION

An increase in oxidative stress and inflammation has a negative influence on overall quality and quantity of life leading to accelerated development of age-associated diseases and a decrease in lifespan. An acute induced stress response leads to worse outcome of organ transplantation procedures due to the development of ischemia-reperfusion injury (IRI), creating a boundary for the possibilities of organ transplantation for patients with end-stage organ failure. A surgery-related stress response might also influence the outcome of patients undergoing elective surgery, especially when comorbidities as in morbid obesity are present. Dietary restriction (DR) has been shown to improve lifespan and reduce age-associated diseases as well as to improve outcome of IRI in various healthy laboratory animal models. Many aspects of DR are still unknown, including which components of the calories are responsible for the effects of DR, the mechanisms underlying DR, as well as the overall applicability of DR in different animal models involving acute stress-related injury. Foremost, the translation of DR into a clinical setting has been proven difficult and evidence of effects in patients is therefore limited. There is a pressing necessity for improving the knowledge about the etiology and clinical applicability of DR to optimize the effects of DR on surgical and disease-related stress resistance and postoperative outcome.

The aims of this thesis were three-fold: One, to assess the effects of current and novel short-term DR regimens in different mouse models of acute stress; two, to gain more insight into the mechanisms underlying DR; and three, to search for a clinically applicable dietary intervention in the surgical setting.

Current and novel short-term dietary restriction regimens

Previously, colleagues showed that two weeks of 30% DR and three days of fasting are able to significantly improve survival and kidney function in male C57BL/6 mice that underwent renal IRI as compared to ad libitum (AL) fed mice¹. These results were among the first that showed a beneficial effect of a short-term DR on a model of acute stress and several questions arose calling for follow-up research. In this section I will subsequently address questions related to the effective components and regimens of short-term DR drawing in part on the results in this thesis.

The aforementioned results were obtained in an optimal model for laboratory research with young-lean male mice¹. However, this model is less suitable to examine whether DR has a broader applicability when it comes to differences in age, gender, obesity and genetic background. The results in **chapter 2** taught us that three days of fasting can indeed be reproduced in an optimal model to study aging and obesity. In this study, fasted hybrid mice showed improvement of both survival and kidney after induction of IRI, which was

accompanied by a reduction of acute tubular necrosis and more tubular regeneration. These effects were not as robust as in young-lean mice, yet sufficient enough to induce protection. In addition, we showed that female mice were able to withstand longer periods of IRI than male mice as an indication that the female gender has a higher endogenous threshold against IRI. Therefore, these data concluded that the presence of comorbidities as in age and obesity are not able to annul the robust beneficial effects of fasting on the outcome after renal IRI.

Although three days of fasting is able to induce its beneficial effects in different mouse models, it does not give insight into which dietary components are precisely responsible for the effects of acute stress. After the first results of calorie restriction and its effects on health span and lifespan, many researchers examined whether the calorie reduction per se, or a specific component, was responsible for these effects. The first studies focused on the macronutrients, being protein, carbohydrates and fat²⁻⁵. Later the ratio of macronutrients became a subject of interest as well^{6,7}. The first evidence of a major role of protein restriction was obtained in fruit flies where long-term protein-restriction resulted in increased lifespan⁸⁻¹¹. In mice, the translation of long-term protein restriction to short-term regimens found that six days of deprivation was sufficient to induce beneficial effects against multiple forms of IRI¹². A major issue with protein restriction proved to be the voluntary calorie restriction that mice imposed during the dietary intervention, which made the effects of protein restriction still indistinguishable from calorie restriction¹². In **chapter 4**, we are the first to show the beneficial effects of protein deprivation for only three days, resulting in significant improved mortality and kidney function after renal IRI. In addition, three days of 30% DR did not induce protection and therefore we could distinguish the effects of protein restriction from calorie restriction. Recent literature also implicated the roles of other macronutrients, in particular in the light of aging and health span^{13,14}. Solon-Biet et al. showed that the ratio of protein to carbohydrates is responsible for the benefits, in which a low amount of protein and high amount of carbohydrates revealed the largest effect on both health span and lifespan whereas reduction of carbohydrates gave an opposite image¹⁵. Several studies followed and pointed towards the same direction^{6,7}. We could also confirm the detrimental effects of carbohydrate reduction, since our carbohydrate-free diet resulted in an aggravation of mortality and kidney function decline compared to control mice fed AL. In comparison, a fat-free diet showed results similar to the control mice fed AL, and was implicated to have no major role in the effects of calorie restriction on renal IRI. Indeed, Solon-Biet et al. came to the same conclusion in the long-term dietary interventions, revealing that fat intake did not contribute to health span and lifespan changes in mice⁶. The authors also pointed towards the role of amino acids, in particular branched chain amino acids, in the effects of protein restriction on aging^{6,15}. In **chapter 5**, we also narrowed down the role of protein restriction by providing mice with a 3-day diet lacking one of

the following essential amino acids (EAA): methionine, leucine or tryptophan. These diets were followed by induction of acute stress in the form of liver IRI. Most literature about amino acids and DR studied a methionine restricted diet, and it showed that the results are slightly in favor of methionine being responsible for the beneficial effects on aging^{13,16,17}. The extent to which tryptophan and leucine deprived diets have been examined is small, however do point towards a favorable role of essential amino acids deprivation on increased lifespan⁵. We showed that hepatic IRI, as a model for acute stress, was significantly reduced by all three EAA-free diets. These effects were already visible six hours after hepatic IRI in the leucine-free and tryptophan-free diets, while all EAA-free diets showed these effects at 24 hours post-IRI. We concluded that it is possible to provide robust protection against IRI with a diet as short as three days lacking only one essential amino acid and that these essential amino acids are able to produce this protection in a similar manner.

In conclusion, by extending current DR regimens we showed that three days of fasting is able to induce protection against renal IRI in different animal models, including aged and overweight mice that more resemble the human population. In addition, by exploring novel DR regimens we could induce the protection against IRI with protein restriction and EAA-restriction as short as three days. Of interest, carbohydrate and fat deprivation were not able to induce protection and even aggravated the detrimental effects of IRI. Therefore, macronutrients are not equally responsible for the beneficial effects of DR and separation of total calorie restriction from protein restriction enabled us to develop a short-term DR regimen that is more specific and could be more suited to use in a clinical setting.

Insight into the mechanisms underlying dietary restriction

Parallel with the vastly increasing number of studies about DR is the amount of studies focusing on the mechanisms underlying DR¹⁸⁻²⁰. Many genes and pathways have been proposed to play an important role in the beneficial effects of DR, however none of those has been validated extensively in different studies^{19,21-23}. Despite the fact that the exact mechanisms underlying DR remain to be elucidated, several pathways and genes have been put forward by many authors and are therefore of particular interest. These pathways include the NRF2-mediated stress response and mTOR nutrient signaling^{24,25}. With an unbiased approach, we collected and analyzed transcriptome profiles of kidney and liver after various short-term dietary interventions that were either protective or non-protective against renal and hepatic IRI in order to examine the responsible mechanisms for ourselves. Interestingly, aforementioned pathways were on our top list of pathways and transcription factors as well. Transcription factor nuclear factor-erythroid like 2 (NRF2) is known to be the initiator of the phase II response, which is a detoxifying response to for instance oxidative and xenobiotic metabolism²⁴. The NRF2-pathway was activated by all our protective diets,

including three days of fasting in the aged-overweight mice in **chapter 2**, the protein-free diet used against renal IRI in **chapter 4**, and all EAA-free diets given prior to hepatic IRI in **chapter 5**. Previous gene expression datasets of three days of fasting in young-lean male mice and two weeks of 30% DR demonstrated the activation of NRF2 as well¹. Despite that the importance of NRF2 in the protection against DR has been described in multiple studies as well as our studies, a *Nrf2* knock-out mice model submitted to DR showed similar increase in lifespan as control mice. Therefore, the exclusive role for NRF2 could not be determined and other factors are of essence in the protection as well²⁶. Another one of those factors could be the nutrient-sensing pathway of mammalian target of Rapamycin (mTOR). mTOR has extensively been linked to an increase of lifespan and stress resistance and several studies that investigated the effects of a mTOR-inhibitor, rapamycin, show promising results^{25,27-29}. In our renal IRI model, the protective diets all activated the transcription factor hepatocyte nuclear receptor factor alpha (HNF4A). HNF4A results in downregulation of metabolic sensors, in particular the mTOR pathway^{30,31}. Using Western blot analysis, we examined S6 phosphorylation as a down-stream target of mTOR through immunoblotting. We showed a significant decrease in S6 phosphorylation after three days of fasting, indicating downregulation of mTOR²⁵. The EAA-free diets downregulated mTOR as well, although not significantly in all diets. Since the mTOR pathway came up downregulated in both kidney and liver, this demonstrates its importance in the overall induction of stress resistance by DR. Moreover, renal and hepatic gene expression profiles showed multiple common features even though different DR regimens were used. The nuclear receptor signaling was proposed to be upregulated via the activation of retinoid acids (RAs), for instance the PPAR-pathway as seen in the aged-overweight fasting mice studied in **chapter 2**, and FOXO3, which is the transcription factor that was activated the most after DR in the kidney in **chapter 4**. Both RAs and FOXO3 are linked to increased stress resistance and protection against various forms of ischemia³²⁻³⁴. The stress resistance pathway mediated by all diets was NRF2, as mentioned before, but also the eukaryotic translation initiation factor 2a (EIF2a). Via activation of general control nonderepressible 2 (*Gcn2*), the EIF2a signaling response activates and mediates genes involved in antioxidant defense, reduction of inflammation and cell survival³⁵. Previously, *Gcn2* was thought to be required for inducing stress resistance in mice, although a more recent study showed that *Gcn2*-deprivation was not sufficient to indeed provide protection against hepatic IRI and other factors might be required^{12,36}. One of these additional factors might be the inhibition of cellular proliferation via inhibition of transcription factors FOXM1 and SMARCB1^{24,37} as seen after the EAA-free diets in **chapter 5**, thereby inducing the adaptive response that shifts resources from growth to maintenance as seen by DR³⁸. We concluded that it is possible to provide robust protection against IRI with a diet as short as three days lacking protein or only one essential amino acid. We propose a mechanism-of-action model, based

on both renal and liver array results, in which this protection is induced by activation of nuclear receptor signaling, stress resistance pathways as well as inhibition of cell growth to a more maintenance state, mediated via key transcription factors mandatory for the beneficial effects.

The transcriptome profile analyses of all diets as done in **chapter 2**, **chapter 4** and **chapter 5**, were performed in biopsies taken after the dietary intervention but before induction of the acute stress of IRI. In **chapter 3**, we focused on the effects shortly after the induction of the stressor, which was in this case the chemotherapeutic agent irinotecan. We applied three days of fasting in C26 colorectal carcinoma (CRC)-bearing BALB/c male mice. Twelve days after tumor inoculation, mice were either fasted for three days or continued to be AL fed after which each group was given one high dose of irinotecan or vehicle. The effects of fasting were investigated on a transcriptional level in liver and tumor tissue collected 12 hours after the administration of irinotecan, when mice were sacrificed. In liver tissue, unbiased transcriptome analysis showed that fasting markedly reduced the number of gene expression changes caused by administration of irinotecan. Together with more homogenous gene expression profiles in liver tissue of mice subjected to fasting, these data point towards a dampening of the changes caused by irinotecan, thereby partially protecting healthy tissue from the response to irinotecan. Further evidence of this hypothesis is provided by the dysregulation of the genotoxic response due to fasting as compared to liver tissue of AL fed mice given irinotecan; the AL fed mice showed activation of DNA damage pathways, including RhoA signaling, as well as cellular stress and cytokine signaling pathways, whereas fasting mice subjected to irinotecan showed indirect inhibition of RhoA via activation of RhoGDI signaling, and vast reduction of chemokine and cytokine pathways³⁹. In addition, pathways involved in growth and proliferation, such as the mTOR signaling via suppression of the p7056 pathway, were downregulated which points once more towards the shift from growth to maintenance as described before^{38,40}. Interesting, the NRF2-pathway remained activated in the fasting mice after the stressor (*i.e.* irinotecan) was given, which may indicate a key role for NRF2 in the protection against acute stress. The fact that these stress-related pathways are already induced before the induction of stress and eventually results in dampening of genotoxicity, implicates that DR is able to induce the right amount of stress to eventually protect against high levels of stress as induced by either IRI or chemotherapy. This hypothesis has been proposed before, and was named hormesis in which low doses of a certain stressor are able to protect against the toxic effects of a stressor in high doses²¹. In this case hormesis is activated via nutrient deprivation, in particular via reduction in proteins or essential amino acids. Even more so, in **chapter 3** we showed that fasting has no effect on the antitumor effect of irinotecan as implied by previous findings. For instance, colleagues showed that fasted APC^{15lox} mutant mice given irinotecan had similar reduction in tumor size, and inhibited tumor cell proliferation as measured

by markers such as Cyclin D1⁴¹. Although detrimental effects of fasting on the effects of chemotherapy or on the main tumors have not been reported, implications have been made about the additional beneficial effects of DR on tumorigenesis and cancer treatment²⁰. In our data, on a transcriptional level the changes induced by fasting in healthy liver tissue were not present in tumor tissue. The transcriptomic profiles of the tumor tissue were very heterogeneous, and therefore our analyses could not detect specific changes induced by fasting in tumor tissue treated with irinotecan. These data support the differential stress sensitization theory, which states that beneficial alterations in normal cells due to nutrient deprivation protects them against chemotherapy induced toxicity whilst these changes do not occur in cancer cells⁴².

The search for a clinically applicable dietary intervention

The misbalance of increasing body of evidence showing the benefits of both long-term and short-term DR in various animal models, including non-human primates, and only few clinical studies concerning DR is indicative for the problems associated with translation of DR to a clinical setting^{43,44}. Multiple reasons for the absence of clinical implementation have been given over time⁴⁵. Foremost, the metabolic rate of mice is a multitude of that of humans which suggests prolonged periods of DR in humans. The difficulty for humans to comply to such periods of DR is intense, even though a small group of long-term DR-believers has been able to restrict themselves of 30% calories for many years now and do show signs of improved metabolic profile. Moreover, the generally held belief that the advantages of normal to high food intake prior to surgery is in conflict with the principle of preoperative nutrient restriction⁴⁵. Therefore, obtaining more evidence of the safety, feasibility and effects of a dietary intervention in a clinical setting was warranted to change the current preoperative nutritional care in patients.

To start with, a model that is opposite to nutrient deprivation might be of additional value in order to fully understand the effects of DR and the way it affects surgical outcome. Therefore, in **chapter 6**, the link between inflammation, aging and surgery was investigated by examining markers of aging and the immune system in patients with morbid obesity undergoing bariatric surgery. Morbid obesity is known to negatively affect mortality and increases the risk of age-associated diseases, including diabetes mellitus, cardiovascular disease and cancer⁴⁶. This link is thought to be caused by the chronic subclinical inflammatory state as seen in morbidly obese patients, which is caused by an over activation of the immune system as induced by white adipose tissue⁴⁷. This inflammation has a direct effect on the immune system and is thought to cause premature aging of the immune system, a phenomenon called ‘inflammaging’⁴⁸. This is possibly even worse in patients who are metabolically compromised by the presence of the metabolic syndrome, which might be

partially reversed by bariatric surgery. We showed that obesity itself did not affect relative telomere length (RTL), however the presence of metabolic syndrome significantly decreased the RTL of CD4⁺ T-cells. This shortening of RTL was accompanied by an increase of fully matured T cells, indicating that the complete T-cell compartment is affected by obesity. Bariatric surgery, which is the definitive solution for morbid obesity once all other options have failed, could partially forestall this effect⁴⁹. At three and six months after surgery, the significant decrease of RTL seen prior to surgery was no longer present, indicating that the shortening was halted. However, RTL at 12 months postoperatively was similar to the length prior to surgery, suggesting bariatric surgery affects RTL only in the first phase after surgery. These data show that metabolically compromised morbidly obese patients show signs of accelerated immune aging, which gives important insight into the increased risk of morbidity and mortality of these patients. Therefore, the metabolic syndrome predisposes to accelerated T-cell aging and is temporarily reversed by obesity-reducing surgery.

As it comes to DR, previously colleagues showed the feasibility and safety of a preoperative DR regimen in a clinical setting. A preoperative diet including three days of 30% DR followed by 24 hours of fasting was well adhered to by living kidney donors, and no preoperative, perioperative or postoperative complications due to the diet were seen⁵⁰. However, the diet only induced marginal effects on postoperative outcome⁵¹. In **chapter 2** we used an optimal model to study human aging and obesity and demonstrated that DR is applicable independent of age and body weight, although aging did result in a dampening of the transcriptomic response. In addition, we showed that both male and female genders are protected against IRI by DR. **Chapter 4** pointed us towards the additional effects of protein restriction on IRI. With our extended knowledge of protein restriction and handling of such a diet by patients, in **chapter 7** we developed a combined calorie and protein restricted diet to further investigate in a clinical setting. We showed the safety, feasibility and adherence to the diet in two surgical patient populations, namely living kidney donors and morbidly obese patients. A total of 71% of the donors and bariatric surgery patients complied to the restricted diet, which induced minor discomfort in about two-third of the patients. All discomforts, mainly gastro-intestinal changes, scored low on the visual analogue scale and quickly resolved after normal eating pattern was resumed. The patients that did withdraw early from the diet, reported discomfort as the main reason. Especially the morbidly obese patients awaiting bariatric surgery suffered from discomfort, possibly due to the increased prevalence of functional gastrointestinal disorders in obese patients⁵². Adherence to the diet could be objectively measured via metabolic parameters prealbumin (PAB) and retinol binding protein (RBP). Serum levels of both markers significantly decreased due to the restricted diet compared to the placebo diet and control group. Branched chain amino acids leucine and valine were both significantly decreased in the diet group, while no changes occurred in the placebo or control group. One patient in the control group showed no

reduction in any of these markers, and the compliance of this participant could therefore be questioned. Also, the restricted diet induced a significant body weight loss compared to the control groups, what could be seen as another marker for adherence to the diet. No increase in complications or length of hospital stay occurred in the restricted diet group, indicating the safety of the diet. To conclude, in **chapter 8** we were able to show the beneficial effects of a mild adaptation of this diet in living kidney donors. The diet included more protein-free snacks that patients could choose from, which might be the reason for the increased in compliance rate. The combined calorie and protein restricted (CCPR) diet induced vast improvement of kidney function in the living kidney donors, as shown by improved clearance of serum creatinine, estimated glomerular filtration rate (eGFR) and serum levels of urea in the first postoperative period. In addition, kidney transplant recipients of donors whom had received the diet showed an even more remarkable improvement of their graft function and outcome, with an average decrease in serum creatinine levels of 70% in the CCPR group compared to 40% in the control group. This improvement was accompanied by a significant lower incidence of acute rejection and slow graft function in the first postoperative period. Transcriptome profiles of kidneys subjected to the calorie and protein-restricted diet showed more heterogeneity compared to the profiles obtained in mice. Even so, the analysis of the human biopsies marked activation of the NRF2-mediated stress response and inhibition of various cytokine signaling pathways, indicative of a reduction of cellular stress and DNA damage, and therefore revealed a high overlap with our data obtained in mice²⁴. Especially the activation of the NRF2-mediated stress response indicated the important role of this transcription factor. Furthermore, EIF2 signaling was significantly upregulated as well, which is a pathway strongly regulated by fasting in the irinotecan-subjected mice as well³⁵. These data provide the effectiveness of a diet to activate the stress response in order to increase stress resistance against surgery-related injury. Overlaying our data with previously performed transcriptome analyses in human kidney biopsies found various genes of interest to the beneficial effect against kidney-related injury, including *ASB15*, *EGR2* and *AXNA*^{53,54}. However, no other studies investigated gene expression changes in kidney biopsies subjected to DR up-to-date and an exact comparison of studies could therefore not be made. A recent pilot study did show signs of reduced hematological toxicity and improved DNA damage recovery in breast cancer patients whom were fasted 24 hours before undergoing chemotherapy⁵⁵. Our study also successfully translated DR in a clinical setting, and provided the evidence that short-term DR is able to increase stress resistance in humans. Therefore, it paves the way for future implementation of DR in elective surgery patients and perhaps in cancer patients undergoing chemotherapy as well.

FUTURE PERSPECTIVES

The cornerstone of the studies described in this thesis is the effects of dietary restriction (DR) on acute stress-related injury. We demonstrated the beneficial effects of three days of fasting, a 3-day protein-free diet as well as a 3-day essential amino acid-free diet on renal and hepatic ischemia-reperfusion injury (IRI) as well as on chemotherapy induced toxicity, and linked the phenotypical protective response to a differentiated network of pathways and transcription factors on a transcriptional level. We successfully translated the preclinical data to a safe, feasible and effective diet in living kidney donors and their kidney transplant recipients, and showed that it improves graft outcome and function. These data show a unique comprehensive picture of the effects of nutritional preconditioning from a phenotypical, transcriptional and clinical point of view, and has brought us a step further to develop the optimal preoperative DR strategy in an elective clinical setting.

We showed that the beneficial effects of three days of fasting on IRI can be reproduced in an animal model that represents human aging and obesity. The effects of DR were more pronounced in young-lean mice and female mice were able to resist longer periods of renal IRI, indicating that the intensity of stress resistance is dependent on factors as age, body weight and gender. Future studies including a large cohort of female and male mice of different ages and body weights, could point us further towards understand the extent of which these factors play a role in the protection. As a result, factors including age, body weight and gender should be held into account when applying DR in the clinic, and future studies should include a sufficient number of patients to correct for and investigate the exact role of these factors.

As described, the protective effects of a short-term fasting regimen could also be applied to reduce the adverse effects of chemotherapy⁵⁶. Since fasting did not affect the antitumor efficacy of chemotherapy treatment, the concept of differential stress sensitization (DSS) was confirmed in our studies⁴². Huisman et al. proposed the role of phase II proteins in the increased stress resistance in normal cells, including NRF2 and upregulation of xenobiotic metabolism⁴¹. We could partially verify this hypothesis with the activation of the NRF2 stress response in healthy liver cells, whereas the transcriptional changes as seen in the liver did not occur in tumor tissue. The role of NRF2 as sole contributor to the beneficial effects of fasting on stress resistance has not yet been demonstrated²⁶. Extending the experimental setup to different chemotherapeutics, larger groups and various time points of analysis could further elucidate the mechanisms responsible for this DSS. As a consequence, higher dosages of chemotherapeutics might be applied in the near future, thereby increasing the chance of an effective treatment for cancer and survival benefits in cancer patients.

We are the first to show the beneficial effect of protein deprivation for only three days and this diet could be further narrowed down by showing the beneficial effects of individual essential amino acid deprivation on hepatic IRI, suggesting an essential role of amino acid sensing in the increased stress resistance. As a final step, transcriptome analyses of all these diets enabled us to study their induced changes on mRNA level. However, these data did not reveal one mechanism in particular but instead a network of multiple pathways activated by a number of transcription factors, evoking the protective response of short-term nutrient deprivation. In all studies, we could disentangle a similar pattern of pathway regulation. Future studies focusing on overexpression and knock-down of transcription factors such as FOXO3, should further elucidate the role of these transcription factors and the pathways they activated in the protection of DR.

We examined the effects of morbid obesity on aging of the immune system, in particular the T-cell immune system. Our data suggest that that morbid obesity in combination with the presence of metabolic syndrome indeed leads to premature aging of the immune system as determined by attrition of telomere length and an increase in T-cell maturation in peripheral white blood cells. These changes could be forestalled by applying obesity-reducing bariatric surgery, and were already present in the first three to six months following surgery. This pilot study indicates that morbid obesity is a risk factor for premature aging of the immune system, and that bariatric surgery is a valuable treatment to counteract this effect. Studying the effects of morbid obesity, the metabolic syndrome and bariatric surgery in a larger cohort and on a molecular level in tissue collected during surgery, could increase our understanding of the effects of obesity and inflammation on aging as well as on stress resistance during a situation of food deprivation, either via DR or via surgery. In addition, extending the follow-up period after bariatric surgery could give insight whether the decrease in telomere length at 12 months postoperatively is an indication of the short-term effect of bariatric surgery on immunological aging or the effect of the small sample size and therefore not representative.

We showed the safety, feasibility and objective adherence to the diet in two surgical patient populations, namely living kidney donors and bariatric surgery patients. We were able to show the beneficial effects of a mild adaptation of this diet in living kidney donors, and showed vast improvement of kidney function in both donors and recipients. Transcriptome profiles of human kidney biopsies revealed high overlap with our preclinical data, and highlighted the importance of gender on the effects on stress resistance. Future studies are needed in order to validate these results, and these studies should focus on larger cohorts, different patient populations as well as other DR regimens.

In overall conclusion, in this thesis we provide new evidence that various short-term dietary restriction interventions are able to induce beneficial effects on acute-stress related injury in various mouse models, human living kidney donors and their transplant recipients, and substantiated these results with promising new insights into the molecular mechanisms using gene expression analyses. We are only a few steps away from the successful application of nutritional precondition in elective surgery. Future studies should finalize these steps by validating the clinical results in larger and different patient cohorts as well as provide posttranscriptional mechanisms underlying dietary restriction. These data should bring us to the optimal preoperative nutritional regimen, either via dietary restriction or a dietary restriction mimetic, to implement in standard care for elective surgery patients.

REFERENCES

1. Mitchell, J.R., et al. Short-term dietary restriction and fasting precondition against ischemia-reperfusion injury in mice. *Aging Cell* 9, 40-53 (2010).
2. Good, R.A., et al. Nutritional deficiency, immunologic function, and disease. *Am J Pathol* 84, 599-614 (1976).
3. Macrae, F.A. Fat and calories in colon and breast cancer: from animal studies to controlled clinical trials. *Prev Med* 22, 750-766 (1993).
4. Sohal, R.S. & Weindruch, R. Oxidative stress, caloric restriction, and aging. *Science* 273, 59-63 (1996).
5. Spindler, S.R. Caloric restriction: from soup to nuts. *Ageing Res Rev* 9, 324-353 (2010).
6. Solon-Biet, S.M., et al. Dietary Protein to Carbohydrate Ratio and Caloric Restriction: Comparing Metabolic Outcomes in Mice. *Cell Rep* 11, 1529-1534 (2015).
7. Le Couteur, D.G., et al. The impact of low-protein high-carbohydrate diets on aging and lifespan. *Cell Mol Life Sci* 73, 1237-1252 (2016).
8. Partridge, L., Piper, M.D. & Mair, W. Dietary restriction in *Drosophila*. *Mech Ageing Dev* 126, 938-950 (2005).
9. Fontana, L., Partridge, L. & Longo, V.D. Extending healthy life span--from yeast to humans. *Science* 328, 321-326 (2010).
10. Bruce, K.D., et al. High carbohydrate-low protein consumption maximizes *Drosophila* lifespan. *Exp Gerontol* 48, 1129-1135 (2013).
11. Jensen, K., McClure, C., Priest, N.K. & Hunt, J. Sex-specific effects of protein and carbohydrate intake on reproduction but not lifespan in *Drosophila melanogaster*. *Aging Cell* 14, 605-615 (2015).
12. Peng, W., et al. Surgical stress resistance induced by single amino acid deprivation requires *Gcn2* in mice. *Sci Transl Med* 4, 118ra111 (2012).
13. Lee, C. & Longo, V. Dietary restriction with and without caloric restriction for healthy aging. *F1000Res* 5(2016).
14. Simpson, S.J., et al. Dietary protein, aging and nutritional geometry. *Ageing Res Rev* (2017).
15. Solon-Biet, S.M., et al. The ratio of macronutrients, not caloric intake, dictates cardiometabolic health, aging, and longevity in ad libitum-fed mice. *Cell Metab* 19, 418-430 (2014).
16. Brown-Borg, H.M. & Buffenstein, R. Cutting back on the essentials: Can manipulating intake of specific amino acids modulate health and lifespan? *Ageing Res Rev* (2016).
17. Ables, G.P. & Johnson, J.E. Pleiotropic responses to methionine restriction. *Exp Gerontol* 94, 83-88 (2017).
18. Shimokawa, I., Chiba, T., Yamaza, H. & Komatsu, T. Longevity genes: insights from calorie restriction and genetic longevity models. *Mol Cells* 26, 427-435 (2008).
19. Longo, V.D., et al. Interventions to Slow Aging in Humans: Are We Ready? *Aging Cell* 14, 497-510 (2015).

20. Cangemi, A., et al. Dietary restriction: could it be considered as speed bump on tumor progression road? *Tumour Biol* 37, 7109-7118 (2016).
21. Turturro, A., Hass, B.S. & Hart, R.W. Does caloric restriction induce hormesis? *Hum Exp Toxicol* 19, 320-329 (2000).
22. Masoro, E.J. Caloric restriction and aging: controversial issues. *J Gerontol A Biol Sci Med Sci* 61, 14-19 (2006).
23. Cavallini, G., Donati, A., Gori, Z. & Bergamini, E. Towards an understanding of the anti-aging mechanism of caloric restriction. *Curr Aging Sci* 1, 4-9 (2008).
24. Hine, C.M. & Mitchell, J.R. NRF2 and the Phase II Response in Acute Stress Resistance Induced by Dietary Restriction. *J Clin Exp Pathol* S4(2012).
25. Yuan, M., Pino, E., Wu, L., Kacergis, M. & Soukas, A.A. Identification of Akt-independent regulation of hepatic lipogenesis by mammalian target of rapamycin (mTOR) complex 2. *J Biol Chem* 287, 29579-29588 (2012).
26. Pearson, K.J., et al. Nrf2 mediates cancer protection but not longevity induced by caloric restriction. *Proc Natl Acad Sci U S A* 105, 2325-2330 (2008).
27. Geissler, E.K. & Schlitt, H.J. The potential benefits of rapamycin on renal function, tolerance, fibrosis, and malignancy following transplantation. *Kidney Int* 78, 1075-1079 (2010).
28. Esposito, C., et al. Sirolimus prevents short-term renal changes induced by ischemia-reperfusion injury in rats. *Am J Nephrol* 33, 239-249 (2011).
29. Zhang, C., et al. Rapamycin protects kidney against ischemia-reperfusion injury through recruitment of NKT-cells. *J Transl Med* 12, 224 (2014).
30. Hirota, K., et al. Hepatocyte nuclear factor-4 is a novel downstream target of insulin via FKHR as a signal-regulated transcriptional inhibitor. *J Biol Chem* 278, 13056-13060 (2003).
31. Daemen, S., Kutmon, M. & Evelo, C.T. A pathway approach to investigate the function and regulation of SREBPs. *Genes Nutr* 8, 289-300 (2013).
32. van den Berg, M.C. & Burgering, B.M. Integrating opposing signals toward Forkhead box O. *Antioxid Redox Signal* 14, 607-621 (2011).
33. Fusco, S. & Pani, G. Brain response to calorie restriction. *Cell Mol Life Sci* 70, 3157-3170 (2013).
34. Obrochta, K.M., Krois, C.R., Campos, B. & Napoli, J.L. Insulin regulates retinol dehydrogenase expression and all-trans-retinoic acid biosynthesis through FoxO1. *J Biol Chem* 290, 7259-7268 (2015).
35. Lageix, S., Rothenburg, S., Dever, T.E. & Hinnebusch, A.G. Enhanced interaction between pseudokinase and kinase domains in Gcn2 stimulates eIF2alpha phosphorylation in starved cells. *PLoS Genet* 10, e1004326 (2014).
36. Harputlugil, E., et al. The TSC complex is required for the benefits of dietary protein restriction on stress resistance in vivo. *Cell Rep* 8, 1160-1170 (2014).
37. Kalimuthu, S.N. & Chetty, R. Gene of the month: SMARCB1. *J Clin Pathol* 69, 484-489 (2016).
38. Shanley, D.P. & Kirkwood, T.B. Calorie restriction and aging: a life-history analysis. *Evolution* 54, 740-750 (2000).

39. Aghajanian, A., Wittchen, E.S., Campbell, S.L. & Burridge, K. Direct activation of RhoA by reactive oxygen species requires a redox-sensitive motif. *PLoS One* 4, e8045 (2009).
40. Kim, J., Kundu, M., Viollet, B. & Guan, K.L. AMPK and mTOR regulate autophagy through direct phosphorylation of Ulk1. *Nat-cell Biol* 13, 132-141 (2011).
41. Huisman, S.A., Bijman-Lagcher, W., JN, I.J., Smits, R. & de Bruin, R.W. Fasting protects against the side effects of irinotecan but preserves its anti-tumor effect in *Apc15lox* mutant mice. *Cell Cycle* 14, 2333-2339 (2015).
42. Lee, C., et al. Fasting cycles retard growth of tumors and sensitize a range of cancer cell types to chemotherapy. *Sci Transl Med* 4, 124ra127 (2012).
43. Robertson, L.T. & Mitchell, J.R. Benefits of short-term dietary restriction in mammals. *Exp Gerontol* 48, 1043-1048 (2013).
44. Ingram, D.K. & de Cabo, R. Calorie restriction in rodents: Caveats to consider. *Ageing Res Rev* (2017).
45. Brandhorst, S., Harputlugil, E., Mitchell, J.R. & Longo, V.D. Protective effects of short-term dietary restriction in surgical stress and chemotherapy. *Ageing Res Rev* (2017).
46. Follow-up to the Political Declaration of the High-level Meeting of the General Assembly on the Prevention and Control of Non-Communicable Diseases 2013. (2013).
47. Cao, H. Adipocytokines in obesity and metabolic disease. *J Endocrinol* 220, T47-59 (2014).
48. Frasca, D. & Blomberg, B.B. Inflammaging decreases adaptive and innate immune responses in mice and humans. *Biogerontology* 17, 7-19 (2016).
49. Lopes, E.C., et al. Is Bariatric Surgery Effective in Reducing Comorbidities and Drug Costs? A Systematic Review and Meta-Analysis. *Obes Surg* 25, 1741-1749 (2015).
50. van Ginhoven, T.M., et al. Pre-operative dietary restriction is feasible in live-kidney donors. *Clin Transplant* 25, 486-494 (2011).
51. van Ginhoven, T.M., et al. Dietary restriction modifies certain aspects of the postoperative acute phase response. *J Surg Res* 171, 582-589 (2011).
52. Ho, W. & Spiegel, B.M. The relationship between obesity and functional gastrointestinal disorders: causation, association, or neither? *Gastroenterol Hepatol (N Y)* 4, 572-578 (2008).
53. O'Connell, P.J., et al. Biopsy transcriptome expression profiling to identify kidney transplants at risk of chronic injury: a multicentre, prospective study. *Lancet* 388, 983-993 (2016).
54. Azevedo, H., et al. Intragraft transcriptional profiling of renal transplant patients with tubular dysfunction reveals mechanisms underlying graft injury and recovery. *Hum Genomics* 10, 2 (2016).
55. de Groot, S., et al. The effects of short-term fasting on tolerance to (neo) adjuvant chemotherapy in HER2-negative breast cancer patients: a randomized pilot study. *BMC Cancer* 15, 652 (2015).
56. Huisman, S.A., et al. Fasting protects against the side effects of irinotecan treatment but does not affect anti-tumour activity in mice. *Br J Pharmacol* 173, 804-814 (2016).

CHAPTER 10

NEDERLANDSE SAMENVATTING

NEDERLANDSE SAMENVATTING

Een toename in oxidatieve stress en inflammatie heeft een nadelig effect op de kwaliteit en kwantiteit van leven en leidt zowel tot versnelde ontwikkeling van ouderdomsziekten als tot een afname van de levensduur. Een acute toename in oxidatieve stress, de acute stressrespons, resulteert in een slechtere uitkomst van orgaantransplantaties vanwege het optreden van ischemie-reperfusie schade (IRS). Dit leidt tot een beperkte hoeveelheid mogelijkheden voor orgaantransplantatie bij patiënten met eindstadium nierfalen. Een stressrespons gerelateerd aan een operatie kan eveneens de uitkomst van de operatie beïnvloeden bij patiënten die electieve chirurgie ondergaan, in het bijzonder wanneer bijkomende aandoeningen zoals morbide obesitas aanwezig zijn. Dieetrestrictie (DR) heeft een bewezen positief effect op de levensduur en op het verminderen van ouderdomsziekten alsmede een verbeterde uitkomst van IRS in verscheidene gezonde diermodellen. Vele aspecten van DR zijn nog steeds onbekend, zoals welke componenten van de calorie verantwoordelijk zijn voor de effecten van DR, welke mechanismen ten grondslag liggen aan DR en de toepasbaarheid van DR in meerdere diermodellen van acute stress. Daarbij is de translatie van DR naar de klinische setting moeilijk gebleken en blijft het bewijs over de effecten van DR in patiënten vooralsnog beperkt. Om deze redenen is er een dringende behoefte voor het verbreden van de kennis over de etiologie en klinische toepasbaarheid van DR om de effecten van DR op chirurgische- en ziekte-gerelateerde stress alsmede de postoperatieve uitkomst te optimaliseren.

De doelen van dit proefschrift waren: het vaststellen van de effecten van de huidige regimes kortdurende diëten in verschillende muismodellen, het onderzoeken van de effecten van macronutriënten en aminozuren op de effecten van DR, om de kennis te verbreden over de moleculaire mechanismen die ten grondslag liggen aan DR en om een veilig en effectief dieet te ontwikkelen om toe te passen in een klinische, chirurgische setting.

Modellen en mechanismen van nutritionele preconditionering

In **hoofdstuk 2** hebben we de eerdere resultaten van DR op IRS toegepast op een ander muismodel om zo de effecten van DR in een wijder perspectief te plaatsen. Eerder hebben we aangetoond dat 2 weken 30% DR en 3 dagen vasten zorgen voor een significante verbetering van zowel overleving als nierfunctie in C57BL/6 mannetjes muizen die totaal 37 minuten IRS hebben ondergaan in tegenstelling tot muizen die onbeperkt, ad libitum, toegang hadden tot voedsel. In dit hoofdstuk laten we zien dat deze positieve effecten ook geïnduceerd konden worden in een muismodel met een andere genetische herkomst, van oudere leeftijd, met overgewicht en in zowel het mannelijke als vrouwelijke geslacht. Mannetjes en vrouwtjes F1-FVB/C57BL6-hybride muizen die 3 dagen hadden gevast, lieten een verbetering van overleving zien na het toepassen van IRS waarbij de vrouwtjes

muizen tevens in staat waren langere IRS-tijden te weerstaan dan mannetjes. Analyse van de nierfunctie na inductie van IRS liet zien dat vasten zorgde voor significant lagere serum ureum waarden, vermindering van acute tubulaire necrose en meer tubulair herstel. We concludeerden dat een hogere leeftijd en de aanwezigheid van obesitas niet zorgden voor afname van de robuuste effecten van vasten op de uitkomst na IRS in de nier en dat het vrouwelijke geslacht in staat is langere IRS-tijden te kunnen weerstaan.

Vervolgens hebben we deze fenotypische resultaten geanalyseerd op transcriptieniveau door microarray analyse te verrichten op nieren van zowel jonge slanke als oudere mannetjes muizen met overgewicht, nadat ze 3 dagen hadden gevast. Een sterk vergelijkbaar patroon van clusters en richting van genen was zichtbaar in het nierweefsel van zowel de jonge als oudere muizen, alhoewel de genexpressie wel sterker was in de jonge muizen. Dit resultaat suggereert dat de transcriptie effecten van DR minder duidelijk aanwezig zijn in oude muizen met overgewicht maar uiteindelijk wel voldoende zijn voor het induceren van bescherming. Hierdoor werd het mogelijk om de beschermende effecten van DR te onderzoeken door naar de overlappende respons tussen beide groepen te kijken. Een pathway-analyse van deze overlappende respons liet een anti-inflammatoir patroon zien, waarbij er sprake was van activatie van de retinoid X-receptor (RXR), de peroxisome proliferator-activated receptor (PPAR) en de nuclear factor erythroid like 2 (*Nrf2*) pathways. Deze pathways zijn allemaal gerelateerd aan de activatie van de acute fase respons via stimulatie van vetzuur verbranding, vermindering van de ontstekingsprocessen of via de inductie van bescherming door detoxificatie. Met dit hoofdstuk hebben we de inductie van een netwerk van een aantal pathways kunnen bevestigen, wat leidt tot een toename van weerstand tegen oxidatieve stress in zowel jonge slanke als oudere muizen met overgewicht.

In **hoofdstuk 3** hebben we de zoektocht naar de effecten van vasten voortgezet door vasten toe te passen in een ander diermodel en daarbij de mechanismen van vasten op transcriptieniveau verder uit te zoeken. We hebben nogmaals 3 dagen vasten uitgevoerd maar dit keer in BALB/c muizen die subcutaan werden geïnjecteerd met C26 colorectale carcinoomcellen. Twaalf dagen na tumor injectie werden de muizen verdeeld in een groep die 3 dagen ging vasten en een groep die ad libitum toegang had tot eten. De muizen in beide groepen werden vervolgens weer onderverdeeld in een groep die een hoge dosis van het chemotherapeuticum irinotecan kreeg of een placebo injectie. De effecten van vasten op irinotecan werden onderzocht in zowel het bloed, lever- als tumorweefsel dat was verzameld op het moment van opoffering van de muizen, namelijk op tijdstip 12 uur na de injectie. Analyse van de lever- en nierfunctie in de controle muizen liet duidelijke lever- en nierschade zien samen met beenmergdepressie als gevolg van de gift irinotecan, terwijl de gevaste muizen significante vermindering van deze schade liet zien en geen beenmergdepressie optrad. In gezond leverweefsel werd vervolgens een transcriptoom analyse verricht na

dieetinterventie en chemotherapie behandeling. Hierbij werd zichtbaar dat 3 dagen vasten zorgde voor zowel een verminderd aantal genexpressie veranderingen door irinotecan als een gelijkmatiger genexpressie profiel. Deze data suggereren dat vasten leidt tot een verminderde respons zoals veroorzaakt door irinotecan, daarbij het gezonde leverweefsel deels beschermend tegen de toxische respons geïnduceerd door het chemotherapeuticum. Deze hypothese werd verder bevestigd door de dysregulatie van de genotoxische respons van irinotecan door vasten in vergelijking met de controlegroep. Met name de expressie van meerdere DNA-schade pathways, zoals de RhoA en MAPK signaling, was geremd door vasten. Zowel RhoA als MAPK zijn gelinkt aan ziekte winst bij kanker in de literatuur en meerdere klinische studies worden momenteel verricht betreffende MAPK-remmers als behandeling tegen kanker. Ook pathways die geassocieerd zijn met stress resistentie waren aangedaan door vasten, zoals remming van de mTOR pathway via demping van de p7056 pathways en de activatie van de NRF2-gemedieerde stress respons. Naar aanleiding van deze data stelden we de hypothese dat de bijwerkingen van chemotherapie kunnen worden geremd door vasten in gezond leverweefsel via inbreuk doen op de regulatie van de celcyclus en de remming van DNA-schade alsmede de activatie van anti-inflammatoire en stressrespons pathways in gezonde cellen om zo de weerstand tegen stress te verhogen.

Eerdere resultaten hebben laten zien dat vasten geen verandering geeft op het anti-tumor effect van irinotecan, en deze resultaten konden worden gevalideerd in onze transcriptoom analyse. Tumorweefsel liet namelijk grote heterogeniteit tussen weefsels zien en daardoor kon geen duidelijk patroon worden gezien zoals geïnduceerd door vasten. Daarom waren de veranderingen geïnduceerd door vasten zoals in gezond leverweefsel niet zichtbaar in tumorweefsel. Deze data ondersteunen de differentiële stress sensitatie theorie, welke inhoudt dat veranderingen in normale cellen als gevolg van vermindering van voeding zorgen voor bescherming tegen chemotherapie-gerelateerde toxiciteit terwijl deze veranderingen niet zichtbaar zijn in kankercellen.

In **hoofdstuk 4** hebben we vervolgens de rol van macronutriënten onderzocht in de effecten van DR, waarbij we gebruikt hebben gemaakt van nier IRS als model voor schade als gevolg van acute stress. Het eerste bewijs van de rol van eiwitrestrictie werd gezien in fruitvliegen, waarbij eiwitrestrictie op lange termijn zorgde voor een verlenging van de levensduur. Wij gaven mannetjes C57BL/6 muizen een van de volgende diëten: 3 of 10 dagen eiwitvrij, 3 of 14 dagen koolhydraatvrij en 3 of 14 dagen vetvrij. De diëten werden gevolgd door inductie van IRS van de nier. Zowel mortaliteit als nierfunctie verslechterden door een koolhydraatvrij en een vetvrij dieet, terwijl een 10-daags eiwitvrij dieet een verbetering van overleving en nierfunctie liet zien na IRS. Wel gaf eiwitrestrictie tevens een restrictie van calorieën van ongeveer 30%, waardoor de effecten van calorische en eiwitrestrictie niet van elkaar konden worden onderscheiden. Een eiwitvrij dieet gedurende 3 dagen zorgde tevens

voor bescherming tegen IRS, vergelijkbaar met 2 weken 30% DR, terwijl 3 dagen 30% DR geen bescherming bood. Hierdoor konden we alsnog bescherming tegen IRS toeschrijven aan de eiwitrestrictie. Vervolgens hebben we de eerdere mRNA genexpressie datasets uitgebreid met array data na een 3 dagen eiwitvrij, koolhydraatvrij en vetvrij dieet. Door het excluseren van alle genen die tevens gereguleerd werden door de niet-beschermende diëten (koolhydraatvrij, vetvrij en 3 dagen 30% DR), kwamen slechts marginale veranderingen in genregulatie naar voren die niet verder konden leiden naar inzicht in het beschermende mechanisme van DR. We stelden de hypothese op dat de genexpressie profielen van de niet-beschermende diëten deels zouden overlappen met die van de beschermende diëten en dat de bescherming werd geïnduceerd door additionele veranderingen dan wel sterkere regulatie van pathways. Met deze hypothese hebben we een meta-analyse uitgevoerd met alle diëten, waarna een pathway en upstream transcriptiefactor analyse volgden. Hieruit kwam naar voren dat bij het beschermende effect pathways betrokken zijn die invloed hebben op nucleaire receptoren, stressrespons, stress-gerelateerde schade en biosynthese. Ook kwam de NRF2-gemedieerde stressrespons pathway naar voren, een pathway die tevens naar voren kwam in onze vorige studies. Deze pathways werden gereguleerd door activatie van verscheidene transcriptiefactoren, de belangrijkste daarbij FOXO3, HMGA1 en HNF4A, waarbij een gedetailleerde meta-analyse liet zien dat deze transcriptie factoren niet of minimaal werden gereguleerd in het niet-beschermende koolhydraatvrije dieet. FOXO3 speelt een belangrijke rol in meerdere processen waaronder die van weerstand tegen cellulaire stress en die van celcyclus regulatie. Deze beider processen zijn eerder beschreven als belangrijke pionnen in het induceren van de beschermende effecten van DR op IRS. HMGA1 is een van de factoren betrokken bij de insuline receptor pathway die is aangedaan door DR. Daarbij kan HMGA1 ook de binding van FOXO's aan nucleaire receptoren bevorderen, waarbij de nucleaire signalering wordt geactiveerd. Activatie van HNF4A leidt tot remming van metabole sensoren, met name die van de mTOR pathway. Zoals eerder beschreven is remming van mTOR gerelateerd aan verlenging van levensduur en toename van weerstand tegen stress. Via Western blot analyse hebben we deze remming van mTOR gevalideerd. Samenvattend hebben we met deze analyse de betrokkenheid van verscheidene bekende en eerdergenoemde pathways betrokken bij de bescherming van DR tegen IRS kunnen valideren en zijn nieuwe transcriptiefactoren aan het licht gekomen die waarschijnlijk aan de basis staan van de regulatie van deze pathways. Desalniettemin zijn meer studies in verschillende diermodellen van DR en stress tezamen met het uitbreiden van de genexpressie analyses nodig zijn om het optimale dieet te vinden wat uiteindelijk ook toepasbaar is in mensen.

Om die reden hebben we in **hoofdstuk 5** de rol van eiwitrestrictie en de effecten op transcriptieniveau verder onder de loep genomen in een ander IRS-model. We hebben muizen een dieet van 3 dagen gegeven waarbij een van de volgende essentiële aminozuren

ontbrak: methionine, leucine of tryptofaan. Vervolgens hebben deze muizen IRS van de lever ondergaan via afklemmen van een groot deel van de bloedtoevoer van en naar de lever gedurende 75 minuten. Het meten van de voedselinname, gewichtsveranderingen, markers voor leverschade en genexpressie analyses werden verricht en vergeleken met een controlegroep zonder dieet. Alhoewel alle diëten zorgden voor 30% reductie in calorie inname, waren markers voor leverschade significant verlaagd in alle dieetgroepen. Deze effecten waren al na 6 uur na IRS zichtbaar in de leucine- en tryptofaangroepen, en na 24 uur in alle dieetgroepen. Op transcriptieniveau lieten de leucine- en tryptofaangroepen een hoge mate van overlap zien wat betreft genvariatie, pathway en transcriptiefactor analyse. Deze respons was minder sterk in de methionine groep. Desalniettemin was een duidelijk vergelijkbaar patroon van genexpressie en –richting zichtbaar tussen alle dieetgroepen. Pathway en upstream transcriptiefactor analyses van de overlappende genen wezen weer richting de rol van nucleaire receptoren en pathways betrokken bij weerstand tegen cellulaire stress, waarbij er grote gelijkenis te zien was tussen de nier en lever modellen van IRS. NRF2 en mTOR waren bekende factoren die tevens gereguleerd waren in de lever en versterkten zo hun belangrijke rol die zij spelen in de beschermende effecten van DR op IRS in beide diermodellen. Ook FOXO was geactiveerd, echter was dit niet significant in alle dieetgroepen. Een model voor bescherming op transcriptieniveau werd ontworpen dat was gebaseerd op de gezamenlijke resultaten in de nier en lever. Dit model beschrijft de effecten van DR die geïnduceerd zijn via regulatie van nucleaire receptoren, pathways betrokken bij weerstand tegen acute stress en de remming van cellulaire proliferatie. Aan de basis van het beschermende effect staat daarbij de nucleaire receptor signalering die zorgt voor activatie van retinoïde zuren, FOXO en remming van steroïden wat leidt tot toename van de stressresistentie en bescherming tegen verscheidene vormen van ischemie. Andere stressresistentie pathway waren tevens sterk geactiveerd door de aminozuurvrije diëten, waaronder de eerdergenoemde NRF2 pathway alsook de EIF2 α signalering via Gcn2. De activatie van de EIF2 α pathway via Gcn2 zorgt voor regulatie van genen die betrokken zijn bij de activatie van antioxidanten, de afname van inflammatie en bij cellulaire overleving. Eerder werd gedacht dat Gcn2 essentieel was voor de inductie van stressresistentie in muizen, echter werd dit in een recentere studie weer ontkracht. Als laatste speelt remming van cellulaire proliferatie door DR een belangrijke rol, waarbij deze remming werd bewerkstelligd door remming van transcriptiefactoren FOXM1 en SMARCB1. Hierdoor werd een adaptieve respons geïnduceerd die zorgt voor de verschuiving van celgroei naar onderhoud.

We concluderen dat het weglaten van een essentieel aminozuur voor 3 dagen dezelfde bescherming biedt tegen lever IRS als een eiwitvrij dieet. Deze data worden ondersteund door een model waarin de bescherming wordt geïnduceerd door activatie van nucleaire

receptoren, stressresistentie pathways alsmede de verschuiving van celgroei naar onderhoud en wordt gemedieerd door transcriptiefactoren die essentieel blijken voor het ontstaan van bescherming.

De connectie tussen inflammatie, veroudering en chirurgie

Om de effecten van DR op chirurgie en het postoperatieve herstel in zijn volledigheid te kunnen begrijpen, is een model dat lijnrecht tegenover DR staat daarbij van toegevoegde waarde. Daarom hebben we in **hoofdstuk 6** de connectie tussen inflammatie, veroudering en chirurgie onderzocht door te kijken naar markers van veroudering en het immuunsysteem in patiënten met morbide obesitas die bariatrische chirurgie ondergaan. De aanwezigheid van morbide obesitas heeft een negatief effect op zowel mortaliteit als morbiditeit, waarbij het met name gaat om het risico op het ontstaan van ouderdomsziekten zoals diabetes mellitus, hart- en vaatziekten en kanker. De veronderstelling bestaat dat deze connectie wordt veroorzaakt door het ontstaan van chronische en subklinische inflammatie in patiënten met morbide obesitas. Deze inflammatie wordt veroorzaakt door een overactiviteit van het immuunsysteem geïnduceerd door wit vetweefsel en heeft een direct effect op het immuunsysteem. Deze overactiviteit zou de oorzaak zijn van de versnelde veroudering van het immuunsysteem en is in ergere mate aanwezig bij mensen die het metabool syndroom hebben. Bariatrische chirurgie zou een rol kunnen spelen in het tegenhouden van deze versnelde veroudering. Twee maten voor veroudering zijn telomeerlengte enerzijds en de T-cel differentiatiestatus anderzijds, wat de rijping van het T-cel immuunsysteem vaststelt. Om uiteindelijk de effecten van morbide obesitas, het metabool syndroom en bariatrische chirurgie op de versnelde veroudering van het immuunsysteem te onderzoeken, hebben we telomeerlengte en de T-cel differentiatiestatus gemeten in patiënten met morbide obesitas die wel of niet het metabool syndroom hadden. Deze metingen zijn gedaan in bloedmonsters die zowel voor als op meerdere tijdstippen na bariatrische chirurgie zijn afgenomen. Zowel relatieve telomeerlengte (RTL) als meerdere markers voor de T-cel differentiatiestatus zijn bepaald. Deze bepalingen lieten zien dat alleen morbide obesitas de RTL niet aantast, maar dat de aanwezigheid van het metabool syndroom wel de RTL in CD4⁺ T-cellen significant verkort. Deze verkorting ging gepaard met een toename van volledig gerijpte T-cellen, waarbij duidelijk werd dat het gehele T-cel compartiment was aangedaan door obesitas en het metabool syndroom. Bariatrische chirurgie, de definitieve oplossing voor morbide obesitas op het moment dat alle andere opties hebben gefaald, zorgde voor het deels terugdringen van dit effect. Op 3 en 6 maanden na chirurgie was de significante verkorting van RTL, zoals zichtbaar was voor chirurgie, niet meer aanwezig als teken van het tot staan brengen van de verkorting. Echter was de RTL na 12 maanden wel weer gelijk aan de lengte zoals gemeten vóór chirurgie, wat suggereert dat bariatrische chirurgie de RTL alleen in de eerste fase beïnvloedt. De veroudering van het T-cel systeem

zoals zichtbaar vóór chirurgie, was in een minder sterke mate aanwezig na chirurgie. Deze data laten zien dat patiënten met morbide obesitas en het metabool syndroom tekenen van versnelde veroudering laten zien. Dit geeft een belangrijk inzicht in de mogelijke redenen voor het toegenomen risico op mortaliteit en morbiditeit in deze patiënten. Het feit dat deze negatieve effecten deels kunnen worden tegengegaan door chirurgie is een indicatie dat bariatrische chirurgie bevorderlijk kan zijn voor zowel gezondheid als levensduur. Om deze reden zou de versnelde veroudering bij mensen met morbide obesitas en het metabool syndroom een criterium kunnen zijn om bariatrische chirurgie toe te passen, naast het al bekende criterium van gewichtsreductie. De criteria voor het ondergaan van bariatrische chirurgie zouden daarom onder de loep moeten worden genomen om de behandeling voor morbide obesitas in de toekomst te kunnen optimaliseren.

Klinische toepasbaarheid van nutritionele preconditionering

De eerste klinische vertaling van alle diëten zoals verricht in de diermodellen is verricht in **hoofdstuk 7**. In dit hoofdstuk hebben we de haalbaarheid en veiligheid van een calorie- en eiwitbeperkt dieet onderzocht in mensen. Daarvoor hebben we zowel levende nierdonoren als bariatrische chirurgie patiënten gerandomiseerd in één van de volgende 3 groepen: de eerste groep kreeg een experimenteel, synthetisch vloeibaar dieet met 30% calorische restrictie en 80% eiwitrestrictie voor 5 dagen; de tweede groep kreeg een placebo synthetisch vloeibaar dieet voor 5 dagen wat isocalorisch was aan hun dagelijkse energiebehoefte; de derde groep was de controlegroep en deze mensen kregen geen restricties wat betreft voedsel inname. De haalbaarheid en veiligheid van de diëten werden bepaald aan de hand van gerapporteerde ongemakken, gewichtsveranderingen en metabole parameters zoals gemeten in bloedmonsters voor en na alle dieetinterventies. Totaal had 71% van de donoren en bariatrische chirurgie patiënten zich aan het restrictie-dieet gehouden, waarbij het dieet in 2/3 van de gevallen voor lichte ongemakken zorgde. Deze ongemakken, voornamelijk gastro-intestinaal van aard, werden laag gescoord en verdwenen snel op het moment van hervatten van het normale eetpatroon. Het merendeel van de patiënten dat het dieet echter niet had volgehouden, gaf wel aan dat de ongemakken hiervan de reden waren. Met name de bariatrische chirurgie patiënten gaven deze ongemakken vaker aan, mogelijk vanwege de connectie tussen obesitas en functionele gastro-intestinale klachten.

De haalbaarheid van het dieet kon objectief worden gemeten via de metabole parameters prealbumine (PAB) en retinol binding protein (RBP): serumwaarden van beide parameters waren significant verlaagd na het volgen van het restrictieve dieet in tegenstelling tot de groepen met het placebodieet en geen dieet. De vertakte keten aminozuren leucine en valine waren ook beide significant verlaagd in de dieetgroep in tegenstelling tot de placebo- en controlegroep. De dieetgroep liet geen hoger percentage complicaties of een langere

opnameduur zien, als indicatie van de veiligheid van het dieet. Deze eerste klinische studie laat zien dat een gecombineerd calorie- en eiwitbeperkt (GCEB) dieet haalbaar en veilig is in een klinische setting en dat de haalbaarheid objectief gemeten kan worden aan de hand van een combinatie van parameters. Kleine aanpassingen aan het dieet zouden de gastro-intestinale ongemakken kunnen verminderen waardoor de haalbaarheid van een dergelijk dieet verbeterd kan worden. Deze aanpassingen zou gedaan kunnen worden door bijvoorbeeld meer eiwitvrije snacks aan het dieet toe te voegen naar wens van de patiënt. Tevens kan het toevoegen van vast voedsel ook de haalbaarheid verhogen, de ongemakken verminderen en kan het dieet zo verder worden geoptimaliseerd om nutritionele preconditionering in een klinische setting te onderzoeken.

Tenslotte hebben we in **hoofdstuk 8** de perioperatieve en postoperatieve effecten van een GCEB-dieet onderzocht in levende nierdonoren en hun transplantaat ontvangers. Dit GCEB-dieet was een kleine aanpassing ten opzichte van het eerdergenoemde dieet en gaf de mogelijkheid voor meer variatie in eiwitvrije snacks. In totaal werden 35 donoren gerandomiseerd in ofwel de GCEB-groep (n=15) ofwel de controlegroep zonder voedingsrestricties (n=20). Het dieet werd gedurende de 5 dagen voor de operatie aan de donoren gegeven. Alle donoren hadden zich aan het dieet gehouden en lieten geen ernstige bijwerkingen zien. De primaire eindkomstmaat van deze studie was de postoperatieve nierfunctie van de donoren. Deze nierfunctie was significant beter in de GCEB-dieet groep vanaf dag 2 tot aan maand 1 postoperatief en werd gezien als verbeterende klaring van het serum creatinine, de filtratiesnelheid en serumwaarden van ureum. De levende nierdonoren in beide groepen lieten geen verschil zien tussen de opnameduur of de postoperatieve complicaties. De nierontvangers van de donoren die het GCEB-dieet hadden gevolgd lieten tevens een significante verbetering van de nierfunctie zien, waarbij de gemiddelde daling van het serum creatinine 70% bedroeg in de GCEB-groep in vergelijking met 40% in de controlegroep. Deze verbetering van nierfunctie ging gepaard met een significant lagere incidentie van acute afstoting, zichtbaar in nierbiopten die op indicatie waren afgenomen, en een significant lagere incidentie van een vertraagde functie van het transplantaat in de eerste postoperatieve periode. Vervolgens werden de transcriptoom profielen tussen beide dieetgroepen vergeleken in nierbiopten die direct na preservatie en voor implantatie van de nier in de ontvanger waren afgenomen. Deze vergelijking liet de grootste variatie van de genexpressie zien als gevolg van het geslacht van de donor. Door de verdeling van geslacht te maken, bleek de groep van mannelijke donoren in de GCEB-groep te klein om verdere analyse te verrichten. De analyse werd alleen verricht in de vrouwelijke donoren en hieruit werd zichtbaar dat het dieet zorgde voor een remming van genexpressie in het algemeen. Pathway analyse liet een remming van meerdere immunoregulatorische pathways zien, waaronder de Primary Immundeficiency Signaling, en een activatie van verscheidene stressrespons pathways zoals de NRF-gemedieerde stressrespons en de EIF2 α signaling

respons. De resultaten van deze klinische gegevens laten een grote gelijkens zien met onze preklinische data en tonen aan dat de effectiviteit van het GCEB-dieet wordt bewerkstelligd via de activatie van de stressrespons om zo meer weerstand tegen chirurgisch geïnduceerde stress te geven. Deze klinische data werden vervolgens vergeleken met data van eerdere genexpressies verricht in nierbiopten zoals beschreven in de literatuur, en bij deze vergelijking kwamen enkele interessante genen naar boven waaronder ASB15. Echter zijn er nog geen andere studies verricht waarin is gekeken naar veranderingen in genexpressie in nierbiopten na het volgen van een dieet. Samenvattend is deze studie de eerste in zijn soort die de positieve effecten van kortdurende DR op de stressresistentie heeft kunnen vertalen naar de kliniek en zorgt voor het bewijs dat kortdurende DR inderdaad in staat is om stressresistentie te verhogen in mensen.

Concluderend heeft dit proefschrift het bewijs geleverd dat verscheidene kortdurende dieetinterventies kunnen zorgen voor positieve effecten op de acute stressrespons in meerdere muismodellen, levende nierdonoren en hun transplantaat ontvangers en hebben deze resultaten bijgedragen aan de voortschrijdende inzichten in de moleculaire mechanismen achter dieetrestrictie via genexpressie analyses. We zijn nu slechts een aantal stappen verwijderd van de succesvolle implementatie van nutritionele preconditionering bij electieve chirurgie. Toekomstige studies moeten de genoemde resultaten gaan valideren in grotere en andere patiënten cohorten en moeten op post-transcriptioneel niveau de mechanismen achter dieetrestrictie verder gaan ontrafelen. Uiteindelijk zullen al deze studies leiden tot het optimale preoperatieve dieet, ofwel via dieetrestrictie of wel via een dieetvervanger, om te kunnen implementeren in de standaardzorg voor electieve patiënten.

APPENDICES

Dankwoord
List of publications
Curriculum Vitae
Portfolio

DANKWOORD

Dit proefschrift in deze hoedanigheid is tot stand gekomen door de bijdrage van vele mensen. Voor deze bijdrage wil ik iedereen bedanken; enkelen wil ik graag in het bijzonder bedanken.

Mijn copromotor, dr. R.W.F. de Bruin. Beste Ron, ruim 6 jaar geleden belde je me in de avond op om te zeggen dat ik was aangenomen. Zelf had ik nooit bedacht dat ik er nu zo voor zou staan, maar uiteraard riep jij het al vanaf jaar 1. Waarschijnlijk had ik wat vaker en wat eerder naar je moeten luisteren, maar daarover discussiëren we later nog weleens. Bedankt voor het veelvuldig nakijken van mijn 'poëzie', en het feit dat het altijd beter kan. Bedankt voor je meest waardevolle input en je support op de juiste momenten, je onuitputtelijke bron van verhalen en de borrels die het een onvergetelijke tijd op het lab hebben gemaakt.

Mijn promotor, Prof. dr. J.N.M. IJzermans. Beste prof., vooral het laatste jaar waren onze gesprekken veelvuldiger en intensiever. Op de juiste momenten kwam u altijd wel een met een kritische noot, waardoor ik zelf weer anders naar de analyses ging kijken. Bedankt voor de ruimte om het onderzoek grotendeels mijn eigen draai te geven. Tevens bedankt voor het vertrouwen en de aanbevelingen, ook op het moment dat ik de keuze had gemaakt om mijn carrière over een hele andere boeg te gaan gooien.

Mijn andere copromotor, dr. M.E.T. Dollé. Beste Martijn, jij hebt je vanaf dag 1 ingezet om mij welkom te laten voelen op het RIVM. Hierdoor werd het RIVM mijn tweede thuis wat betreft onderzoek. Bij elke vraag die we niet direct konden beantwoorden, wist jij binnen no-time de expertise in huis te vinden wat ervoor heeft gezorgd dat we alles uit het onderzoek hebben gehaald wat mogelijk is. Jouw oog voor detail is niet te evenaren. Bedankt voor alle tijd, (financiële) support en gezelligheid tijdens mijn onderzoektijd.

Mijn andere promotor, Prof. dr. H. van Steeg. Beste Harry, onze besprekingen waren niet veelvuldig, maar zijn mij wel stuk voor stuk bijgebleven. Je kijk op het onderzoek (en op het leven) heeft ook mijn kijk hierop zo nu en dan doen veranderen. Binnenkort mag je gaan genieten van je welverdiende pensioen. Het is een eer voor mij dat je nog in mijn commissie plaats zal nemen voor die tijd. Hartelijk dank hiervoor!

Beste Prof. dr. J.H.J. Hoeijmakers. Beste Jan, dank voor de correcties van mijn artikelen, de hernieuwde kijk op het onderzoek en het enthousiasme voor alles wat betreft veroudering en dieetrestrictie. Tevens dank voor het zitting nemen in mijn leescommissie.

Beste Prof. dr. A.H.J. Mathijssen, beste Prof. dr. H. Pijl, zeer veel dank voor het zitting nemen in mijn leescommissie.

Beste Prof. dr. R. Zietse, ons eerste contact stamt nog van het keuzeonderzoek tijdens mijn studie jaren waarbij u mij heeft begeleid vanuit Nederland terwijl ik van mijn tijd in Milaan aan het genieten was. Het feit dat u nu zitting wilt nemen in mijn commissie voelt daarom als vertrouwd; hartelijk dank hiervoor.

Beste Prof. dr. K. Willems van Dijk, hartelijk dank voor het zitting nemen in mijn commissie.

Mijn grootste dank gaat uit naar alle nierdonoren, niertransplantatie patiënten en bariatrische chirurgie patiënten die hebben deelgenomen aan mijn klinische studies en dit onderzoek mogelijk hebben gemaakt.

Beste dr. E. van der Harst. Beste Erwin, dankzij de betrokkenheid van het Maasstad en de bariatrische chirurgie heeft het onderzoek een unieke vorm aangenomen. Met je initiële idee over de telomeren hebben we samen de succesvolle Telomeerstudie opgezet en uitgevoerd. Graag blijf ik betrokken bij het vervolg! Veel dank voor de begeleiding bij het uitvoeren van mijn onderzoek in het Maasstad.

Beste dr. R.A. Klaassen. Beste René, vooral in het begin ben je betrokken geweest bij de opzet en uitvoering van alle klinische studies in het Maasstad waarbij de logistiek ook op langere termijn perfect bleef verlopen. Dank voor de begeleiding en het mogelijk maken van het onderzoek in het Maasstad.

Veel dank aan alle poli-assistenten, physician assistants, assistenten en chirurgen die betrokken zijn geweest bij de uitvoering van mijn studies in het Maasstad! In het bijzonder bedank ik graag Daisy Verhoeven, Corry van Rooijen en Wouter Roosink.

Beste Conny, iedereen weet eigenlijk wel dat jij de spil bent van de laboratoria van A3/A4 op het RIVM. Jouw hulp bij de uitvoering van alle RNA-isolaties en PCRs is van grote waarde geweest. Bedankt voor al je tijd, geduld, uitleg en gezelligheid op het lab!

Beste Jeroen, jij hebt mij alle beginselen van microarray analyses met het geduld van de wereld uitgelegd. Bedankt dat je te pas en te onpas klaar stond voor het beantwoorden van mijn vragen en het oneindig aanpassen van alle PCA-plots en heatmaps.

Beste Sandra, dank voor de uitvoering van de Western blots en de gezelligheid op het RIVM!
Beste Paul, dank voor je hulp bij de transcriptoom analyses van de humane nierbiopten.

Beste Nicolle, dankzij jouw kennis op het gebied van de telomeren is de Telomeerstudie een groot succes geworden. Het is ontzettend fijn om te weten dat jij altijd beschikbaar bent voor vragen en brainstormen. Heel veel dank voor je input en je begeleiding!

Beste Ruud, onze kortstondige samenwerking met de Telomeerstudie was ontzettend gezellig. Zowaar gaan we de studie tot een succes brengen! Heel veel succes met je verdere carrière.

Veel dank aan alle poli-assistenten, verpleegkundigen van 9-Zuid en alle transplantatiechirurgen die betrokken zijn geweest bij de opzet en uitvoering van de PROTECT-studie. Sabrina van Unnik en Linda van Duijvenbooden, bedankt voor de hulp bij de voedingsdagboeken.

Carola, jij bent de beste en meest gezellige secretaresse die een onderzoeker zich mag wensen. Altijd en overal wist jij een antwoord op mijn vragen en had je tijd om tijdens mijn 'wachtijd' voor een volgende afspraak koffie te drinken. Veel succes nu in de Z-flat!

Alle onderzoekers van labje #1: bedankt voor alle gezelligheid, dankzij jullie was ik altijd op de hoogte van alles wat er op Facebook gebeurde. Stef, Eline, Ruth, Chloë, Daniël, Hester: bedankt en veel succes met jullie onderzoek! Büttner, bedankt en tot snel in het SFG. Sander, jouw kijk op alles heeft er bij mij ook voor gezorgd dat ik alles wat meer cum grano salis ging bekijken. Bedankt voor je gezelligheid en onze samenwerking. Van je bruine vest op het lab kunnen we inmiddels wel soep koken. Jeroen, jij kwam op het laatst even binnenstormen en walste iedereen plat met je wervelwind aan publicaties. Bedankt voor je gezelligheid en al onze (vaak onzinnige) gesprekken. Veel succes met je opleiding!

Tanja, onze samenwerking op het lab was nog wel het meest intensief. Al was het alleen al maar omdat we 3 jaar lang een tafel hebben moeten delen op het lab zonder daglicht. Er zijn maar weinig mensen die zo hard werken als jij, waardoor onze artikelen samen zeker succesvol zijn geweest. Ik weet zeker dat je er gaat komen, daar hoeft je niet over te twifelen. Bedankt voor je hulp en gezelligheid!

Lieve Sandra en Gisela, jullie zijn allebei absoluut onmisbaar op het lab. Bedankt voor alle gezelligheid op het lab tijdens het plakken, knippen en vullen van alle materialen voor de studies maar ook tijdens de koffie- en lunchpauzes en de labuitjes; het was nooit saai!

Alle collega-onderzoekers uit de Z-flat en de Daniel: bedankt voor de gezelligheid!

Dear dr. Maurizio Gallieni, dear Prof. dr. Diego Brancaccio: thank you so much for the perfect research master I had in Milan, it will be remembered!

Alle collega's uit het Ikazia: heel erg bedankt voor de gezellige, intensieve maar vooral leerzame tijd! Dr. P.T. den Hoed, beste Ted, de leerschool van de chirurgie in het Ikazia heeft de perfecte basis gelegd voor mij als arts, dank voor de begeleiding hierbij. Dr. A.M.E. van

Well, beste Annemarie, dank voor je input als mentor. Nina, dank ook, voor de gezelligheid en de raadzame koffiemomenten. Heel veel succes nog, ook! Inge en Mostafa, de tijd met jullie in de PKV-tussenruimte was fantastisch. Ilse en Marja, met jullie op de SEH was het altijd feest, dank voor alle gezellige diensten!

Alle collega's in het Alrijne Leiderdorp: bedankt voor de gezellige tijd! Beste dr. A.M. Zeillemaker, dank voor het vertrouwen en de kortstondige begeleiding. Laura, het was altijd leuk om met jou samen de acute poli/SEH te runnen!

Lieve collega's uit het SFG: bedankt dat jullie me vanaf dag 1 al welkom hebben laten voelen bij de interne. Ik kijk ernaar uit om nog lang met jullie samen te werken! Beste dr. Y.C. Schrama, bedankt voor het vertrouwen.

Jeff, jij en je poloshirt of -overhemd waren onmisbaar voor de gezelligheid tijdens alle congressen maar ook tijdens onze tijd samen in het Ikazia. Altijd even tijd om te zeuren op alles, vooral op mijn (beperkte) Apple skills en jouw (eenkennige) smaak als het gaat om mooie kleding en goed eten. Bedankt voor al je steun!

Kirsten, het is altijd gezellig met jou, vooral als we (net niet) gaan sporten. Gelukkig hebben we niet als doel om zwemkampioenen te worden. Bel me gerust over alle elektrolytstoornissen op de afdeling; voor jou doe ik het graag.

Natasja, mijn oud-huisgenootje, onze dinersessies aan de gammele bar in de keuken van de Hofdijk zullen me altijd bijblijven. Gelukkig zijn we contact blijven houden. Worden we ook nog eens collega's! Bedankt voor al je steun en gezelligheid!

Hanna, al het lief en leed wat ik met je deel, kan jij weer zo'n draai geven dat we altijd lachend eindigen. Jouw ironie, never-ending doorzettingsvermogen en positiviteit zijn en zullen altijd een voorbeeld voor me blijven. Ik kijk met smart uit naar ons volgende lunch/borrel avontuur!

Jochem, of Wosti, hooikist, cobblestone. Ik had nooit gedacht dat we een week lang vakantie konden vullen met onzinverhalen en er zo hard om konden lachen ook. En dat inmiddels alweer meerdere keren; ik kijk uit naar de volgende keer! Bedankt dat je zo'n ongelofelijk goede vriend bent en altijd voor me klaarstaat!

Romy, jij komt voor in al mijn herinneringen aan het Maerlant. Van de eeuwigdurende fietstochten ernaartoe, de meezinguren tijdens Aardrijkskunde, de skireizen en de vele uren buiten schooltijd om. Een avond met jou staat altijd gevuld met gezelligheid, overheerlijk (zelf gebrouwen) eten, en wijn. Met jou kan ik echt alles delen. Bedankt dat je al zolang mijn vriendinnetje bent!

Myrthe, mijn basisschool-vriendinnetje. Bij jou gaat er niets boven Groningen, maar gelukkig is daar de digitale wereld. Beloofd, ik kom snel een keer langs!

Mijn lieve beste vriendinnetjes, jullie zijn geweldig! Hanke, jou ken ik nog het ‘minst lang’ maar ik kan echt alles met je delen. Elke keer weer raak ik gefascineerd door je fantastische kapsel, je collectie schoenen en je aanstekelijke lach. Zjwan, met jouw kleine Adam is je droom uitgekomen. Wat heb jij een transformatie doorgemaakt vanaf het moment dat ik je ken! Ik ben trots op je dat jij je hart bent blijven volgen en gelukkig dat je er altijd voor me bent. Michelle, onze reis naar Italië was onvergetelijk en onze tijd samen in het Ikazia was fantastisch, maar onze wekelijkse tot bijna dagelijkse koffiemomenten tijdens onderzoek hebben ervoor gezorgd dat ik gekomen ben waar ik nu sta. Ik kan niet wachten om je nieuwe huisje in Oostvoorne te bewonderen. Bedankt dat je mijn paranimf wilt zijn!

Lieve familie, bedankt voor jullie steun. Oma, Anne Marie en Aart, bedankt voor het vertrouwen in mijn kunnen en alle bemoedigende woorden.

Arnold, het was altijd weer een verrassing vanaf welke coördinaten ergens op zee je weer contact zocht. Van de avonden gevuld met pogingen om Jamie Oliver te evenaren en analyses hoe alles altijd beter kan, gevolgd door een ‘biosje’, heb ik genoten. Patrick, als het eens tegenzat wist jij wel met je non-stop verhalen overal weer een positieve draai aan te geven op het moment dat het nodig was. Vele uren van geluk heb ik doorgebracht met jou, Sandra en mijn lieve nichtjes Emily en Lily. Gerda, je staat altijd achter me en je bent de allerliefste zus die ik me kan wensen. Met de kleine Lize kan het geluk niet meer op; wat ben ik verliefd op je fantastische dochter! Bedankt dat je mijn paranimf wilt zijn, zonder jou was dit niks geworden.

Tot slot: lieve papa en mama, lieve Piet en Francien. Echt alles wat ik bereikt heb, wijt ik aan jullie onvoorwaardelijke steun, liefde en eeuwige geduld. Hoe jullie het altijd maar weer voor elkaar krijgen voor ons allemaal is bewonderenswaardig. Lieve Piet, alle telefoontjes in de avond- en nachturen, alle technische problemen, even zinloos kletsen bij een biertje: altijd en overal sta je voor me klaar. Lieve Francien, wat heb je toch altijd alles voor ons over. Jij weet overal het goede antwoord op en bent er altijd voor me. Dankzij jou weet ik dat ik uitzicht heb en ga hebben op het beste leven wat ik me kan wensen. Zei ik het niet? Het komt altijd goed. Ik hou van jullie.

LIST OF PUBLICATIONS

Jongbloed F, Galassi A, Cozzolino M, Zietse R, Chiarelli G, Cusi D, Brancaccio D, Gallieni M. **Clinical significance of FGF-23 measurement in dialysis patients.** *Clin Nephrol.* 2011 Sep;76(3):201-9.

Jongbloed F, de Bruin RWF, Pennings JLA, Payán-Gómez C, van den Engel S, van Oostrom CT, de Bruin A, Hoeijmakers JHJ, van Steeg H, IJzermans JNM, Dollé MET. **Preoperative fasting protects against renal ischemia-reperfusion injury in aged and overweight mice.** *PLoS One.* 2014 Jun 24;9(6):e100853.

Jongbloed F, IJzermans JNM, de Bruin RWF. **Letter to the Editor: Permissive underfeeding or standard enteral feeding in critical illness.** *N Engl J Med.* 2015 Sep 17;373(12):1175.

Jongbloed F, de Bruin RWF, Klaassen RA, van Steeg H, Dor FJMF, van der Harst E, Dollé MET, IJzermans JNM. **Preoperative calorie and protein restriction is feasible and safe in live kidney donors and morbidly obese patients: a pilot study.** *Nutrients.* 2016 May 20;8(5).

Jongbloed F*, Saat TC*, Verweij M, Payan-Gomez CE, Hoeijmakers JHJ, van den Engel S, van Oostrom CT, Ambagtsheer G, Imholz S, Pennings JLA, van Steeg H, IJzermans JNM, Dollé MET, de Bruin RWF. **A signature of renal stress resistance induced by short-term dietary restriction, fasting, and protein restriction.** *Sci Rep.* 2017 Jan 19;7:40901.

Jongbloed F, Meijers RWJ, Klaassen RA, IJzermans JNM, Betjes MGH, van der Harst E, de Bruin RWF, Litjens NHJ. **Effects of morbid obesity, metabolic syndrome and bariatric surgery on aging of the immune system.** *Submitted.*

Jongbloed F, Dollé MET, Huisman SA, Luijten M, van Steeg H, Pennings JLA, Rodenburg W, IJzermans JNM, de Bruin RWF. **The transcriptomic response to irinotecan in fasted colon carcinoma bearing mice.** *Submitted.*

Jongbloed F, de Bruin RWF, Beekhof P, Wackers P, Hesselink DA, van Steeg H, Hoeijmakers JHJ, Dollé MET, IJzermans JNM. **Combined calorie and protein restriction improves outcome in living kidney donors and kidney transplant recipients.** *Submitted.*

Shushimita S*, Kotimaa JP*, Jongbloed F, de Bruin RWF, IJzermans JNM, van Kooten C, Dor FJMF. **Dietary restriction modulates hepatic and renal expression of complement system genes in mice.** *Submitted.*

Jongbloed F*, Saat TC*, Dollé MET, van den Engel S, van Oostrom CT, Imholz S, van Steeg H, IJzermans JNM, de Bruin RWF. **The role of protein and essential amino acids in the protection against hepatic ischemia-reperfusion injury in mice.** *Manuscript.*

CURRICULUM VITAE

Franny Jongbloed werd geboren op 11 juni 1987 te Rotterdam, Nederland. In 2005 behaalde zij het Gymnasium aan het Maerlant College te Brielle. Na enkele weken te zijn gestart met de studie Biofarmaceutische Wetenschappen in Leiden werd zij alsnog ingeloot voor de studie Geneeskunde aan het Erasmus Universiteit te Rotterdam. Als keuzeonderzoek ging zij voor 21 weken naar het Ospedale San Paolo in Milaan en werkte op de afdeling Nefrologie onder leiding van Prof. Diego Brancaccio en dr. Maurizio Gallieni. Hierna behaalde zij het Doctoraalexamen en begon met coschappen in de regio Rotterdam. In oktober 2011 behaalde zij het Artsexamen. In september 2011 begon zij aan een promotietraject bij de afdeling Transplantatiechirurgie in het Erasmus MC onder leiding van Prof. dr. Jan IJzermans en dr. Ron de Bruin. Tevens was het promotietraject onderdeel van het RIVM en werkte zij bij het Centrum van Gezondheidsonderzoek onder leiding van Prof. dr. Harry van Steeg en dr. Martijn Dollé. Het promotieonderzoek breidde zich vervolgens ook uit naar het Maasstad Ziekenhuis, waarbij zij onder leiding van dr. Erwin van der Harst en René Klaassen heeft gewerkt. Na vier jaar fulltime onderzoek is zij in oktober 2015 gestart als ANIOS bij de afdeling chirurgie in het Ikazia ziekenhuis te Rotterdam en werkte zij daar tot en met eind december 2016. In januari 2017 heeft zij nog enkele maanden als ANIOS gewerkt op de afdeling chirurgie bij de Alrijne Zorggroep in Leiderdorp. Tijdens deze werkervaring ontstond de voorkeur voor de interne geneeskunde. Daarom heeft zij in juli 2017 de overstap gemaakt en is zij begonnen als ANIOS bij de interne geneeskunde in het Franciscus Gasthuis te Rotterdam, waar zij tot op heden met veel plezier werkt. Zij zal per 1 januari 2018 dan ook de opleiding Interne Geneeskunde starten in het Franciscus Gasthuis te Rotterdam onder leiding van Dr. Yvonne Schrama.

PHD PORTFOLIO



Summary of PhD training and teaching

Name PhD student: Franny Jongbloed Erasmus MC Department: Surgery Research School: Molecular Medicine	PhD period: September 2011 – September 2015 Promotors: Prof. dr. J.N.M. IJzermans, Prof. dr. H. Van Steeg Copromotors: Dr. R.W.F. de Bruin, Dr. M.E.T. Dollé	
1. PhD training	Year	Workload (ECTS)
General courses - Biomedical English Writing and Communication - BROK ('Basiscursus Regelgeving Klinisch Onderzoek')	2014 2012	5.7 1.5
Research courses - Basic introduction course on SPSS - Basic course on R - Ingenuity course - Basic data analyse on gene expression arrays	2012 2015 2014 2013	1.0 1.0 0.5 1.1
Seminars and workshops - Photoshop and Illustrator CS5 Workshop - Adobe InDesign Workshop	2013 2013	0.3 0.15
Presentations - National conferences - International conferences	2012 2013 2014 2015 2013 2014 2015	0.8 4.9 3.0 0.8 0.8 3.6 0.6
2. Teaching	Year	Workload (ECTS)
Supervising practicals and excursions, Tutoring - Supervising first aid examinations (Medical Students)	2012 2013 2014 2014	0.2 0.2 0.2 0.2
Supervising Master's theses - Supervising student Bachelor's thesis - Supervising students in the lab / clinic	2015 2015	2.0 5.0

